

STRUCTURAL AND PAIN MODIFICATIONS IN MODELS OF OSTEOARTHRITIS

Lilian Ngozi Nwosu, BSc

Arthritis Research UK Pain Centre

School of Medicine

**Department of Rheumatology, Orthopaedics and
Dermatology**

**Thesis submitted to the University of Nottingham
for the degree of Doctor of Philosophy**

December 2015

DECLARATION

This is to certify that the work submitted in this thesis is the result of original research which was conducted by me. Any help received with undertaking the in-vivo studies here has been fully acknowledged and referenced were appropriate.

Study design, data collection, analysis and writing were conducted primarily by me. Paul Mapp did the MNX surgeries used in this thesis. Peter Gowler, Junting Huang, Seyed Shahtaheri and Pongsatorn Meesawatsom conducted some macroscopic and/ or microscopic scoring on knee tissues from my experiments which I used in comparison to my data for some of the validation of pathological assessment systems used here.

Supervision of this thesis was undertaken by Professors David Walsh and Victoria Chapman. This thesis has not already been accepted for any degree.

ABSTRACT

Background: Despite the extensive research into the pathophysiology of osteoarthritis (OA), pain still represents a significant unmet clinical need. Current treatments for OA target symptomatic relief, but pharmacological analgesia is often not sustained. Pathological characteristics associated with OA pain include chondropathy, synovitis, subchondral bone marrow lesions and osteophytes. Concurrent with the development of OA, sensitisation of nociceptive pathways augments pain. Pain in OA therefore depends on a combination of pathology within the joint, peripheral and central neuronal sensitisation.

Objectives: This thesis explores the effects of a tropomyosin related kinase A receptor (TrkA) inhibitor and an anti-nerve growth factor (NGF) antibody as interventions to modify inflammation, structural pathology and pain behaviour in rat models of OA. It also describes methods development and validation for assessing joint pathology in these rat models.

Hypothesis: Pain behaviour and structural pathology are features of OA models that are mediated by NGF-TrkA signalling. NGF may mediate OA pain by joint function and structure, including neuronal sensitisation, inflammation and subchondral osteoclast activation.

Methods: Rat models of inflammation and OA (carrageenan, monosodium iodoacetate - MIA and medial meniscal transection – MNX) were assessed for pain behaviour, inflammation and structural pathology. In the MIA model, two doses were investigated. A lower 0.1mg dose representing milder OA and a standard 1mg dose representing more severe OA. Scoring of knee joint pathology macroscopically was developed and applied. Reliability, reproducibility and validity of both macroscopic and microscopic (histological) scoring systems for knee joint pathology were determined. Effect of interventions on pain behaviour (weight bearing asymmetry and paw withdrawal thresholds) and structural pathology (macroscopic and microscopic scoring of articular surfaces) to include inflammation were assessed using inhibitors of the NGF-TrkA pathway. Pain Data were analysed longitudinally using area under the curve or independently with Kruskal Wallis test followed by Dunns post hoc. Other data were analysed with Kruskal Wallis test followed by Dunns post hoc. Data are presented as mean (95% confidence interval).

Results: The carrageenan, MIA and MNX models all exhibited inflammation and pain behaviour. The MIA and MNX models displayed both macroscopic and microscopic pathology. The pain phenotypes (weight bearing asymmetry and hind paw withdrawal threshold) observed in the MIA model were dependent on the MIA dose. The 0.1mg MIA injected rats displayed reduced

paw withdrawal threshold (0.1mg MIA v saline; day 20 = 187 [115-259] v 282 [265–298] *p<0.05) but not weight bearing asymmetry (0.1mg MIA v saline; day 20 = 52.8 [4.79-101] v 49.8 [14–85.5]) whereas the 1mg MIA injected rats displayed both (paw withdrawal threshold; 1mg MIA v saline; day 20 = 187 [160-215] v 282 [265–298] **p<0.01 and weight bearing asymmetry; 1mg MIA v saline; day 20 = 189 [118-261] v 49.8 [14–85.5] *p<0.05).

The Guingamp method of macroscopic scoring permitted discrimination between OA disease group and normal controls. This method of scoring had a higher reliability and reproducibility than other macroscopic scoring methods. The Janusz and modified OARSI histopathology scoring systems for cartilage damage were reliable and reproducible with similar variability and had strong correlations to each other.

Following preventive or therapeutic treatment with the tropomyosin receptor kinase (Trk) A inhibitor AR786, pain behaviour was inhibited in both MIA (MIA + Vehicle v MIA + drug; day 21 = 27 [21-23] v 3.7 [-1.4 – 8.8] **p<0.01) and MNX (MNX + Vehicle v MNX + drug; day 21 = 27 [21-32] v 4.8 [1.1-8.6] **p<0.01) models. Synovitis was attenuated only in the MIA model (MIA + Vehicle v MIA + drug; day21 = 2.3 [2-2.6] v 1.2 [0.32-2.1] *p<0.05). Analgesia was sustained for up to 10 days in the MNX model following AR786 treatment discontinuation. AR786 administration reduced the numbers of tartrate resistant acid phosphatase (TRAP) positive multinucleated osteoclast cells in the MIA model (MIA + Vehicle v MIA + drug; day 21 = 68 [59-76] v 51 [46-56] **p<0.01) but not the MNX model. AR786 did not significantly alter macroscopic measures of structural pathology in either model. Preventive and therapeutic treatment with the anti-NGF monoclonal antibody M911 did not alter changes to cartilage pathology.

Conclusions: Manifestation of pain, inflammation and alterations in knee joint structure are characteristic features of OA models and these alterations in joint structure can be measured reliably and reproducibly by both macroscopic visualization and assessment of histological sections. NGF might contribute to OA pain through the NGF-TrkA pathway. This contribution might be as a result of facilitating nociception, inflammation, and activation of osteoclasts. Further investigation into the mechanisms by which NGF contributes to OA pain through the TrkA receptor might increase therapeutic potential for OA chronic pain relief.

PUBLICATIONS AND PRESENTATIONS

PUBLICATIONS

- Devi Rani Sagar, Lilian Nwosu, David A. Walsh, Victoria Chapman. Dissecting the contribution of knee joint NGF to spinal nociceptive sensitization in a model of OA pain in the rat. *Osteoarthritis and Cartilage* 2015.
- Lilian N. Nwosu, Paul Mapp, Victoria Chapman, David A. Walsh. Blocking the Tropomyosin receptor kinase A (TrkA) receptor inhibits pain behaviour in two rat models of osteoarthritis. *Annals of the Rheumatic Diseases* 2015 (accepted).

PRESENTATIONS

ORAL

- Nwosu LN, Mapp PI, Bouhana KS, Andrews SW, Chapman V, Walsh DA. Effects of anti-NGF strategies in two animal models of osteoarthritis (OA). ACR/ARHP annual meeting, Boston 2014.

POSTER

- Nwosu LN, Mapp PI, Chapman V, Walsh DA. Alterations in central pain processing are not restricted to end stage osteoarthritis in the monosodium-iodoacetate model of osteoarthritis (OA). OARSI world congress on OA, Paris 2014.
- Nwosu LN, Mapp PI, Chapman V, Walsh DA. Tropomyosin receptor kinase (Trk) A receptor inhibition reduces pain behaviour in a rodent model of osteoarthritis (OA). European pain federation EFIC, Vienna Austria, September 2015.

ACKNOWLEDGMENTS

Firstly I would like to thank God for giving me the opportunity and carrying me through this PhD, I would not have been able to do it without him.

I am grateful to the Arthritis Research UK Pain Centre for funding my project. I would most like to thank my supervisors Professors David Walsh and Victoria Chapman for their excellent supervision and guidance throughout my PhD. The project and thesis would not have been possible without their support and helpful discussions in the preclinicals and one to one meetings. David, your sense of humour from my thesis comments always made me laugh “This section is a bit long (indeed, the whole thesis risks being a dinosaur)”

I would like to thank Dr Paul Mapp and the rest of the Pain Centre team for all their help with my in-vivo studies especially Tracy, Devi, Junting, Adrian, Den, Paul Millns and James Burston who was always there (including weekends) when I needed him. Thanks to Karyn Bouhana, Steven Andrews and colleagues from Array BioPharma (Colorado, USA) for providing the compounds (AR786 and Gelucire 50/13 vehicle) used in this thesis.

To my pal Laura Stoppiello soon to be Wyatt who was always a constant reminder that I wasn't in it alone. I am grateful for all your help.

It was a pleasure to have had the opportunity to meet and work with the amazing multidisciplinary team of researchers and non-researchers in the department of Academic Rheumatology.

Lastly and most importantly, I dedicate this thesis to my dad and mum for their encouragement and always believing that I could do it. To the rest of my family (Tonia, Emeka, Kate, Kingsley, Kenny and Anthony) and friends for all their love and support.

Give honour to whom honour is due (Romans 13:7)

TABLE OF CONTENTS

DECLARATION	i
ABSTRACT	ii
PUBLICATIONS AND PRESENTATIONS	iv
ACKNOWLEDGMENTS	v
TABLE OF CONTENTS	vi
LIST OF FIGURES	xii
LIST OF TABLES	xv
ABBREVIATIONS	xvi
CHAPTER 1; INTRODUCTION.....	1
1.1 OSTEOARTHRITIS	1
1.1.1 Epidemiology.....	2
1.1.1.1 Risk factors.....	2
1.1.2 Pathophysiology	4
1.1.2.1 Articular cartilage.....	5
1.1.2.2 Subchondral bone	7
1.1.2.3 Synovium.....	8
1.1.3 Diagnosis, detection and treatment of OA.....	10
1.1.3.1 Current treatments for OA.....	11
1.2 INFLAMMATION; ROLE OF INFLAMMATION IN OA PATHOGENESIS	14
Synovitis precedes structural change.....	15
1.2.1 Innate immunity in OA.....	15
1.2.2 Inflammatory cells and cytokines in OA	16
1.2.2.1 Role of synovial macrophages in inflammation and OA	16
1.2.3 Anti-inflammation therapy	17
1.3 PAIN AND OA.....	21
1.3.1 Innervation of the normal and the arthritic knee joint and its link to pain	23

1.3.2	The normal joint	23
1.3.3	Mechanisms involved in the development of joint pain.....	25
1.3.4	Inflammatory mediators and modulators of pain.....	26
1.3.4.1	Nerve growth factor.....	27
1.3.4.2	General roles of NGF	28
1.3.4.3	Actions of NGF	30
1.3.4.4	Current strategies for targeting NGF-TrkA signalling	36
1.4	PRECLINICAL ANIMAL MODELS	38
1.4.1	Monosodium iodoacetate (MIA) model of OA	39
1.4.2	Medial meniscal transection (MNX) model of OA	39
1.5	PAIN BEHAVIOURAL MEASUREMENTS.....	41
1.6	HYPOTHESIS AND OBJECTIVES OF THESIS	42
1.6.1	Hypothesis	42
1.6.2	Objectives	42
	CHAPTER 2; MATERIALS AND METHODS	44
2.1	INTRODUCTION	44
2.2	ANIMALS	44
2.3	ANIMAL MODELS	44
2.3.1	Anaesthesia.....	44
2.3.2	Intra-articular injections.....	45
2.3.3	Intra-peritoneal injections.....	46
2.3.4	Oral gavage.....	47
2.3.5	Medial meniscal transection.....	49
2.4	ACUTE INFLAMMATION	51
2.4.1	Joint swelling.....	51
2.5	PAIN BEHAVIOUR MEASUREMENTS	52
2.5.1	Weight bearing.....	53
2.5.2	Distal (static) allodynia.....	54
2.6	TISSUE COLLECTION AND PROCESSING.....	55

2.6.1	Euthanasia (overdose by CO ₂ or anaesthetic-pentobarbital)	55
2.6.2	Systemic transcardiac perfusion fixation.....	55
2.6.3	Harvesting and mounting of rat synovia.....	56
2.6.4	Harvesting and mounting of rat tibiofemoral joints	57
2.7	HISTOCHEMISTRY	62
2.7.1	Histological stains.....	62
2.7.1.1	Haematoxylin and eosin (H&E)	62
2.7.1.2	Safranin-O fast green.....	63
2.7.1.3	Alcian blue-pas.....	65
2.7.2	Enzyme histochemistry.....	67
2.7.2.1	Tartrate resistant acid phosphatase (TRAP).....	67
2.7.3	Immunohistochemistry (IHC).....	68
2.7.3.1	Introduction	68
2.7.3.2	Limitations, difficulties and problems of IHC	68
2.7.3.3	Principles of IHC.....	69
2.7.3.4	Staining procedures	72
2.8	IMAGE ANALYSIS AND QUANTIFICATION.....	74
2.8.1	Synovia	74
2.8.1.1	Synovitis.....	74
2.8.1.2	Macrophage infiltration.....	74
2.8.2	Cartilage and subchondral bone.....	75
2.8.2.1	Macroscopic chondropathy scoring.....	75
2.8.2.2	Microscopic scoring	75
2.8.2.3	TRAP (osteoclast) counting	77
2.9	STATISTICAL ANALYSIS	78
2.10	REAGENTS	79
CHAPTER 3; THE CARRAGEENAN MODEL OF INFLAMMATORY ARTHRITIS		80
3.1	INTRODUCTION	80
3.2	AIMS.....	83

3.3	METHODS	84
3.4	RESULTS	88
3.4.1	Effect of intra-articular injection of carrageenan.....	88
3.4.1.1	Body weight	88
3.4.1.2	Pain behaviour.....	89
3.4.1.3	Acute inflammation.....	91
3.4.2	Macrophage markers are associated with inflammatory pain	98
3.5	DISCUSSION	99
3.6	CONCLUSIONS.....	103
CHAPTER 4; RELIABILITY, AGREEMENT AND VALIDITY OF THE		
GUINGAMP MACROSCOPIC CHONDROPATHY SCORING SYSTEM IN		
RAT MODELS OF OA		
104		
4.1	INTRODUCTION	104
4.2	AIMS.....	107
4.3	MATERIALS AND METHODS.....	108
4.3.1	Indian ink and modified SFA classification	108
4.3.2	Modified SFA and Guingamp classification	111
4.3.3	Validation of the macroscopic scoring systems.....	111
4.4	RESULTS	116
4.4.1	Macroscopic chondropathy scoring on 0.1mg or 1mg MIA injected knee joints	116
4.4.1.1	Direct visual scoring;.....	117
4.4.1.2	Photographic scoring.....	118
4.4.2	Validity testing of the macroscopic scoring systems.....	119
4.5	DISCUSSION	126
4.6	CONCLUSIONS.....	131
CHAPTER 5; THE MONOSODIUM-IODOACETATE (MIA) MODEL OF		
OA PAIN; COMPARISON BETWEEN TWO MIA DOSES AND TIME		
POINTS		
132		
5.1	INTRODUCTION	132
5.2	AIMS.....	135

5.3	METHODS	136
5.3.1	Characteristic features of a low and standard dose of MIA injections in naïve animals	136
5.3.2	Validation of histopathology scoring systems.....	140
5.4	RESULTS	142
5.4.1	Effects of a low 0.1mg and standard 1mg MIA dose	142
5.4.1.1	Body weight	142
5.4.1.2	Intra-articular injection of MIA induces changes in pain behaviour; pain phenotypes depend on severity of disease	143
5.4.1.3	Inflammation	146
5.4.1.4	Osteochondral pathology.....	152
5.4.2	Heterogeneity of OA pathology in the MIA model.....	157
5.4.3	Reliability of histological scoring systems	160
5.4.4	Comparison between Safranin-O and Alcian blue in the detection of matrix proteoglycan.....	164
5.5	DISCUSSION	166
5.5.1	Symptomatic features of OA in the MIA model	166
5.5.2	Heterogeneity of OA pathology in the MIA model.....	170
5.5.3	Reliability of histological scoring systems	171
5.5.4	Sensitivity of histological stains in the detection of matrix proteoglycan	173
5.6	CONCLUSIONS.....	175
CHAPTER 6; CONTRIBUTION OF NGF IN OA PAIN: TARGETING THE NGF-TRKA PATHWAY IN TWO RAT MODELS OF OA		176
6.1	INTRODUCTION	176
6.2	AIMS.....	179
6.3	METHODS	180
6.4	RESULTS	187
6.4.1	Effects of AR786 in the MIA and MNX models of OA pain... 187	
6.4.1.1	Body weight	187
6.4.1.2	Pain behaviour.....	189

6.4.1.3	Inflammation	195
6.4.1.4	Macroscopic pathology	201
6.4.1.5	Numbers of TRAP positive osteoclasts.....	204
6.4.2	Therapeutic and preventive administration of a monoclonal NGF antibody M911 in the MIA model	209
6.4.2.1	Structural (microscopic) pathology	209
6.5	DISCUSSION	215
6.6	CONCLUSIONS.....	221
CHAPTER 7;	GENERAL DISCUSSION.....	222
7.1	MAIN STUDY FINDINGS	222
7.2	NGF; A MEDIATOR OF INFLAMMATION, OSTEOCHONDRAL PATHOLOGY AND PAIN IN OSTEOARTHRITIS	224
7.2.1	Inflammation.....	224
7.2.2	Osteochondral pathology	226
7.2.3	Pain	226
7.2.4	Targeting NGF or TrkA for OA	229
7.3	LIMITATIONS OF CURRENT RESEARCH	230
CHAPTER 3	230
CHAPTER 4	231
CHAPTER 5	232
CHAPTER 6	232
7.4	DIRECTIONS FOR FUTURE RESEARCH.....	234
7.5	CONCLUSION.....	237
REFERENCES	239
APPENDICES	272
Materials and Reagents.....		272
Buffers and solutions used for immunohistochemistry		274
Antibody list		276

LIST OF FIGURES

Figure 1.1 Normal and osteoarthritic knee.	1
Figure 1.2 Risk factors for OA.	4
Figure 1.3 The articular cartilage.....	5
Figure 1.4 The pathology of osteoarthritis	9
Figure 1.5 Neurotrophins and their preferred Trk receptors.....	28
Figure 1.6 NGF-TrkA signalling.	35
Figure 1.7 Therapeutic strategies for targeting NGF/TrkA for OA pain relief.	37
Figure 2.1 Intra-articular injections into rat knees.....	46
Figure 2.2 Administration of compounds intra-peritoneally	47
Figure 2.3 Compound administration by oral gavage	48
Figure 2.4 Transection of the medial meniscus of the knee	51
Figure 2.5 Measurement of knee joint swelling	52
Figure 2.6 Incapacitance meter used for recording weight bearing.....	53
Figure 2.7 Wire bottom test cages for measuring allodynia.....	54
Figure 2.8 Harvested synovia	57
Figure 2.9 Harvested and embedded rat joints	61
Figure 2.10 Haematoxylin and Eosin stained section of a tibia.	63
Figure 2.11 Safranin-O Fast green stained section of a tibia.....	65
Figure 2.12 Tibia plateau with Alcian blue PAS stain.	66
Figure 2.13 Indirect immunohistochemistry.....	72
Figure 3.1 Time course of carrageenan induced inflammation and pain behaviour	85
Figure 3.2 Weight gain of rats	88
Figure 3.3 Effect of intra-articular injection of 2% carrageenan on weight bearing asymmetry.....	89
Figure 3.4 Effect of intra-articular injection of 2% carrageenan on paw withdrawal threshold	90
Figure 3.5 Effect of intra-articular injection of 2% carrageenan on joint swelling (Knee diameter).....	92

Figure 3.6 Histologic changes after intra-articular injection of 2% carrageenan	93
Figure 3.7 Macrophage infiltrations after intra-articular injection of 2% carrageenan	94
Figure 3.8 ED2 and ED3-immunoreactive macrophages in normal rat spleen	95
Figure 3.9 Macrophage infiltrations after intra-articular injection of 2% carrageenan	96
Figure 3.10 Macrophage infiltrations after intra-articular injection of 2% carrageenan	97
Figure 4.1 Original SFA scoring from diagrams obtained from photographs of human knees.	110
Figure 4.2 Example pictures of the Guingamp scoring system for the medial femoral condyle of MNX-operated rats.....	115
Figure 4.3 Macroscopic changes, articular surface lesions after intra-articular injection of 1mg or 0.1mg MIA.....	117
Figure 4.4 Macroscopic changes, articular surface lesions after intra-articular injection of 1mg or 0.1mg MIA.....	118
Figure 4.5 Direct (A and C) and photographic (B and D) scoring of macroscopic chondropathy in MIA injected (A and B) or MNX operated (C and D) rats by one observer (LN).	120
Figure 4.6 Photographic scoring of macroscopic chondropathy in MNX operated (A-C) rats.	121
Figure 4.7 Bland-Altman plots	124
Figure 5.1 Time course of MIA-induced pain behaviour and inflammation..	137
Figure 5.2 Time course of MIA-induced pain behaviour and inflammation..	138
Figure 5.3 Time course of weight gain of rats.....	142
Figure 5.4 Effects of MIA on weight bearing asymmetry.....	144
Figure 5.5 Effects of MIA on paw withdrawal threshold.....	145
Figure 5.6 Evidence of inflammation 20 and 42 days after OA induction.....	148
Figure 5.7 Mild persistent synovitis is a feature both of standard and low dose MIA model.....	151
Figure 5.8 Structural changes in the articular cartilage in the MIA model ...	154
Figure 5.9 IpA and IpP scores for cartilage damage in the MIA model.....	158
Figure 5.10 IpA and IpP scores for chondrocyte morphology in the MIA model	159

Figure 5.11 Cartilage chondropathy in the MIA model as scored by the Janusz and modified OARSI classification methods.	163
Figure 5.12 Proteoglycan content in the cartilage matrix of the MIA model, comparing the Safranin-O Fast green stain to the Alcian blue-PAS stain.....	165
Figure 6.1 NGF-TrkA complex formed by binding of NGF to the TrkA receptor.	179
Figure 6.2 Time course of experiment investigating the effect of a therapeutic administration of the TrkA inhibitor AR786 in the MIA and MNX models of OA.....	182
Figure 6.3 Time course of experiment investigating the effect of preventive administration of the TrkA inhibitor AR786 in the MNX model.....	183
Figure 6.4 Time course of weight gain of rats.....	188
Figure 6.5 Effects of therapeutic AR786 on pain behaviour in the MIA and MNX models of OA	190
Figure 6.6 Effect of preventive AR786 on pain behaviour in the MNX model of OA.....	193
Figure 6.7 Effect of AR786 on MIA- or MNX-induced inflammation.....	197
Figure 6.8 Synovitis in the MIA and MNX models of OA	200
Figure 6.9 Macroscopic chondropathy scoring in the MIA and MNX models of OA.....	202
Figure 6.10 Macroscopic appearances of chondropathy in the MIA and MNX models of OA.....	203
Figure 6.11 TRAP positive multinucleated osteoclasts in MIA and MNX models of OA.....	205
Figure 6.12 TRAP positive multinucleated osteoclasts in the MIA and MNX models of OA.....	208
Figure 6.13 Microscopic pathology in the MIA model of OA.....	211
Figure 6.14 Microscopic appearances of pathology in the MIA model of OA	214

LIST OF TABLES

Table 1.1 Osteoarthritis management involving non-pharmacological, pharmacological, and surgical treatment options; adverse effects/safety profiles for the different pharmacological treatment options	13
Table 1.2 Evidence of the role of synovitis in OA	19
Table 3.1 Correlations between pain, synovitis and ED macrophage markers	98
Table 4.1 OA cartilage histopathology assessment – pros and cons	104
Table 4.2 Outline of classification systems used for macroscopic chondropathy scoring of OA	114
Table 4.3 Inter-rater reliability analysis for macroscopic chondropathy scoring as measured by two scoring methods and between observers	122
Table 4.4 Associations of macroscopic scores with other OA histological severity scores and synovitis	125
Table 5.1 Pathological features in articular cartilage and subchondral bone 20 days after intra-articular injection of MIA (study 1)	155
Table 5.2 Pathological features in articular cartilage and subchondral bone 20 and 42 days after intra-articular injection of MIA (study 2)	156
Table 5.3 Inter observer agreement between four histological scoring investigators as measured by two different statistical methods.....	161

ABBREVIATIONS

ABC	Avidin-biotin peroxidase complex
ACLT	Anterior cruciate ligament transection
ACR	American college of rheumatology
ADAMTS	A Disintegration and Metalloproteinase with Thrombospondin-like Motifs
AIDS	Acquired immune deficiency syndrome
AMPA	α -amino-3-hydroxy-5-methyl-4- isoxazolepropionic acid
ASIC	Acid sensing ion channel
ASPA	Animals Scientific Procedures Act
ATP	Adenosine triphosphate
BDNF	Brain derived neurotrophic factor
BMP	Bone morphogenic protein
BSA	Bovine serum albumin
CFA	Complete Freund Adjuvant
CGP-39	Cartilage glycoprotein 39
CGRP	Calcitonin gene related peptide
CI	Confidence interval
CIPA	Congenital insensitivity to pain with anhidrosis
CNS	Central nervous system
CO ₂	Carbon dioxide
COX	Cyclooxygenase
CRP	C-reactive protein
CSF	Cerebrospinal fluid
CT	Computed tomography
DAB	Diaminobenzidine
DAMP	Danger associated molecular pattern
DH ₂ O	Distilled water

DMM	Destabilization of the medial meniscus
DRG	Dorsal root ganglion
ECM	Extracellular matrix
EDTA	Ethylenediaminetetraacetic acid
EGF	Endothelial growth factor
EULAR	European League against Rheumatism
FG	Femoral groove
GAG	Glycosaminoglycan
GAPDH	Glyceraldehyde 3-phosphate dehydrogenase
GI	Gastrointestinal
HA	Hyaluronan
H&E	Haematoxylin and Eosin
HCL	Hydrochloric acid
HHGS	Histological Histochemical Grading System
HIV	Human immunodeficiency virus
IA	Intra-articular injection
ICAM	Intracellular adhesion molecule
ICC	Intraclass correlation
IgG	Immunoglobulin G
IHC	Immunohistochemistry
IL	Interleukin
IPA	Ipsilateral anterior
IPP	Ipsilateral posterior
IQR	Inter quartile range
JSN	Joint space narrowing
K/C	Kaolin/carrageenan-induced arthritis
K	Kappa
LFC	Lateral femoral condyle
LTB ₄	Leukotriene B ₄

LTP	Lateral tibial plateau
mAb	Monoclonal antibody
MAC	Minimum alveolar concentration
MCL	Medial collateral ligament
MFC	Medial femoral condyle
MIA	Monosodium-iodoacetate
MMP	Matrix metalloproteinase
MMT	Medial meniscal tear
MNX	Meniscal transection
MRI	Magnetic resonance imaging
MTP	Medial tibial plateau
NGF	Nerve growth factor
NHS	Normal horse serum
NMDA	N-Methyl-D-aspartate
NSAIDS	Non-steroidal anti-inflammatory drugs
NT3/4/5	Neurotrophin 3/4/5
O ₂	Oxygen
OA	Osteoarthritis
OACH	Osteoarthritis cartilage histopathology
OARSI	Osteoarthritis Research Society International
OCT	Optimal cutting temperature
PAL	Periarteriolar lymphoid sheet
PAMP	Pathogen associated molecular pattern
PAS	Periodic acid schiff
PBS	Phosphate buffered saline
PDGF	Platelet derived growth factor
PFA	Paraformaldehyde
PGE ₂	Prostaglandin E ₂
PLC	Phospholipase C

PNS	Peripheral nervous system
PRR	Pattern recognition receptor
PVP	Polyvinylpyrrolidone
PWT	Paw withdrawal threshold
RT	Room temperature
RA	Rheumatoid arthritis
RANKL	Receptor activator of nuclear factor kappa-B ligand
RPOA	Rapidly progressive OA
SD	Sprague Dawley
SEM	Standard error of mean
SFA	Société Française D'Arthroscopie (French society of arthroscopy)
SNP	Single nucleotide polymorphism
SP	Substance P
THR	Total hip replacement
TIMP	Tissue inhibitor of metalloproteinase
TKR	Total knee replacement
TLR	Toll-like receptor
TNF	Tumour necrosis factor
TRAP	Tartrate resistant acid phosphatase
TrkA/B/C	Tropomyosin receptor kinase A/B/C
TRPV1	Transient receptor potential vanilloid 1
UKA	Unicondylar knee arthroplasty
VCAM	Vascular cell adhesion molecule
VEGF	Vascular endothelial growth factor

CHAPTER 1; INTRODUCTION

Arthritis is a disease characterised by inflammation and pain to one or more joints. There are many different types of arthritis, with the most common form being osteoarthritis, which is degenerative but also inflammatory.

1.1 OSTEOARTHRITIS

Osteoarthritis (OA) is a painful chronic disease that affects the whole joint; subchondral bone, cartilage, synovium, synovial fluid, tendon, ligaments, menisci and joint capsule (Fig.1.1) (Little and Smith, 2008). OA is caused by progressive joint degeneration which includes loss of articular cartilage surface integrity, subchondral bone remodelling and sclerosis with osteophyte formation (Fig.1.1) (Buckwalter and Mankin, 1998).

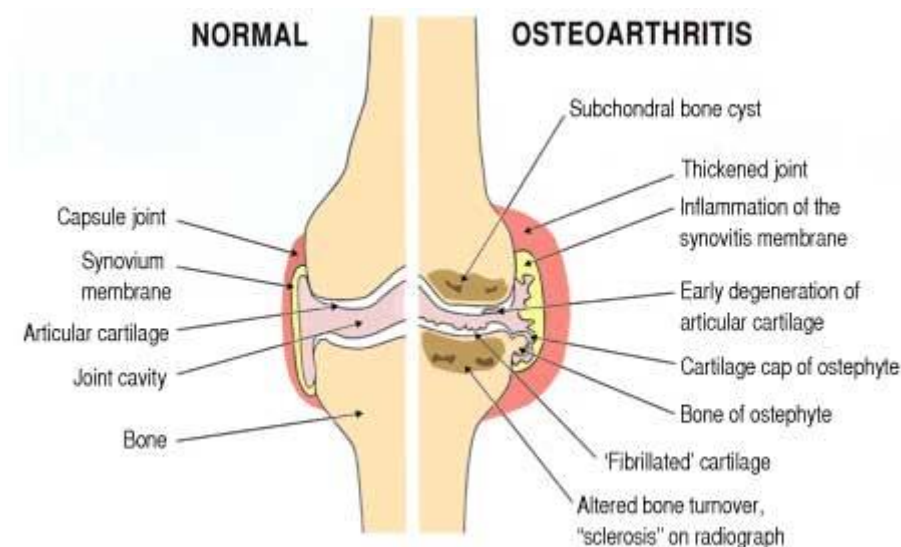


Figure 1.1 Normal and osteoarthritic knee. The OA knee is characterised by subchondral bone cyst formation, synovitis, cartilage fibrillation, subchondral bone remodelling, osteophyte formation etc. Figure taken from (MendMeShop.com, 2006-2015)

In OA, joint degeneration represents the disease while symptoms of aching, discomfort, pain, and stiffness for which patients seek medical care represent the illness (Hochberg, 2013). Although the pathophysiology of joint degeneration in OA is extensively studied, there is still a gap in our knowledge of how it leads to the clinical syndrome of OA and as a result, efforts to prevent the disease or slow its progression are hampered. Even more complex are the mechanisms by which the OA joint becomes painful. The available therapeutic treatments do not prevent or cure OA and symptomatic treatments do not offer effective pain relief in everyone. OA therefore becomes a substantial economic burden for sufferers (as it reduces their quality of life), health care systems and countries (Reginster, 2002, Leigh et al., 2001, Buckwalter and Martin, 2006). Finding better treatments for the prevention and cure of OA would require more research into the modification of structural pathology and pain in order to slow down disease progression and reduce joint pain and dysfunction.

1.1.1 Epidemiology

OA may develop in any joint but most commonly occurs in the knee, hip, hand, spine and foot. It is a major cause of disability and morbidity in people aged 45 and above in developed countries (Helmick et al., 2008). The incidence of hand, hip and knee OA increases with age, with women having higher rates than men (Cooper et al., 2013). In England and Wales approximately 1.3 – 1.75 million people are affected by symptomatic OA, while in France about 6 million people are newly diagnosed each year (KO and CO, 2008, Reginster, 2002). Knee OA occurs less frequently than hand OA, although as previously mentioned, it occurs more frequently in females with female to male ratios varying between 1.5:1 and 4:1. US population studies on prevalence rates report that severe radiographic changes affect around 1% of people aged between 25 and 34 years and that this figure increases to nearly 50% in those aged 75 years and above (Jordan et al., 2007).

1.1.1.1 Risk factors

Primary OA is OA in the absence of a known cause. Variations occur in the proportions of individuals with primary OA within a particular OA population.

The risk of developing OA is largely driven by systemic or local factors. Systemic factors may increase the likelihood of injury to the joint by direct damage to joint tissues or by preventing the repair process in damaged joint tissues. The most obvious of the systemic factors is age as the likelihood of primary OA increases exponentially with age (Cicutini and Spector, 1997). Other systemic factors include sex, being more prevalent in women than men. For example in the Aboriginal community in Queensland, Australia, 88% of women were found to have primary OA, whereas 82% of men had secondary OA (Cooper et al., 2013). Reports from twin studies and family clustering provide strong evidence that OA has a genetic component (Valdes et al., 2006, Spector and MacGregor, 2004). For example genetic and/or life style factors was reported to contribute to the racial and ethnic differences in the occurrence of OA. The prevalence of hip and knee OA was found to be higher in African Americans compared to Caucasians, whereas the Chinese had a lower prevalence of hand and hip OA (Jordan, 2012). Other systemic factors include obesity, diet and malnutrition, metabolic diseases, osteoporosis.

Local factors such as joint overload, joint deformity, sarcopenia, malnutrition, joint trauma and injury etc. tend to be biomechanical in nature and adversely affect forces applied to the joint. OA risk factors can be grouped into two; those that show an increased likelihood of developing OA (predisposition) and those that may influence the development of OA (susceptibility) (Fig.1.2).

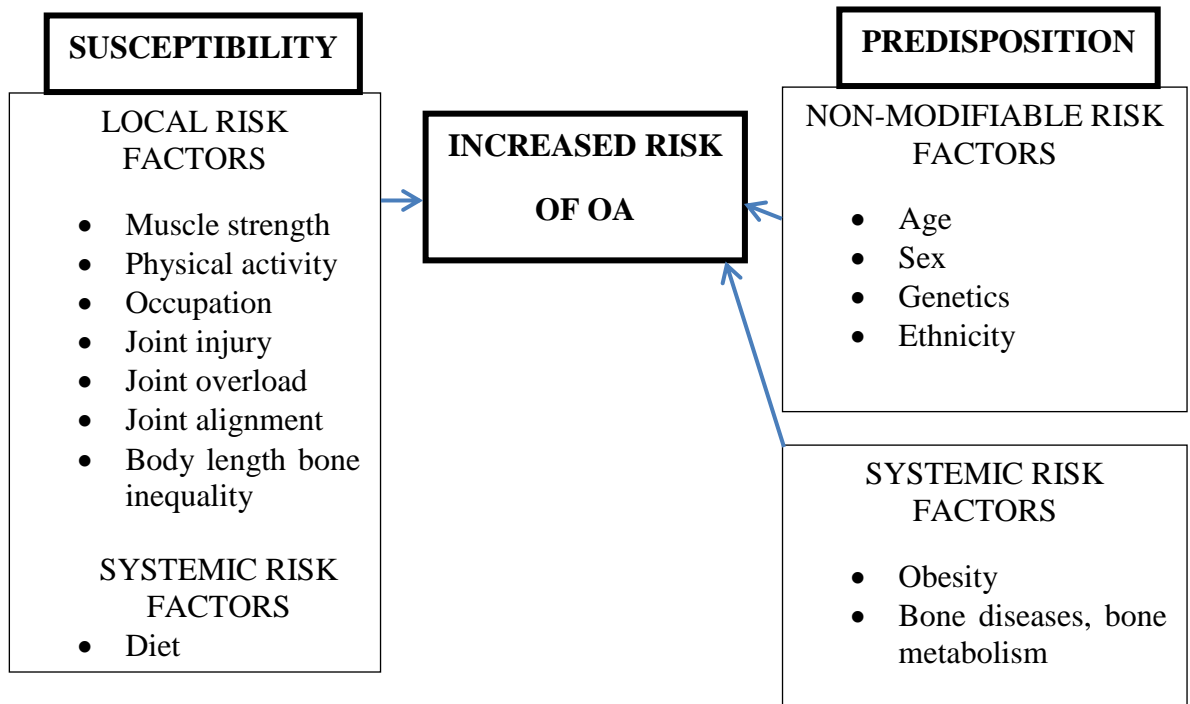


Figure 1.2 Risk factors for OA. The major risk factors that may lead to the increased susceptibility or predisposition to develop OA. Figure adapted from (Musumeci et al., 2015).

1.1.2 Pathophysiology

The process of OA development involves the whole joint and redefines the definition of OA being a degenerative joint disease exclusively characterised by wear and tear but rather involves the remodelling of joint tissues which may be driven by a host of inflammatory mediators within the affected joint. OA may initially arise from changes within the cartilage or the underlying subchondral bone and subchondral bone pathology may drive cartilage pathology (Burr, 2004). The reason for the above statement is due to the speculation of the close relationship between the articular cartilage and subchondral bone, which relates to the intimate contact that exists between the two (Goldring and Goldring, 2010a). A controversy still exists on whether bone pathology precedes cartilage pathology or if it further occurs during the development of the disease, but there have been reports of bone remodelling

detected in early OA in animal models (Pastoureau et al., 1999, Hayami et al., 2006a) and humans (Hochberg et al., 1995, Day et al., 2001).

1.1.2.1 Articular cartilage

The articular cartilage is the protective connective tissue that lines the ends of long bones. It acts as a shock absorber and reduces friction during movement. It is made up of four layers (Fig. 1.3). Each layer is differentiated by chondrocyte shape, proteoglycan content and arrangement of collagen fibres; the superficial tangential, middle (transitional), deep (radial) and calcified layers (Fig.1.3). The first three layers make up the non-calcified cartilage and are separated from the calcified cartilage by a tidemark (Fig.1.3).

Cartilage pathology also known as chondropathy may be characterised by fibrillations, fissuring, diminished cartilage thickness or erosions. Progressive loss of the articular cartilage eventually leads to exposure of the underlying subchondral bone. The medial compartment of the knee is reported as the commonest site observed to manifest overall tibiofemoral OA possibly due to heavier loading on the medial than lateral compartment (Wise et al., 2012). Most research studies including animal studies focus on the medial compartment especially the medial tibial plateau (Stoppigliello et al., 2014, Mapp et al., 2013).

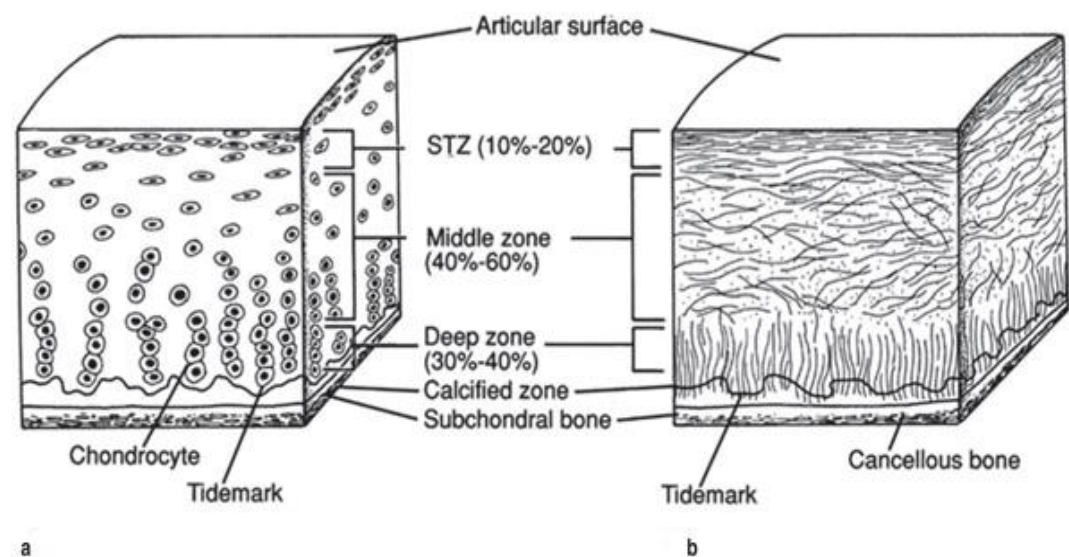


Figure 1.3 The articular cartilage. Chondrocyte (a) and collagen fiber organisation (b). Superficial tangential zone (STZ). Figure taken from (Steward et al., 2011).

In the resting state of normal adult cartilage, chondrocytes are inactive and there is little cartilage matrix turnover. In OA, these cells become activated and exhibit proliferation and cloning, increased production of matrix proteins and degradation enzymes are also released (Goldring and Marcu, 2009). This change in state of chondrocytes may be viewed as an injury response that may eventually lead to matrix remodelling, abnormal hypertrophy of chondrocytes and calcification of the cartilage (Goldring and Marcu, 2009). The cartilage matrix consists of water and ground substance (proteoglycan and collagen). The breakdown of cartilage matrix is complex and may involve interplay of genetic, environmental, mechanical and biochemical input. One of the biochemical factors proposed to be involved are the degradative enzymes known as matrix metalloproteinases (MMPs) which break down collagen and proteoglycans. Of this family, aggrecanases (ADAMTS4, -5 and -10), collagenases (MMP1, -8 and -13), stromelysins (MMP3) and gelatinases (MMP2) have been identified and reported to be elevated in OA (Hassanali and Oyoo, 2011, Loeser et al., 2012, Murphy and Nagase, 2008). The aggrecanase (A Disintegration and Metalloproteinase with Thrombospondin-like Motifs) – ADAMTS5 and MMP3 which degrade aggrecan followed by MMP13 which degrades type II collagen may be responsible for matrix breakdown in early OA (Loeser et al., 2012). Once the collagen matrix degenerates, a non-reversible state may be reached. Chondrocytes express receptors for extracellular matrix components. Mechanical stimulation of these receptors contributes to the synthesis and release of matrix-degrading proteinases, inflammatory cytokines and chemokines. These chemokines or cytokines involved in cartilage homeostasis may be produced by the synovium. During cartilage break down MMPs increase and their inhibitors are decreased by interleukins (IL) -1, 17, 18 and tumour necrosis factor (TNF)- α (Martel-Pelletier, 2004). Tissue inhibitors of metalloproteinases (TIMPS) are responsible for controlling the activity of MMPs. TIMP1 which is found in normal cartilage inhibits MMP1 while TIMP3 inhibits ADAMTS4 and -5 (Davidson et al., 2006, Kashiwagi et al., 2001). An imbalance in the regulation of MMPs and TIMPS may lead to increased chondropathy (Franses et al., 2010).

The pathological process of chondropathy in OA can be divided into 3 stages (Martinek, 2003). The first stage, matrix degradation occurs initially at the molecular level with the water content increasing and aggrecan decreasing and as a result the cartilage network becomes damaged and results in reduced stiffness. In the second stage, chondrocytes try to repair the damage by proliferating and increasing their metabolic activity, as a result chondrocytes clusters (cloning) with newly synthesised matrix molecules are formed. This state can remain for several years. In the last stage, the chondrocytes cannot compensate for the matrix breakdown, thus complete loss of cartilage occurs as a result (Lorenz and Richter, 2006).

1.1.2.2 Subchondral bone

Bone underlying the cartilage is made up of the cortical plate, trabecular bone and subarticular bone. Each region may contribute to cartilage pathology. There is active bone formation at joint margins which may lead to osteophyte formation in primary and secondary OA or bone erosion in inflammatory arthritis (Roman-Blas and Herrero-Beaumont, 2013). The close relationship between the articular cartilage and bone both in location and mechanism makes them a functional unit that contributes greatly to normal joint function. An imbalance in the mechanical or biological state of the subchondral bone may alter changes in the articular cartilage and vice versa (Goldring and Goldring, 2010b). In the course of OA, the architecture and properties of the cortical and trabecular bone may enter a cell mediated state of remodelling. This process is initiated by the quiescent bone surfaces and bone resorption mediated by osteoclasts. This resorption process is followed by bone formation mediated by osteoblasts. In physiological conditions, there is a balance between bone resorption and bone formation (Goldring and Goldring, 2010a).

Subchondral bone changes in OA include; thickening of the bone plate, trabecular bone remodelling, osteophytes, and development of subchondral bone sclerosis or cysts. There is also evidence of tidemark (line that separates the non-calcified and calcified cartilage) duplication which occurs as a result of vascular invasion of the calcified cartilage from the subchondral bone (Walsh et al., 2007). These bone changes may result in increased alterations in the

contour of adjacent articulating surfaces which can lead to changes in the joint that can further contribute to an adverse biomechanical environment (Radin and Rose, 1986, Burr, 2004, Bullough, 2004). The subchondral bone may be a source of pain in OA as it is richly innervated by sensory nerves. Innervation by sensory nerves which express the neuropeptide calcitonin gene related peptide (CGRP) was found co-localised with nerve growth factor (NGF) alongside blood vessels in vascular channels associated with osteocondral angiogenesis (Walsh et al., 2007, Walsh et al., 2010). Recent reports also point to the involvement of the bone resorbing cells osteoclasts in their contribution to chondropathy and pain as their inhibition prevented cartilage pathology and pain behaviour in a rat model of OA (Strassle et al., 2010, Sagar et al., 2014).

1.1.2.3 Synovium

The synovium is an important component of the knee and plays a key role in cartilage degeneration (Scanzello and Goldring, 2012). Other of its roles includes regulating immune function, phagocytosis, lubrication and cartilage nutrition. This thesis will focus on the role of the synovium in OA pathology. Synovial inflammation will be referred to here as synovitis. Evidence show that inflammation is an integral component of OA progression contributing to its development and symptoms (Bonnet and Walsh, 2005) and reports from histological studies account the occurrence of synovitis in early OA (Benito et al., 2005) and after joint injuries (Pessler et al., 2008, Scanzello et al., 2011). Specific characteristic features of synovitis e.g. infiltration by macrophages may be higher in early OA (Benito et al., 2005) but the prevalence of synovitis increases with advancing OA (Krasnokutsky et al., 2011, Scanzello et al., 2011). Other characteristic features of synovitis in addition to macrophage infiltration include lymphocyte infiltration (Pearle et al., 2007), lining and villous hyperplasia, fibrosis, cartilage/bone detritus and increased vascularity which may be a therapeutic target (Ashraf et al., 2011b). Soluble mediators of inflammation such as chemokines and cytokines (IL-1, -6 and TNF- α) which promote synovitis are increased in OA and in post injury joint tissues. Inflammation may result from the phagocytosis of shed cartilage debris by synovial cells. Released cytokines can inhibit matrix synthesis and promote

cartilage break down (Goldring and Marcu, 2009). Synovitis is discussed further in section 1.2.

Alterations in the cartilage, subchondral bone and synovium are interconnected and are essential in understanding the pathogenesis of progressive joint destruction in OA (Fig. 1.4). Although, whether events in cartilage precede those in bone and synovium or vice versa or they actually occur around the same time in the development of OA are all topics of interest and may have valuable therapeutic implications in the setting of OA.

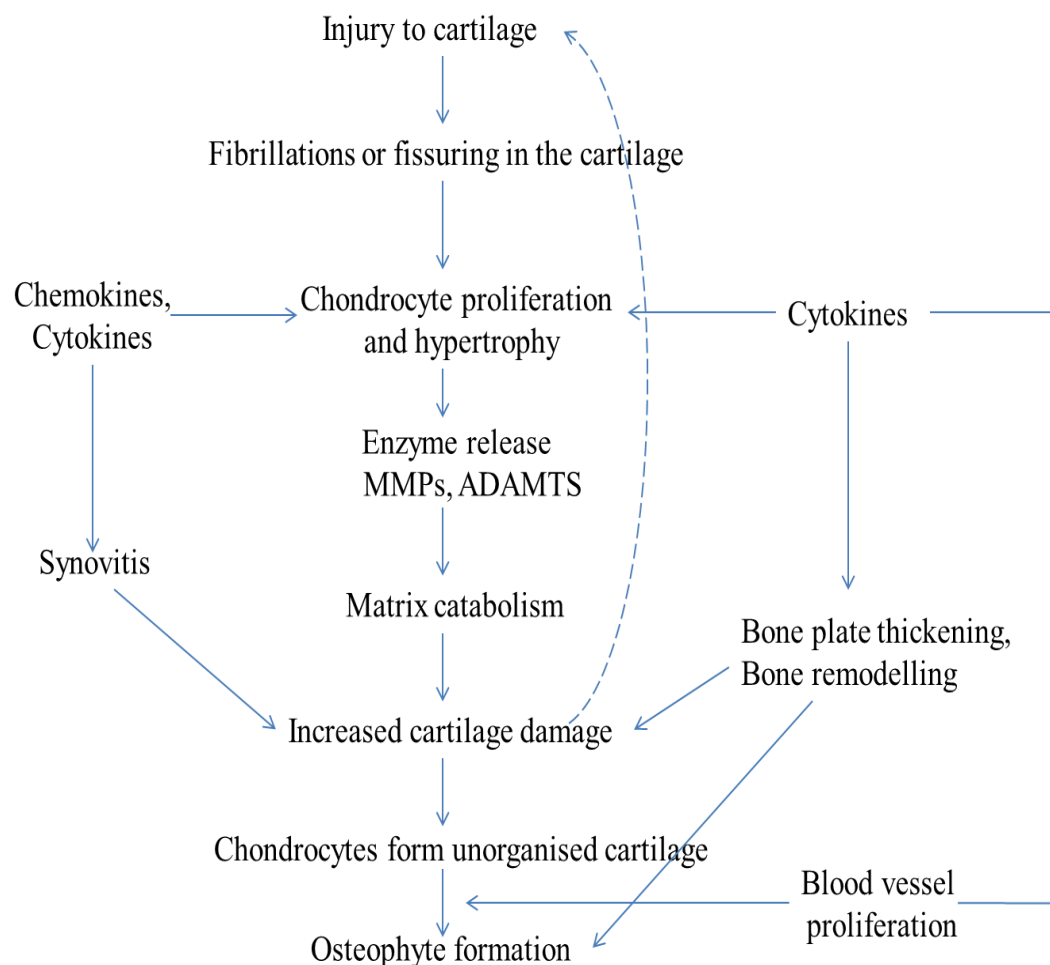


Figure 1.4 The pathology of osteoarthritis. Cartilage breakdown, bone remodelling and synovitis lead to weakening of joint protectors. The release of cytokines and degradative enzymes lead to further cartilage breakdown, producing a vicious cycle that causes rapid progression of OA. Figure adapted from (Agnihotri, 2009).

1.1.3 Diagnosis, detection and treatment of OA

Imaging for assessment of all the structures of the joint using conventional radiography is still the most widely used technique for evaluation of a patient with a known or suspected diagnosis of OA. However, recent magnetic resonance imaging (MRI) based knee OA studies have begun to reveal the limitations of radiography. The ability of MRI to image the entire knee as a whole organ (cartilage, meniscus, subarticular bone marrow, and synovium) and to directly and three-dimensionally assess cartilage morphology and composition plays an important role in understanding the natural history of the disease and in the search for new treatments (Guermazi et al., 2013). This approach has detected abnormalities to the cartilage, menisci, bone (bone marrow lesions and osteophytes), synovium and ligaments in OA patients who show no radiographic changes (Conaghan et al., 2006).

Radiography which is the simplest and least expensive imaging technique is used by physicians to frequently diagnose OA together with patient reported symptoms, particularly pain and stiffness (Gignac et al., 2006). Although the radiographic changes observed confirm the diagnosis of OA, there is often poor correlations between clinical symptoms and these changes, as some people with severe radiographic changes have minimal symptoms, whereas others with minimal radiographic changes have severe symptoms (McAlindon et al., 1992). Examples of radiographic changes associated with OA are; joint space narrowing (JSN), osteophytes, subchondral bone sclerosis, subchondral bone cysts (Altman and Gold, 2007). Another disadvantage to the use of radiography is that it is insensitive in detecting early stage OA. Other imaging techniques other than MRI which can be useful in evaluating early OA are; ultrasound, computed tomography (CT), arthroscopy, but are rarely used for diagnosis.

Ultrasound enables multiplanar and real time imaging at a relatively low cost, without radiation exposure. It is able to image soft tissue and thus is used to detect synovial pathology. The ability to detect synovial pathology may be a major advantage over radiography in regards to early changes in OA. A disadvantage is that the physical properties of sound hinder its application to deeper articular structures and the subchondral bone (Guermazi et al., 2013).

CT is a valuable tool for the characterization of OA, for the imaging of bone changes. Cortical bone and soft tissue calcifications are better depicted than on MRI. CT has an established clinical role in assessing facet joint OA of the spine (Hechelhammer et al., 2007). A major limitation is the relatively high dose of radiation it delivers.

Arthroscopy can reveal cartilage changes before bone changes, however it is an invasive technique and so rarely used for OA diagnosis (Ayril et al., 1996, Dougados et al., 1994).

The American College of Rheumatologists (ACR) developed classification systems for hand (Altman et al., 1990), knee (Altman et al., 1986) and hip (Altman et al., 1991) OA with the aim of differentiating OA from other forms of arthritis. The clinical classification for knee OA was based on knee pain in addition to 3 of the following 6 criteria: > 50 years of age, < 30 minutes of morning stiffness, crepitus, bony tenderness, bony enlargement and an absence of palpable warmth (Altman et al., 1986). A similar criterion for diagnosing knee OA to those developed in 1986 by ACR were recommended in 2009 by the European League against Rheumatism (EULAR). The recommendations were that when the following 3 symptoms (persistent knee pain, limited morning stiffness and reduced function) and 3 signs (crepitus, restricted movement and bony enlargement) were detected, it was sufficient to correctly diagnose 99% of knee OA (Zhang et al., 2010a).

1.1.3.1 Current treatments for OA

OA has no cure as of yet, and although structure-modifying treatments remains a significant unmet need in OA, several symptomatic treatments are available. These treatments are directed at modifying the signs and symptoms of the disease especially pain and inflammation, to improve quality of life, joint function and mobility and if possible, delay disease progression (Altman, 2010). There is not a single therapy adequate enough for OA; therefore, the recommended therapy includes both non-pharmacological and pharmacological treatments (Table 1.1).

The non-pharmacological treatments include patient education, exercise programs, injury prevention, weight loss, orthotic devices (special foot wear, knee bracing, canes etc.), all of which in combination to pharmacological treatments aid in managing OA (Roubille et al., 2013) (Table 1.1). Alternative strategies such as acupuncture (Zhang et al., 2010b) and transcutaneous electrical stimulation (Zhang et al., 2008) have been reported to show some short term pain relief efficacy.

Pharmacological treatments include analgesics (paracetamol, opioids, duloxetine, and capsaicin), anti-inflammatory agents with analgesic properties (non-selective non-steroidal anti-inflammatory drugs -NSAIDs, cyclooxygenase -COX-2 inhibitors, topical NSAIDs and intra-articular corticosteroids) (Michael et al., 2010, Vad and Dysart, 2012). These treatments are prescribed with care due to their adverse effects and unfavourable safety profiles (Table 1.1). Paracetamol and/or topical NSAIDS are considered as the first-line of treatment for mild to moderate pain (Zhang et al., 2010b) before oral NSAIDS (NICE). NSAIDS are among the most widely used medications and are prescribed to non-responders of paracetamol (Zhang et al., 2008). COX inhibitors were developed to decrease GI toxicity and used for pain relief in place of non-selective NSAIDS (McKenna et al., 2001), but pose a potential cardiovascular risk as do non-selective NSAIDS (Trelle et al., 2011). Tramadol and stronger opioids are recommended for the management of moderate to severe OA pain in patients intolerant to NSAIDS or unresponsive to NSAIDS and paracetamol (Zhang et al., 2008). Intra-articular injection of corticosteroids is effective for symptomatic treatment of OA patients with synovitis (Pasquali Ronchetti et al., 2001), but there is no evidence to support disease-modifying activity for these agents (McGarry and Daruwalla, 2011)

The available drug treatments for OA have limited success, in that although they may reduce pain in some patients, others may often eventually end up with joint replacement. This is in part due to the complex nature of OA and our incomplete knowledge of the association of joint pathology with pain experience in OA. Pain in OA is discussed further in section 1.3.

Table 1.1 Osteoarthritis management involving non-pharmacological, pharmacological, and surgical treatment options; adverse effects/safety profiles for the different pharmacological treatment options

Treatment type	Component		Adverse effects/safety profile
Non-pharmacological	Education, exercise, injury prevention, weight loss, orthotic devices		
Symptomatic drugs	Oral	Paracetamol	Hepatotoxicity
		NSAIDS (co-therapy with proton pump inhibitor), COX-2 inhibitors	GI ulcer/bleeding, cardiovascular events, renal toxicity, worsening asthma
		Opioids	Constipation, vomiting, somnolence, increased risk of fracture, morbidity and mortality in the elderly, possible addiction
		Duloxetine	Constipation, nausea, hyperhidrosis, dry mouth, fatigue
	Topical	Topical NSAIDS	Skin reactions, GI events
		Capsaicin	Skin burning sensation, long term skin desensitization?
	Injectable	Intra-articular corticosteroids	Local infection, systemic effects, chondrodegeneration
		Intra-articular hyaluronic acid or viscosupplementation	Local reactions at the site of injection, swelling, flares of pain
Surgical	Cartilage repair, osteotomy with axis correction, arthroplasty (UKA, TKR, THR)		Postoperative pain, infection, deep vein thrombosis, death

Abbreviations: GI, gastrointestinal; NSAID, nonsteroidal anti-inflammatory drug, THR, total hip replacement; TKR, total knee replacement; UKA, unicompartmental knee arthroplasty. Table adapted from (Roubille et al., 2013)

1.2 INFLAMMATION; ROLE OF INFLAMMATION IN OA PATHOGENESIS

Inflammation is implicated in the pathogenesis of OA (Scanzello and Goldring, 2012, Sohn et al., 2012). A study by Soren and colleagues showed synovial inflammation in so-called 'post-traumatic' synovitis (Soren et al., 1976) and later, reports of similar histological synovial changes among at least a subset of patients with primary OA were published (Myers et al., 1990, Ayril et al., 2005). Given that synovitis is now widely appreciated in OA patients (Table 1.2), it does not imply that the pathogenesis of OA is related to only the synovium. Rather synovitis might be a secondary process initiated by the activation of the innate immune system following chondropathy that creates a critical link in the cycle of development and progression of OA.

Synovitis is defined as inflammation of the synovial membrane. Synovitis can be diagnosed by imaging and histology (Table 1.2). The normal human synovium is made up of 1-4 cell layers at the surface with a loosely arranged zone of fibrocollagenous tissue consisting of adipocytes, fibroblasts, mast cells and macrophages (Wenham and Conaghan, 2010). There is an abundant vascular supply also containing nerves spread throughout the sublining of the fibrocollagenous tissue (Walsh et al., 2007). Synovial biopsies from knee pain and joint replacement patients demonstrate characteristic changes in the synovium (Stoppiello et al., 2014). These changes are present both in early and late stage OA where they become more pronounced (Loeuille et al., 2005). They include; proliferation and thickening of the lining layer, increase in the number of vascular channels and dense inflammatory cell infiltration composed largely of lymphocytes and monocytes (Haraoui et al., 1991). Surface fibrin deposition and fibrosis are present in late stage OA (Loeuille et al., 2005). Joint swelling is another clinical feature of OA caused by inflammation (Table 1.2). Joint swelling may reflect synovitis as a result of thickening of the synovial lining layer or effusion. Joint effusion which is the presence of increased intra-articular fluid may occur in parallel with OA flares (night pain, morning stiffness) in some patients (Sellam and Berenbaum, 2008).

Synovitis precedes structural change

Although OA is considered a condition manifest by significant cartilage loss and joint space narrowing (JSN) or osteophytes, it is now clear that inflammation occurs well in advance before radiographic changes in OA. The combination of imaging and arthroscopy suggest the presence of inflammation in OA even before the occurrence of visible cartilage degeneration (Sokolove and Lepus, 2013). One study reported a clear association between the presence of synovitis and the future development of medial cartilage loss by arthroscopy (Ayril et al., 2005). Another study reported increased mononuclear cell infiltration and over expression of inflammatory mediators in early compared to late OA (Benito et al., 2005). Other studies using MRI report associations between synovitis and OA progression (Krasnokutsky et al., 2011, Roemer et al., 2011).

1.2.1 Innate immunity in OA

Unlike rheumatoid arthritis (RA), changes in the adaptive immune system in OA are less robust but the activation of this system is central to both diseases. Innate immunity is activated by pattern-recognition receptors (PRRs) in response to invading pathogens such as bacteria, viruses and fungi (Kawai and Akira, 2010). PRRs are composed of family members of cells surface, endosomal and cytosolic receptors e.g. toll-like receptors (TLRs) (Kawai and Akira, 2010). PRRs also recognise endogenous ‘danger signals’ arising from damaged tissues. Pathogen-associated molecular patterns (PAMPs) and danger (damage) associated molecular patterns (DAMPs) are members of PRRs that signal to the immune system and thus initiates a protective response to fight infection or initiate repair (Sokolove and Lepus, 2013). In addition to DAMPs, PAMPs and TLRs, other molecules have been implicated in the initiation of the innate immune system in response to joint damage, thus potentially contributing to chronic inflammation in OA. Examples are; extracellular matrix (ECM) break down products including fibronectin (Okamura et al., 2001), hyaluronan (Termeer et al., 2002), and known (S100 proteins) and novel plasma DAMPs (Sohn et al., 2012, van Lent et al., 2012).

1.2.2 Inflammatory cells and cytokines in OA

More than a decade ago, Benito and co reported the infiltration into the synovium by activated B and T cells and the increased expression of pro-inflammatory mediators in both early and late stage OA (Benito et al., 2005). Another study reported B cell infiltration in the synovium of OA patients who fulfilled the ACR criteria for knee OA and presented with knee pain and/or joint swelling (Da et al., 2007). Following on from then, there have been other reports of the involvement of mononuclear cells including macrophages and the production and release of pro inflammatory mediators in OA synovium (Table 1.2). Interestingly, work by Benito et al (2005) reported that mononuclear cell infiltration in the synovium and expression of inflammatory mediators such as IL-1, TNF- α , vascular endothelial growth factor (VEGF) and intercellular adhesion molecules were higher in early OA than late OA (Benito et al., 2005) thus contributing to the evidence of the involvement of inflammation in early OA. IL-1 and TNF- α may promote inflammation in OA as well as promoting the initiation and progression of cartilage degeneration in OA (Goldring, 2001). These mediators may stimulate chondrocytes to produce matrix and collagen breakdown proteins (MMPs). The further production of IL-1 by chondrocytes in turn further stimulates MMP production. IL-1 and TNF- α are reported to also contribute to the increased expression of other catabolic enzymes and markers including prostaglandins, nitric oxide etc. (Goldring, 2001, Malemud, 2010). VEGF was reported to be involved in regulating angiogenesis in the synovium. Angiogenesis has been suggested to contribute to chronic synovitis and may occur at all stages (Haywood et al., 2003). Angiogenesis and inflammation are intercorrelated process that may facilitate disease progression and contribute to pain in OA (Walsh et al., 2007, Ashraf and Walsh, 2008).

1.2.2.1 *Role of synovial macrophages in inflammation and OA*

Synovial macrophages may contribute to synovitis and OA pathology. Histological studies have reported that synovial macrophages exhibit an activated phenotype in OA. These activated macrophages were observed to

contribute to the increased production of proinflammatory cytokines and VEGF (Haywood et al., 2003, Benito et al., 2005). In-vivo studies where synovial lining macrophages were depleted showed that, macrophage depletion was linked to fibrosis and osteophyte formation (Van Lent et al., 2004). In-vitro studies of depleted synovial macrophages demonstrated a reduction in the amount of macrophage derived- cytokines (IL-1, TNF- α) as well as those produced by fibroblasts (IL-6 and 8) and the down regulation of matrix enzymes (MMP-1, -3) (Bondeson et al., 2006). These findings show the contribution of synovial macrophages in perpetuating the production and release of proinflammatory cytokines and destructive enzymes (Bondeson et al., 2010). In addition a clinical study by Kraus and co which used imaging by ^{99m}Tc-Etarfolatide (folate receptor-targeted companion diagnostic imaging) reported the involvement of activated macrophages in OA. Activated macrophages were reported to be detected in 76% of OA patients and that these detected macrophages were strongly associated to JSN, osteophyte severity pain and stiffness (Byers Kraus et al., 2013). Soluble macrophage markers (CD14 and CD163) were also reported to be positively associated with JSN, osteophyte, pain and osteophyte progression (Daghestani et al., 2015). All of these findings support the idea (or hypothesis) that macrophages may contribute to joint degeneration and is a likely promoting factor of OA pathogenesis and pain.

In conclusion, the synovium in OA joints is abnormal, even from the earliest clinical stages. This abnormality is reflected by the (1) activation of innate immunity by TLRs, DAMPs, PAMPs, (2) production of inflammatory cytokines IL-1, IL-6, TNF-a and VEGF, (3) infiltration of mononuclear cells and (4) thickening of the synovial lining layer and fibrosis. Thus, the targeting of the inflamed synovium would be beneficial in OA. Early targeting should potentially delay or prevent the breakdown of cartilage and osteophyte formation, especially in early OA.

1.2.3 Anti-inflammation therapy

NSAIDS were reported to be efficacious in reducing OA pain in randomized clinical trials. This analgesic efficacy is thought to be due to effect on

inflammation or the inflamed synovium (Zhang et al., 2008). Other reports of NSAIDs have demonstrated their efficacy in reducing joint effusion and pain (Brandt et al., 2006) and cartilage and synovial turnover markers (Gineyts et al., 2004). Intra-articular corticosteroids are commonly used in OA (Bellamy et al., 2006, Arden et al., 2008) for pain relief with the presumption that the effect is via effect on the synovium (Jones and Doherty, 1996). Steroidal and non-steroidal anti-inflammatory treatment however have their limitations as periodical use can result in unwanted effects such as peptic ulcers, hypertension, myopathy, oedema etc. Other potential anti-inflammatory therapies include biologic molecules such as anti-TNF agents, anti-NGF antibodies, anti-proteases (anti-MMPs and ADAMTS) and bradykinin blocking agents (Roach et al., 2007, Abdiche et al., 2008, Berenbaum, 2010, Malesud, 2010).

Table 1.2 Evidence of the role of synovitis in OA

Level of evidence	Observation
Clinical	Effusion, joint swelling or palpable synovitis. Localised inflammation. Increased pain especially at night and morning stiffness
Imaging	Gadolinium-enhanced synovium and increased synovial volume by MRI detection. Correlation between MRI and histological observations. Synovitis observed in symptomatic joints by ultrasonography. Association between synovitis detected by ultrasound and clinical symptoms of synovitis. Macroscopic synovial changes present in half of knee OA patients detected by arthroscopy. Associations between arthroscopic synovitis and OA knee progression.
Histological	Synovial hypertrophy and hyperplasia. Infiltration by monocytes, macrophages, activated B and T cells. Adaptive immune T and B cell responses to extracellular matrix fragments. Increased angiogenesis. Synovitis localised to degenerative cartilage.
Molecular	Production and/or release of proinflammatory cytokines (TNF, IL-1 β , IL-6, IL-8, IL-15, IL-17, IL-21) Increased production of Prostaglandin (PG) E ₂ and nitric oxide. Increased expression of adhesion molecules (ICAM-1, VCAM-1) in the synovium. Increased activity of MMPs (MMP-1, MMP-3, MMP-9, and MMP-13) and ADAMTS. Production of adipokines (visfatin, leptin, adiponectin). Release of EGF and VEGF. Involvement of macrophages in osteophyte formation via BMPs. Insufficient release of anti-inflammatory cytokines (IL-4, IL-10, IL-13, IL-1Ra). Release of proinflammatory and pain neurotransmitters (substance P, NGF).

Biological markers

Elevated levels of CRP (detected by ultrasensitive assay). Elevated levels of MMP-3 and MMP-9 in synovial cells of patients with rapidly destructive hip arthropathy. Potential surrogate biomarkers of inflammation; CGP-39 and fragments of type II collagen and aggrecan.

Abbreviations: ADAMTS, a disintegrin and metalloproteinase with thrombospondin motifs; BMP, bone morphogenetic protein; CGP-39, cartilage glycoprotein-39 (also known as chitinase-3-like protein 1 and YKL-40); CRP, C-reactive protein; EGF, endothelial growth factor; ICAM-1, intercellular adhesion molecule 1; IL, interleukin; IL-1Ra, interleukin 1 receptor antagonist; MMP, matrix metalloproteinase; NGF, nerve growth factor; PGE2, prostaglandin E2; TNF, tumour necrosis factor; VCAM-1, vascular cell adhesion molecule 1; VEGF, vascular endothelial growth factor.

Table adapted from (Sellam and Berenbaum, 2010, Sokolove and Lepus, 2013), see references to evidence in the referenced reviews.

1.3 PAIN AND OA

Pain is the major symptom suffered by arthritic patients and the reason why they seek medical help. This may be caused by the presence of nerves that have undergone peripheral sensitization, and increase in the release of inflammatory mediators of pain, for example NGF (Suri et al., 2007, Konttinen et al., 2006, Iannone et al., 2002).

Pain as defined by the International Association for the Study of Pain “is an unpleasant sensory and emotional experience associated with actual or potential tissue damage or described in terms of such damage” (Merskey and Bogduk, 1994). This definition emphasises the perception rather than sensation of pain and that the process of pain perception is not a simple ‘hard-wired’ system with a single ‘stimulus-response’ relationship but involves complex interactions between sensory, emotional and behavioural factors (Hudspith et al., 2006).

One of the important functions of the nervous system is to provide information about the occurrence of a potential threat or injury. This information is provided by small-diameter sensory afferent fibres called nociceptors. Nociception, which is derived from the Latin word ‘*nocere*’ meaning to harm is the intermediate sensory process between a noxious stimulus and pain response. It is an afferent activity produced by a stimulus that can be potentially damaging. Nociceptors can respond to chemical, thermal and mechanical changes above their normal threshold. The nociceptive signal is passed via the spinal cord to the brain (McMahon et al., 2013). The perception of acute pain begins suddenly and is usually sharp in quality and nociceptive fibres respond accordingly depending on the noxious stimuli. In acute pain, potentiation of pain would encourage rest and thus prevent further tissue injury (Woolf, 1991). On the other hand chronic pain commonly persists long after healing of an injury (Ready and Edwards, 1992, Woolf, 2011). Chronic pain is often idiopathic and lacks the physiological protective role of pain. It therefore becomes a pathological condition that is not only useless but also greatly distressing (Neogi et al., 2013).

Chronic pain may arise from the sensitization of peripheral nerves and spinal neurones (Ji et al., 2014). Peripheral nerve endings become more sensitive to noxious stimuli through tissue damage, action of local hormones e.g. prostaglandins, histamine, serotonin and bradykinin, and also by direct nerve damage. This process is known as peripheral sensitization and is usually associated with localised pain from the damaged tissue. The changes in key proteins and ion channels (transduction proteins) determine the excitability of peripheral nerve endings. Two processes occur during peripheral sensitization; post-translational processing; this involves changes to the existing nociceptor proteins, and altered gene expression of new nociceptor proteins (Woolf) (further discussed in section 1.3.4.3).

Central sensitization represents an increase in the function of neurones and circuits in nociceptive pathways of the central nervous system (CNS) (Woolf, 2011, Latremoliere and Woolf, 2009). Central sensitization plays a role in many acute and chronic pain states and is responsible for the temporal, spatial and threshold changes in pain mechanisms and thus highlights the fundamental contribution of the CNS in the generation of pain (McMahon et al., 2013). Central sensitization has been implicated to occur in two stages; an immediate but shorter phase and a gradual onset but longer lasting phase. The earlier phase reflects changes to synaptic transmissions within the spinal cord and involves neurotransmitters e.g. glutamate, neuropeptides e.g. substance P and CGRP and synaptic modulators e.g. brain derived neurotrophic factor (BDNF) (Woolf). These transmitters or modulators act on specific receptors found on spinal neurones thereby activating intracellular signalling pathways that further lead to the phosphorylation of membrane receptors e.g. α -amino-3-hydroxy-5-methyl-4-isoxazolepropionic acid (AMPA) and N-Methyl-D-aspartate (NMDA) which bind the excitatory neurotransmitter glutamate. These changes lower the activation thresholds of the above receptors thus leading to the excitation of neurones. The later phase involves increased levels of protein production (Woolf). Example proteins are dynorphin; an endogenous opioid that augments neuronal excitability, COX2; an enzyme that leads to the production of prostaglandin (PG) E2. In addition to the involvement of PGE2 in mediating peripheral sensitization, it also contributes to central sensitization

(Woolf). The overall effect of the above changes results in the activation of neurones by stimuli which would otherwise not activate neurones in the normal healthy state. In this case, pain sensibility is drastically altered.

Pain can arise spontaneously in many chronic pain states and can be grouped into; those that are elicited by a normally non-painful stimuli (allodynia), those that are enhanced in response to a painful stimuli (hyperalgesia), and finally those that spread beyond the site of tissue injury (secondary hyperalgesia) (Latremoliere and Woolf, 2009, Woolf, 2011).

Chronic pain continues to be the commonest cause of disability as it limits joint use in OA patients and impairs their quality of life. More specifically, OA and RA patients together were reported to make up 42% of all chronic pain sufferers (Breivik et al., 2006). Although sensitisation may trigger a transition from acute to chronic pain (Basbaum et al., 2009), understanding this transition is still a crucial challenge yet to be overcome in pain research in order to allow for the improvement of targeted treatment to the long lasting debilitating condition known as chronic pain.

1.3.1 Innervation of the normal and the arthritic knee joint and its link to pain

Joints are innervated by both the afferent sensory and efferent sympathetic branches of the nervous system as evidenced by early studies in animals (Buma et al., 2000, Heppelmann, 1997, Samuel, 1952, Hukkanen et al., 1991, Freeman and Wyke, 1967). The knee joint of the cat proved a useful model for studying joint innervations in both the normal and inflamed joint (Freeman and Wyke, 1967, Heppelmann, 1997). The normal knee joint receives its supply from two articular nerves. These nerves may be grouped into primary nerves (posterior, medial and lateral) and accessory nerves (branches of intra muscular nerves) (Mapp, 1995, Freeman and Wyke, 1967).

1.3.2 The normal joint

The parts of the normal healthy adult knee that are richly innervated by nerves are the muscle, synovium, articular capsule, tendons, ligaments and

subchondral bone (but not the hyaline cartilage nor the inner two thirds of the meniscus) and may be sources of pain in OA (Hunter et al., 2008). The pattern of innervation is made up of four groups (I – IV) of sensory afferents (~60%) and sympathetic fibres and arises from several locations on the spinal cord (Heppelmann, 1997, Schaible and Straub, 2014). The sympathetic fibres which are postganglionic help to regulate vascular tone in the joint, since blood flow was observed to be increased after elimination of the sympathetic innervation and was decreased during electrical stimulation of joint nerves (Schaible and Straub, 2014). Sensory nerves which also have afferent vasoregulatory functions are responsible for detecting and transmitting mechanical information and also chemical information during inflammation between the joint and the central nervous system (CNS) (McDougall, 2006).

Groups I and II are the large diameter (5 μ m) myelinated fibres; A α and A β fibres. These fibres are proprioceptive (they can be activated by innocuous light pressure and stretch) with a conduction velocity of 20-100 m/s. These nerve fibres have their nerve endings terminating in the fat pad, capsule, ligaments, menisci, and periosteum (Hunter et al., 2008, McMahon et al., 2013).

Group III (A δ) fibres are small diameter (2-3 μ m) myelinated fibres that have their myelin sheaths terminating in the terminal region to become free nerve endings. These fibres have a conduction velocity of <20 m/s. Some of the A δ fibres are low mechanical threshold fibres thus they tend to respond to passive joint movements as compared to the high mechanical threshold fibres which respond more to extreme noxious stimuli (Hunter et al., 2008).

Lastly the **group IV** fibres are the thinly unmyelinated C fibres. These fibres have a conduction velocity of <1 m/s (Hunter et al., 2008, McMahon et al., 2013)

Some A δ and C (high threshold) fibres are nociceptive in nature because they are responsible for carrying nociceptive information. Most nociceptors are polymodal i.e. they may respond to painful mechanical stimuli (intense pressure or stretch), painful thermal stimuli (hot or cold) or to chemical stimuli (Schaible et al., 2006). Both the nociceptive A δ and C fibres supply the

capsule, ligaments, menisci, periosteum and mineralized bone (mostly areas of high mechanical load) (Hunter et al., 2008), whereas only C fibres innervate the synovial membrane (Loeser et al., 2012, Heppelmann, 1997). It has been estimated that of the total number of nerves that supply the joints, ~80% are C fibres and that sympathetic efferent C fibres make up half of this 80% as they disappear after surgical sympathectomy (Hassanali and Oyoo, 2011, Loeser et al., 2012).

C fibres are responsible for the slow burning, throbbing pain experienced by OA sufferers. Nociceptors can be categorized based on their expression of molecular and neurochemical markers. For example C fibres have been sub-grouped as either peptidergic or non-peptidergic. Peptidergic fibres are defined by their expression of the neuropeptides; substance P (SP), calcitonin gene related peptide (CGRP), NGF receptor (tropomyosin-related kinase A; TrkA). Non-peptidergic fibres are classed as those that express the growth factor receptor c-Ret and bind to lectin IB4 (Canetta, 2010, Miller et al., 2015).

1.3.3 Mechanisms involved in the development of joint pain

Joint nociceptors are usually localized to specific articular structures while having their receptive field in the joint, but during inflammation this receptive field may expand to include other adjacent areas such as the surrounding muscle. An example of this case is a spinal neurone with its receptive field in the joint responding to physical stimulation of the surrounding muscle of the joint (Hunter et al., 2008). Pain in arthritis may originate from the innervated areas of the joints such as the synovium, periosteum, subchondral bone, ligament and muscle (Hunter et al., 2008). The cartilage is normally without innervations, but in diseased conditions such as in knee OA, the normally aneural cartilage may be innervated by peptidergic nerve fibres which contain the neuropeptides SP and CGRP (Suri et al., 2007, Hunter et al., 2008). A study which investigated neurovascular invasion in knee joint confirmed the localisation of sympathetic and sensory nerves to the cartilage, this may suggest that nerve innervation in the aneural tissue in the knee joint may be a potential source of pain for OA patients (Suri et al., 2007). The neuropeptides

SP and CGRP can lead to neurogenic inflammation which is inflammation that arises as a result of the local release of inflammatory mediators from sensory fibres and immune cells e.g. mast cells and macrophages (Tore and Tuncel, 2009). Release of SP and CGRP can result in vasodilatation, plasma extravasation, leukocyte chemotaxis and phagocytosis (Zegarska et al., 2006). The process of neurogenic inflammation plays an important role in the pathogenesis of numerous diseases including OA (Saito, 2003).

Joint nociceptors may become activated by responding to noxious mechanical stimuli such as when the normal joint is hit, over rotated or over stretched, although there are a few nociceptors that do not respond at all to noxious mechanical stimuli of the normal joint (Hassanali and Oyoo, 2011, Schaible et al., 2006). These nerve fibres are called 'silent nociceptors' because they are dormant in normal healthy joint, but become active and begin to send nociceptive inputs to the CNS following tissue injury or inflammation. This supplementary input by silent nociceptors accounts for one of the factors that contribute to the generation of arthritis pain as it contributes to the increased afferent inflow (recruitment) into the spinal cord during inflammation (McDougall, 2006, Schaible et al., 2002).

1.3.4 Inflammatory mediators and modulators of pain

Numerous inflammatory mediators contribute to both the degradative and nociceptive pathways associated with OA progression. During inflammation, a cascade of events occurs which includes the release of cytokines by chondrocytes or synovium; as a result, a complex biochemical and mechanical interplay with other biological mediators leads to the induction of OA and pain (Dray and Read, 2007, Schaible et al., 2011). Some particular mediators are known to stimulate hyperalgesia by a number of direct and indirect mechanisms of actions, including the sensitization of primary afferent fibres following mechanical stimuli. Examples include pro-inflammatory mediators; interleukins (IL-1, IL-6, and IL-17), tumour necrosis factor- α (TNF- α), and prostaglandin E2 (PGE2). Other mediators include SP, VEGF, nerve growth factor (NGF) etc. (Lee et al., 2013a). The focus of this thesis was on NGF as an inflammatory mediator of pain through TrkA.

1.3.4.1 Nerve growth factor

NGF is a member to a family of molecules known as neurotrophins. These neurotrophins are 12.5-kd proteins that are usually associated as homodimers and are responsible for controlling the survival, development and function of subsets of sensory and sympathetic neurones; in general they play roles in the maintenance or regeneration of the nervous system (Mantyh et al., 2011, Anand, 1995). The other members of the neurotrophin family are BDNF, neurotrophin-3 and neurotrophin-4/5 (Mantyh et al., 2011). NGF is synthesised as pro-NGF and cleaved by endoproteases e.g. MMP-7 (Le and Friedman, 2012), tryptase (Spinnler et al., 2011) into the mature form of NGF (Fahnestock et al., 2004). NGF is made up of an α and β chain, with the NGF β chain being responsible for its neurotrophic effects (Freemont et al., 2002). NGF has two receptors which it binds to; the high affinity receptor TrkA which binds only to NGF and the low affinity receptor (p75 receptor) which binds all members of the neurotrophin family (Mantyh et al., 2011). In addition to the p75 receptor, the other neurotrophins bind the other two Trk receptors B and C (Fig.1.3). NGF binds to the extracellular region of the TrkA receptor. This region comprises of three leucine and two cysteine rich motifs, followed by two immunoglobulin like domains (Ig-like) (HoldenPaul et al., 1997, Robertson et al., 2001). On release of NGF by cells in target organs such as skin, blood vessels and bladder, NGF is taken up by sympathetic and small sensory nerve fibres by binding to TrkA. This is achieved by the formation of NGF-TrkA complex which is then internalised and transported in a retrograde fashion i.e. from peripheral terminals to sensory cell bodies in the dorsal root ganglion (DRG) (Anand, 1995, Delcroix et al., 2003, Mantyh et al., 2011).

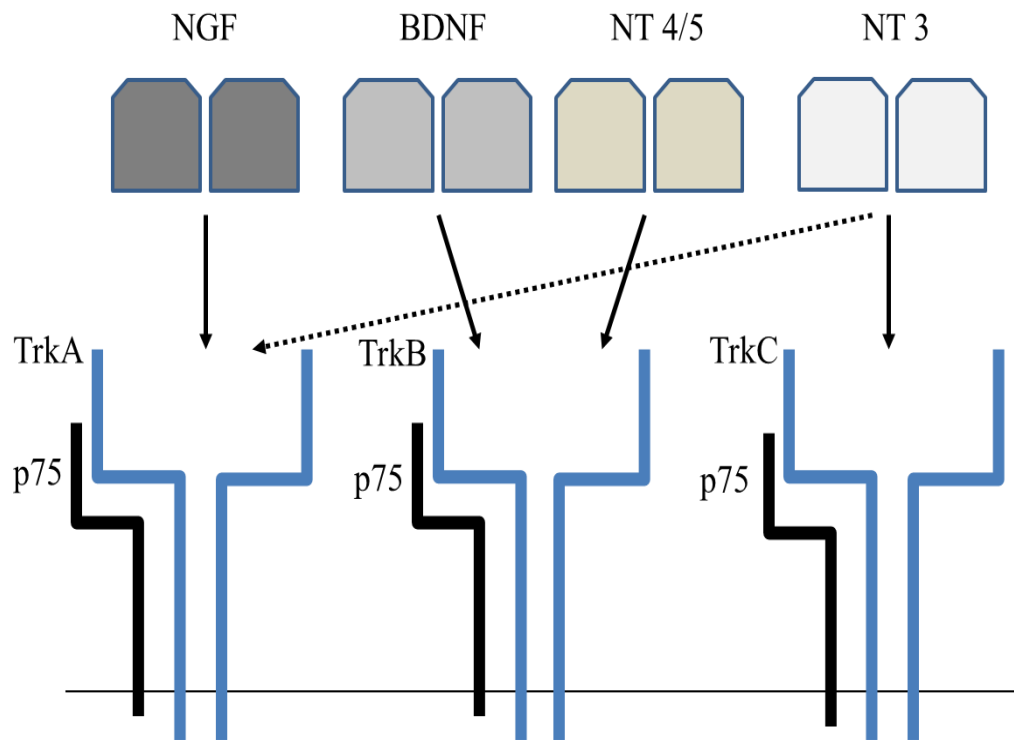


Figure 1.5 Neurotrophins and their preferred Trk receptors. NGF binds TrkA, BDNF and NT4/5 bind TrkB and NT3 binds TrkC but can bind other Trk receptors albeit with different potencies. All neurotrophins bind p75 with equal affinity.

1.3.4.2 General roles of NGF

NGF IN NEURONAL GROWTH AND DEVELOPMENT

It has been more than 60 years since the discovery of the role of NGF in neuronal development. This role which it plays in the development of the peripheral nervous system (PNS) is to support the growth and survival of some neural-crest derived cells in developing embryos especially those of the sympathetic and sensory neurones (Levi-Montalcini and Hamburger, 1951, Mantyh et al., 2011). A study was published in 1996 regarding the importance of NGF in developing neurones (Indo et al., 1996). Congenital insensitivity to pain with anhidrosis (CIPA) was witnessed in a single family who had a mutation in the gene encoding the TrkA receptor that resulted in structural neuropathy of unmyelinated peripheral nerve fibres. This mutation was seen to disrupt the normal signalling functions of NGF. The patients who had this condition had normal proprioception and normal sensitivity to innocuous

pressure but abnormal sensitivity to thermal stimuli (McMahon and Bevan, 2005, Indo et al., 1996).

Other cases of this congenital insensitivity to pain have also been seen in genetically altered mice that either have mutations to NGF or its high affinity receptor TrkA (Mardy et al., 2001). These 3-day-old genetically modified mice that are either lacking NGF or TrkA were born without the neural crest-derived small diameter sensory neurones because all of them undergo cell death. Therefore these animals were seen to be highly unresponsive to painful stimuli as the above neurones are mostly nociceptive in nature or that the nociceptors that express TrkA fall into this group (Brown and Podosin, 1966, Crowley et al., 1994, Smeyne et al., 1994, Mantyh et al., 2011, Pezet and McMahon, 2006).

Apart from its role in neuronal development and survival, NGF has other roles which it plays, an example is its involvement in the phenotypic expression of peptidergic primary afferent neurones soon after birth (early postnatal period). Here A δ high threshold mechanoreceptors were absent in animals that were deprived of NGF in the critical postnatal period. The animals were deprived of NGF by immunizing them with neutralizing antibodies (anti-NGF) against NGF. This revealed that neurones in the DRG could survive without NGF shortly after birth but that within 10 days of birth the high threshold mechanoreceptors that were seen in non-deprived animals were switched to sensitive mechanoreceptors in deprived animals. Other changes that occurred were to the C-fibres which were seen to lose their heat sensitivity (McMahon and Bevan, 2005, Mantyh et al., 2011, Rueff and Mendell, 1996).

NGF AS A NOCICEPTIVE AGENT (ADULT)

NGF is a sensitizer and modulator of the expression of a variety of components such as neurotransmitters, ion channels and receptors expressed by adult nociceptors (Mantyh et al., 2011). Evidence for NGF being a sensitizing agent has being demonstrated in acute, short-lived nociceptive responses and in longer term, chronic pain (Aloe and Levi-Montalcini, 1977, Taiwo et al., 1991, Mantyh et al., 2011). NGF becomes involved in sensitization of nerves only after sensory neurones are no longer dependent on it for survival. This involves

the NGF-TrkA pathway. This pathway plays an important role in the early, intermediate and long-term generation and maintenance of a variety of acute and chronic pain states (Zhu et al., 2004, Mantyh et al., 2011).

1.3.4.3 Actions of NGF

NGF sensitizes nerves, thus an increase in NGF expression in OA may lead to increased activity of the nerves in the subchondral bone. As a result of this, pain is increased both structurally (increased and abnormal innervations at the osteochondral junction), and through peripheral sensitization (Walsh et al., 2010). Blood vessels and nerve growth may be induced by other growth factors such as VEGF. NGF produced by vascular cells may contribute to the growth of nerves along newly formed vessels (Walsh et al., 2010, Nico et al., 2008). Recent clinical trials using the monoclonal antibody; Tanezumab which blocks NGF, demonstrated the ability to inhibit OA knee pain thus confirming the involvement of NGF in arthritis (Lane et al., 2010), although the drug's rapid analgesic effect may have been due to an action on sensitization rather than nerve growth (Ashraf et al., 2011b, Cattaneo, 2010). The occurrence of adverse effects (rapidly progressive OA – RPOA; osteonecrosis) with this NGF antibody (Brown et al., 2012) once led to their being put on hold by the federal drug administration (FDA).

NGF receptors have been detected on murine CD4 T cells, human B lymphocytes, human keratinocytes, fibroblasts etc. In respect to the above, NGF may be a possible mediator of cross-talk between the nervous and immune systems (Iannone et al., 2002). This may enable it to maintain and exacerbate inflammatory disease (Iannone et al., 2002, Raychaudhuri et al., 2011). Levels of NGF have been observed to increase in some immune diseases such as systemic sclerosis and chronic arthritides (Iannone et al., 2002). Raised levels of NGF in the synovium may contribute to joint inflammation by activating inflammatory cells (Halliday et al., 1998).

Finally endogenously produced NGF can lead to increased destruction of normal joint tissue by enabling the inward movement and degranulation of neutrophils thus raising elastase levels leading to overall joint destruction and ultimately pain (Raychaudhuri et al., 2011). Evidence suggest the involvement

of NGF in inducing RANKL-independent osteoclastogenesis and its potential contribution to normal and pathological subchondral bone remodelling (Hemingway et al., 2011).

MECHANISM OF ACTION; NGF-TRKA SIGNALLING (PROTEIN PHOSPHORYLATION AND ALTERATIONS IN GENE EXPRESSION)

The binding of released NGF to TrkA expressed on sensory neurones after tissue injury leads to the occurrence of early transcriptional changes in the sensory signalling pathway. NGF principally signals via retrograde transport of the internalized NGF-TrkA complex, so there is thus a delay (from hours to days) before the effect of NGF's contribution to hypersensitivity is seen. After retrograde transport of the NGF-TrkA complex to the dorsal root ganglia (DRG), changes in sensory phenotypes occur through the switching on (and off) of gene promoters (Fig. 1.4), which leads to the increased synthesis of peptides (e.g. SP, CGRP, and BDNF), and of nociceptor-specific ion channels (Nav 1.8, Cav 3.2, -3.3) at the DRG (Kerr et al., 2001). For example it was observed that exposing sensory neurones expressing TrkA to NGF led to an increase in the synthesis and expression of acid sensing ion channel (ASIC) 3 through the control of the promoter region of its gene (Mamet et al., 2002). Also NGF-induced altered gene expression can result in the phenotypic switch of non-peptidergic neurones to peptidergic neurones (Woolf and Costigan, 1999). These peptidergic fibres express increased levels of SP, CGRP and BDNF. Stimulation of peptidergic fibres may lead to an enhanced inflammatory response and further sensitisation of nociceptors by SP and CGRP (Donnerer et al., 1992).

Downstream signalling of NGF can lead to central sensitization. The involvement of NGF in mediating central sensitization can occur as a result of the indirect effect of NGF on synaptic transmission between nociceptors and second-order cells in laminae I and II of the spinal cord via its effect on the release of peptides such as BDNF (Fig. 1.4) (Garraway et al., 2003). Released BDNF acts as a central modulator via post synaptic TrkB (Thompson et al., 1999). BDNF-TrkB binding on second-order neurones can lead to the

activation of intracellular protein kinases. These protein kinases can mediate the phosphorylation of glutamate AMPA receptors. Phosphorylation of AMPA receptors was observed to contribute to central sensitization at the dorsal horn synapse, particularly in combination with SP and CGRP acting on postsynaptic receptors (Fig. 1.4) (Mantyh et al., 2011). BDNF upregulation after peripheral inflammation was observed to be NGF-dependent as upregulation was inhibited by NGF antibody (Obata et al., 2003). Involvement of BDNF in mediating central sensitization was reported after it was observed that inhibition of central BDNF led to the attenuation of second (delayed) phase of hyperalgesia (Kerr et al., 1999). The delayed hyperalgesia was induced by formalin and thermal hyperalgesia in carrageenan rats in an NGF-dependent manner (Kerr et al., 1999). The involvement of NGF in mediating nociception either by peripheral or central sensitization or both, points to the fundamental difference between the role of NGF during neuronal embryonic growth and differentiation, and its role in the adult sensory system.

NGF modulation of TRPV1: TrkA-expressing sensory neurones are known to also express transient receptor potential vanilloid 1 (TRPV1) (Ramsey et al., 2006). TRPV1 is a non-selective ligand-gated cation channel that plays a role in pain transmission and modulation (Szolcsányi and Sándor, 2012, Kelly et al., 2013a). There is evidence of its involvement in contributing to inflammatory pain in arthritis (Brain, 2011). TRPV1 may be activated by exogenous and endogenous mechanical, thermal and chemical (i.e. acid, lipids) stimuli. Stimulus-induced opening of TRPV1 results in the influx of calcium ions and the generation of an action potential (i.e. thus transmission of pain signals) by the nociceptive neuron (Ramsey et al., 2006). The binding of NGF to TrkA during injury or inflammation leads to the activation of the phospholipid cleaving enzyme phospholipase C (PLC). Activation of PLC leads to TRPV1 sensitization by decreasing the threshold at which it opens. Furthermore NGF upregulates the expression of TRPV1 on plasma membranes of neurones. NGF action on TRPV1 activation and expression results in a decrease in threshold for action potential generation in nociceptive neurons (McKelvey et al., 2013).

Effect of NGF on mast cells: NGF contributes to pain facilitation indirectly by binding to TrkA-expressing mast cells. This results in the release of pain

mediators such as histamine, prostaglandins, and including NGF which may contribute to inflammation or create a positive feedback loop that sensitizes adjacent nociceptive neurones (Kawamoto et al., 2002) (Fig. 1.4). The prominent role which NGF plays in contributing to driving nociception creates a scientific rationale for interrupting NGF-TrkA signalling as a target for pain relief therapeutics.

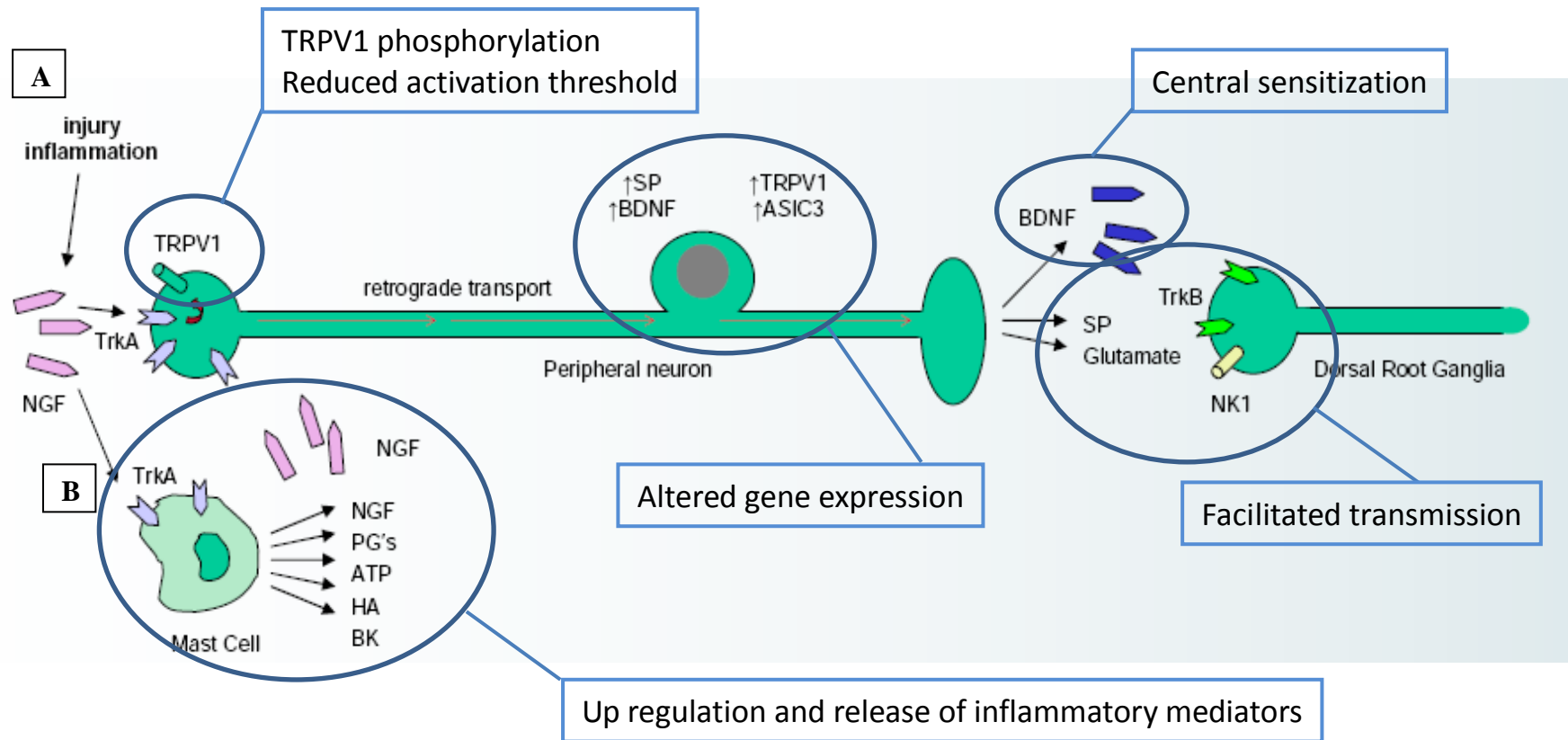


Figure 1.6

Figure 1.6 NGF-TrkA signalling. Neurotransmitters, receptors and ion channels are modulated and up-regulated by NGF binding to TrkA-expressing sensory neurones. TrkA-positive nerve fibres have their cell body in the dorsal root ganglia (DRG) and transmit sensory information from the periphery to the spinal cord and brain. During inflammation, injury, or certain diseases, inflammatory, immune, or Schwann cells release NGF. Released NGF binds to TrkA, which in turns directly activates and/or sensitizes nociceptors (A). The formed NGF-TrkA complex is transported retrogradely to the DRG, resulting in increased synthesis of neuropeptides (e.g., substance P [SP], brain-derived neurotrophic factor [BDNF], calcitonin gene-related peptide [CGRP]), receptors, ion channels, and anterograde transport of certain neurotransmitters, receptors, and ion channels from the DRG to the periphery tissue and spinal cord. Alternatively NGF may be released from mast cells but also from other recruited inflammatory cells (B). Indirect action of NGF in mediating sensitization occurs by NGF-TrkA binding on mast cells. This results in the release of inflammatory mediators; histamine, serotonin (5HT), and protons (H⁺), hyaluronan (HA), adenosine triphosphate (ATP) as well as NGF. NGF-TrkA binding on TrkA expressing fibre terminals activates intracellular signalling pathways. This results in the increased expression and/or modulation of a number of receptors, e.g. bradykinin (BK) receptors (B₂R); ion channels, e.g. transient receptor potential vanilloid 1 (TRPV1); acid-sensing ion channels (ASIC) 2/3 at the membrane surface of the fibre terminal. These rapid changes (minutes to hours) in the afferent terminal modify the sensory fibre's response to sensory stimuli and the propagation of sensory impulses to the dorsal horn of the spinal cord. Figure adapted from (Mantyh et al., 2011).

1.3.4.4 Current strategies for targeting NGF-TrkA signalling

Analgesic efficacies of NGF blockers continue to make the targeting of NGF attractive for OA chronic pain relief (Lane et al., 2010, Sanga et al., 2013, Tiseo et al., 2014). There are four major strategies currently being pursued for targeting NGF/TrkA (Fig. 1.5) and each one has its pros and cons (Hansel et al., 2010, Opar, 2010). For example, while monoclonal antibodies (mAbs) are very specific in their targeting, there are reports of immune reactions such as acute anaphylaxis, serum sickness and the generation of antibodies against the therapeutic agent from their use. In contrast, small molecule inhibitors of kinase activity do not require intravenous or intramuscular administration, might be more cost effective to produce than mAbs and allow greater flexibility in dosing as they are mostly administered orally, but are generally less selective than mAbs (Opar, 2010, Ghilardi et al., 2010, Ghilardi et al., 2011). With the lack of selectivity being said, this thesis provides results using a very selective TrkA (AR786) inhibitor (chapter 6). It also investigates the effects of a mAb (Mumab911) - chapter 6. Mumab 911 reported by Shelton et al (2005) completely reversed established pain in auto-immune arthritic rats without having any effect on joint destruction and inflammation.

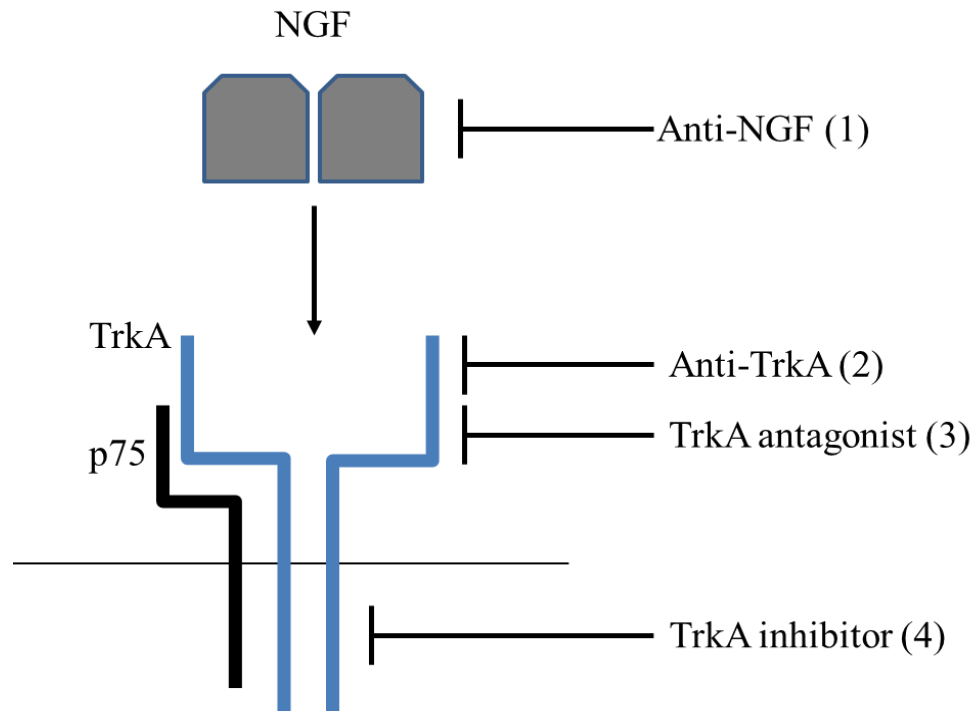


Figure 1.7 Therapeutic strategies for targeting NGF/TrkA for OA pain relief.

Available therapeutic targeting of NGF or its cognate receptor TrkA include; monoclonal antibodies or peptibodies that sequester NGF (1), monoclonal antibodies that target TrkA and prevent NGF from binding to TrkA (2), small molecule TrkA antagonist therapy (3) and small molecule kinase inhibitors of TrkA (4). The anti-NGF used in this thesis is Mumab 911 while the TrkA inhibitor is AR786. Figure adapted from (Ghilardi et al., 2010).

1.4 PRECLINICAL ANIMAL MODELS

The use of animal models has increased our understanding of the basic mechanisms of joint disease. There are variations that occur within the different models, and also because arthritis is induced by different stimuli. These include; autoimmunity production to cartilage components, nonspecific targeting of autoimmunity with adjuvants, and stimulating effects with exogenous noxious agents such as bacteria, viruses and mono-iodoacetate, including inducing post trauma by surgery. In addition, the recent use of focused manipulation of transgenics has introduced novel variants (Berg, 2009).

There is not one animal model of arthritis that truly portrays the human disease, but each one models a different aspect and thus can be useful tools to comprehend particular pathways (Berg, 2009). This includes their use in drug testing of anti-arthritis agents in the pharmaceutical industry. The important criteria in the selection of an ideal animal model are; (a) efficiency for therapeutic prediction in humans, i.e. what is effective in the animal should be effective in the patient, (b) similarity to human disease in all tissues of the articulating joint, (c) mammalian species that is inexpensive, easy to use and house, (d) reproducible disease that occurs in a suitable time frame to allow for high through put studies and also for reproducibility of data and, (e) reasonable test duration period, thus allowing for the study of early, mid and late pathophysiology and treatment effects (Bendele et al., 1999, Little and Smith, 2008).

A number of animal models have been developed for the different types of arthritis; examples of the models for OA include; naturally occurring Dunkin Hartley Guinea pigs, surgically-induced rat medial meniscal tear (MNX), anterior cruciate ligament transection (ACLT) in rats and dogs, less surgically invasive destabilization of the medial meniscus (DMM) in mice and chemically-induced intra-articular monosodium-iodoacetate (MIA) model etc. (Bendele, 2001, Malfait et al., 2010).

It is widely accepted that the naturally occurring (spontaneous) OA models may mimic the causes, histopathological features, and slow progression of

human disease better than surgical or chemical models (Poole et al., 2010). However like in humans, there is a high degree of variability in the onset and the rate and extent of structural progression between animals in spontaneous models. This thus leads to a heterogeneous population and the need for larger experimental group sizes. In addition, appropriate age-matched, non-arthritic controls from which meaningful and ultimately translatable comparisons can be made are not always possible to achieve, therefore, experimenter-induced models of OA pain which share similar pathological features of human OA especially when fully established can be used instead (Sagar et al., 2013).

1.4.1 Monosodium iodoacetate (MIA) model of OA

MIA is an inhibitor of the enzyme glyceraldehyde-3-phosphate dehydrogenase hence it inhibits glycolysis, thus it kills chondrocytes. Intra-articular injection of MIA leads to the destruction of cartilage and can be induced in any species (rat, mouse, guinea pig). Different degrees of chondrocyte killing and thus cartilage destruction can be achieved depending on the concentration and frequency used. Two intra-articular injections of MIA (0.1ml of 3mg/ml) at 24 hour intervals were reported to result in death of all chondrocytes in the tibial plateaux and femoral condyles (Williams and Brandt, 1985, Bendele, 2001). Chondrocytes / osteocytes are also formed. Other characteristic occurrences in the joint are; progressive proteoglycan loss (evidence seen as a reduction in toluidine blue or Safranin-O matrix staining), and atrophy of the remaining collagenous matrix. Fibrillation occurs at a later stage as well as collagen matrix resorption and subchondral bone degradation. This model is useful for the evaluation of agents that inhibit matrix breakdown and induction of repair (Bendele, 2001). Another advantage to this model is that it reduces hind-paw withdrawal thresholds within a week of induction, so it is useful in studying pain related behaviours (Fernihough et al., 2004, Anemaet, 2008). A disadvantage is that this model does not fully mimic the OA process (Little and Smith, 2008).

1.4.2 Medial meniscal transection (MNX) model of OA

The MNX is a model that results in the rapid degeneration of cartilage characterized by loss of chondrocytes and proteoglycans, formation of

osteophytes, fibrillation and chondrocyte cloning in rats that have had their medial collateral ligament and meniscus transected and removed. These degenerative cartilage changes are seen to occur within 3 - 6 weeks post-surgery. Tibial cartilage degeneration may be severe compared to the surrounding matrix. An advantage to using this particular model is that it produces rapid, reproducible changes, and can be used to investigate disease modifying OA drugs, as well as studying the induction and inhibition of osteophyte formation as osteophyte formation is a prominent feature (Bendele, 2001). A disadvantage of this model is that cartilage degeneration progresses rapidly compared to the human OA progression which is slow (Anemaet, 2008, Bendele, 2001). Rats are also known to have very little spontaneous knee joint degeneration, thus the observed lesions are assumed to be as a result of surgical manipulation only. (Bendele, 2001).

Despite there being a variety of animal models of OA that mimic different aspects of the disease, there is not yet an ideal model that would truly represent the human disease because of its complexity. Each model and disease onset and pathology has its own advantages and disadvantages, and there are still gaps in our knowledge of the disease and its pathogenesis. With that been said, animal models are still required because of the ethical limitations to the use of humans, lack of readily available human samples and also because the available human samples are obtained from patients with advanced disease at total knee replacement (tkr) surgery or post mortem in the case of OA. This thus limits our knowledge into the mechanisms that contribute to the development and maintenance of OA pain (Ghilardi et al., 2012).

1.5 PAIN BEHAVIOURAL MEASUREMENTS

Pain is a major symptom of OA, therefore assessment and quantification of pain in experimental animal models would be useful in investigating OA mechanisms and assessing effect of anti-arthritic medication for the development of effective analgesics for OA pain treatment. A number of behavioural tests have been developed for pain assessment in rodent models of arthritis. These include; weight bearing by the affected foot, foot position and gait analysis, paw elevation time, heat sensitivity of the paw (secondary hyperalgesia), locomotor activity scoring either subjectively or by computer, and paw withdrawal threshold to punctuate stimulation indicative of distal mechanical allodynia (Yu et al., 2002, Min et al., 2001, Tonussi and Ferreira, 1992, Malfait et al., 2013).

Weight bearing asymmetry, an indicator of standing pain is brought about by the tendency to lean away or put less weight on the affected joint in OA (Christiansen and Stevens-Lapsley, 2010). This phenomenon does occur in animals with unilateral joint injury and can be measured (Bove et al., 2003). On the other hand, mechanical thresholds which indicate widespread or referred pain for example in the affected and non-affected limb (Arendt-Nielsen et al., 2010) can also be measured in animals (Sagar et al., 2010). Weight bearing and paw withdrawal threshold were the pain measurements of choice in this thesis as they broadly represent nociceptive, peripheral and central sensitisation pain mechanisms and also because they generate robust and reproducible measures of joint pain and secondary allodynia respectively. (Andruski et al., 2008, Suokas et al., 2012). Weight bearing is both peripherally and centrally driven while paw withdrawal threshold is mainly centrally driven.

1.6 HYPOTHESIS AND OBJECTIVES OF THESIS

1.6.1 Hypothesis

Pain behaviour and structural pathology are features of OA models that are mediated by nerve growth factor (NGF). NGF may mediate OA pain by altering joint function and structure, including neuronal sensitisation, inflammation and subchondral osteoclast activation.

1.6.2 Objectives

To investigate the relationship between structural pathology including inflammation and associated pain in models of OA.

To explore the effects of a TrkA inhibitor and an anti-NGF antibody on inflammation, structural pathology and pain behaviour in models of OA.

The thesis has been structured as follows;

- **Chapter 2;** describes in detail all the methodology used in this thesis and why they were selected for use.
- **Chapter 3;** Investigates the characteristic features of the carrageenan model as a model of inflammatory arthritis. These features include pain behaviour and acute inflammation observed as joint swelling, synovitis and synovial macrophage infiltration. Three macrophage markers are explored in this chapter and they provide the rationale for the use of the selected macrophage marker in the subsequent chapters.
- **Chapter 4;** Describes in detail the methodology development of assessing joint pathology macroscopically in the MIA and MNX models of OA. Determines the reliability, reproducibility and validity of the selected macroscopic scoring system and provides an additional method of assessing pathology in OA. The selected macroscopic scoring system was applied in the subsequent chapters.
- **Chapter 5;** Investigates the characteristic features of symptomatic (structural pathology, inflammation and pain behaviour) OA in two MIA models (0.1mg and 1mg). Determines the reliability and validity

of histopathological scoring systems. Validated scoring system was applied in the next chapter.

- **Chapter 6;** Evaluates the effect of inhibitors of NGF (Mumab 911) and its cognate receptor TrkA (AR786) in modifying pain behaviour, inflammation and structural joint damage in the MIA and MNX models of OA. It also explores the duration of sustained analgesia following discontinued treatment with AR786.
- **Chapter 7;** General discussion of the results, relevance of the studies to the existing literature and how the current work of preclinical research may impact on clinical research. This chapter concludes with the limitations met in this thesis and an outline of possible research arising from this thesis.

CHAPTER 2; MATERIALS AND METHODS

2.1 INTRODUCTION

This chapter outlines all the methods carried out in this thesis, with descriptions of the sources of rats, tissues, consumables and equipment. All studies including pilot experiments were carried out on rats in line with the 3R's (reduction, refinement and replacement).

2.2 ANIMALS

Male Sprague-Dawley rats obtained from Charles River U.K were used. Rats weighed between 200-400g at the start of the experiments. Rats were housed in groups of 4 per cage and habituated in the animal holding room for at least 5 days after delivery. All procedures carried out on the rats including housing, handling and testing were conducted within the Guidelines for the Ethical use of animals in experimental pain (Zimmermann, 1983) and with accordance to the UK Home Office regulations, and were in line with the Animals Scientific Procedures Act (ASPA) 1986. Body weights of rats were measured before, during and after each experiment. All experiments were carried out in a randomised and blinded fashion; the experimenter was blind to arthritic and non-arthritic rats, treated and untreated groups. Rats were randomised following baseline pain behaviour measurements. Experiment start dates were staggered to permit pain assessment and tissue collection, ensuring balanced representation of each of the experimental and control groups in each cohort of rats.

2.3 ANIMAL MODELS

2.3.1 Anaesthesia

Anaesthesia was thought traditionally as an all or nothing binary phenomenon (Pandit, 2014). This view was put forward in an editorial by Prys-Roberts

where he wrote, “*There cannot be degrees of anaesthesia nor for that matter can there be variable depths of anaesthesia*” (Prys-Roberts, 1987). This statement although not supported by other references, became a sentiment widely repeated in standard texts (Miller, 2010). Anaesthesia has now been redefined as the state of the brain in complete mental oblivion with no recall in memory, thoughts or experience of sensory perception (Pandit, 2014). In reality, however, ‘*anaesthesia*’ is any drug-induced mental state that makes surgery acceptable at the time, and later, whether or not that includes some awareness and recall of events (Pandit, 2014).

General anaesthesia by inhalation was administered to rats undergoing recovery procedures (intra-articular administration of compounds or surgery) or an overdose by injection in non-recovery experiments (as recommended in the schedule 2.4 of the Animals Scientific Procedures Act 1986 (ASPA) (Wolfensohn and Lloyd, 2003). Isoflurane (halogenated ether), the inhalant anaesthetic of choice is a volatile compound delivered in conjunction with oxygen (O₂). Isoflurane induces and maintains general anaesthesia by depression of the central nervous system (CNS). It is less soluble in blood so it has a high rate of rapid induction and recovery of anaesthesia. Its circulatory margin of safety is the largest compared to all other potent halogenated agents as it produces the least myocardial depression at a given minimum alveolar concentration (MAC) multiple (Eger, 1984). Each rat was placed in a chamber and anaesthetised with isoflurane mixture (2% in 1L/min of O₂) until areflexic. Areflexia was confirmed by pinching of the fore and hind paws.

2.3.2 Intra-articular injections

Each rat was anaesthetised with isoflurane mixture (2% in O₂) (section 2.3.1). The rat was then placed in a supine position and the skin directly above and around the joint of the left leg was shaved and swabbed with chlorhexidine (Animal care Ltd, Dunning ton, York). The white tendon below the skin of the knee joint was identified. Injection of 50µl was then given into the left joint of the rats using a 27-gauge 12.7-mm needle inserted through the suprapatellar ligament with the joint held in 90° flexion (Mapp et al., 1996, Walsh et al., 1998a, Seegers et al., 2003). Administered compounds were dissolved in sterile

0.9% normal saline (pH 7.4). After injection, the injected area was then massaged to allow proper dispersion of the drug. Un-injected and saline-injected knee joints were used as controls.

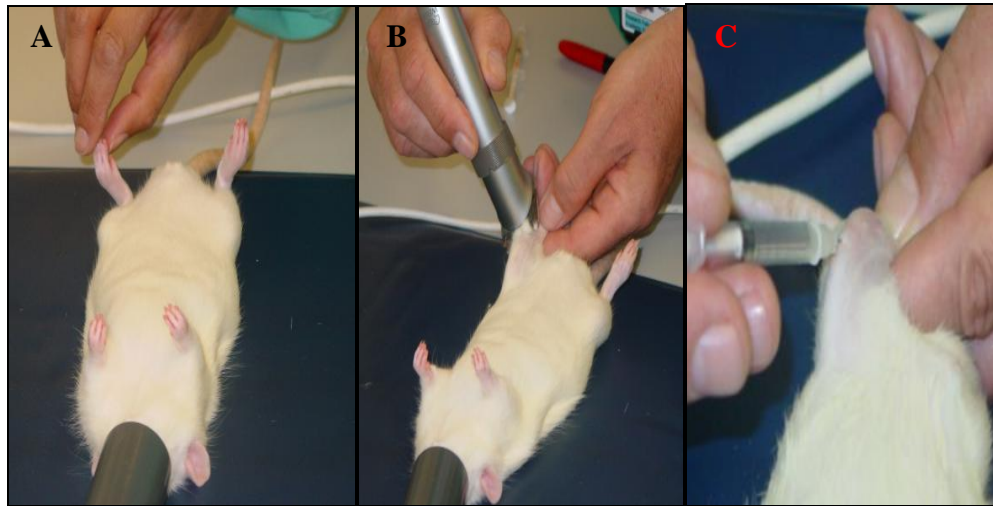


Figure 2.1 Intra-articular injections into rat knees

Anaesthetised rat in an areflexic state, judged by pinching of the fore and hind paws (A). Skin above knee joint is shaved and swabbed with chlorhexidine ready for injection (B). Compound administered using a 27G, 12.7mm needle inserted through the suprapatellar ligament or inserted straight in the joint space through the infrapatella ligament with the joint held in 90° flexion (C). Picture taken from (Ashraf, 2011).

2.3.3 Intra-peritoneal injections

Each rat was restrained by the scruff in the non-dominant hand or by another person in cases where the rat was too big to be restrained by the same person administering the injection. The rat was positioned with the head angled toward the floor or on its back. This allowed intestines to move away from injection site, with the position maintained throughout procedure. In the case of a rat, a 23-25 g, 0.5 to 1 inch needle, volume limit 10ml/kg was used. The syringe was held in the dominant hand (thumb, bevel & measurement lines up). The needle was then inserted to the hub into the lower abdominal quadrant between the midline and leg at a 45° angle. Aspiration was done gently to ensure that the needle was not inserted into a blood vessel, urinary bladder or intestine. If this was the case, the needle was removed and with a different needle, a new

solution was injected with as little movement as possible, after which the needle was carefully removed (AWHLA, 2005-2014). This procedure was used at the end of the studies for termination by an overdose of pentobarbital anaesthetic (5ml/kg).



Figure 2.2 Administration of compounds intra-peritoneally

Procedure carried out by two people, one holding the rat in the correct position and the other doing the injecting in the lower abdominal quadrant with needle placed at a 45° angle. Picture taken from (AWHLA, 2005-2014).

2.3.4 Oral gavage

Gavage or stomach catheters are used to introduce liquids directly into the stomach of animals. They are stainless steel needles with a protective rounded tip or soft flexible plastic tubes to prevent any internal damage to the animal during oral dosing. The maximum volume that could be administered to a rat was calculated based on the Home Office guidance (20ml/kg up to three times daily). For a 200-350g rat, a 14G-3inch and 4mm ball diameter needle is used. The rat was restrained by scruffing with its neck extended, so that the head was well controlled and the forelimbs immobilised (Wolfensohn and Lloyd, 2003). Distance from the oral cavity to the end of the xyphoid process (caudal point of the sternum) was measured outside of the restrained rat with the feeding needle

to ensure that the needle to be used was of appropriate size and at the same time giving an idea of how far the needle was to be inserted when dosing. Inappropriate sized needles could lead to damage of the oesophagus or the stomach of the rat as well as resulting in the drug being delivered to a site other than the stomach. The needle attached to a 1ml syringe containing the appropriate drug in a 500 μ l volume was passed gently down along the roof of the rat's oral cavity on the left side thus enabling the needle to slide down the oesophagus with ease. The needle was rotated slightly to enable smooth passage throughout the sphincter of the epiglottis and into the oesophagus. Once the needle was at the premeasured distance, the contents of the syringe were slowly administered to prevent reflux of the fluid. The needle was then gently removed in the opposite direction from insertion and the rat returned to its cage and observed for potential complications such as gasping and frothing at the mouth or nose.

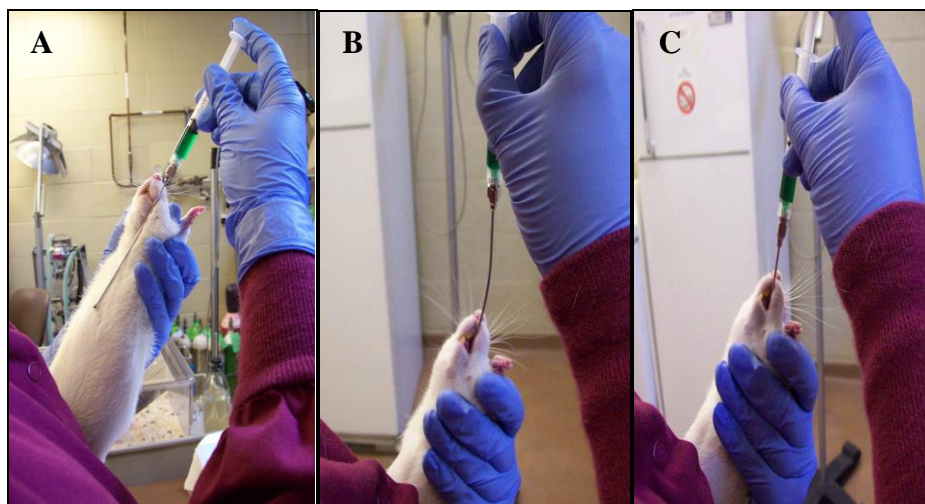


Figure 2.3 Compound administration by oral gavage

Rat is restrained with the non-dominant hand or by another person, and the dosing needle measured from the oral cavity to the stomach to see if the needle was the right size and what distance the needle should be inserted (A). Dosing needle carefully inserted through the oral cavity (B). When the correct distance was reached, the compound was then administered slowly (C). Picture taken from (Jones, 2012).

2.3.5 Medial meniscal transection

OA was induced on day 0 by surgical transection of the medial meniscus as previously described (Janusz et al., 2002, Ashraf, 2011).

Briefly, prior to surgery, each rat was anaesthetized (section 2.3.1); the left leg was shaved and swabbed with chlorhexidine, so as to provide a sterile area to operate on. The rat was appropriately positioned over a heat blanket to keep it warm during surgery. A nose cone was used to deliver the anaesthetic and keep the rat anaesthetised during surgery. A sterile op-cover (Kruuse Ltd, Sherburn in Elmet, North Yorkshire) was placed over the leg to be operated on, covering all but the area to be operated on, thus minimising the risk of sterile items becoming non-sterile due to contact with areas close to the surgical field. All instruments were autoclaved a day before the surgery and re-autoclaved between rats during surgery.

A section of skin medial to the joint was lifted using straight forceps (InterFocus Ltd, Linton, Cambridge, 11370-40) and a single cut made underneath the joint cavity with straight iris scissors (InterFocus Ltd, Linton, Cambridge, 14558-11). The medial collateral ligament (MCL) could be seen as a white shadow buried under the muscle layers following the cut. Any haemorrhage from the skin edge was stopped by firmly applying pressure with a sterile swab. Connective tissue (CT) directly above the MCL was grasped with straight forceps and cauterized using small vessel cauteriser (InterFocus Ltd, Linton, Cambridge, 18000-00) edged in a straight line from one corner of the cut to the other so as to easily access the MCL. The muscle layers were held before being cauterized in the same way as the CT. If any bleeding occurred during this process, it was arrested by cauterizing the bleeding vessel. When the MCL was clearly visible, the distal end was grasped with rat teeth forceps (InterFocus Ltd, Linton, Cambridge, 11084-07) and cut using a straight spring scissors (InterFocus Ltd, Linton, Cambridge, 15000-00) held flat to the joint. The MCL was lifted until the meniscus was clearly seen and then cut and partly removed (3mm) to uncover the meniscus.

The procedure was stopped and the wound sutured if SHAM surgery was being performed. Otherwise the procedure was continued and the meniscus was freed

from its surrounding tissues by making two cuts on either side, anterior and posterior of the meniscus, at the top and two cuts at the bottom using straight spring scissors. The ankle of the rat was twisted gently to clearly visualize the joint space and the meniscus was then held with rat teeth forceps before being cut through its full thickness at its narrowest point (middle) using straight spring scissors. The procedure was done with care so as to ensure that the underlying articular cartilage did not suffer any forced damage whilst the meniscus was being cut during the surgery. Following the transection of the meniscus, the bone ends were inspected thoroughly under the microscope to ensure no damage was sustained. The site was also flushed with saline and dabbed using sterile swabs to remove any blood. Sutures were made using a micro needle holder with cutter (InterFocus Ltd, Linton, Cambridge, 12075-14) and suture tying forceps (InterFocus Ltd, Linton, Cambridge, 18025-10) to pass curved needles through tissues and to tie knots after suturing. The CT layer was closed with interrupted stitches using Ethicon coated vicryl 8/0 sutures (NHS supply chain). The skin was closed using wound clips (Harvard Apparatus) to appose the tissue margins and allow healing (Figure 2.4).

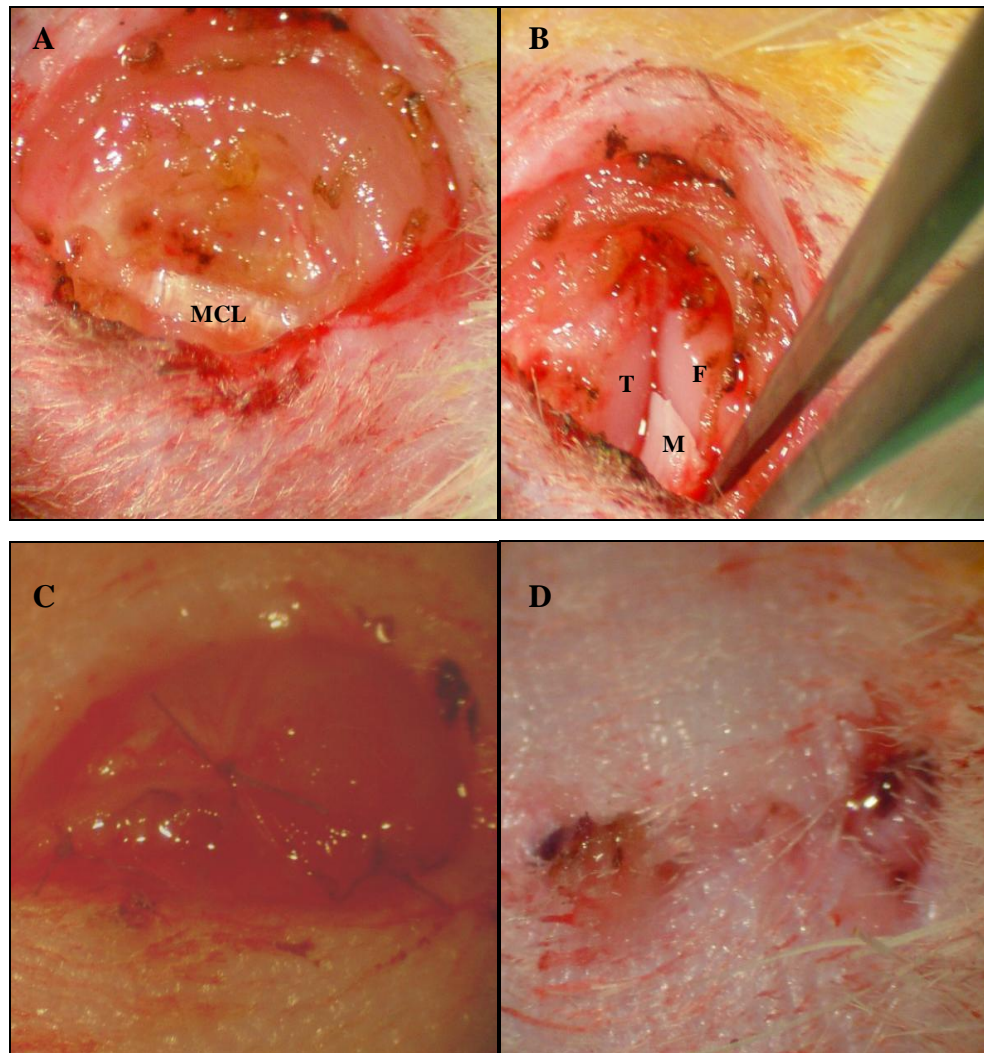


Figure 2.4 Transection of the medial meniscus of the knee

Exposed medial collateral ligament (MCL) was cut and partly removed for easy access to the meniscus (A). Meniscus (M) transected through its full thickness at its narrowest point, femur (F) and tibia (T) are seen and can freely move (B), after which the connective tissue was closed (C), then followed by the skin (D). Picture taken from (Ashraf, 2011).

2.4 ACUTE INFLAMMATION

2.4.1 Joint swelling

OA is a disease of the joint and the procedures carried out on the rats were mostly done to the joint. Joint swelling for each limb (ipsilateral-operated and

contralateral-non operated or control) was measured using a digital electronic calliper (Miyutoyo UK Ltd., Andover, UK) at set time points as differences in knee diameters (mm) representing acute or chronic inflammation.

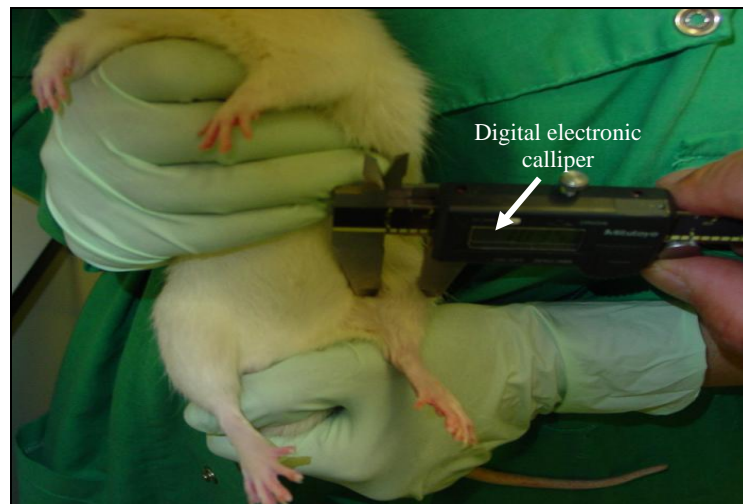


Figure 2.5 Measurement of knee joint swelling

Procedure was carried out by two people, one to restrain the rat in the correct position and the other doing the measurement with a digital electronic calliper. Picture taken from (Ashraf, 2011).

2.5 PAIN BEHAVIOUR MEASUREMENTS

Pain behaviour was measured indirectly as a percentage difference in hind-limb weight bearing asymmetry (peripheral sensitisation) and distal allodynia-hind paw withdrawal threshold (central sensitisation) (Neugebauer et al., 2007). These methods are used in research studies in humans for pain assessments in arthritic patients. Reduced weight bearing is comparable to weight bearing asymmetry. Paw withdrawal threshold (PWT) indicates reduced pain thresholds to mechanical stimuli distal to the affected joint. Similar observations have been made by quantitative sensory testing in man (Hassan and Walsh, 2014, Suokas et al., 2012).

2.5.1 Weight bearing

This technique compares the difference between the weights placed on the ipsilateral limb and contralateral limb of an animal. Rats were first habituated in a Perspex box prior to start of the study where the baseline measurements would be taken thereafter at the start of each study. This enabled the rats to get used to their surroundings and aimed to reduce a rise in stress levels. Stress may confound pain behaviour measurements. Weight bearing asymmetry was measured at different set time-points using an Incapacitance Meter (Linton Instruments, Norfolk, UK). Each rat was placed in a Perspex box such that each paw rests on a separate transducer pad that records the rat's weight distribution over a period of 3 seconds. After 3 consecutive readings an average was taken and expressed as a difference in percentage of force between the hind limbs (Mapp et al., 2010, Bove et al., 2003). Results are presented as calculated by the following equation, so as to take into account the weights of the rats: $(\text{Contralateral} - \text{Ipsilateral} / \text{Contralateral} + \text{Ipsilateral}) \times 100$

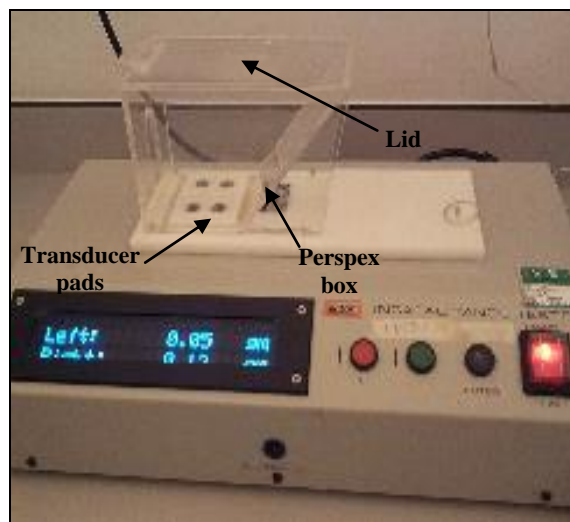


Figure 2.6 Incapacitance meter used for recording weight bearing

The incapacitance meter consists of a Perspex box to hold the rats, transducer pads which record the weight distributed to either hind limb by the rat.

2.5.2 Distal (static) allodynia

Hind paw withdrawal threshold (PWT) which indicates distal mechanical allodynia was measured. Rats were habituated by placing them singly into Plexiglas mesh bottom test cages 15-20 minutes prior to the assessment of allodynia. Measurement was done via the Dixon up-down method using calibrated Semmes-Weinstein monofilaments ranging in strength from 1g, 1.4g, 2g, 4g, 6g, 8g, 10g and 15g as previously described (Chaplan et al., 1994, Sagar et al., 2010, Sagar et al., 2011). Firstly the ipsilateral paw was stimulated with the 2g filament and held for 3 seconds. In the case of a pain response, seen as a rapid lifting of the affected paw and flinching, the next lower filament was used. In the case of a no pain response, the next upper filament was used. After the first threshold response was observed, i.e. a response followed by no response or vice versa, the lowest monofilament that elicited a response was then noted as the PWT. A repeat of the above was then carried out on the contralateral side.



Figure 2.7 Wire bottom test cages for measuring allodynia

Each rat was placed in Plexiglas mesh bottom test cage and paw withdrawal threshold measured by stimulation with von Frey hairs.

2.6 TISSUE COLLECTION AND PROCESSING

2.6.1 Euthanasia (overdose by CO₂ or anaesthetic-pentobarbital)

At the end of each in-vivo study in this thesis, each rat was killed either by a rising concentration of carbon dioxide (CO₂) in the case of fresh tissue collection or by an overdose of the anaesthetic pentobarbital for perfusion fixed tissue collection. These methods of sacrifice are in line with the recommended schedule 1 method (appropriate methods of humane killing) of the Animals Scientific Procedures Act 1986 (ASPA). The following refers only to CO₂ use; each rat was placed in an empty chamber with a transparent lid. Flow of CO₂ was turned on to 2 L/min for a 200-500g rat, gradually introducing 100% CO₂ to result in the replacement of 20% of a small chamber volume per minute while for a big chamber flow of CO₂ was 6 L/min (for two or more rats) (Hewett et al., 1993). The narcotic effect of CO₂ to depress awareness causes the rats to lose consciousness with increasing concentration and then they eventually die from hypoxia (Mackay, 1947). The flow of CO₂ was turned off after 6 minutes and the chamber inverted each time in order to tip out all of the residual CO₂ which would have otherwise sunk to the bottom of the chamber as CO₂ has a higher density than O₂ thus making it heavier than O₂ (Smith and Harrap, 1997). The danger of not performing the above action would result in the respiratory distress and struggling of the next rat put into the chamber as the procedure requires the gradual introduction of CO₂ (Danneman et al., 1997). Death was always confirmed by dislocation of the neck.

2.6.2 Systemic transcardiac perfusion fixation

Each rat was fully anaesthetised 15 minutes prior to the fixation procedure with intraperitoneal injection (section 2.1.3) of 2ml sodium pentobarbital (Euthatal). The rat was left until there were no corneal and hind paw withdrawal reflexes but not left too long that the heart was no longer beating, as maintained circulation was needed for the procedure. The rat was restrained on a perfusion tray with needles so that the fixative would easily access the joint tissues, and the skin directly above the rib cage was cut exposing the muscle underneath.

The cartilage below the sternum was held with a forceps and the ribcage cut through gently to expose the heart without damaging the lungs. The auricle above the heart was excised to allow for the clear visibility of the ascending aorta. The heart was then grasped gently with forceps and a small incision made in the left ventricle and a cannula was then passed through it into the ascending aorta. A small incision was made in the right atrium to allow drainage of returning blood (in the case blood collection was needed) and fluid from the systemic circulation. 300ml phosphate buffered saline (PBS) was pumped through the cannula to wash out any remaining traces of blood in the rat. After the fluid ran clear, 400ml Zamboni's fixative was then pumped through the rat to fix the tibiofemoral knee joints (Hukkanen et al., 1992, Honore and Mantyh, 2000). Tibiofemoral joints were promptly excised by cutting mid-femur and tibia with a bone cutter and post fixed in the same perfusion fixative solution, ready for the decalcification process (section 2.6.4) (Imai et al., 1997).

2.6.3 Harvesting and mounting of rat synovia

Each rat was killed by a rising concentration of CO₂ (section 2.6.1). The skin above the knee was removed for each rat and the synovia with patellae from right and left knees were dissected free from bone. The skin above the patella was sliced using a scalpel. The patella was held using a rat teeth forceps and the skin on either side was sliced to expose the fat pad below the patella that houses the synovium. The synovium was then held by the patella end and embedded perpendicularly on its side in Tissue Tek Optimum Cutting Temperature (OCT®) mounting medium (Raymond Lamb, Eastbourne, UK) onto cork blocks before being snap frozen in melting isopentane and stored at -80°C until use (Ashraf, 2011, Walsh et al., 1993).

For Zamboni-fixed synovia, samples were transferred to 15% [w/v] sucrose in PBS/Sucrose-azide solution at 4°C for 5 days. The PBS/Sucrose solution was changed daily until the yellow appearance of the solution cleared. Once cleared, the PBS/Sucrose-azide was replaced with 1:1 mixture of PBS/Sucrose-azide and OCT® mounting medium for 2 days and then into 100% OCT® for another two days after which it was embedded in OCT onto cork blocks and

snap frozen in melting isopentane and stored at -80°C until use. The samples were placed in PBS/Sucrose-azide, to cryoprotect the tissue and also prevent any bacteria growth with sodium azide. The synovium were put in OCT before being embedded so that the OCT would coat the cells and prevent the section from drying out and will also prevent ice crystal from forming during embedding.

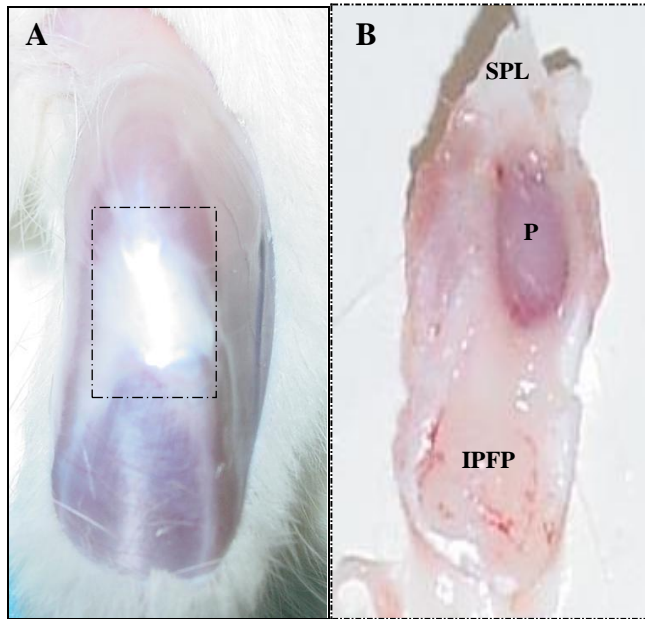


Figure 2.8 Harvested synovia

Rat knee with removed skin to expose tendon directly above joint (A). Dissected synovium with patella (B). Picture adapted from (Ashraf, 2011). Supra-patellar ligament (SPL), patella (P), infra-patellar fat pad (IPFP).

2.6.4 Harvesting and mounting of rat tibiofemoral joints

Tibiofemoral joints were excised by cutting mid-femur and tibia with a bone cutter and excess skeletal muscle dissected off. Joints taken fresh were immersed in neutral buffered formalin containing 4% formaldehyde at room temperature for 48h while perfusion fixed joints were post fixed in Zamboni's fixative (4% paraformaldehyde, 15% (v/v) saturated (1.3% picric acid), 0.1M phosphate buffer, pH 7.3) for 48h at 4°C (Imai et al., 1997), ready for the decalcification process. The joints were placed on a roller mixer and continuously agitated during the decalcification process, as mechanical

agitation is thought to hasten the decalcification process (Russell, 1963) and also to prevent the formation of artefact crystals due to stagnation (Mephram, 1991).

Decalcification is the process by which heavily mineralised tissues are softened in order to obtain satisfactory thin sections for histological purposes. This process is usually carried out by treatment of tissues with reagents which react with calcium; either by use of acids (weak acids - formic acid) to produce soluble calcium salts or the use of chelating agents (ethylenediaminetetraacetic acid [EDTA]) which take up calcium salts (Mephram, 1991). The choice of decalcification is dependent on a few different factors; the hypothesis of the experiment, the staining techniques required and the urgency of the case. In this thesis, EDTA decalcification was mainly used because it was a less harsh and slower method of decalcification compared to formic acid. EDTA has less of an effect on many immunohistochemical stains e.g. for detection of TRAP positive osteoclasts – section 2.7.2.1. It also allows the detection of nerve structures. Formic acid was used only once to rapidly decalcify the tibiofemoral joints to be used for histological (Safranin-O fast green) stains (section 2.7.1.2) in order to analyse the proteoglycan content of the joint as it has been reported that there is increased wash out of proteoglycan with the slower EDTA method (Kiraly et al., 1996, Chevrier et al., 2005).

Weak acid fixation; formic acid is the only weak acid extensively used primarily for decalcification. It can be used as a simple 5-10% aqueous solution or in addition with a buffer or formalin which has the benefit of simultaneous fixation and decalcification. Decalcification occurs rapidly within 1-10days depending on the size and nature of the tissue, and the acidity of the solution.

Chelating agents; EDTA is the most commonly used agent in the form of its disodium salt. Although an acid, it does not act as a mineral or organic acid but can only capture and bind ionised calcium. It acts only on the outer layer of the apatite crystal at the start of decalcification. As decalcification proceeds, the crystal becomes smaller as the layers become depleted, and thus it is a slower process (6-8weeks). This method of decalcification has less effects on other

elements making it a better method for immunohistochemistry as some enzymes are still active after EDTA decalcification (Mephram, 1991).

Formalin-fixed tibiofemoral joints were decalcified in 10% formic acid in neutral buffered formalin (containing 4% formaldehyde), changed twice a week, for 7 days at room temperature or in 10% EDTA in 10mM Tris buffer with 7.5% [w/v] polyvinylpyrrolidene [PVP], pH 6.95). The joints were decalcified for approximately 6 weeks at room temperature. The decalcification fluid was changed twice a week.

Zamboni-fixed tibiofemoral joints were transferred to 15% [w/v] sucrose in phosphate buffered saline (PBS/Sucrose) solution at 4°C for 5 days. The PBS/Sucrose-azide solution was changed daily until the yellow appearance of the solution cleared. Once cleared, the PBS/Sucrose-azide was replaced with decalcification fluid (10% EDTA in 10mM Tris buffer with 7.5% [w/v] polyvinylpyrrolidene [PVP], pH 6.95). The joints were then decalcified for approximately 6 weeks at 4°C.

After decalcification of the formalin fixed joints, the joints were then split in a frontal plane and placed in cassettes (Figure 2.9). These trimmed joint tissues were then processed by standard histological techniques and mounted in paraffin wax blocks for sectioning. Briefly, the joint samples were secured (flat side down) in labelled plastic cassettes. The cassettes were then placed in the Shandon Pathcentre enclosed tissue processor (Shandon ThermoScientific, Leicestershire, UK) at King's Mill Hospital by an experienced laboratory technician (Roger Hill) to undergo a series of dehydration (in alcohol) and clearing (in xylene) steps. The joint tissues were impregnated with molten wax for the final embedding stage of setting the tissues in blocks of paraffin wax. For this, the tissues were left in the respective cassettes in molten wax. Metal moulds were placed on a hot-plate and molten wax was dispensed into them from a Tissue Tek ® embedding centre (model TEC5 EME2; Sakura Finetek Europe, The Netherlands). Tibiofemoral joint or tibia joint tissues only (in the case of disarticulated joints) were then placed flat side down into the centre of the mould using warm forceps and transferred briefly to a cold-plate to allow the wax to slightly solidify at the bottom of the mould and at the same time the

section was pressed down to enable an even flat tissue surface to be achieved with the wax. Labelled plastic cassettes were then placed on top of the mould, pressed down and more wax poured on top to evenly fill the cassettes. Moulds were then placed on the cold-plate for quick cooling of the wax. Once the wax set, the wax blocks were removed from the metal moulds, excess wax trimmed from the cassettes and the wax blocks were stored at room temperature until required for sectioning (Figure 2.9).

After decalcification of the Zamboni's fixed joint, and after radiography, the frontal split trimmed joints were transferred to PBS/Sucrose solution for 5 days at 4°C, then through to 1:1 mixture of PBS/Sucrose and OCT® embedding matrix for 7 days, then into 100% OCT for a further 7 days at 4 °C. The sections were continuously agitated on a roller-mixer throughout this process before being mounted onto cork blocks and then snap frozen in melting isopentane on liquid nitrogen and stored at -80 °C until use.

Frontal sectioning is the most commonly used method of splitting, embedding and sectioning of rat knees for microscopic evaluation by histology (Gerwin et al., 2010, Janusz et al., 2002, Hayami et al., 2006b). In this process, the joints were split into two equal halves, anterior and posterior, along the MCL in the frontal plane. The knee joint was placed in between blunt forceps on its side with the MCL facing up. The forceps were then squeezed to straighten the joint and allowing for aligning the cut through the middle of the arms of the forceps with a scalpel. The two resulting anterior and posterior halves were embedded separately in two different blocks. The resulting histological section included both femoral condyles, tibial plateaux and menisci (Gerwin et al., 2010) or in most of the cases in this thesis, it included only the tibial plateau as macroscopic scoring (Chapter 4) were carried out on the joints hence the joints were disarticulated before splitting and only the tibia embedded.

Following the osteoarthritis research international (OARSI) histopathology initiative recommendations for histological assessments of osteoarthritis in the rat, three 5µm sections were cut from each paraffin block at approximately 200µm levels in order to obtain 6 sections in total (3 from each anterior and posterior block of one rat) but that 3 of the sections from a part was scored

(Gerwin et al., 2010). This protocol was tested in Chapter 5 and it was found that in order to obtain sufficient power to demonstrate structural changes to the cartilage surface and chondrocyte appearance, 6 sections to include both anterior and posterior joints was required (detailed explanation and results in chapter 5).

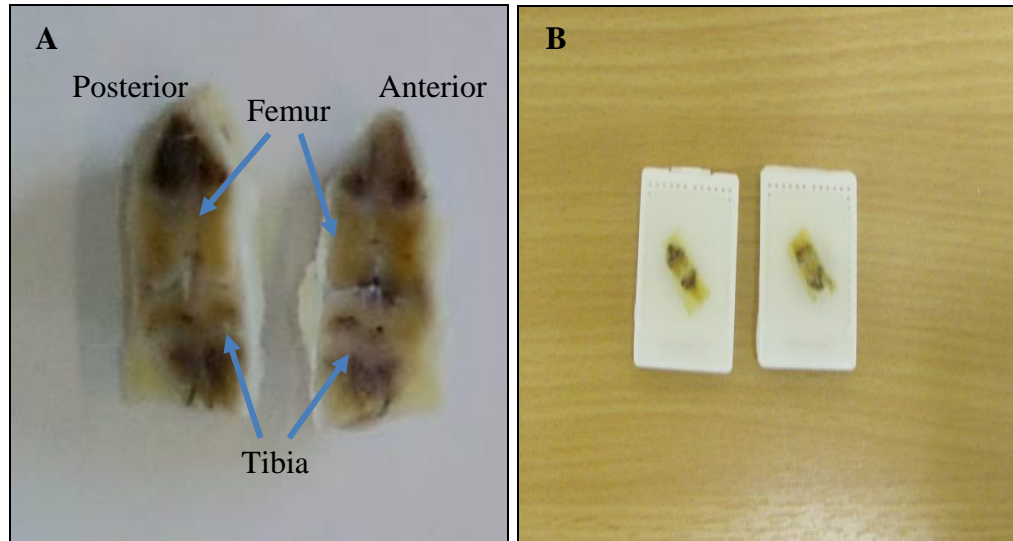


Figure 2.9 Harvested and embedded rat joints

Knee joints split frontally into anterior and posterior halves with femur and tibia intact (A). Tissue samples subsequently embedded in paraffin wax blocks for storage and sectioning (B) Picture adapted from (Ashraf, 2011).

2.7 HISTOCHEMISTRY

Histochemistry is the study of the identification of chemical components of cells and tissues using histological techniques. Histochemistry is useful in the evaluation of diseases that involve the bone e.g. OA.

2.7.1 Histological stains

The most frequently used stains are haematoxylin and eosin (H&E), Safranin-O-Fast green, toluidine blue and alcian blue PAS. It is recommended that for a method of scoring, the stain used should be sensitive enough to detect the tidemark. In this case, the H&E stain is used, although the tidemark is more clearly seen in humans than rats (Gerwin et al., 2010).

2.7.1.1 *Haematoxylin and eosin (H&E)*

H&E is often used to analyse tissue morphology. The haematoxylin dye is basic and has a high affinity for acidic structures; examples are the cell nucleus which it stains blue/black. The acidic eosin dye stains more of basic structures; the cell cytoplasm and connective tissue fibres in different hues of pink, red or orange (Mephram, 1991). There are different types of the haematoxylin dye; Ehrlich's, Harris's, Mayer's and Weigert's haematoxylin. The Harris haemalum is used for fresh frozen tissue in a progressive staining method while the Mayer's haemalum is used for fixed frozen or paraffin (wax embedded) tissues in a regressive stain. A progressive stain is when the tissue is stained long enough to reach the desired endpoint, while a regressive stain is when the tissue is over stained and then later differentiated in acid alcohol to the desired endpoint (King and King, 1986, Millikin, 2005). Unfixed tissues such as synovia cannot be stained by the regressive method as the acid alcohol step will damage the tissue, hence the Harris haemalum is used.

Frozen tissue sections were cut using the cryostat and paraffin sections using the microtome. 5µm thick frozen sections were washed for 5 minutes in PBS and another 5 minutes in distilled water. Paraffin wax embedded tissue sections (5µm thick) were first dewaxed in xylene and then rehydrated in graded ethanol (100% and 70%) before being washed in distilled water for 5 minutes. Nuclear staining was then achieved by immersing the sections in Mayer's

haematoxylin for 10 minutes or Harris haematoxylin for 5 minutes, rinsing in running tap water to differentiate the staining, dipping the sections in 1% acid alcohol solution for 10 seconds (for wax sections) and back into tap water for further 3 minutes before being immersed in 1% eosin for 1 minute (fresh tissue step is from water to eosin) to stain all other tissue structures varying degree of red. Staining was then differentiated with running tap water and the sections were dehydrated through graded ethanol (70% and 100%) into xylene and mounted in DePeX and covered with cover-slips and allowed to dry.



Figure 2.10 Haematoxylin and Eosin stained section of a tibia.

2.7.1.2 Safranin-O fast green

Safranin-O fast green is a widely used technique for studying cartilage and bone (Bulstra et al., 1993, Pedersen et al., 2013). Safranin-O is a cationic dye that binds specifically to sulphated glycosaminoglycans (GAGs) and proteoglycan. A product of the binding is the intense red stain which indicates the presence of proteoglycan content. Varying intensity of the red colour is what is measured in histological sections assessing cartilage damage. Fast

green provides a contrasting counterstain, it stains the underlying subchondral bone a blue/green colour (Rosenberg, 1971). In normal cartilage, Safranin-O staining is known to be directly proportional to proteoglycan content and therefore have been used to investigate changes in articular disease. In cartilage, where the levels of GAGs have been severely depleted, sensitivity to proteoglycan content is reduced (Camplejohn and Allard, 1988). The result may vary in staining intensity between individuals of the same species, hence another proteoglycan stain could be used in parallel (Alcian blue PAS stain, section 2.7.1.3). As proteoglycans are usually washed out during decalcification, especially with prolonged methods, other quicker decalcification methods (Formic acid-Formalin method instead of the EDTA method) could be applied to preserve proteoglycan content so as to achieve high quality quantitative assessment results (Schmitz et al., 2010, Encfeldt and Hjertquist, 1967).

Paraffin wax embedded sections were cut using the microtome. Five µm thick sections were first dewaxed in xylene and then rehydrated in graded ethanol (100% and 70%) before being washed in distilled water twice for 5 minutes. Sections were then immersed for 2 minutes in Weigert's haematoxylin, rinsed for 1 minute in running tap water and submerged in acid alcohol solution for 20 seconds. The sections rinsed again in tap water for further 3 minutes. Sections were subsequently immersed in Fast Green for 5 minutes, dipped in acetic acid solution for 1 minute and immersed in Safranin-O for 5 minutes. Staining was then differentiated with running tap water and the sections were dehydrated through graded ethanol (70% and 100%) into xylene and mounted in DePeX, then covered with cover-slips and allowed to dry.

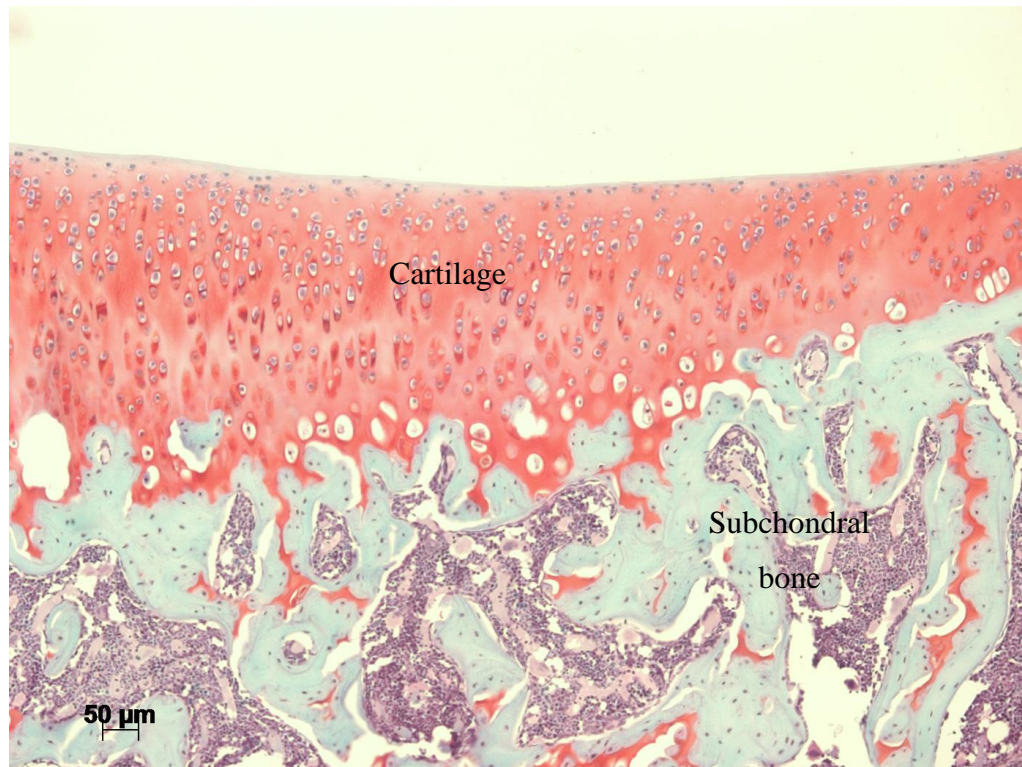


Figure 2.11 Safranin-O Fast green stained section of a tibia. Scale bar = 50µm.

2.7.1.3 Alcian blue-pas

Toluidine blue, Safranin-O and alcian blue are cationic dyes. Alcian blue with the periodic acid Schiff (PAS) reaction is widely used in histological studies of connective tissue for both light and electron microscopy (Ippolito et al., 1983, McIlwraith and Van Sickle, 1981). There are extensive investigations in in-vitro studies of the chemical interactions of GAGs with alcian blue (Scott and Dorling, 1965). The PAS reaction is used to indicate the presence of carbohydrates in tissues. The reaction occurs by oxidative cleavage of the carbon-to-carbon bond in 1,2-glycols or their amino or alkylamino derivatives by periodic acid, thus resulting in dialdehyde formations (Mephram, 1991). These aldehydes react with fuchsin-sulphurous acid, combining with the basic pararosaniline to give the magenta colour (Stoward, 1967).

The tissue parts (non-calcified cartilage) that stain blue to bluish green in the alcian-blue pas reaction are alcianophilic and contain acidic mucins, the parts

that contain neutral mucins stain magenta (calcified cartilage). A mixture of the above stain the underlying bone bluish-purple and the nuclei appear dark blue.

Paraffin wax embedded sections were cut using the microtome. 5µm thick sections were first dewaxed in xylene and then rehydrated in graded ethanol (100%, 96% and 90%) before being washed in distilled water twice for 5 minutes. Sections were then immersed for 5 minutes in acetic acid solution, and incubated in alcian blue for 1 hour. Sections were then rinsed for 5 minutes in running tap water and distilled water. They were then immersed in periodic acid solution for 10 minutes and rinsed thereafter for 5 minutes in distilled water. Sections were subsequently immersed in Schiff reagent for 15 minutes and rinsed thereafter for 5 minutes in distilled water. The sections were then dehydrated through graded ethanol (90%, 96% and 100%) into xylene and mounted in DePeX, then covered with cover-slips and allowed to dry.

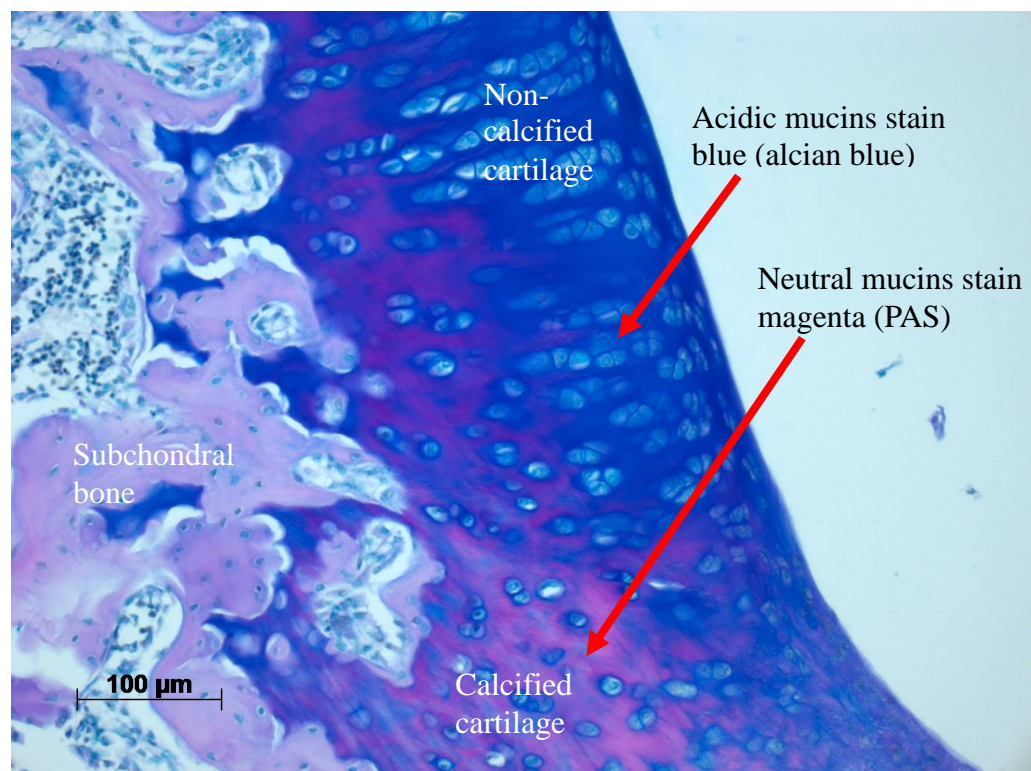


Figure 2.12 Tibia plateau with Alcian blue PAS stain. Scale bar = 100µm

2.7.2 Enzyme histochemistry

Enzyme histochemistry is one subclass of histochemistry. In general, enzymes are the proteins being studied in enzyme histochemistry and are the rate determining factor for most biochemical reactions.

2.7.2.1 Tartrate resistant acid phosphatase (TRAP)

Tartrate resistant acid phosphatase (TRAP) is a histochemical marker for osteoclasts, and is involved in diverse pathological conditions to include hairy cell leukaemia, AIDS, encephalopathy, OA etc. (Summers and Jaffe, 2011, Schindelmeiser et al., 1989, Sagar et al., 2014). It is also expressed by other mono histocytes such as macrophages. These cells express the band 5 isozyme of TRAP (Minkin, 1982). Expression of TRAP is associated with the activation and differentiation of osteoclasts. Commercially available TRAP test kits have been designed to detect TRAP on osteoclast. The TRAP enzyme is higher in disease conditions where bone breakdown is enhanced e.g. Paget's disease, hyperthyroidism and OA (Lau et al., 1987, Chamberlain et al., 1995, Sagar et al., 2014).

Paraffin wax embedded sections were cut using the microtome. 5µm thick sections were first dewaxed in xylene and then rehydrated in graded ethanol (100% and 70%) before being washed in distilled water twice for 5 minutes. Sections were then incubated overnight in a mixture of 1mM CaCl₂ and 1mM MgCl₂ solution, after which they were rinsed for 5 minutes in distilled water. TRAP solution was applied on each individual section in a humidified box and incubated at 37°C for 1 hour. The TRAP substrate consisted of 2ml acetate solution, 2ml Naphthol AS-BI phosphoric acid, 2ml Tartrate solution, contents of 1 capsule of Fast Garnet GBC salt, all of which were dissolved in 44ml of distilled water, stirred and filtered before use. Following incubation, the sections were rinsed in tap water and then in distilled water. Acid haematoxylin was used to counterstain the sections for 5 minutes and then the rinsing process was repeated in both tap water and distilled water before being mounted in 1:1 ratio of PBS/glycerol and then vanish applied around coverslips to seal the edges.

The contents of the TRAP solution including Acid Haematoxylin all came premade in a TRAP kit (Sigma Aldrich).

2.7.3 Immunohistochemistry (IHC)

2.7.3.1 Introduction

Immunohistochemistry comprises of various methods used to detect tissue constituents (antigens such as, amino acids and proteins, infectious agents and specific cell populations) when specific antibodies are employed. For example, in cell preparations it is known as immunocytochemistry (Matos et al., 2010, Coons and Kaplan, 1950).

The IHC technique consists of two phases: (1) slide preparation and staining: specimen fixation, tissue processing and storage, antigen retrieval, non-specific site block, endogenous peroxidase block, primary antibody incubation, secondary antibody incubation (whether the antibody is conjugated to an enzyme example, a peroxidise labelled antibody or is tagged with a fluorophore; fluorescein example in immunofluorescence), employment of detection systems, counterstaining (optional) and slide mounting; (2) analysis and quantification of obtained expression (Matos et al., 2010, Renshaw, 2007).

2.7.3.2 Limitations, difficulties and problems of IHC

Although IHC is useful for scientific research and employs relatively simple immunostaining techniques, there are some limitations to it and the result outcome obtained usually depends on a variety of different factors. The usefulness and contribution that IHC brings to scientific research depends on the expertise of the experimenter carrying out the IHC technique and the observer who interprets the results expressed (Leong and Wright, 1987, Werner et al., 2000, Jaffer and Bleiweiss, 2004, Matos et al., 2010). Thus IHC may have simple immunostaining methods but it requires efficient execution and in order to prevent significant bias, the results obtained should be interpreted with caution (Matos et al., 2010). A review presented the different bias that can occur with analysing IHC reactions; they are reaction bias and interpretation bias (Yaziji and Barry, 2006). In reaction bias, the different conditions are;

- Specimen fixation (long periods of tissue fixation may cause tissues to lose their antigenicity or some fixations may mask some of the important antigens e.g. formalin fixations)
- Tissue processing (this may also compromise tissue antigenicity if not carried out properly).
- Antigen retrieval (this helps to unmask antigens in e.g. formalin fixed tissues, but this may also damage the tissue structure).
- Detection systems (the secondary antibody employed and the amplification system used; the avidin-biotin peroxidase complex - ABC method etc. is among one of the best amplifications systems because it is relatively low cost and more flexible).

In interpretation bias, there are; the types of antibodies to be used, the sensitivity of the antibodies selected and their use in the literature (interpretation of the outcomes) (Yaziji and Barry, 2006, Shi et al., 2007, Rickert and Maliniak, 1989, Giorno, 1984, Matos et al., 2010).

Irrespective of the limitations, difficulties and problems which may be encountered in IHC, the use of immunohistochemical methods in scientific research for the diagnosis of pathologic conditions still continues to rise as evidenced by the high number of scientific publications that use the IHC technique (Matos et al., 2010, Werner, 2005). A way in which this can be achieved is by standardizing the IHC methods protocol so as to minimize the occurrence of undesirable outcomes (Matos et al., 2010).

2.7.3.3 Principles of IHC

Tissues were initially harvested and processed (section 2.6.3) after each study. Thin sections were then cut and stained with labelled antibodies. Processing the tissue samples are necessary to preserve the tissue architecture and also fix the antigen in place so as to protect them from deteriorating or leaking out of the tissue during the staining procedure. In this thesis, sections used for IHC were cut from unfixed (fresh) frozen tissue samples. The sections were always immersed in acetone prior to staining. Acetone is an organic solvent that removes lipid molecules while dehydrating cells. It also precipitates protein molecules onto the cell surface in the process. There are other crosslinking

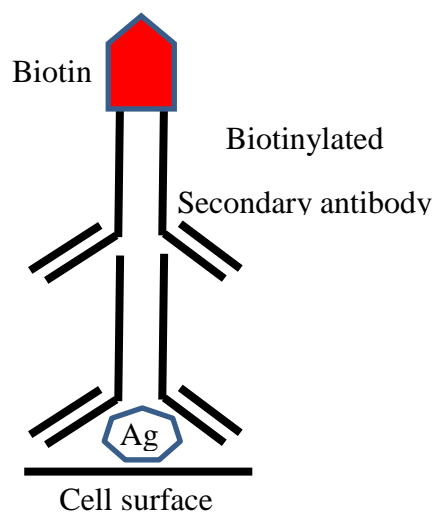
reagents used for fixation, examples are paraformaldehyde (PFA). Although PFA is better at preserving the structure of tissues and cells, it may reduce the antigenic properties of some of the cell components due to crosslinking, thereby preventing the binding of an antibody. In this case, antigen retrieval methods may be applied.

The fundamental principles of IHC staining are the incubation of tissue samples with primary antibodies directed to preferred antigens of interest. The binding of these antibodies to form an antigen-antibody complex and the detection of said antibodies. There are several methods of visualising bound antibody to an antigen; a) direct method, b) indirect method, c) unlabelled antibody enzyme method with peroxidase-anti-peroxidase complex (PAP), d) immunogold method, e) Avidin biotin complex (ABC) method and f) new direct technique (enhanced polymer one-step staining system) (Mepham, 1991). In this thesis we have used the indirect method with the ABC method.

The indirect method requires the application of an unconjugated primary antibody which is then followed by a labelled antibody directed against the first antibody (Figure 2.10). This technique is more sensitive than the direct method and relatively cost effective. In this thesis, we used the indirect method. Here the labelled secondary antibodies are biotinylated and raised against the immunoglobulin G (IgG) of the animal species of which the primary antibodies were raised. This enables the reaction between both primary and secondary antibodies. The specific antigen-antibody complex formed due to the above interactions can be visualised using the ABC method (Hsu and Raine, 1981). The ABC method greatly depends on the affinity of the glycoprotein avidin for the low molecular weight vitamin, biotin. Avidin is made up of four subunits in a tertiary structure possessing four biotin-binding hydrophobic pockets, thus amplifying the antigen-antibody signal (Mepham, 1991). Biotin (Vitamin H) easily binds to antibodies and enzyme markers and up to 150 biotin molecules can bind to one antibody molecule. Labelled variants of the avidin –biotin system include peroxidase and alkaline phosphatase which directly bind avidin or streptavidin (Guesdon et al., 1979). Alternatively, the enzymes maybe labelled with biotin and three-quarter of the avidin binding sites are then occupied by the biotinylated label to form the avidin-biotin complex (Hsu and

Raine, 1981). As a number of biotins attach a single antibody, it enables the labelled avidin molecules to bind to it. This results in increased sensitivity compared to the techniques previously mentioned. In order to be able to visualise ABC, it can be developed by incubating with diaminobenzidine (DAB) substrate to give a brown coloured stain. Furthermore, the DAB stain can be enhanced using the enzyme glucose oxidase and nickel to obtain a final deep purple to black colour (Shu et al., 1988).

A) Indirect method



B) Avidin-biotin complex method

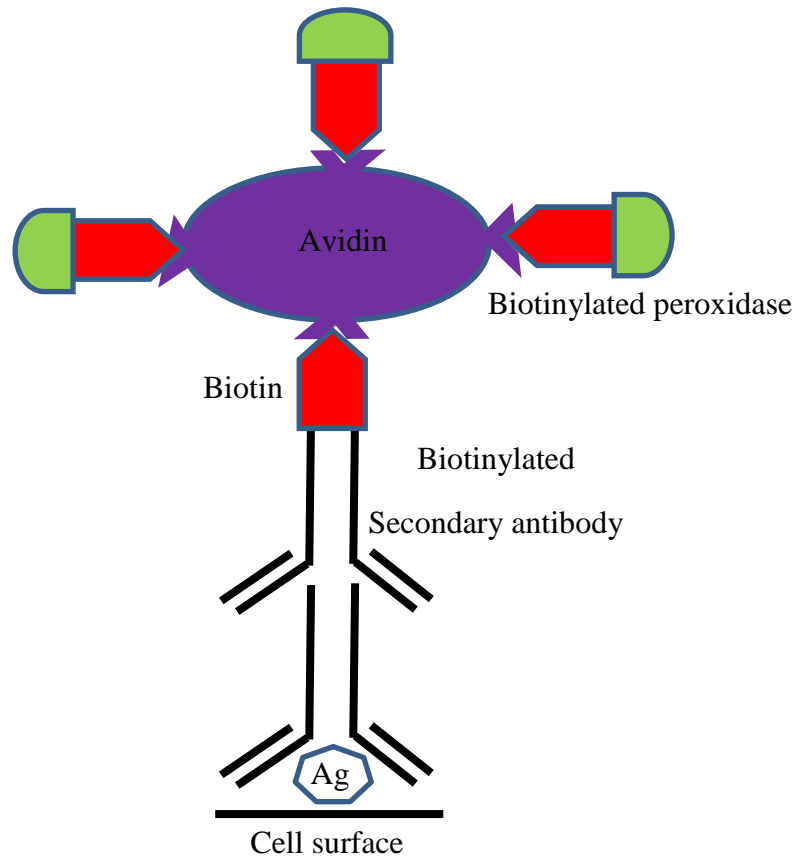


Figure 2.13 Indirect immunohistochemistry. Indirect method, biotin labelled secondary antibody binds the unconjugated primary antibody (A). Avidin-biotin complex method, the biotinylated secondary-primary antibody complex is detected with the preformed avidin-biotin complexes (B). Four biotin vitamins bind with high affinity to one avidin glycoprotein, thus intensifying the antigen-antibody signal. Peroxidase (P), antigen (Ag).

2.7.3.4 Staining procedures

Unfixed fresh frozen tissues were used. All tissue samples were sectioned to 5µm thickness in this thesis unless otherwise stated. Details of primary and secondary antibodies can be found in the appendix. Synovial sections were cut using a motorised cryostat, mounted on diagnostic microscopic slides and briefly air dried. Preparations were mounted in DePeX. Unfixed tissue sections were fixed firstly in acetone for 10 minutes at 4°C and washed twice for 5 minutes in 0.01M PBS, pH 7.4. The sections were then incubated for 30 minutes at room temperature in 0.33% hydrogen peroxide/methanol solution so

as to block the effect of endogenous peroxidase and thus reducing the chances of false positive reactions (Streefkerk, 1972). After the blocking step, they were rinsed twice in 0.01M PBS for 5 minutes.

Primary antibodies to macrophage clone ED1, ED2 or ED3, were initially diluted in 0.01M PBS with 5% bovine serum albumin (BSA) and 3.3% normal serum obtained from the species in which the secondary antibody was raised. These antibodies were applied onto sections and left for 1h in a humidified box, after which the sections were rinsed twice in 0.01M PBS for 5 minutes. The secondary antibody was then applied onto the sections and the sections placed in a humidified box for 45 minutes at room temperature. After which they were then rinsed twice in 0.01M PBS for 5 minutes. ABC was then applied in the required concentration to the sections and incubated for 30 minutes at room temperature. ABC was made 30 minutes and left to stand at room temperature before use. ABC peroxidase comes in a kit containing solution A and B. depending on the number of sections needed to be stained, ABC was made appropriately. 100µl of solution A was added to 5ml 0.01M PBS and mixed by vortexing, the same volume of solution B was then added to the mixture. Following ABC incubation, the sections were rinsed in 0.01M PBS twice for 5 minutes. They were then incubated in 0.1M sodium acetate buffer solution, pH 4.6 for 5 minutes before being developed with the glucose oxidase/nickel DAB solution. The development process was monitored directly using a light microscope and the reaction time was mostly at 7 minutes maximum, after which the sections were rinsed in 0.01M PBS, thus stopping the reaction and then dehydrated in graded alcohols and mounted in DePeX..

The glucose oxidase/nickel DAB solution comprised of 25mg DAB in 5ml of distilled water, 1.25g di-ammonium nickel II sulphate, 25ml of 0.2M sodium acetate buffer (pH 6.0), 20mg ammonium chloride, 100mg β-D-glucose and 0.5mg glucose oxidase. The glucose oxidase was always added last minute to the solution before been applied to the sections in an incubation box as the reaction of glucose oxidase to nickel DAB begins as soon as glucose oxidase is added.

2.8 IMAGE ANALYSIS AND QUANTIFICATION

All image analysis and quantification were carried out using a Zeiss Axioscop-50 microscope (Carl Zeiss Ltd, Welwyn Garden City, UK) with the experimenter blinded to experimental group and sections randomised by an independent researcher. Images were captured using a video camera (AxioCam MRm ZEISS) and analysed using Axiovision image analysis software.

2.8.1 Synovia

2.8.1.1 *Synovitis*

Using a 20x objective lens, synovitis was scored according to the thickness of the synovial lining layer and synovial cellularity as follows;

Grade 0 = Lining cell layer 1–2 cells thick. Grade 1 = Lining cell layer 3–5 cells thick. Grade 2 = Lining cell layer 6–8 cells thick and/or mild increase in cellularity. Grade 3 = Lining cell layer >9 cells thick and/or severe increase in cellularity (Mapp et al., 2008).

2.8.1.2 *Macrophage infiltration*

Using a 20x objective lens, data were obtained from four fields of view on one section per rat. The optimum number of fields per section and sections for each case had already been determined by Walsh and co (1998a). The fields were chosen dependent on the areas that displayed the highest densities of macrophages. Colour transmitted light image of a selected area was captured and directly changed to a monochrome image. An outline was then made on the surrounding positive area and measured. The image was thresholded according to hue to include all positive cells and measured. Macrophage area was defined as a percentage of positive synovial area for the subsets of macrophages (ED1, ED2, or ED3) (Seegers et al., 2003, Ashraf, 2011, Walsh et al., 1998a).

2.8.2 Cartilage and subchondral bone

2.8.2.1 Macroscopic chondropathy scoring

The severity of loss of articular cartilage integrity for the medial and lateral femoral condyles, tibial plateaus and femoral groove were determined for each knee joint by a single assessor blinded to both OA and treatment groups immediately following tissue harvesting (Guingamp et al., 1997). All five chondral (medial and lateral femoral condyles, tibial plateaus and femoral groove) surfaces were photographed using a video camera (model W30X-HD, 30x zoom full HD (1080p) - Vet Tech solutions limited). Severity of chondropathy was analysed directly using a dissecting microscope and later on from the photographs. A graded score of 0 to 4 were given as follows:

Grade 0 = Normal appearance. Grade 1 = Slight yellowish discolouration of the chondral surface. Grade 2 = small cartilage erosions in load bearing areas. Grade 3 = Large cartilage erosions extending down to subchondral bone. Grade 4 = Large cartilage erosions with large areas of subchondral bone exposure.

The grade from each articular surface was summed to give a total maximum possible score of 20 for a joint, with 0 indicating no evidence of chondropathy.

A detailed explanation of the above method can be found in Chapter 4 of this thesis.

2.8.2.2 Microscopic scoring

The modified Mankin scoring system is what is mostly used as microscopic scoring systems for rat OA (Gerwin et al., 2010). The Mankin scoring system was developed from a grading system using femoral heads removed at arthroplastic surgery in humans and might not be a suitable method of scoring in rats (Mankin et al., 1971). Although modified for use in rats, the scoring system restricted the evaluation of OA cartilage changes while a few included OA related changes in synovium and bone (Appleton et al., 2007, Yorimitsu et al., 2008). Even though we conclude that the Mankin score may not be ideal for use in rats, there are still structural features in the cartilage that require the use of the Mankin score. In this thesis the monosodium iodoacetate (MIA) rat

model which is a model that affects chondrocytes in the cartilage was used hence chondrocyte morphology was assessed. The level of GAGs (proteoglycan content) in the cartilage was also of interest. The Mankin scoring system delineates the grades and criteria needed to measure these features.

Simplicity, utility, scalability, extendability and comparability are the five principles for an ideal cartilage histopathology scoring system. The method should be simple, reproducible and easily applied by different investigators. It should be a useful assessment of both clinical and experimental OA. It should be a method that would correlate easily with cartilage macroscopic appearance. It should be a method capable of being applied successfully by qualitative assessment and finally, it should be capable of being harmonized with histological assessment systems of other cartilage disorders to include those associated with cartilage repair (Pritzker et al., 2006).

The entire lateral and medial tibial plateau (in the case of the MIA model) or the medial tibial plateau only (MNX model) of frontal sections stained with H&E were used to assess chondropathy through a $\times 10$ objective lens under transmitted light, While Safranin-O fast green or alcian blue was used to assess proteoglycan content. Chondropathy was evaluated using the system of Janusz et al., as previously described (Janusz et al., 2002) or the modified OARSI osteoarthritis cartilage histopathology assessment system (Pritzker et al., 2006). Both scoring methods were tested and validated (detailed explanation in Chapter 5).

Janusz method; cartilage pathology was scored on a scale of 0 to 5 as follows:

Grade 0 = Cartilage of normal appearance. Grade 1 = Minimal fibrillation in superficial zone only. Grade 2 = Mild, extends into the upper middle zone. Grade 3 = Moderate, well into the middle zone. Grade 4 = Marked, into the deep zone but not to the tidemark. Grade 5 = Severe, full thickness degeneration to the tidemark

The extent of medial tibial plateau involved in the damage was also taken into account; 1/3, 2/3 or 3/3. The cartilage damage score was then multiplied by 1, 2 or 3 respectively to give an overall chondropathy score.

OARSI method; cartilage pathology was scored based on a scale of 0–6 as follows:

Grade 0 = normal. Grade 1 = surface intact. Grade 2 = surface discontinuity. Grade 3 = vertical fissures (cleft). Grade 4 = erosion. Grade 5 = denudation. Grade 6 = deformation

A stage score (scale of 0–4) indicating the surface extent of joint involvement (0 = no activity, 1 = <10%, 2 = 10–25%, 3 = >25–50%, and 4 = >50%) was multiplied by the grade to give an overall chondropathy score.

Integrity of the osteochondral junction was measured as the number of channels crossing the osteochondral junction into the articular cartilage per millimetre length of the tibial plateau of an H&E stained section using a ×20 objective lens. Channels were accepted as being in the cartilage if they had either entered into the cartilage or were not separated from cartilage by bone. To measure the length of the tibial plateau, a digital electronic calliper (Miyutoyo UK Ltd., Andover, UK) was used.

Morphology of chondrocytes and proteoglycan content were scored using the Mankin scoring system (Mankin et al., 1971).

Chondrocyte morphology:

Grade 0 = Normal. Grade 1 = Hypercellularity. Grade 2 = Cloning (occurrence of 2 or more cells with 4 or more nuclei). Grade 3 = Hypocellularity

Proteoglycan content:

Grade 0 = Normal. Grade 1 = Mild loss. Grade 2 = Moderate loss. Grade 3 = Severe loss. Grade 4 = Complete loss

2.8.2.3 TRAP (osteoclast) counting

Tartrate resistant acid phosphatase (TRAP) positive osteoclast cell counting was developed in-house (Luting Xu). The effective area to count was from one end of the growth plate to the other end, underneath the cartilage and/or around the bone marrow cavities. In the event of cartilage break down under pathological conditions, cells in between the bone marrow circles were

counted. A positive osteoclast cell was always found in a dark purplish or reddish area and was counted if it had least 3 or more nuclei. The cells and area to count was initially visualised under a 4x objective lens but counted at x20 magnification. In cases where 2 nuclei aggregates shared a positive stained area border and the cell membrane was discernible between them, this was counted as 2 osteoclasts. Also, in cases when the stained area was too dark to identify the number of nuclei, the size of the area was compared to the negative cells adjacent to it. If it was larger than twice of the adjacent cells, it was counted one positive osteoclast. Light stained area with no identifiable nuclei was never counted.

2.9 STATISTICAL ANALYSIS

Synovial inflammation, lining thickness and cellularity were scored as previously described, one synovial section per rat and overall grade that best represented the section given (Ashraf et al., 2011a). Infiltration by macrophages was quantified on 4 fields of view per synovial section per rat (Walsh et al., 1998a). Data for each experiment were presented graphically as mean \pm SEM and analysed using Prism V.6 (GraphPad, San Diego, California, USA). The different groups were compared using non-parametric tests either Mann-Whitney U test when only comparing two groups or Kruskal Wallis tests with post hoc Dunn's test (when comparing more than two groups). Weight bearing asymmetry and PWT data were firstly analysed using area under the curve (AUC). Numerical data were presented as mean (95% confidence interval - CI) or median (Interquartile Range - IQR). Associations between variables were analysed using Statistical package for the Social Sciences v.21 (SPSS Inc., Chicago, Illinois, USA). Data were presented as Spearman's correlation coefficients. A two-tailed P value of less than 0.05 was taken as significant in all cases.

Sample Size

A power calculation was performed to determine the minimal number of rats required to test for a significant difference in the data. A power of 80% was decided to show a difference of 10% at P value of 0.05. Pilot data was used to

determine mean and standard deviation. The formula used was; $(u + v)^2 (\sigma_1^2 + \sigma_2^2) / (\mu_1^2 + \mu_2^2)$, where u is the one sided percentage point of the normal distribution corresponding to 100% minus the power. In this case 100-80 = 20%, so u = 0.84. V is the percentage of the normal distribution corresponding to the two sided significant level. In this case the significant level used was 5% i.e. p = 0.05, so v = 1.96. σ is standard deviation and μ is the mean. Sample size was increased from n = 6 to n = 10 following power calculations.

2.10 REAGENTS

Monoclonal antibodies to macrophages (clone ED1, ED2 and ED3) were from Serotec (Oxford, UK). Biotinylated rat-adsorbed horse anti-mouse antibody (BA 2001) and avidin-biotin complexes (Vectastain Elite ABC Kits) were from Vector laboratories (Peterborough, UK). DePeX mounting medium, Schiff reagent and PBS were from VWR Ltd (Lutterworth, UK). OCT®, Mayers and Harris haematoxylin and eosin were from Raymond Lamb (Eastbourne, UK). Carrageenan, BSA, Tris, EDTA, tartrate resistant acid phosphatase (TRAP) kit, neutral buffered formalin, formic acid, PFA, alcian blue, periodic acid and other chemicals were obtained from Sigma-Aldrich (Poole, UK). AR456786-06 and Gelucire (vehicle) compounds were kindly provided by Array Biopharma (Colorado, USA) for use in collaboration.

CHAPTER 3; THE CARRAGEENAN MODEL OF INFLAMMATORY ARTHRITIS

3.1 INTRODUCTION

Osteoarthritis (OA) is primarily thought to be a degenerative disease; however, more often observed through imaging and histology (Ayril et al., 2005, Scanzello and Goldring, 2012), inflammation is increasingly recognized as being a major contributor to the pathology of OA hence making it clinically important in OA. Synovitis is a feature of OA and is characterised by marked hyperplasia of the lining cells of the synovium, infiltration by inflammatory cells such as macrophages, a subset of B and T cells, mast cells and natural killer cells (Sokolove and Lepus, 2013). Synovitis can be both episodic (flares characterized by local warmth, tenderness and effusion) and persistent (Bonnet and Walsh, 2005, Mapp and Walsh, 2012). Inflammation under physiological conditions is needed to maintain homeostasis. It does this by controlling tissue damage which can occur as a result of traumatic, pathogenic and toxic insults or injury (Benelli et al., 2006). The initial response to cellular injury is known as acute inflammation. Acute inflammation occurs rapidly within minutes of trauma occurring and is characterised by coagulation, increased blood flow and vascular permeability at the affected site, which resolves with time. Chronic inflammation is prolonged inflammation characterised by release of inflammatory cells, blood vessel growth (angiogenesis), neovascularization etc. Development of chronic inflammation in OA is understood as a recurring vicious cycle of tissue damage, inflammation and repair (Dallegrì and Ottonello, 1997, Scanzello et al., 2008).

Carrageenan (Sigma Aldrich) is often used in research to induce tissue inflammation. Carrageenan is one of a family of linear sulphated polysaccharides obtained from red seaweed. There are three main commercial classes of carrageenan; kappa, iota and lambda (λ). Intra-articular injection of λ carrageenan in rat knees induces synovitis in the rat knee and pain behaviour when injected into the foot (Lam and Ferrell, 1991, Lam and Ferrell, 1989,

Walsh et al., 1998a). Histological evidence of synovitis is represented by increased synovial lining thickness, macrophage infiltration and angiogenesis (Mapp and Walsh, 2012).

Macrophage precursors originate in the bone marrow as monocytes, when monocytes are released into the peripheral blood, they circulate for a few days before becoming localized to different tissues, where they undergo differentiation into macrophages (Dijkstra et al., 1985, Gordon and Taylor, 2005). Different subpopulations (immature resident or mature resident) of macrophages can be distinguished by different monoclonal antibodies (Kool et al., 1992, Richards et al., 1999). The monoclonal antibody ED1 identifies immature resident or exudate macrophages while ED2 and ED3 monoclonal antibodies identify mature resident macrophages. ED1 is the rat homologue of human CD68 a single chain glycoprotein of 90-110 kDa. CD68 immunoreactivity is mostly found on the lysosomal membrane of myeloid cells. The majority of tissue macrophages express CD68. ED2 recognises CD163, a 175 kDa cell surface glycoprotein expressed by about 50% of peritoneal macrophages, which are group of macrophages found in the spleen and by macrophages in most other tissues. However, monocytes, alveolar macrophages or microglia do not express CD163. ED3 recognises CD169, a 185 kDa molecule expressed by macrophages which are closely associated with T cells predominantly confined to lymphoid organs only (Dijkstra et al., 1985, Richards et al., 1999)). Depending on the local microenvironment, macrophages differentiate into M1, which are the classically activated (pro-inflammatory) form or M2 which are the alternatively activated (immunomodulatory and tissue remodelling) form. The M2 form can further be subdivided into M2a (alternative), M2b (type II) and M2c (deactivated). The antibody clone ED1 (CD68) is a pan macrophage marker that stains all phagocytic macrophages, ED2 (CD163) is an M2c macrophage marker and ED3 (CD169) is known to be expressed by activated macrophages in chronic inflammatory diseases such as rheumatoid arthritis, multiple sclerosis, HIV etc. (Ito et al., 2014, Hartnell et al., 2001, van der Kuyl et al., 2007). Evidence suggests that the ED3 (CD169) marker is not restricted to all M1 macrophages but is rather a marker of interferon (IFN)-induced inflammatory M1

macrophages (Ohnishi et al., 2013). High expressions of CD169 in IFN-stimulated M1-type human macrophages were observed from peripheral blood mononuclear cells.

All three macrophages markers have been reported to be expressed in complete Freund's adjuvant (CFA) – induced rat knees (Dijkstra et al., 1987) and the ED1 antigen expressed in carrageenan induced rat synovium but the ED2 and ED3 macrophage markers have not been reported to be expressed in the rat synovium in the carrageenan model.

Synovitis is reported to play an important role in driving OA pathology (Bondeson et al., 2010). There is evidence from imaging studies that suggest the role of synovitis in structural degradation of the OA joint (Ayril et al., 2005, Roemer et al., 2009, Atukorala et al., 2014). Synovitis contributes to OA pathology and has also been reported to contribute to OA pain. Imaging studies have reported possible associations between synovitis and pain (Torres et al., 2006, Hill et al., 2007, Baker et al., 2010). Synovitis might contribute to pain by the release of pain related mediators e.g. serotonin, substance P (SP), prostaglandin E₂ (PGE₂), bradykinin, leukotriene B₄ (LTB₄), nerve growth factor (NGF) etc. which act on pain receptors on sensory nerves, sensitizing or activating them. Studies have shown that the carrageenan model including the kaolin/carrageenan-induced model have a neurogenic component as reduced responses to carrageenan-induced inflammation was observed after surgical denervation or capsaicin pre-treatment (Lam and Ferrell, 1991, Neugebauer and Schaible, 1990). Neurogenic and acute inflammation caused by these models leads to sensitization of spinal neurons with input from the inflamed joint as the neurons in the joint showed altered responses to stimulation (Lam and Ferrell, 1989, Neugebauer and Schaible, 1990). Altered responsiveness to stimulation were also observed in non-inflamed regions of the leg in these models, showing expansion of the receptive field of these neurons (Neugebauer and Schaible, 1990). This allows for pain measurements of secondary allodynia and makes the carrageenan model of monoarthritis a suitable model of inflammation.

The carrageenan model was reported to cause a reduction in weight bearing by the affected limb (Valenti et al., 2010a) and reduced paw withdrawal threshold (Lee et al., 2013b) when injected to the joint. The macrophage markers ED1, ED2 and ED3 have been used extensively but none of these studies have investigated their associations to synovitis and pain behaviour in this model or elsewhere.

The hypothesis was that intra-articular injection of carrageenan into the knee would induce acute inflammation (seen as joint swelling, synovitis with ED1, ED2 and ED3 macrophage expression) and increased pain behaviour (weight bearing asymmetry and reduced hind paw withdrawal threshold) and that associations between synovitis and pain may be as a result of macrophages.

3.2 AIMS

- To characterise the effect of intra-articular injection of carrageenan on pain behaviour and inflammation.
- To investigate ED1, ED2 and ED3 macrophage expression in the synovium of carrageenan injected rats. ED2 and ED3 markers have not been explored previously in the synovium of carrageenan rats.
- To explore possible associations between pain behaviour, synovitis and ED macrophage markers, which have not been previously explored.

3.3 METHODS

Refer to Chapter 2 for general methodology. Experiments were carried out on male Sprague Dawley rats (Charles River, UK) $n = 25$, weighing 220-370g at time of carrageenan injection. This chapter consists of two studies.

Induction of inflammatory arthritis

25 male rats were anaesthetised with isoflurane mixture (2% in O₂) and then given intra-articular injections of either 50µl of 2% carrageenan (Lam and Ferrell, 1989, Walsh et al., 1998a) in sterile 0.9% saline or 0.9% saline into their left knee joints ($n=22$) or 0.9% normal saline into their right knee joints ($n=6$). Naïve rats ($n=3$) were also anaesthetised but not injected. Study 1 investigated the effect of intra-articular carrageenan for 24h while study 2 went up to 3 days post injection (Fig. 3.1).

Pain measurements

Pain behaviour was measured as hind limb weight-bearing asymmetry and distal allodynia to punctuate stimulation of the hind paw using von Frey filaments (Semmes-Weinstein monofilaments 1 - 15g). Measurements were taken pre-injection and also at 2h, 6h, 24h, 1, 2 and 3days post injection.

Tissue collection

At end of each study, rats were killed by a rising concentration of CO₂. Synovia with patella from the rat joints were then harvested and immediately snap frozen in isopentane on day 3 for histology and immunohistochemistry. Frozen synovial tissues were stored at -80°C until when needed. The controls used were the saline injected right knees and naïve un-injected knees.

Time course of experiment

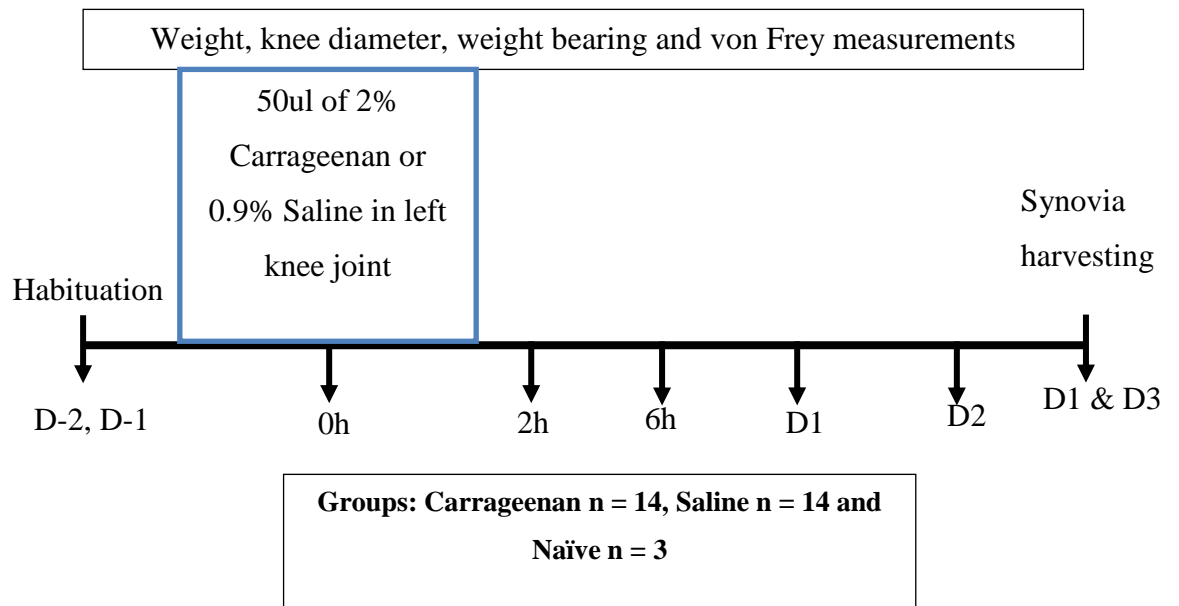


Figure 3.1 Time course of carrageenan induced inflammation and pain behaviour

Rats were habituated to pain assessment (incapacitance meter and von Frey box) for 2 days prior to baseline measurements. 2% carrageenan or saline was injected intra-articular at time point 0. Knee diameter and pain behaviour measurements were taken prior to injection, then at 2h, 6h, day 1, day 2 and day 3 post injection. Weights of rats were measured at similar time points except at 2h and 6h. Synovia harvesting was carried out day 1 and day 3 post injection

Inflammation

Inflammation was assessed as joint swelling, synovial histological score and macrophage infiltration.

Knee diameter (joint swelling) of the right and left knee joints were measured at 2h, 6h, days 1, 2 and 3 post intra-articular injection.

Synovial sections (5µm), 1 section/rat were stained with haematoxylin and eosin (H&E) to assess its lining thickness and cellularity (Mapp et al., 2008). Synovitis scoring was performed using a 20× objective lens of a Zeiss Axioscop-50 microscope (Carl Zeiss Ltd, Welwyn Garden City, UK).

Macrophage infiltrations were assessed in synovial sections stained by immunohistochemistry. Frozen synovia sections (5µm thick) were placed in a trough containing cold acetone for 10 minutes to fix the sections. They were then washed in PBS twice for 5 minutes and then endogenous peroxidase blocked by placing in hydrogen peroxide/methanol (1:4) solution for 30 minutes. Mouse monoclonal primary antibodies for ED1 (1:1000), ED2 (1:1600) and ED3 (1:400) were applied to each individual section for 1h. Biotinylated horse anti-mouse (1:100) was added for 45 minutes. Sections were then placed in ABC peroxidase solution for 30 minutes and then 0.1M sodium acetate solution for 5 minutes. Nickel DAB solution was made and applied following the sodium acetate and incubated until desired endpoint (Shu et al., 1988). PBS washes were done at room temperature twice for 5 minutes in between steps except for the sodium acetate and Nickel DAB step. After PBS wash, staining was then differentiated with running tap water and the sections dehydrated through graded ethanol (70% and 100%) into xylene and mounted in DePeX and covered with cover-slips. ED2 and ED3 macrophages had never been stained in the carrageenan synovium. Normal rat spleen was reported to express ED2 and ED3 macrophages (Denham et al., 1990), therefore the rat spleen was used as a positive control in this experiment (Fig. 3.8). Negative controls were the primary antibody was missed out were also included.

Statistical analysis

Synovial inflammation, lining thickness and cellularity were scored as previously described, one synovial section per rat and overall grade that best represented the section given (Ashraf et al., 2011a). Infiltration by macrophages was quantified on 4 fields of view per synovial section per rat (Walsh et al., 1998a, Walsh et al., 1998b).

Data for each experiment were presented graphically as mean \pm SEM or median and analysed using Prism V.6 (GraphPad, San Diego, California, USA). The different groups were compared using the non-parametric Kruskal-Wallis test followed by post hoc Dunn's test for each parameter. A two-tailed p value of less than 0.05 was taken as significant in all cases. Numerical data were presented as mean (95% CI) or median (IQR).

Data for correlations between variables were obtained using scores observed at and after day of sacrifice for all groups of rats and analysed using Statistical package for the Social Sciences v.21 (SPSS Inc., Chicago, Illinois, USA). Data were presented as Spearman's correlation coefficients.

3.4 RESULTS

Two studies were carried out in this chapter. Study 1 investigated the effect of intra-articular carrageenan for 24h while study 2 went up to 3 days post injection

3.4.1 Effect of intra-articular injection of carrageenan

3.4.1.1 Body weight

Rats given 50µl carrageenan or saline into their left knee joint had equal weights (Fig. 3.2A). Those given carrageenan or saline into their left and right knee joints respectively had higher weights than the naïve rats. The weights of these rats on day 0 when the treatments were given were already higher than the naïve rats, and continued to increase with no loss in weight (Fig. 3.2B).

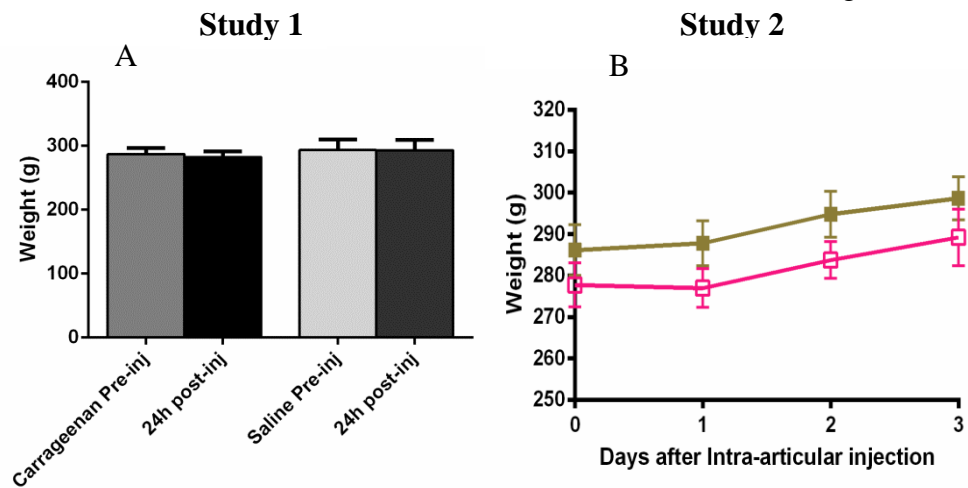


Figure 3.2 Weight gain of rats

Bar graph shows mean \pm SEM of weights from carrageenan or saline injected rats (n = 8). Line graph shows mean \pm SEM of weights from carrageenan (left knee - ■) and saline (right knee) injected rats (n = 6) and naïve rats (n = 3 - □)

3.4.1.2 Pain behaviour

Weight bearing asymmetry (%) increased from 6h after carrageenan injection and this was significant at 24h [7 (4.5 – 9.4)] compared to saline injected rats [1.2 (0.2 to 2.1) $p < 0.01$] (Fig. 3.3A).

Weight bearing asymmetry (%) significantly increased at 6h following intra-articular injection of 2% carrageenan [17 (6 to 28)] compared to naïve controls [-1 (-7 to 5) $p < 0.05$]. The significant increase in weight bearing asymmetry was maintained at a plateau till day 3 [19 (3 to 35)] v [2 (-0.2 to 5) $p < 0.05$] (Fig. 3.3B).

Hind paw withdrawal threshold (g) was significantly reduced at day 3 post carrageenan injection [3 (1 to 5)] compared to saline-injected [9 (5 to 12) $p < 0.05$] and naïve controls [8 (3 to 13) $p < 0.05$] (Fig. 3.4B).

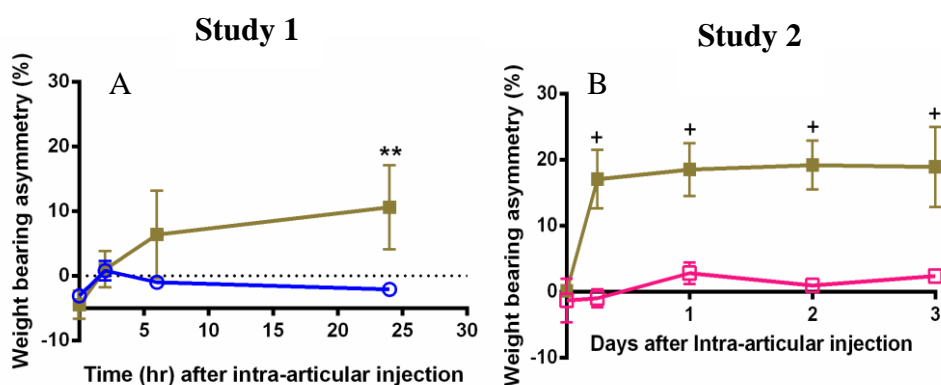


Figure 3.3 Effect of intra-articular injection of 2% carrageenan on weight bearing asymmetry

Pain behaviour was measured in two separate experiments as a % difference in weight bearing between left and right hind limb from 0 to 24h (A) or 0 to 3 days (B) after carrageenan injection. Intra-articular carrageenan (■) injection induced weight bearing asymmetry compared to saline injected (A - ○) or naïve rats (B - □). Data are expressed as mean \pm SEM, carrageenan (n = 8) and saline (n = 8) (A) or carrageenan (left knee) and saline (right knee) injected rats (n = 6) and naïve rats (n = 3) (B). Differences between groups were analysed using a Mann Whitney-U test. ** $p < 0.01$ compared to saline and + $p < 0.05$ compared to naïve controls.

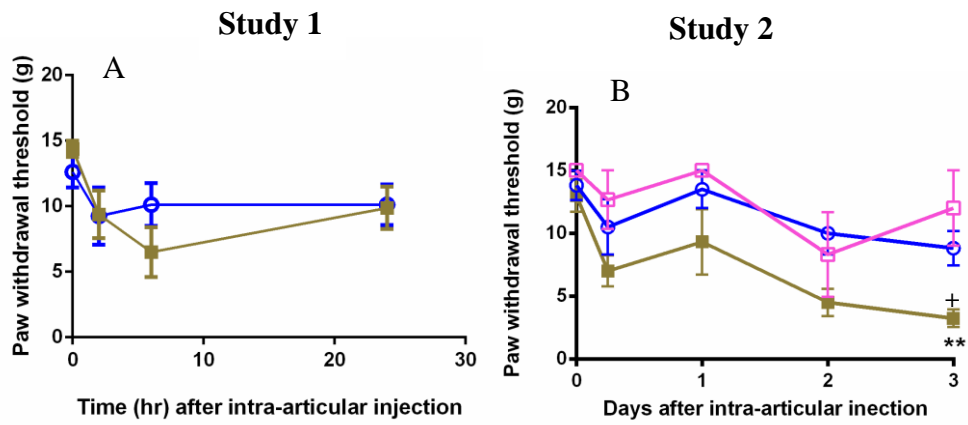


Figure 3.4 Effect of intra-articular injection of 2% carrageenan on paw withdrawal threshold

Pain behaviour was measured in two separate experiments as a rapid lifting of the paw when von Frey filaments were applied from 0 to 24h (A) or 0 to 3 days after injection (B). Intra-articular carrageenan (■) injection induced paw withdrawal threshold compared to saline injected (B - ○) or naïve rats (B - □). Data are expressed as mean \pm SEM, carrageenan (n = 8) and saline (n = 8) (A) or carrageenan (left knee) and saline (right knee) injected rats (n = 6) and naïve rats (n = 3) (B). Differences between groups were analysed using a Kruskal Wallis test with Dunn's multiple comparison. **p < 0.01 comparing all groups, * or +p < 0.05 compared to saline and naïve controls.

3.4.1.3 Acute inflammation

Knee joint diameter (joint swelling) increased following intra-articular injection of 2% carrageenan and was significantly different to saline injected rats within 3 to 24h of administration (Fig. 3.5A). Joint swelling was also increased in another group of carrageenan injected rats [0.4 (0.3 to 0.6) mm] and was significantly different at day 2 compared to naïve controls [-0.003 (-0.07 to 0.06) mm, $p < 0.05$] (Fig. 3.5B).

Normal rat synovium lining region is 1-2 cells thick but 3 days after intra-articular injection of 2% carrageenan, there was increased synovial lining thickness with intense cellular infiltration. Carrageenan induced a significant increase in synovial inflammation compared to naïve controls [3 (2 to 3)] v [0 (0 to 1) $p < 0.05$] (Fig. 3.6).

Synovial macrophage fractional area (%) was higher for rats that received intra-articular carrageenan compared to normal saline and naïve controls. ED1; carrageenan [31 (15 to 47)] v saline [10 (6 to 15) $p < 0.05$] v naïve [12 (5 to 19) $p < 0.05$], ED2; carrageenan [33 (29 to 37)] v naïve [26 (22 to 30) $p < 0.05$] and ED3; carrageenan [44 (36 to 51)] v saline [21 (14 to 28) $p < 0.05$] v naïve [14 (9 to 19) $p < 0.01$] (Fig. 3.7, Fig. 3.9, Fig. 3.10).

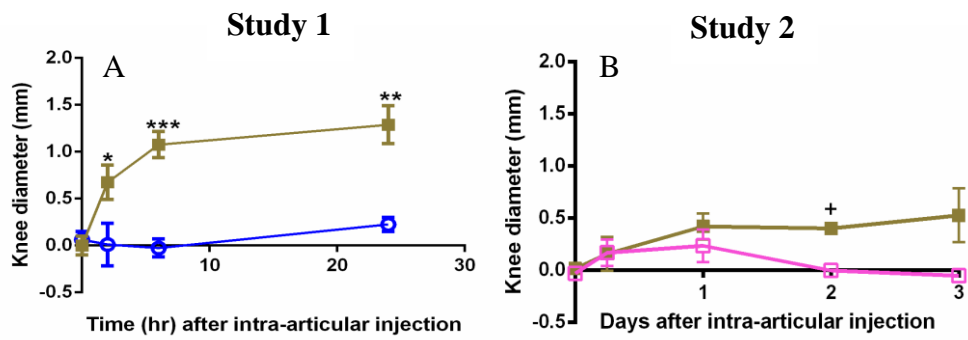


Figure 3.5 Effect of intra-articular injection of 2% carrageenan on joint swelling (Knee diameter).

Joint swelling representing acute inflammation was measured as an increase in knee diameter using an electronic knee calliper from 0 to 24h (A) and 0 to 3 days (B) after injection. Increased joint swelling for carrageenan (■) injected rats compared to saline injected (A - ○) or naïve rats (B - □). Data are expressed as mean \pm SEM, carrageenan (n=8) and saline (n = 8) (A) or carrageenan (left knee) and saline (right knee) injected rats (n = 6) and naïve rats (n = 3) (B). Differences between groups were analysed using a Mann Whitney-U test. * or +p < 0.05, **p<0.01, ***p<0.001 compared to saline or naïve controls.

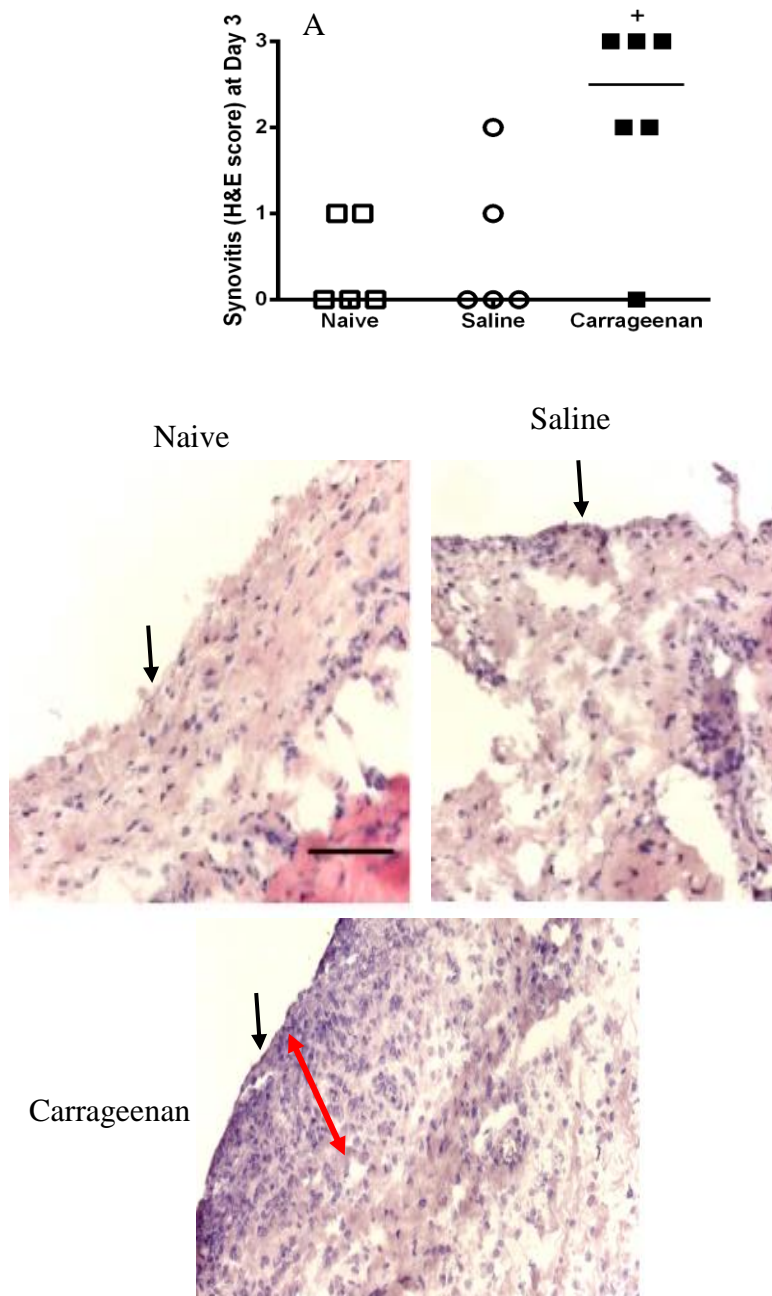


Figure 3.6 Histologic changes after intra-articular injection of 2% carrageenan

Synovium from carrageenan-injected rats showing an increase in synovial lining thickening (red arrow), with an intense increase in cellular infiltration. Synovia from saline-injected and naïve rats showing normal histologic appearances with a thin lining region, 1-2 cells deep (black arrows) and sparse number of cells. Scale bar = 100µm. Data are expressed as median, carrageenan (n = 6), saline (n = 5) and naïve synovia (n = 5). Differences between groups were analysed using a Kruskal Wallis test with Dunn's multiple comparison. +p < 0.05 compared to naïve controls.

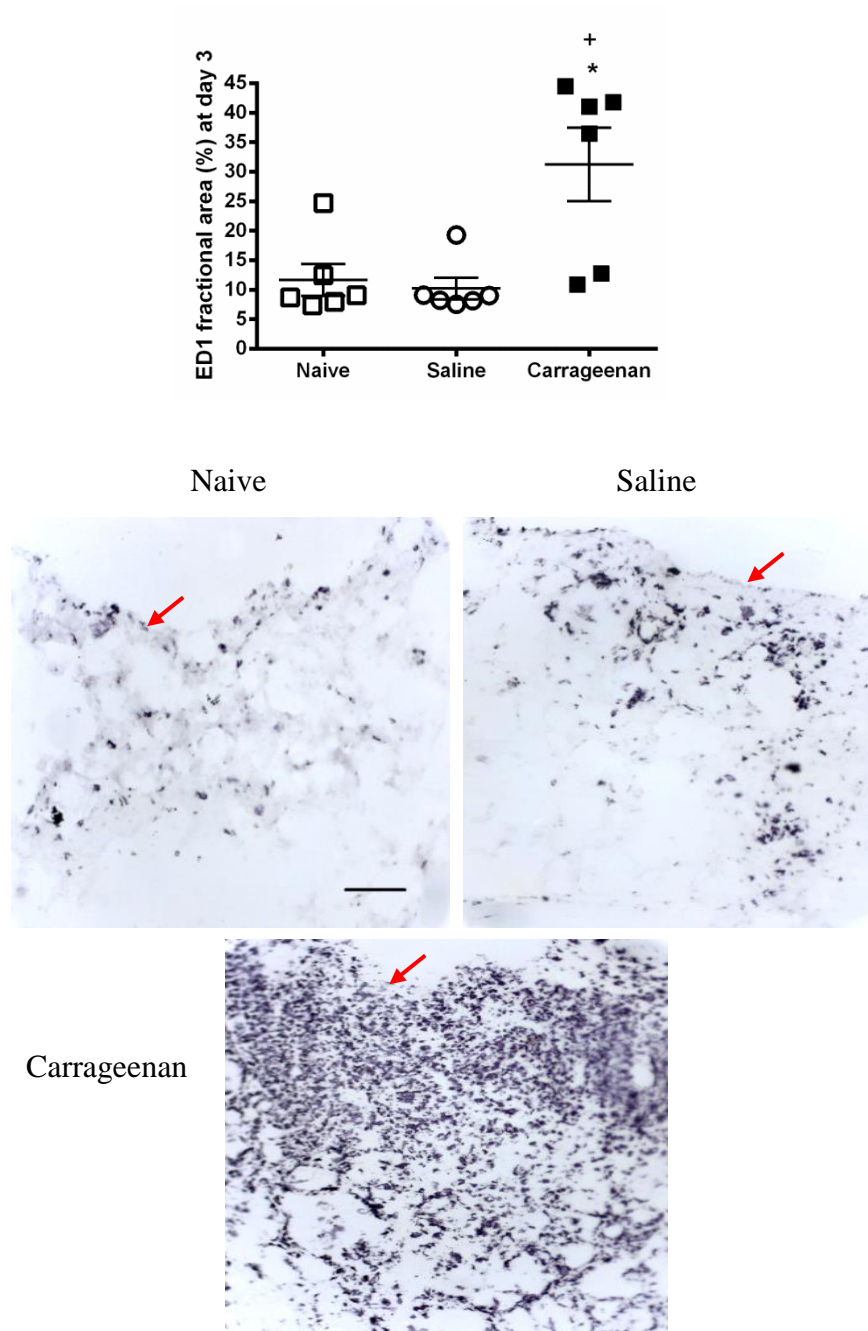


Figure 3.7 Macrophage infiltrations after intra-articular injection of 2% carrageenan

Synovium from carrageenan-injected rats showing dense infiltration by ED1-immunoreactive macrophages (black dots). Synovia from saline-injected and naïve rats showing sparse infiltration by ED1-immunoreactive macrophages (black dots). Red arrows indicate synovial lining. Scale bar = 100µm. Data are expressed as mean ± SEM, carrageenan (n = 6), saline (n = 6) and naïve synovia (n = 6). Differences between groups were analysed using a Kruskal Wallis test with Dunn's multiple comparison. * or +p < 0.05 compared to saline and naïve controls.

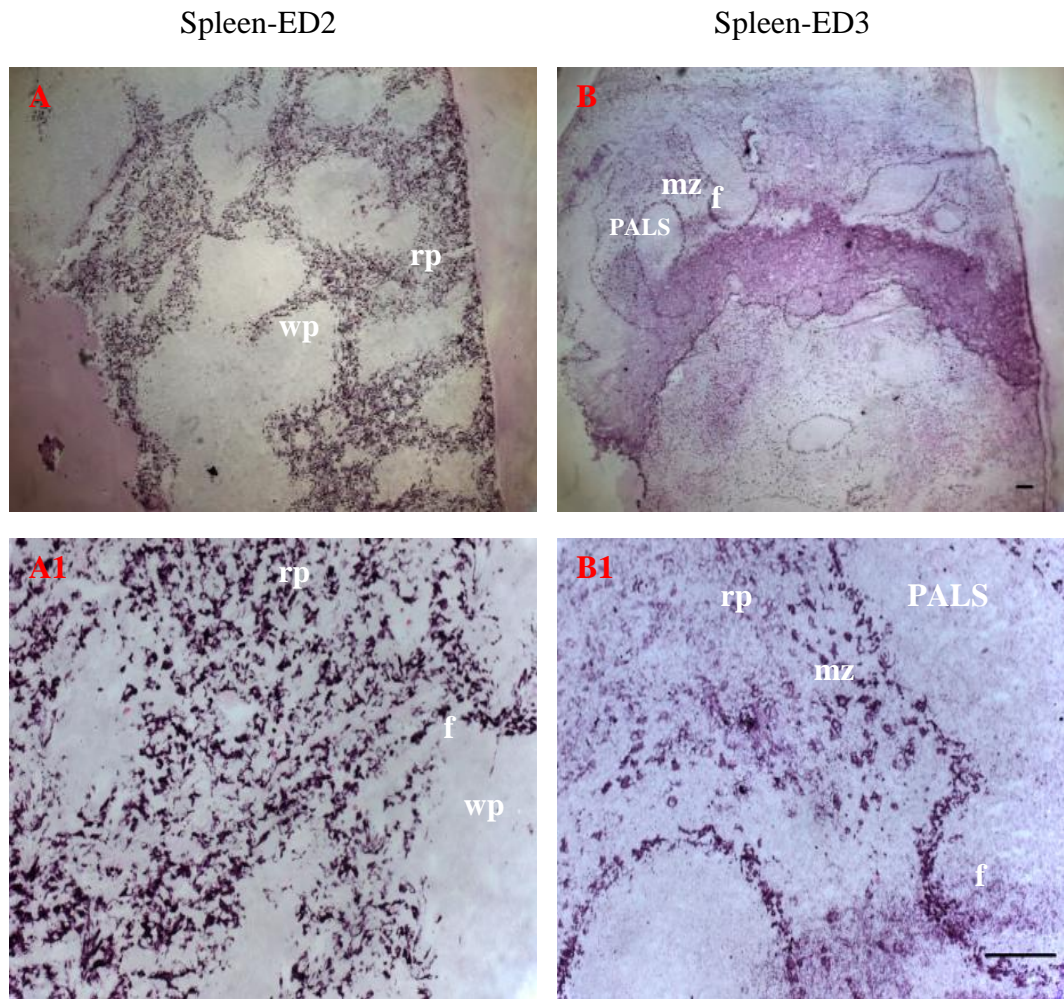


Figure 3.8 ED2 and ED3-immunoreactive macrophages in normal rat spleen

Positive staining for ED2 in red pulp (rp) of spleen and negative stain in the white pulp (wp). Positive staining for ED3 on the rim of the periarteriolar lymphoid sheet (PALS), follicle (f) and marginal zone (mz) as well as some staining of the red pulp of the spleen. Scale bar = 100µm.

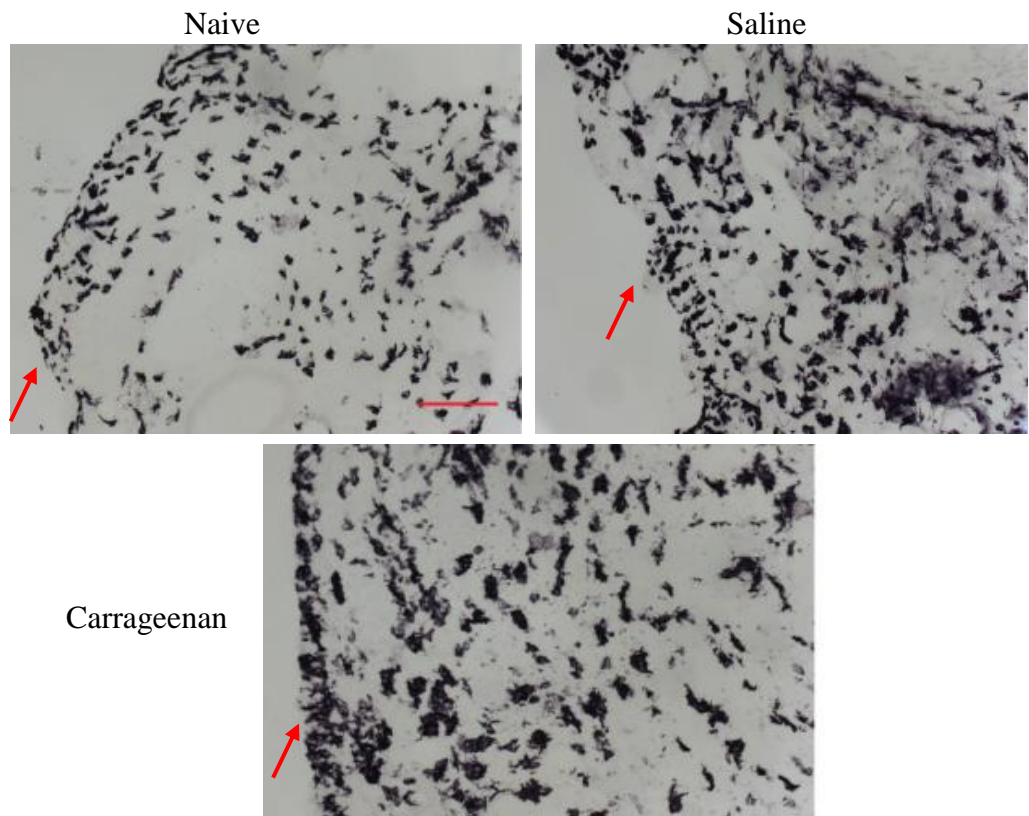
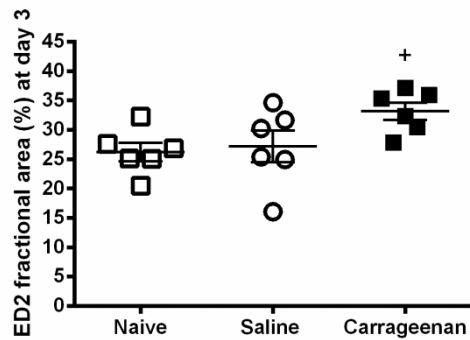


Figure 3.9 Macrophage infiltrations after intra-articular injection of 2% carrageenan

Synovium from carrageenan-injected rats showing dense infiltration by ED2-immunoreactive macrophages (black dots). Synovia from saline-injected rats show similar infiltration to the carrageenan-injected rats by ED2-immunoreactive macrophages (black dots). Naïve synovia showing less intense ED2 infiltration. Red arrows indicate synovial lining. Scale bar = 100µm. Macrophage quantification from previous published method. Data are expressed as mean ± SEM, carrageenan (n = 6), saline (n = 6) and naïve synovia (n = 6). Differences between groups were analysed using a Kruskal Wallis test with Dunn's multiple comparison. +p < 0.05 compared to naïve controls.

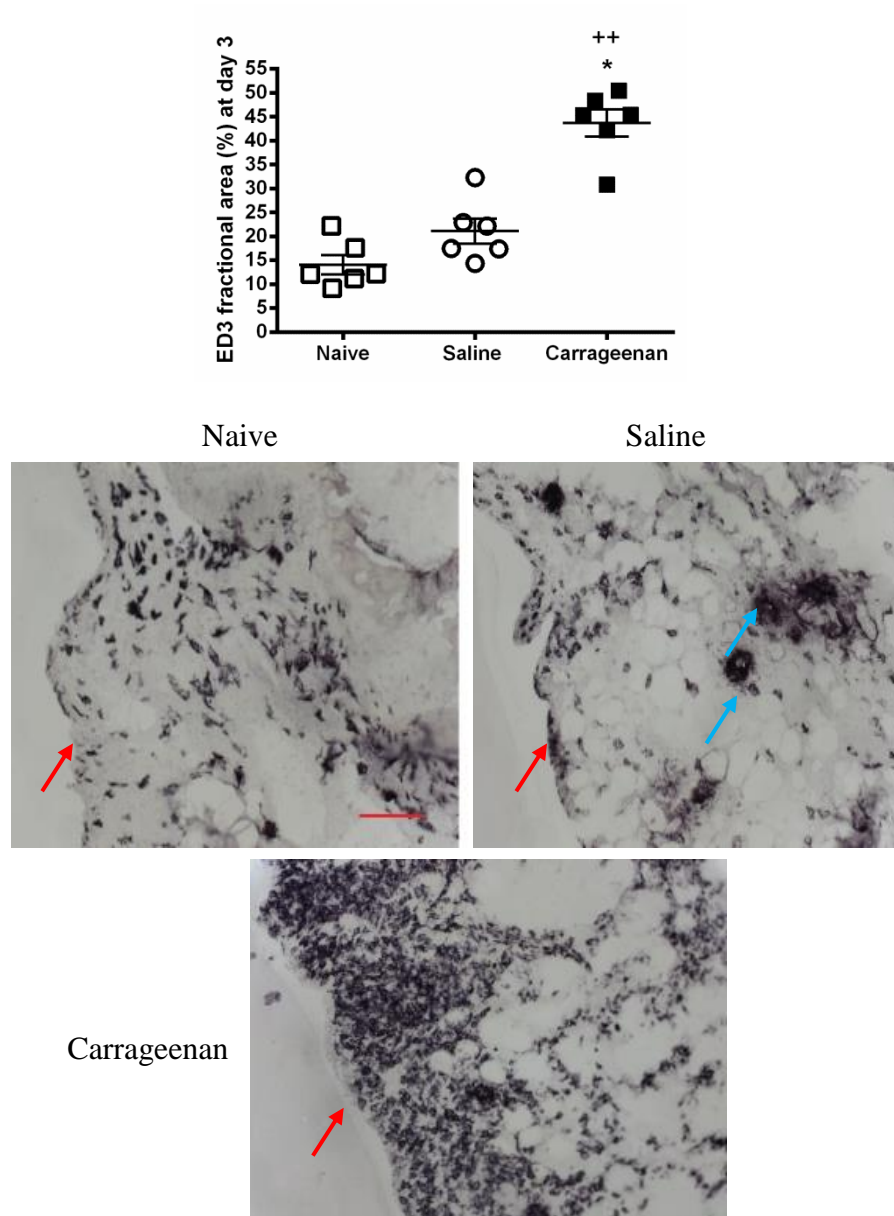


Figure 3.10 Macrophage infiltrations after intra-articular injection of 2% carrageenan

Synovium from carrageenan-injected rats showing dense infiltration by ED3-immunoreactive macrophages (black dots). Synovia from saline-injected and naïve rats showing sparse infiltration by ED3-immunoreactive macrophages (black dots). Red arrows indicate synovial lining; blue arrows indicate artefact and not macrophages. Scale bar = 100µm. Data are expressed as mean \pm SEM, carrageenan (n = 6), saline (n = 6) and naïve synovia (n = 6). Differences between groups were analysed using a Kruskal Wallis test with Dunn's multiple comparison and Wilcoxon signed rank (paired t-) test respectively. ++p < 0.01 compared to naïve controls, * p<0.05 compared to saline controls.

3.4.2 Macrophage markers are associated with inflammatory pain

Associations were observed between synovitis and weight bearing asymmetry. Macrophages expressing ED3 were associated with weight bearing asymmetry, paw withdrawal threshold and synovitis while macrophages expressing ED1 were associated with paw withdrawal threshold only. Macrophages expressing ED2 were associated with weight bearing asymmetry and synovitis (Table 3.1).

Table 3.1 Correlations between pain, synovitis and ED macrophage markers

	Weight bearing asymmetry	Paw withdrawal threshold	Synovitis
Synovitis	0.69*	-0.37	NA
ED1 (CD68)	0.47	-0.53*	0.31
ED2 (CD163)	0.7*	-0.28	0.57*
ED3 (CD169)	0.82**	-0.53*	0.72**

Associations are expressed as Spearman's rank correlation coefficients. **p≤0.01, *p<0.05.

3.5 DISCUSSION

This present study demonstrated that intra-articular injection of carrageenan induced acute inflammation seen as joint swelling, synovitis with macrophage infiltration and increased pain behaviour observed as increased weight bearing asymmetry and reduced paw withdrawal threshold. An interesting and novel finding in this chapter was that macrophages were observed to be associated to both synovitis and pain behaviour.

A constant occurrence in OA is recurrent inflammatory flares (phases). The kaolin/carrageenan-induced knee joint arthritis model (K/C arthritis) imitates the acute inflammatory phase observed in OA. Injection of K/C into the knee causes damage to the cartilage, synovitis and synovial fluid exudates which develops rapidly within hours and is maintained for weeks (Neugebauer et al., 2007). Electrophysiological studies have shown the induction of acute inflammation in the joint of cats within 1-3h following K/C injections (Neugebauer and Schaible, 1988, Neugebauer and Schaible, 1990). Intra-articular injection of carrageenan alone is the modified version of the K/C monoarthritis model, here the time course of carrageenan arthritis is much shorter (hours to days) (Tonussi and Ferreira, 1992, Min et al., 2001, Neugebauer et al., 2007).

Chronic inflammatory arthritis may be characterised by chronic synovitis and joint swelling. Histology is a commonly used method for diagnosing synovitis (Wenham and Conaghan, 2010). Histology, arthroscopy and imaging studies show a marked increase of synovitis in a third of symptomatic OA patients (Mapp and Walsh, 2012). Biopsies from these patients exhibit a variety of changes in the synovium, which although are more pronounced in the late stages of OA, are also present in the earlier stages. These changes include; thickening of the lining layer, increased vascularity and inflammatory cell (e.g. macrophage) infiltration (Wenham and Conaghan, 2010).

Intra-articular injection of 2% carrageenan has been shown to induce joint swelling and synovitis in the rat knee (Lam and Ferrell, 1989, Lam and Ferrell, 1991, Walsh et al., 1998a, Valenti et al., 2010b). Similarly in the present study, joint swelling and synovitis were observed following carrageenan injection.

Intense cellular infiltration by macrophages which occurs 3 days after intra-articular injection of 2% carrageenan is similar to what was previously published (Walsh et al., 1998a). In both Walsh et al, 1998 and Valenti et al, 2010 publications, acute joint swelling was present within 3 days of carrageenan injection. This is in line with the present study which showed joint swelling within 24h of carrageenan injection and was present until the end of the study (day 3).

A characteristic feature of synovitis is the infiltration into the synovium by immune cells such as macrophages. Three days after intra-articular injection of 2% carrageenan, there was increased infiltration by ED1 immunoreactive macrophages. This is similar to what was reported by Walsh and colleagues (1998a). Using rat models of antigen-induced arthritis, ED1, ED2 and ED3 immunoreactive macrophages were seen in the superficial layers of the synovium located at the joint space and articular cartilage (Dijkstra et al., 1987). A similar dense infiltration by ED2 and ED3 immunoreactive macrophages at 3 days post carrageenan injection was observed in the synovium located at the infra patellar fat pad in the current study.

Macrophages may be responsible for contributing to maintaining synovial inflammation in OA (Bondeson et al., 2010). The implication of synovial lining macrophages in OA progression was reported from studies that used liposome-encapsulated clodronate injections to deplete these macrophages in a mouse model of OA (OA was induced by injection of collagenase) (van der Kraan et al., 1990, Bondeson et al., 2010). Another study reported the use of clodronate injections in depleting ED1, ED2 and ED3 immunoreactive macrophages in a rat model of antigen-induced arthritis (Richards et al., 1999). Production of proinflammatory cytokines and vascular endothelial growth factor (VEGF) show that synovial macrophages are activated in OA as shown by histological studies (Haywood et al., 2003, Benito et al., 2005, Bondeson et al., 2010). Using model cultures from the OA synovium, it was seen that macrophages spontaneously produce pro-inflammatory and anti-inflammatory cytokines such as TNF- α , IL-1 β , IL-10 including the major matrix metalloproteinases (MMPs) and tissue inhibitors of metalloproteinases (TIMPs) (Amos et al., 2006, Bondeson et al., 2010).

The antibody clone ED1 is a pan macrophage marker and thus stains all phagocytic macrophages (Damoiseaux et al., 1994) while the clone ED2 stains macrophages involved in the resolution of inflammation (Fabriek et al., 2005). The clone ED3 stains macrophages involved in chronic inflammation (Hartnell et al., 2001). In regards to the above statement on the ED macrophage markers, it is highly likely that the ED1 and ED2 but not the ED3 macrophage markers would be expressed by macrophages in the carrageenan model of acute synovitis. In contrast, all ED macrophage markers were expressed. The association of the macrophages expressing ED2 and ED3 to synovitis may suggest the involvement of these macrophages in inflammation in this model. The association of all 3 markers to either pain phenotypes (weight bearing asymmetry or paw withdrawal threshold) may suggest the involvement of macrophages in contributing to pain in this model. However, the mechanisms by which macrophages contribute to pain behaviour needs further investigation. A role of CD163 (ED2) in host immunity is the regulation of cytokine release by macrophages (Fabriek et al., 2005). These cytokines may then contribute to inflammation and pain. Studies have reported the involvement of macrophages in contributing to the development of neuropathic pain following peripheral nerve injury (Myers et al., 1996) and that the complete or partial depletion of macrophages yield beneficial effects in alleviating nerve injury associated chronic pain (Liu et al., 2000, Mert et al., 2009).

Pro-inflammatory molecules such as tumour necrosis factor alpha (TNF α), interleukins (IL) etc. released into the joint during synovitis initiate local inflammatory vasodilatation and increased vascular permeability thereby facilitating inflammation and as a result pain molecules which sensitize or activate sensory nerves are in turn released. Intra-articular injection of 2% K/C was shown to cause a reduction in weight bearing by the affected limb and allodynia in the rat (Andruski et al., 2008). Similarly, intra-articular injection of 2% carrageenan caused a reduction in weight bearing by the affected limb (Zhang et al., 2004, Kissin et al., 2005, Valenti et al., 2010a). In the present study, intra-articular injection of 2% carrageenan induced a weight bearing deficit of the ipsilateral limb and a reduced nociceptive threshold to punctuate

stimulation of the hind paw thus confirming increased pain sensitivity in this rat model. The weight bearing asymmetry observed here develops early with significant differences seen at 6h, 1, 2 and 3 days post intra-articular injection compared to the paw withdrawal threshold which developed later on, with significant differences to saline injected control observed at day 3. This is different to what was reported by Lee et al, who reported weight bearing asymmetry and reduction in hind paw withdrawal thresholds within 3h of intra-articular injection of 1% carrageenan (Lee et al., 2013b). The reason for the lack of reduced paw withdrawal threshold observed in the present study may be because hind paw withdrawal threshold which is driven mainly by central sensitization of second order neurons in the spinal cord may occur later on, i.e. distal allodynia requires the development and spread of spinal sensitization (Schaible and Grubb, 1993, Schaible et al., 2002). Weight bearing asymmetry on the other hand is a measure of localised joint nociceptive pain and is usually driven by peripheral and central sensitization, thus it may tend to occur earlier in this model. Pain in OA may arise from the different tissues (subchondral bone, ligaments, muscle etc.) within the joint that contain nociceptive fibres; one of such tissue is the synovium. The synovium is richly innervated and can be a likely source of nociception in OA (Hunter et al., 2013). Synovitis was found to be associated with weight bearing asymmetry. The association observed between synovitis and weight bearing asymmetry might be as a result of macrophages as the ED macrophage markers were observed to be associated with both pain behaviour and synovitis but this requires further work.

3.6 CONCLUSIONS

Carrageenan induced inflammation is characterised by joint swelling, synovitis and infiltration by macrophages expressing ED1, ED2 and ED3 immunoreactivities.

Associations of macrophages expressing ED markers with synovitis, weight bearing asymmetry and paw withdrawal threshold may suggest the involvement of macrophages in contributing to inflammation which can then further contribute to nociception and central sensitization.

The ED1 antibody clone is recommended for use in research studies as it labels all active phagocytic macrophages but if the study is specific to chronic inflammatory diseases, then the ED3 antibody clone is highly recommended.

Although this model may have limited validity as a model of human disease, it has potential for the screening of novel interventions that aim to modify pain and joint inflammation in pathological processes such as arthritis.

CHAPTER 4; RELIABILITY, AGREEMENT AND VALIDITY OF THE GUINGAMP MACROSCOPIC CHONDROPATHY SCORING SYSTEM IN RAT MODELS OF OA

4.1 INTRODUCTION

In osteoarthritis (OA), histological grading is the gold standard for investigating pathological change. Mankin, Janusz and a few others have described methods that show sensitivity to changes caused by disease pathology (Mankin et al., 1971, Janusz et al., 2002, Pritzker et al., 2006, Ostergaard et al., 1999) and a number of ways for the measurement of structural changes have been reported. Structural changes to the articular cartilage, chondrocyte morphology and loss of matrix components are normally detected by histology. Although histological methods are often used in characterising structural changes in OA, it is limited by a few disadvantages (Table 4.1).

Table 4.1 OA cartilage histopathology assessment – pros and cons

Pros	Cons
Assesses pathology occurring in the cartilage	Requires invasive tissue sampling
Assesses pathology occurring below the cartilage e.g. in the underlying subchondral bone	Time consuming: length of time for tissue processing
Provides insights into chemical and cellular changes with the joint	Assesses one articular surface instead of the whole joint
	Always requires the use of histological stains for identifying pathology

Macroscopic chondropathy scoring allows for the gross evaluation of the appearance of the joint, and have been mostly developed from arthroscopic studies in man (Oakley and Lassere, 2003). Most macroscopic and histopathology assessment systems are derived from the Collins's classification (Collins, 1950) based on autopsy material of femoral condyles. His classification included 4 pathological grades which roughly followed Fisher's classification (Fischer, 1929), which mainly considered cartilage destruction, marginal proliferation and alterations in bony contour. Of this classification system, Collins mentioned that his grading system was arbitrary and was in no way representing fixed stages of disease progression. Following on from Collins, macroscopic grading has since then progressed.

The Société Française D'Arthroscopie (SFA) system (Dougados et al., 1994) – revised to a simpler score by Aryal et al 1994 (Aryal et al., 1996) builds on the Collins classification system. The SFA system is based on an overall assessment of severity of change to articular surfaces of the tibiofemoral joint in OA and is validated for use across the scale from mild to severe OA chondropathy (Dougados et al., 1994, Aryal et al., 1996). The SFA system involved reporting the observed severity score on an articular diagram (Fig. 4.1) dependent on 3 baseline variables; localization, depth and size.

- Localization: patella, trochlea (femoral groove), medial femoral condyle (MFC), lateral femoral condyle (LFC), medial tibial plateau (MTP) and lateral tibial plateau (LTP).
- Depth: based on the classification by Beguin and Locker (Benguin and Locker, 1983) (Table 4.2).
- Size: lesions evaluated as a % of the whole articular surface, which is then reported on a special form.

The SFA score is a continuous variable between 0-100, obtained for each compartment and 0-400 for the total score. SFA score = size (%) of each grade x severity of grade. Formula is as follows = % (Grade 1 x 0.14) + % (Grade 2 x 0.34) + % (Grade 3 x 0.65) + % (Grade 4 x 1).

Most of the other classifications systems to include Outerbridge classification reported in a publication on the aetiology of chondromalacia patellae

(Outerbridge, 1961) and Pelletier classification (Pelletier and Martel-Pelletier, 1989) follow the 3 baseline variables criteria. The Outerbridge and Pelletier classifications were not used in this thesis because they did not meet the criteria required for classification systems to be used in rats. Both systems involved measuring the fragmentation and fissuring observed in the cartilage in length (cm or mm). This would have not been feasible due to the size of the rat knee.

Use of Indian ink; as described by Yoshioka et al (Yoshioka et al., 1996), assesses gross morphological changes after the application of Indian ink. The Indian ink method was originally carried out by Meachim on preparations made from patellofemoral articulations taken at necropsy done on 29 subjects (Meachim, 1972) (Table 4.2). He was looking for a way to indicate how minimal fibrillations were initiated and he assessed this using transmitted light microscopy. His work showed that articular surfaces with minimal fibrillations exhibited a variety of patterns when examined by stereomicroscopy and by transmission light microscopy of tangential slices. Macroscopic scoring using Indian ink was selected because application of Indian ink to articular surfaces makes areas of mild damage more readily apparent than in unstained surfaces. Another advantage to its use is its aid in the interpretation of histological cut sections after fixation and preparation of tissue. Since the Indian ink is retained at the site of cartilage fibrillation, it helps to distinguish between real and artefactual irregularities of the articular surface (Meachim, 1972).

Finally a macroscopic scoring published by Guingamp et al (Guingamp et al., 1997) was the last of the classification systems chosen because it fits the criteria when taking joint size into consideration. It follows the general theme of localization and depth (Table 4.2) and it was published for use in the monosodium iodoacetate (MIA) model of OA. This classification system is graded from 0-4. These grades are for the 6 chondral compartments of the knee: patella, femoral groove (FG), LTP, MTP, LFC and MFC, with the grades and 6 compartment scores summated for a maximum possible score of 24.

Principles of an ideal macroscopic chondropathy scoring system

Macroscopic chondropathy scoring should be based on the following principles; simplicity, feasibility, scalability, validity and discrimination.

- Simplicity; a system which is simple and reproducible and can be easily applied by investigators with varying levels of experience for macroscopic scoring.
- Feasibility; a system that allows for the scoring of articular surfaces from photographic recordings by a single observer and contemporaneous validation by another observer irrespective of the duration of time (often months or years) over which the samples were harvested. It must also be easily modifiable based on what is required from it e.g. knee joint size of species taken into consideration.
- Scalability; a system that can be correlated with cartilage histopathology and other disease severity.
- Validity; a system that measures what it intends to measure and can show consistency and repeatability by the same observer, between observers and between different modes of scoring.
- Discrimination; a system that has a high sensitivity and can distinguish between disease groups and healthy controls or changes over time.

4.2 AIMS

- To identify a macroscopic scoring system from the literature, that will be suitable for use in rat models of OA.
- To validate this system for reproducibility, to determine inter-observer and intra-observer reliabilities.
- Using this system to explore possible associations with other histological measures of OA structural severity and synovitis.

4.3 MATERIALS AND METHODS

General methodology can be found in chapter 2. Experiments were performed on male SD rats (Charles River, Margate, Kent, UK). Two studies were carried out for this chapter, and tissues from subsequent studies are also reported here. Criteria for choosing the classification systems were based on the method that was feasible when taking the small size of the rat knee into consideration as compared to the size of a larger animal or human knee.

4.3.1 Indian ink and modified SFA classification

This study comprised of 12 Male SD rats, 6 per group (housed 4/cage) weighing approximately 200-250g. The rats were anaesthetised with isoflurane mixture (2% in O₂) and then given intra-articular injections of either 50µl of 0.1mg MIA or 1mg MIA into their left knee joints.

Dissection and grading; Two weeks post treatment, all rats were killed by a rising concentration of CO₂. The left knees of all the rats were dissected and examined for gross morphologic changes which included articular cartilage surface lesions. Using a dissecting microscope, patella with synovium was gently removed and snap frozen in isopentane as previously described. Frozen synovial tissues collected at day 14 for histology and immunohistochemistry were stored at -80°C until when needed. The controls used were the right un-injected (contralateral) knees. With a bone cutter, the bone was cut mid femur and tibia far away from joint as possible. Scissors was then used to remove excess skeletal muscle on either side of the joint so as to see the bone properly. The tip of the scalpel blade was then used to cut the lateral and medial collateral ligaments. The anterior and posterior cruciate ligaments were also cut to slightly free the femur and tibia. Placing the scalpel on the side of the joint directly on the meniscus, the scalpel was gently pressed down, watching out for the cartilage on the femoral condyle and tibia plateau on the side which the blade was placed. The joint was then turned over to the other side and the same procedure was applied. When the femur and tibia became freer, the joint was gently twisted and sliced completely through the meniscus to disarticulate the femur from the tibia. Excess ligament or meniscus left on the bone or cartilage surface was removed with a small scissors. Both femur and corresponding tibia

bones were placed in PBS and then viewed individually under the microscope. The same procedure was applied to the other knee.

All chondral surfaces, MTP, LTP, MFC, LFC and FG (for both knees) were scored using the corresponding scoring sheets i.e. Indian ink, SFA scoring sheet (Table 4.2). The SFA scoring system used here was modified to score the worst grade observed on an articular surface instead of the percentage damage observed for each grade multiplied by the severity of grade for all the grades observed on an articular surface as per the original scoring system (Fig. 4.1). The reason for this was because the rat knee joint is small in size so it would not have been feasible to do this and also scoring the worst grade reflects the true state of the joint at the end of the study or at the time of tissue collection.

Indian ink preparation; The joint was rinsed in PBS and then painted with Indian ink diluted in saline. Excess Indian ink was removed with moistened cotton. The joint was then placed in a standing position to view the cartilage. The painted surface of the cartilage was examined visually at a magnification (X10) using a dissecting microscope (Olympus SZ40-SZ-STU1) with reflected light from table top lamps.

After scoring, the joints were then immediately placed in 20ml vials containing formalin for fixing.

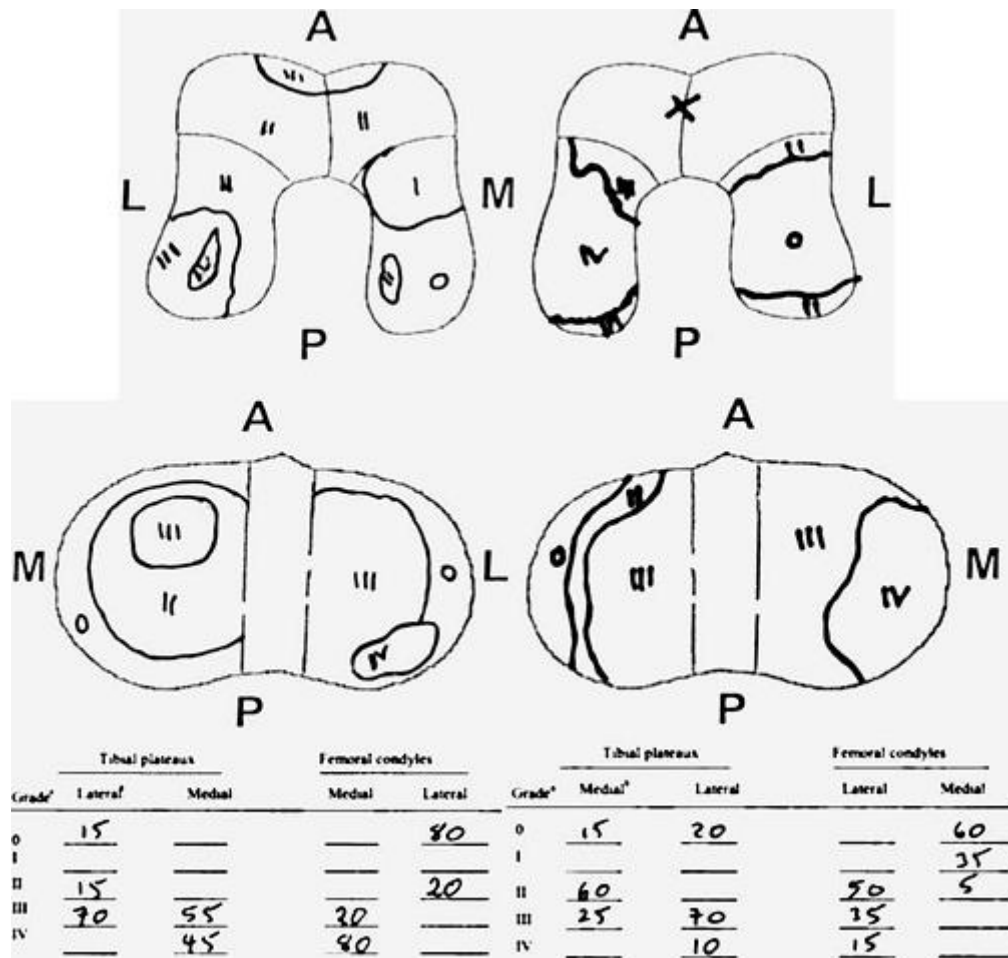


Figure 4.1 Original SFA scoring from diagrams obtained from photographs of human knees.

The SFA method requires reporting on an articular diagram the macroscopic changes based on their location (patella, femoral groove, MTP, LTP, MFC and LFC), depth of chondropathy (from mild to severe) and the size in percentage from 0-100 of lesions detected. The SFA score is a continuous variable between 0-100, obtained for each compartment and 0-400 for the total score. SFA score = size (%) of each grade x severity of grade. Formula is as follows = % (Grade 1 x 0.14) + % (Grade 2 x 0.34) + % (Grade 3 x 0.65) + % (Grade 4 x 1). Picture of diagrams taken from (Walsh et al., 2008)

4.3.2 Modified SFA and Guingamp classification

Knee joint tissues from another study which can be found in chapter 5 were used here. 40 Male SD rats, 10 per group (housed 4/cage) and weighing approximately 200-250g were anaesthetised and then given intra-articular injections of either 50ul of 0.1mg, 1mg MIA or 0.9% saline into their left knee joints.

Dissection and grading; At end of study, rats were killed by a rising concentration of CO₂. Synovia with patella from the rat joints were then harvested and immediately snap frozen in isopentane on day 20 and 42 for histology and immunohistochemistry. Macroscopic scoring was carried out in a similar procedure as the above, excluding the Indian ink. The controls used were the saline-injected knees. After scoring the joints directly using a dissecting microscope, the joints were then fixed and after fixation they were photographed using a video camera (model W30X-HD, 30x zoom full HD (1080p) - Vet Tech solutions limited). The pictures were then graded using the modified SFA and Guingamp classifications.

Note: The complete description of the methodology, behaviour results of the rats used in the second study can be found in chapter 5.

4.3.3 Validation of the macroscopic scoring systems

Knee joint sections stained with H&E or Safranin-O Fast green were used to explore associations between OA structural severity (cartilage damage, chondrocyte morphology, osteochondral junction integrity, matrix proteoglycan content) and macroscopic scores. H&E stained synovial samples were also explored for associations to synovitis.

In another experiment, knee samples from an intervention study which can be found in chapter 6 were used to validate the Guingamp method of scoring. In order to evaluate the validity of using photographs for scoring articular surface changes, macroscopic scores were compared between direct visualisation and photographic images for MIA or saline injected and MNX or sham operated rats.

Inter and Intra-observer reliability was determined by two independent observers (Lilian Nwosu - scorer1 and Pongsatorn Meesawatsom - scorer2), who independently derived scores from photographic images of knee joints from MIA or saline injected, MNX or sham operated rats. Scorer2 was trained and then practised grading 20 photographs of pathological samples.

Statistical analysis

Statistical analysis was performed using Statistical package for the Social Sciences v.21 (SPSS Inc., Chicago, Illinois, USA) or Prism v.6 (Graph Pad, San Diego, California, USA). All data were analysed using a one sample t-test or a Kruskal Wallis test followed by post hoc Dunn's comparison.

Internal consistency for macroscopic chondropathy scoring was determined as Cronbach's alpha and expressed as a number between 0 and 1 (Cronbach, 1951, Tavakol and Dennick, 2011). The closer to 1 the Cronbach's alpha was, the higher the consistency. Intra observer and inter observer agreements were estimated using intraclass correlation coefficients (ICC): intra-rater analysis used a one-way random single measures and an inter-rater analysis used a two-way mixed model, absolute agreement. The reliability was regarded as excellent if $ICC > 0.75$, fair to good if $0.4 < ICC < 0.75$, and poor if $ICC < 0.4$ (Fleiss, 1999, Bruton et al., 2000).

Reliability between macroscopic scores based on direct visualisation of pathological samples and on photographs and between independent observers based on photographs was reported using Bland-Altman plots, which is a graphical illustration that illustrates limits of agreement and repeatability (Bland and Altman, 1986). To construct a Bland-Altman plot, the difference between scoring methods (direct and photographs), between scores by an observer and scores between observers was plotted on the y-axis against the average total between scoring methods (direct and photographs), between scores by an observer and scores between observers on the x-axis. Systematic error in terms of bias (mean difference) and random error in terms of precision

(Mean \pm 2SD) were also calculated to determine agreements between scores (Hanneman, 2008).

Graphs are presented as mean \pm SEM or median. Correlations were presented as Spearman's rank correlation coefficients. A two-tailed $p < 0.05$ was considered significant in all cases.

Table 4.2 Outline of classification systems used for macroscopic chondropathy scoring of OA

Grade	Indian ink (Meachim, 1972)	SFA (Dougados et al., 1994)	Guingamp (Guingamp et al., 1997)
0	Not applicable	Normal appearance	Normal appearance
1	(intact surface) surface appears normal and does not retain any ink	Swelling and/or softening	Slight yellowish discolouration of the chondral surface
2	(minimal fibrillation) site appears normal before staining, but retains ink as elongated specks or light grey patches	Superficial fibrillations	Little cartilage erosions in load bearing areas
3	(overt fibrillation) the cartilage is velvety in appearance and retains ink as intense black patches	Deep fibrillations down to bone	Large erosions extending down to subchondral bone
4	(erosion) loss of cartilage exposing the underlying bone	Exposure of subchondral bone	Large erosions with large areas of subchondral bone exposure

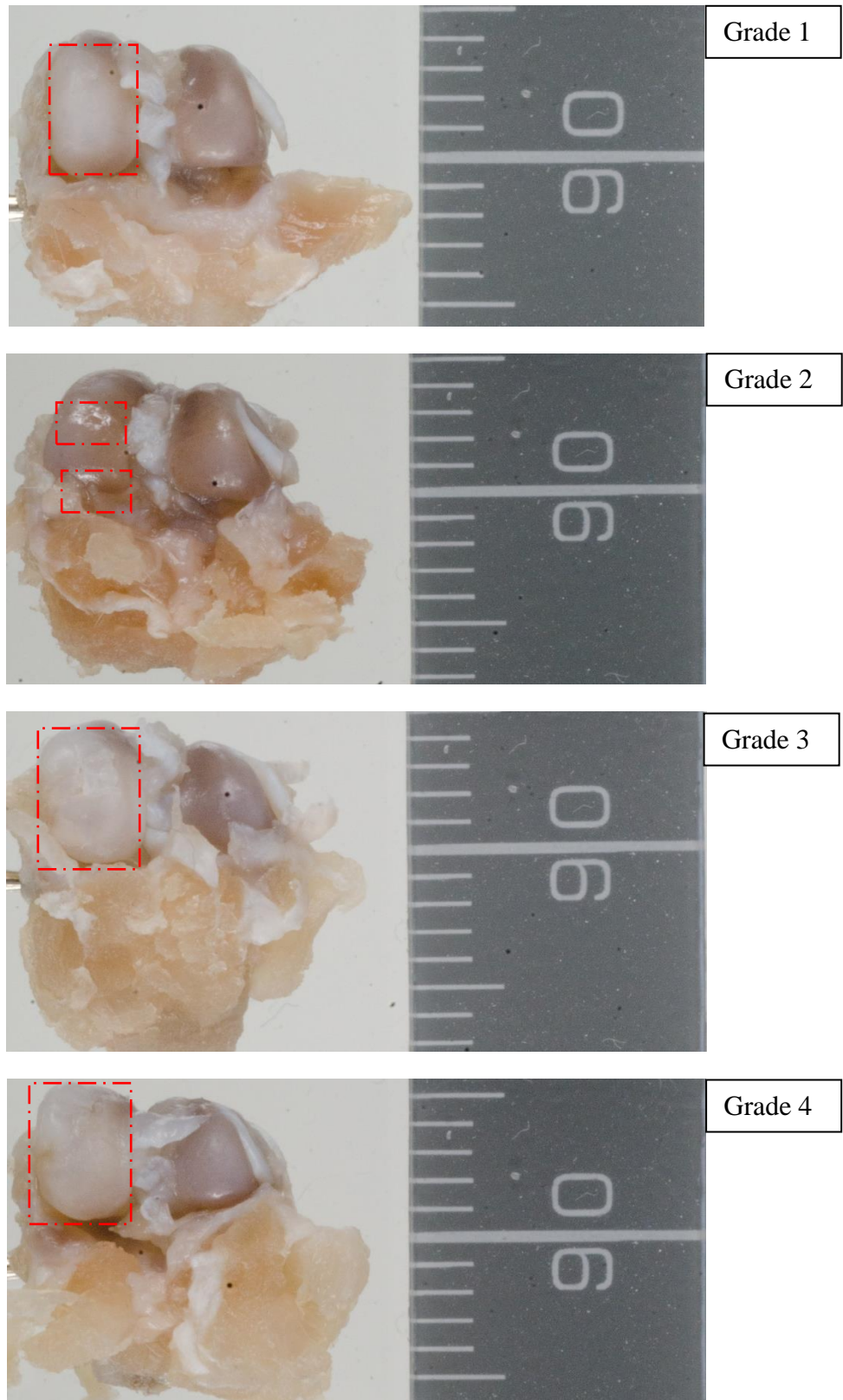


Figure 4.2 Example pictures of the Guingamp scoring system for the medial femoral condyle of MNX-operated rats. 1: Slight yellowish discoloration of the chondral surface. 2: Little cartilage erosions in load bearing areas. 3: Large erosions extending down to subchondral bone. 4: Large erosions with large areas of subchondral bone exposure.

4.4 RESULTS

4.4.1 Macroscopic chondropathy scoring on 0.1mg or 1mg MIA injected knee joints

Intra-articular MIA injection was followed by increased cartilage damage as indicated by increased macroscopic chondropathy scores. There were no significant differences between macroscopic scores for all the experimental groups using the Indian ink direct method of scoring (Fig. 4.3A). Likewise, there were no significant differences in macroscopic scores observed between the experimental groups using the modified SFA direct method of scoring (Fig. 4.3B and C), whereas in the photographic method, only the 1mg MIA injected rats had significantly higher macroscopic scores compared to the saline injected rats (Fig. 4.4A). On the other hand, using the Guingamp photographic method, all groups of MIA injected rats had significantly higher macroscopic scores compared to the saline injected rats but without significant differences between doses and time points (Fig. 4.4B).

4.4.1.1 Direct visual scoring;

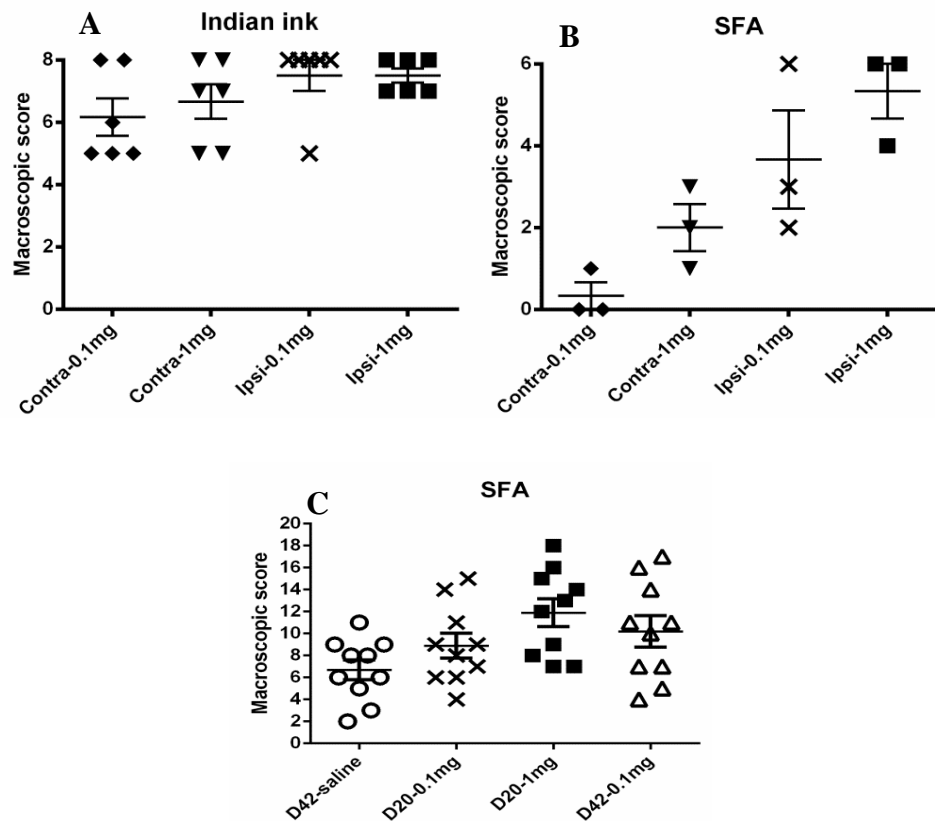


Figure 4.3 Macroscopic changes, articular surface lesions after intra-articular injection of 1mg or 0.1mg MIA.

Intra-articular MIA injections were given in rat knee joints on day 0. At end of study, knee joints were harvested and their articular cartilage surfaces viewed under a dissecting microscope. The worst grade for each chondral surface; MTP, LTP, MFC, LFC and FG were scored at days 14 (**A** and **B**), 20 and 42 (**C**) after MIA injection. Data are expressed as mean ± SEM n = 6 (**A**), n = 3 (**B**) and n = 10 (**C**) knee joints / group. Differences between groups were analysed using a Kruskal Wallis test with a Dunn's post hoc analysis.

4.4.1.2 Photographic scoring

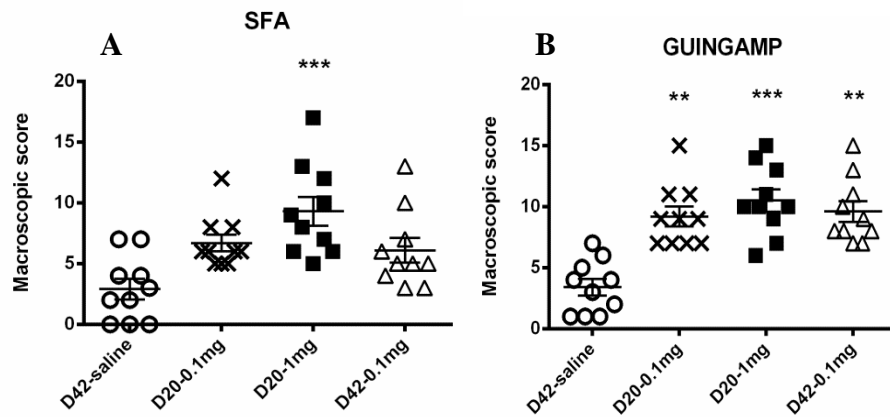


Figure 4.4 Macroscopic changes, articular surface lesions after intra-articular injection of 1mg or 0.1mg MIA.

Intra-articular MIA injections were given in rat knee joints on day 0. At end of study, knee joints were harvested and fixed in formalin before being photographed. Articular cartilage surface changes seen in the photographs were then graded. The worst grade for each chondral surface; MTP, LTP, MFC, LFC and FG were scored at days 20 and 42 after MIA injection. In the modified SFA classification, surface lesions were present in the D20-1mg MIA injected rats (A). In the Guingamp classification, surface lesions were present for all groups (1mg and 0.1mg) and at different time points (20 and 42days) after MIA induction (B). Data are expressed as mean \pm SEM n = 10 knee joints / group. Differences between groups were analysed using a Kruskal Wallis test with a Dunn's post hoc analysis ***p < 0.001, **p < 0.01 compared to D42-saline injected rats (A and B).

4.4.2 Validity testing of the macroscopic scoring systems

Knee samples obtained from an intervention study (chapter 6) were used to further validate the Guingamp method of scoring. MIA injected and MNX operated rats both exhibit significantly higher macroscopic chondropathy scores compared to their corresponding saline injected and sham operated controls either by direct or photographic scoring (Fig 4.5A – D). Positive correlations were also observed between direct and photo scoring methods in both studies (Fig. 4.5E and F), whereas the modified SFA method showed no correlations between direct and photographic methods of scoring ($r = 0.3$, $p = 0.06$). Fig. 4.6 show results from 2 independent observers using the Guingamp photographic scoring method (A and B). Both scorers show higher macroscopic scores for MNX operated rats compared to sham operated rats, individually and when scores were pooled together (C).

Positive correlations were also observed between both observers (D). Inter-rater reliability analysis showed a consensus of scoring with high Cronbach's alpha values for the Guingamp method between direct and photographic methods (0.89 – 0.93) and between 2 independent scorers by photographic method (0.73) (Table 4.3), whereas the modified SFA method showed a lower Cronbach's alpha value of 0.46. Guingamp photographic method of scoring displayed good repeatability between measurements by the same observer using the same photographs (Cronbach's alpha; 0.93 – 0.96) (Table 4.3). Intraobserver agreement comparing photographic Guingamp scoring methods displayed excellent ICCs (0.91 – 0.96), while inter observer agreement between observers displayed a fair to good ICC (0.49) (Table 4.3). The modified SFA method displayed poor interobserver agreements between direct and photographic scoring methods with an ICC value of 0.38.

As shown by the Bland-Altman plots (Fig. 4.7), there were no systematic differences in the direct and photographic scoring methods, between repeated scoring and between observers. Positive correlations were observed between macroscopic chondropathy scores and other OA histological severity scores for both modified SFA and Guingamp photographic scoring methods (Table 4.4).

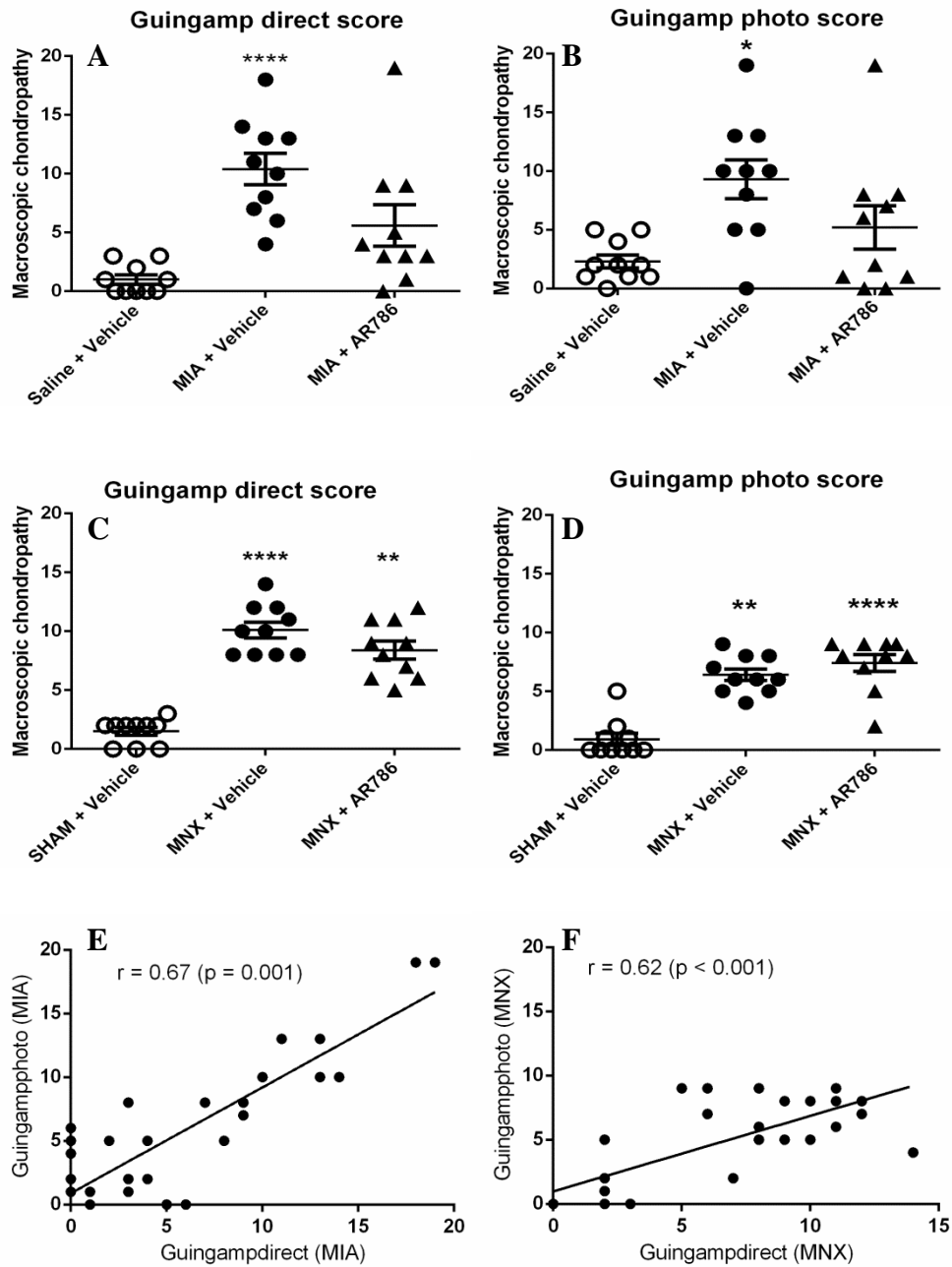


Figure 4.5 Direct (A and C) and photographic (B and D) scoring of macroscopic chondropathy in MIA injected (A and B) or MNX operated (C and D) rats by one observer (LN). Guingamp photo scoring show similar results to direct scoring (A-D) and correlates with the direct scoring for both MIA and MNX models of OA (E and F respectively). Scatter plots show mean \pm SEM of $n = 10$ rats/group (A-D). Scatter plots with regression line show Spearman's correlation coefficients (E and F). Differences between groups were analysed using Kruskal Wallis test followed by post hoc Dunn's comparison. . * $p < 0.05$, ** $p < 0.01$, *** $p < 0.001$ compared with saline-injected or SHAM-operated vehicle controls.

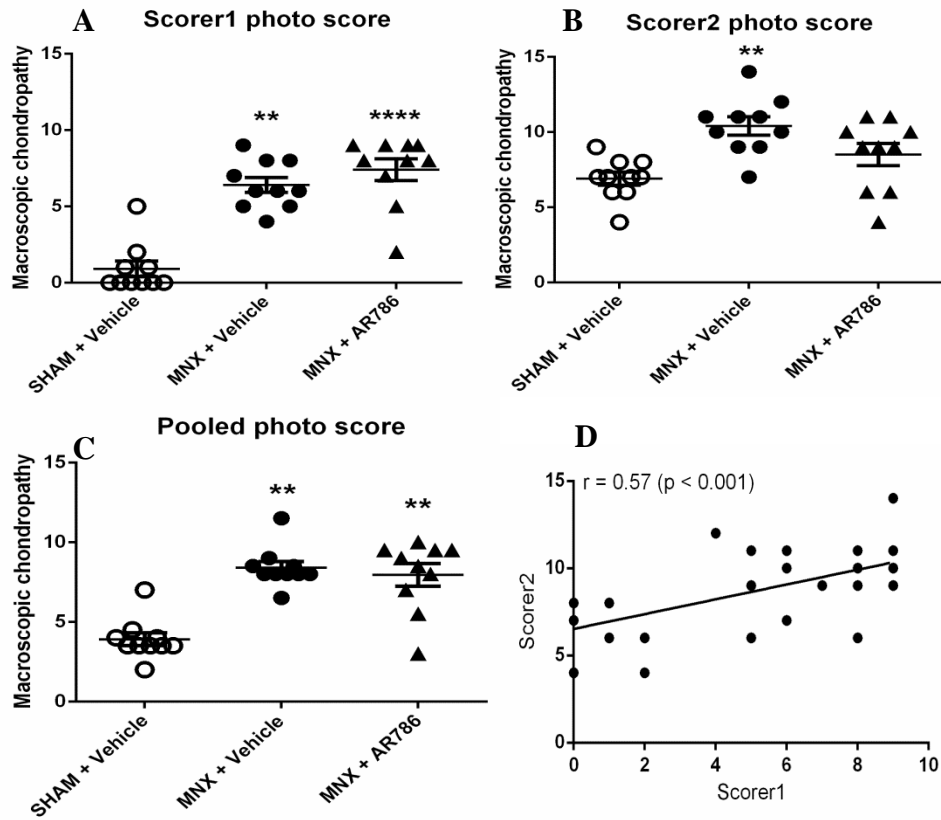


Figure 4.6 Photographic scoring of macroscopic chondropathy in MNX operated (A-C) rats.

Guinamp photo scoring from 2 independent observers show similar results (A and B) and are positively correlated (D). Scatter plots show mean \pm SEM of $n = 10$ rats/group (A-C). Scatter plots with regression line show Spearman's correlation coefficients (D). Differences between groups were analysed using Kruskal Wallis test followed by post hoc Dunn's comparison. * $p < 0.05$, ** $p < 0.01$, *** $p < 0.001$ compared with sham-operated vehicle controls. Scorer 1 (LN), scorer 2 (PM).

Table 4.3 Inter-rater reliability analysis for macroscopic chondropathy scoring as measured by two scoring methods and between observers

Cronbach's alpha	Scorer2 MNX Photo		
	MIA Photo	MNX Photo	
MIA Direct	0.93	NA	NA
MNX Direct	NA	0.89	NA
Scorer1 MNX Photo	NA	NA	0.73
MIA Photo2	0.93	NA	NA
MNX Photo2	NA	0.96	NA

Intra observer agreement

Measure	ICC	95%CI Lower	95%CI Upper
MIA Photo v MIA Photo2	0.91	0.82	0.96
MNX Photo v MNX Photo2	0.96	0.92	0.98

Inter observer agreement

Measure	ICC	95%CI Lower	95%CI Upper
Scorer1 MNX Photo v Scorer2 MNX photo	0.49	-0.23	0.8

Differences between direct and photographic scoring methods and between two independent observers are given as Cronbach's alpha values and ICC (intra-class correlation coefficients) and 95% confidence intervals. The closer to 1 the Cronbach's alpha, the higher the consistency of scoring. The reliability was regarded as excellent if $ICC > 0.75$, fair to good if $0.4 < ICC < 0.75$, and poor if $ICC < 0.4$.

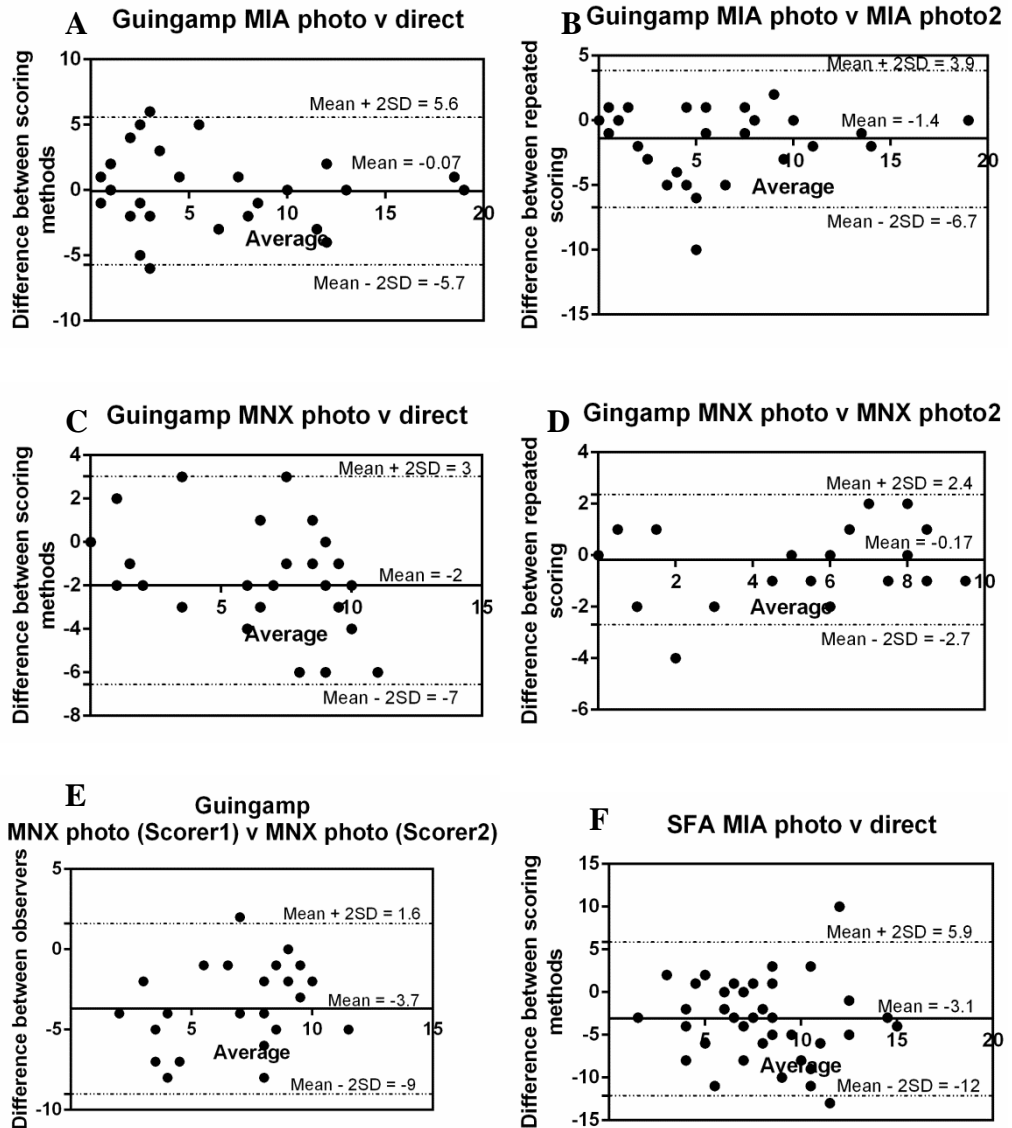


Figure 4.7 Bland-Altman plots illustrating agreement between repeated scoring by an observer, different methods of scoring and between observers. The 95% limits of agreement contain 93% – 100% (28/30 – 30/30) of the difference scores (A – F). Mean+2SD (upper limit of agreement), Mean-2SD (lower limit of agreement), Mean (bias – average of the difference values), values outside the limits of agreements are outliers and values within limits of agreements are individual difference values.

Table 4.4 Associations of macroscopic scores with other OA histological severity scores and synovitis

OA severity scores	SFA Direct	SFA Photo	Guingamp Photo
Cartilage damage (Janusz)	-0.01	0.14	0.37*
Chondrocyte morphology	0.02	0.08	0.29
Osteochondral junction integrity	-0.003	0.32*	0.34*
Matrix proteoglycan content	-0.02	0.37*	0.48**
Synovitis	0.17	0.16	0.51**

No associations between modified SFA direct scoring and OA histopathology. Associations observed for modified SFA photographic scoring and osteochondral junction integrity and proteoglycan scores, whereas by Guingamp photographic method, associations were observed to cartilage damage, osteochondral junction integrity, proteoglycan score and synovitis. Associations are expressed as Spearman's rank correlation coefficients. ** $p \leq 0.01$, * $p < 0.05$.

4.5 DISCUSSION

This chapter investigated macroscopic scoring systems for measuring the severity of OA pathology in tibiofemoral joints already in the literature to identify one that best suits for use in rat models of OA pain. Three (Indian ink, SFA and Guingamp) previously reported methods were selected for the study based on the first two been developed for use in humans with the Indian ink been applied for use in rats and the Guingamp method developed for use in rats. Two (SFA and Guingamp methods) out of the three systems were then slightly modified to fit the criteria based on the size of the rat knee and the chondral compartments (FG, MTP, LTP, MFC, and LFC) available to assess. These systems were based on direct visualisation (using a dissecting microscope) and on photographs of pathological samples.

The findings show that the Guingamp classification method is a reliable method of grading macroscopic chondropathy and it establishes good agreement and validity when compared to Indian ink and the modified SFA methods. The Guingamp direct and photographic methods of scoring were more sensitive than Indian ink direct and modified SFA direct and photographic methods of scoring as it was able to discriminate between normal healthy controls and those with OA disease pathology. It was also able to detect associations between OA structural change and histological synovitis. The Guingamp scoring method, although not directly comparable to man, does display good validity following the range of criteria based on truth, discrimination and feasibility as described in the OMERACT filter (Boers et al., 1998). Truth; if the system measures what it intends to, discrimination; if it can distinguish between groups measured and feasibility; if it can be easily applied.

The Guingamp scoring method based on truth showed good face validity. It showed higher severity scores for the disease group compared to the normal controls that had lower chondropathy scores. Chondropathy is a major pathological process in knee OA and loss of cartilage leads to the exposure of the subchondral bone (Walsh et al., 2008). Sensory nerves within vessels in the subchondral bone are at risk of being exposed and are prone to sensitization by

sensitizing factors (Suri et al., 2007). The photographic scoring system reported in humans by Walsh et al (Walsh et al., 2008) addresses both extent and severity of chondropathy. In contrast, due to the limitation on knee size, the photographic chondropathy scoring system method used in this thesis reports only on severity of chondropathy. This system although limited still measures chondropathy of the whole joint compared to histological systems that measure both extent (involvement of cartilage) and severity but only do so on one articular surface and not the whole joint (Janusz et al., 2002, Pritzker et al., 2006).

The use of photographs did not adversely affect the performance of the Guingamp classification system when compared to the direct scoring method. This is consistent with reports that showed that direct examination of pathological samples using instruments did not add to the direct scoring methods of chondropathy compared to photographic scoring or arthroscopic scoring methods with video assessment (Walsh et al., 2008, Oakley et al., 2005).

Abrasions on the cartilage surface and presence of fibrotic tissue are seen as roughened surfaces which can be highlighted by the use of a dye. Use of Indian ink or Evans blue has been reported extensively as tools for macroscopic chondropathy grading (Richardson C et al., 2001, Tessier et al., 2003, Janusz et al., 2002). Results from these studies report their effectiveness in highlighting fibrillations whether minimal or severe and being able to discriminate normal controls from disease groups. This was not the case in this study as the use of Indian ink did not discriminate between normal controls and disease group. This may have been due to the size of the knee joints of animals used, as the studies reported use of rabbits and guinea pigs. The data from this chapter suggests that using Indian ink is unnecessary and may even reduce the performance of the scoring system compared to the modified SFA or Guingamp scoring methods that do not use dyes for scoring.

The original SFA system was developed for assessing articular surface lesions at knee arthroscopy studies in humans. Although the other two systems, use of Indian ink and Guingamp classification have been reported for use in animals,

the SFA system has only been used in humans. If the modified SFA system was reported here as being a useful system for scoring chondropathy in animals, direct comparisons on pathology would have been facilitated between humans and animals but this did not turn out to be the case.

The modified SFA system was less sensitive to the Guingamp system as it did not discriminate macroscopic pathology between the lower dose (0.1mg) MIA injected rats compared to saline injected control rats but only in the higher dose (1mg MIA) group using the photographic scoring method. Also it was not sensitive at all in discriminating macroscopic pathology in any of the groups by the direct scoring method. This may have been as a result of the modifications made to the SFA system used here. The original SFA method requires reporting on an articular diagram the macroscopic changes based on their location, depth and size. Furthermore, the original SFA system has multiplication factors giving different weights to the different components which results in a total score 0-400 (Ayril et al., 1996). In this thesis, the modified SFA gave a score of 0-20 and reported grades of the worst lesions observed. Modifications were made to this system based on size differences between human and rat knee joints. On the other hand, the Guingamp scoring system which showed sensitivity in discriminating between OA disease groups from normal saline injected or sham operated controls may be forward translated for use in man with comparison to the original SFA scoring system.

The photographic chondropathy scoring method based on the Guingamp scoring system was shown to be a reliable way of scoring macroscopic chondropathy consistent with reports on good agreements with direct scoring method by an observer and between observers based on the original SFA scoring system (Walsh et al., 2008). This highlights the usefulness of photographic scoring as a research tool because it allows for measurements to be carried out on pathological samples that were collected a long time ago and comparison studies to be carried out between observers at different time periods. Macroscopic chondropathy scoring of OA should not just be limited to scoring by photographic method but should also include scoring by direct visualisation method as this provides a better judgement of the depth and severity of pathological changes to articular surfaces than from the assessment

of photographs. Furthermore, there are other aspects of OA pathology (softening of the cartilage or yellowish discolouration of the cartilage) that may not be captured by photographic scoring, but it is currently uncertain what relevance these components may have to patient symptoms or OA pathobiology.

Bland-Altman plots were carried out because the Guingamp method of scoring either directly or through photographs or between observers demonstrated high ICCs in repeated measurements and also because it was the appropriate methodology for this work, based on existing literature on validation methodologies (Hanneman, 2008). In order to obtain a good agreement, the scores between direct and photographic methods, repeated by an observer and between observers should be equal or nearly equal to each other. Bias (mean difference) which represents the measurement differences between the scores should be ideally or close to zero (Bland and Altman, 1995, Hanneman, 2008). Cone or funnel effects at high mean values of the photo or direct scoring were not observed, hence the mean and differences between scoring was said to be consistent and thus the limits of agreement reported appropriate.

Compared to the other two systems (Indian ink and modified SFA), the Guingamp method of scoring was observed to be associated more with other OA structural severity assessments and with synovitis. Macroscopic chondropathy scoring is just one of the methods for measuring OA pathology. Assessments by radiography, for example of osteophytes (bony out growths) give additional information of pathological changes to the cartilage. Histological grading is a widely used method for investigating pathological change, and it does provide some insights into chemical and cellular changes (Appleton et al., 2007, Yorimitsu et al., 2008). On the other hand, this assessment of pathological change is observed only on one articular surface compared to the whole knee joint. All three (macroscopy, radiography and histology) measuring tools portray different but related aspects of the OA process and their associations with each other show that these measuring systems share common aspects of assessing OA structural severity and might increase the validity of an outcome when used together. Despite this, macroscopic scoring was reported to be more effective than radiography,

computed tomography – CT and magnetic resonance imaging – MRI at detecting all the lesions, especially mild changes present in mechanically induced OA in rabbit knees (Torelli et al., 2004).

Synovitis is a characteristic feature of human knee OA. Imaging and histological studies report on marked synovitis being present in a third of people with symptomatic OA (Haywood et al., 2003, Conaghan et al., 2006). It was reported that severity of inflammation increased with structural changes to articular surfaces independent of patient group (total knee replacement-TKR or post mortem-PM) (Walsh et al., 2008). In this study, an association between synovitis and macroscopic scoring using the Guingamp method of scoring was observed. Synovitis was found to be associated with radiological joint space narrowing (JSN), which is normally regarded as an important marker of OA progression (Altman et al., 1987). This association between JSN and synovitis may suggest that association between OA severity and synovitis may be as a result of cartilage pathology (Walsh et al., 2008). This thesis does not have any radiological measurements to back up the associations observed between OA severity and synovitis. Further work including radiological measurement would be needed to replicate the above statement observed in man.

4.6 CONCLUSIONS

Macroscopic chondropathy scoring provides a faster way of obtaining pathological results on chondropathy in the knee, as this can be undertaken at the end of a study and before tissue fixation and processing for histopathological assessments.

The Guingamp classification system has excellent sensitivity and reliability in the measurement of macroscopic chondropathy in rat models of painful OA. Similarly this system by photographic scoring method was in good agreement with scoring by direct visualisation by an observer and between observers. Therefore the Guingamp classification system either by direct visualisation or through photographs is an effective method for scoring OA pathology in rats and can be used for future studies.

Associations between macroscopic chondropathy scoring and histological scoring despite their low values suggest that other important factors that cause pathology in OA may be measured by one or the other. Therefore the use of multiple methods to assess OA pathology in research studies is highly recommended.

CHAPTER 5; THE MONOSODIUM- IODOACETATE (MIA) MODEL OF OA PAIN; COMPARISON BETWEEN TWO MIA DOSES AND TIME POINTS

5.1 INTRODUCTION

The monosodium iodoacetate (MIA) model was first described for use by Kalbhen in hens and rats to chemically induce degenerative arthritis (Kalbhen and Blum, 1977) before its widespread use in other species such as Guinea pigs, mice, horses etc. (Williams and Brandt, 1984, van der Kraan et al., 1989, Janusz et al., 2001, Penraat et al., 2000). This model involves the intra-articular injection of monosodium iodoacetate. The MIA model is widely used because of its reproducibility and its rapid development of joint pathology. Intra-articular injection of MIA into the rat tibiofemoral joint space produces pathology (cartilage and subchondral bone pathology) with similarities as that seen in human OA knees (Guingamp et al., 1997, Guzman et al., 2003). Pronounced pain related behaviours (weight bearing and allodynia – indicating reduced paw withdrawal threshold) are also characteristic features of this model (Bove et al., 2003, Combe et al., 2004, Sagar et al., 2010, Fernihough et al., 2004). The pain behaviours, weight bearing and reduced paw withdrawal threshold represent peripheral and central processing in OA (Christiansen and Stevens-Lapsley, 2010, Suokas et al., 2012).

Previously OA was considered to be a strictly peripheral condition but other clinical features such as referred pain and sensitivity in areas distant to the joint suggests the possibility of altered central processing of nociceptive stimuli (Gwilym et al., 2009). Central sensitization occurs during inflammation and nerve damage whereby neurons in the superficial and deep regions of the dorsal horn of the spinal cord show marked changes of their response properties (Schaible, 2007, Sharif Naeini et al., 2005, Pinto et al., 2007). The changes seen are: lowered thresholds of nociceptive spinal neurones, increased

responses to noxious stimulation of inflamed site or non-inflamed site (hyperalgesia), responses to non-noxious stimulation of non-inflamed surrounding tissues (allodynia) and expansion of the receptive field (Schaible, 2007). The pathological models of knee OA including the MIA model are essential in understanding the involvement of central mechanisms leading to pain responses and the associations between structural features and pain.

OA structural severity can be evaluated by the macroscopic appearance of articular surfaces (Guingamp et al., 1997, Walsh et al., 2008), or microscopic changes in tissue sections (Janusz et al., 2002, Mankin et al., 1971, Pritzker et al., 2006). The OA Histological Histochemical Grading System (HHGS) described by Mankin *et al.* in 1971 (Mankin et al., 1971) is the most widely used grading system for scoring OA pathology. This system developed from examining human hip OA has been widely applied directly or with modifications to other synovial joints e.g. knee and to a variety of animal models (Stoppiello et al., 2014, Murat et al., 2007, Wei et al., 2010). Although the HHGS is a widely used system, its reproducibility has been reported to be inadequate and its reliability has been questioned (van der Sluijs et al., 1992, Ostergaard et al., 1999, Custers et al., 2007). Reports have also shown its inability to discriminate between normal and mild to moderate OA pathology (Ostergaard et al., 1997, Pearson et al., 2011).

The OA working group established in 1998 by The Osteoarthritis Research Society International (OARSI) created the Osteoarthritis Cartilage Histopathology (OACH) grading and staging system with the intention of standardizing the assessment of OA histopathology (Pritzker et al., 2006). The system was observed to be reliable with Cronbach alpha scores in the range 0.7-0.8 and reproducible with excellent inter observer agreements (Custers et al., 2007). The OACH system has been compared to the HHGS in a surgically induced cobalt-chrome implant model of knee OA in goats where it was reported to be more reliable than the HHGS (Custers et al., 2007), although similar reliabilities between both systems have also been reported (Pearson et al., 2011). A disadvantage to the OACH system is that it requires assessing multiple features (cartilage surface integrity, chondrocyte morphology, proteoglycan loss etc.) for each individual grade and thus the transition

between regions of OA structural severity may overlap and therefore makes it difficult in assigning a grade (Pritzker et al., 2006, Pearson et al., 2011). In this chapter, the OACH system was modified to score only cartilage surface integrity.

The Janusz system of histopathology scoring (Janusz et al., 2002) was modified and applied from a scoring system described by Bendele and Hulman on spontaneous osteoarthritis in Guinea pigs (Bendele and Hulman, 1991). The Janusz system consisted of scoring cartilage pathology alone and did not include chondrocyte death and proteoglycan loss as described by Bendele and Hulman. This Janusz histopathological scoring system was effective in showing joint lesion development following meniscal tear in rats, but its reliability or reproducibility, with comparison to the modified OACH or OARSI system has not been evaluated.

Loss of matrix proteoglycan observed as loss of stainable proteoglycan is one of the characteristic features of the MIA model (van der Kraan et al., 1989, Janusz et al., 2001, Bove et al., 2003). Proteoglycan loss can be scored in the cartilage of Safranin-O Fast green, Alcian blue-PAS or Toluidine blue stained sections (Pauli et al., 2012, Mokbel et al., 2011, Sun et al., 2012). Safranin-O and Alcian blue are cationic dyes that bind specifically to sulphated glycosaminoglycans (GAGs) and proteoglycan. A product of the binding of Safranin-O is the intense red stain which indicates the presence of proteoglycan content. Varying intensity of the red colour is what is scored in histological sections assessing cartilage damage. In cartilage, where the levels of GAGs have been severely depleted, sensitivity to proteoglycan content is reduced (Camplejohn and Allard, 1988). This can occur as a result of disease, fixation or wash out during decalcification, especially with prolonged methods e.g. ethylenediaminetetraacetic acid (EDTA) (Hyllested et al., 2002, Encfeldt and Hjertquist, 1967, Chevrier et al., 2005). In order to reduce variability, another proteoglycan stain for example Alcian blue-PAS stain or Toluidine blue stain could be used in parallel.

Structural changes in the OA joint are well characterised but their associations with pain behaviour are complex and less understood (Yusuf et al., 2011). This

is represented in some patients who complain of pain without structural damage while some others that show significant changes in their knee joint do not experience any pain. To mimic this, two doses of MIA were used here; a lower dose (0.1mg) to represent subclinical pain and the standard dose (1mg) to represent clinical pain.

The hypothesis was that the low dose (0.1mg) MIA would induce OA pathology including inflammation but not measurable pain behaviour (weight bearing asymmetry and paw withdrawal threshold) while the standard dose (1mg) will do both.

5.2 AIMS

- To characterise the effect of intra-articular injections of a lower (0.1mg) and standard (1mg) dose of MIA on pain behaviour and joint structure including synovial inflammation.
- To investigate if OA pathology is homogeneous or heterogeneous across the whole knee joint in the MIA model (is it right to score only one part of the knee as recommended by the OARSI scoring system)?
- To validate the histological (Janusz and modified OARSI) scoring systems for reproducibility, to determine inter-observer and intra-observer reliabilities.
- To compare the sensitivity of the Safranin-O Fast green stain for detecting proteoglycan content in the cartilage matrix (comparison to the Alcian blue-pas stain).

5.3 METHODS

Refer to Chapter 2 for general methodology. Experiments were carried out on male Sprague Dawley rats (Charles River, UK) n = 64, weighing 220-370g at time of OA induction. Two studies were carried out in this chapter.

5.3.1 Characteristic features of a low and standard dose of MIA injections in naïve animals

OA induction

64 male rats (n = 8 or 10 per group) were anaesthetised with isoflurane (2% in O₂) mixture and received a single intra-articular injection of MIA (0.1mg/50µl or 1mg/50µl, based on previous studies (Guingamp et al., 1997, Bove et al., 2003, Sagar et al., 2010)). Study 1 investigated the effect of intra-articular MIA for 20 days post injection (Fig. 5.1) while study 2 went up to 42 days post injection (Fig 5.2).

OA pain behavioural measurements

The effects of intra-articular injection of MIA or saline on pain behaviour were measured as hind limb weight-bearing asymmetry and distal allodynia to punctuate stimulation of the hind paw using von Frey filaments (Semmes-Weinstein monofilaments 1 - 15g). Baseline measurements were obtained immediately prior to intra-articular injection (day 0) and from day 3 onwards to day 42. In line with the 3Rs (reduction), the 1mg MIA group were sacrificed at day 20 as pain behaviour and OA pathology are already established at 2 weeks after OA induction (Sagar et al., 2010). Development of allodynia was indicated as a decrease in hind paw withdrawal threshold (PWT). Weight bearing asymmetry was assessed as a % difference in weight distribution between hind limbs (non-arthritis knee – arthritis knee) / (non-arthritis knee + arthritis knee) x100 using an incapacitance meter (Linton Instruments, U.K).

Tissue harvesting and decalcification

Rats were sacrificed at the end of each study and tissues collected at day 20 and 42. Fresh synovial and hard joint tissues were collected from ipsilateral arthritic (MIA) and non-arthritic (saline) controls.

Macroscopic scoring of the articular cartilage (Guingamp method) (Guingamp et al., 1997) was undertaken on harvested knee joints.

Time course of experiment 1

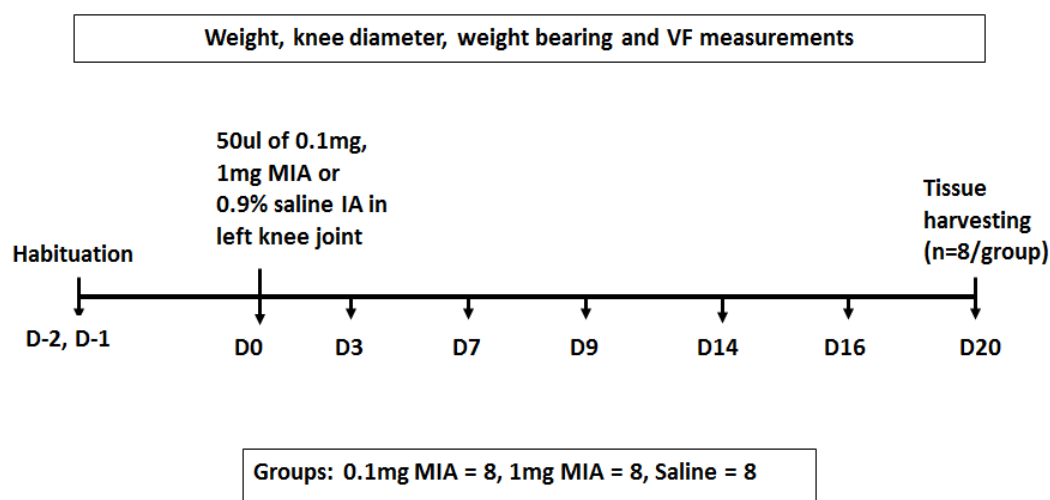


Figure 5.1 Time course of MIA-induced pain behaviour and inflammation.

Rats were habituated to pain assessment (incapacitance meter and von Frey box) two days prior to baseline measurements. MIA was injected intra-articular on day 0. Weights, knee diameters and pain behaviour were measured from day 0 (baseline) until day 20. Tissue (joint) harvesting was carried out on day 20.

Time course of experiment 2

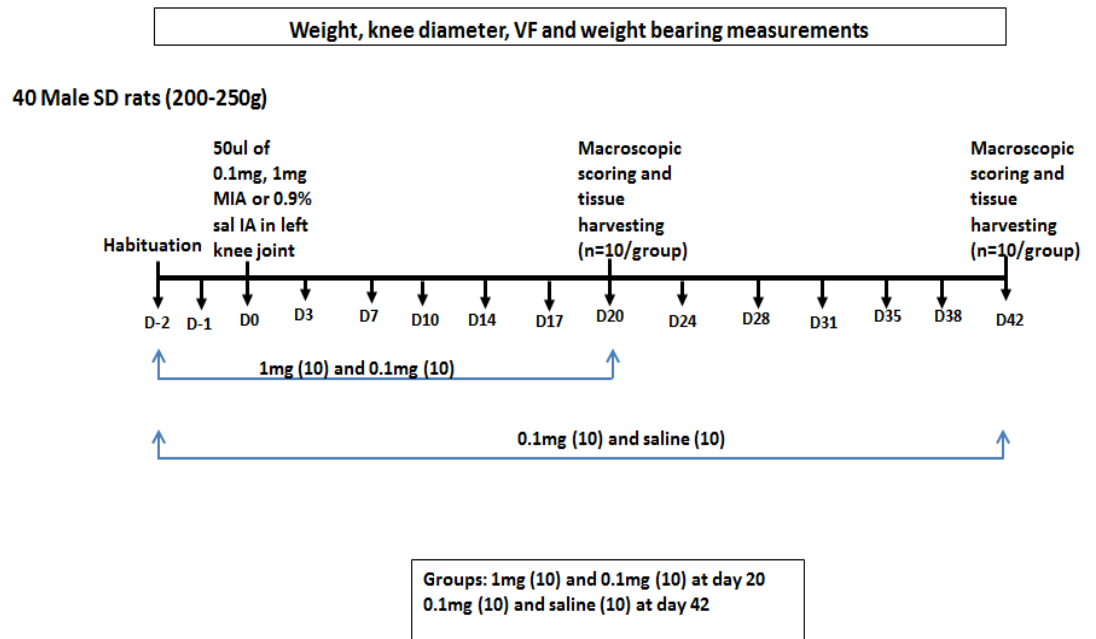


Figure 5.2 Time course of MIA-induced pain behaviour and inflammation.

Rats were habituated to pain assessment (incapacitance meter and von Frey box) two days prior to baseline measurements. MIA was injected intra-articular on day 0. Weights, knee diameters and pain behaviour were measured from day 0 (baseline) until day 20 (for 0.1mg and 1mg MIA groups) and day 42 (for 0.1mg MIA and saline groups). Macroscopic scoring and tissue (joint) harvesting were carried out on day 20 and 42.

Inflammation

Inflammation was assessed as joint swelling, synovial histological score and macrophage infiltration.

Joint swelling was measured at the same time as behavioural measurements using a digital electronic calliper (Mitutoyo, UK), with values representing difference in knee diameters (mm) between the arthritic (left) and non-arthritic (right) knee joints (Ashraf et al., 2010).

Synovial sections (5µm), 1 section/rat were stained with haematoxylin and eosin (H&E) to assess its lining thickness and cellularity as previously described (Mapp et al., 2008, Walsh et al., 1998a). Synovitis scoring was performed using a 20× objective lens of a Zeiss Axioscop-50 microscope (Carl Zeiss Ltd, Welwyn Garden City, UK).

Macrophage infiltration was identified by immunoreactivity for CD68 using the mouse monoclonal antibody clone ED1 (Dijkstra et al., 1985) and the peroxidase-conjugated avidin-biotin-peroxidase complex (ABC) method. Macrophage infiltration was quantified using fractional area and was defined as the percentage of synovial area that was CD68-positive (Walsh et al., 1998a).

Macroscopic chondropathy grading of knee joint pathology

At the end of the experiment at day 20 and day 42, rats were killed by a rising concentration of CO₂. Tibiofemoral joints of the ipsilateral knees were isolated and carefully dissected and disarticulated to assess the severity of damage to the chondral surfaces. Macroscopic lesions were graded using the Guingamp classification as previously described (Guingamp et al., 1997). Grade 0 = normal appearance, 1 = slight yellowish discolouration of the chondral surface, 2 = little cartilage erosion in load bearing areas, 3 = large erosions extending down to the subchondral bone and 4 = large erosions with large areas of subchondral bone exposure. Five chondral compartments of the knee: femoral groove, medial and lateral femoral condyles and medial and lateral tibia plateaus were scored. The 5 compartment scores were combined for a maximum possible score of 20.

Joint histology

Following macroscopic scoring, the joints were fixed in neutral buffered formalin for 48h, then decalcified in EDTA for 6 weeks or 10% formic acid-formalin for 7 days at room temperature and embedded in paraffin. Frontal sections following the OARSI guideline for histological assessment for OA in the rat were cut and stained with H&E, Safranin-O-Fast green or Alcian blue-PAS (Gerwin et al., 2010). These 5µm cut sections were visualised using a 20x objective lens unless stated otherwise. Cartilage chondropathy, chondrocyte morphology and proteoglycan content of the cartilage were evaluated as previously described using a 4x objective lens (Janusz et al., 2002, Ashraf et al., 2011a, Mapp et al., 2010, Kamisan et al., 2013, Pritzker et al., 2006). Osteochondral junction integrity was assessed as the number of vascular channels present in the articular cartilage per length of tibial plateau (mm) (Ashraf et al., 2011a).

5.3.2 Validation of histopathology scoring systems

20 sections out of the 240 sections (n = 6 sections/rat) stained with haematoxylin and eosin or Safranin-O Fast green were scored for cartilage damage (Janusz or modified OARSI methods) (Janusz et al., 2002, Pritzker et al., 2006), chondrocyte appearance, vascular channels crossing the osteochondral junction (osteochondral junction integrity) and proteoglycan content in the cartilage between 4 investigators (LN-scorer1, PG-scorer2, JH-scorer3, SS-scorer4) to test for reliability of histological scoring.

Knee sections from another study (chapter 6) scored for cartilage damage using the Janusz or modified OARSI methods were evaluated for inter observer reliability.

Statistical analysis

Synovial inflammation, lining thickness and cellularity were scored as previously described, one synovial section per rat and overall grade that best represented the section given (Ashraf et al., 2011a). Infiltration by macrophages was quantified on 4 fields of view per synovial section per rat (Walsh et al., 1998a).

Data for each experiment were presented graphically as mean \pm SEM and analysed using Prism V.6 (GraphPad, San Diego, California, USA). The different groups were compared using the non-parametric Kruskal-Wallis test followed by post hoc Dunn's test for each parameter or the Wilcoxon matched-pairs signed rank test. A two-tailed P value of less than 0.05 was taken as significant in all cases. Numerical data were presented as mean (95% CI) or median (IQR).

Internal consistency for histological scoring was determined as Cronbach's alpha and expressed as a number between 0 and 1 (Cronbach, 1951, Tavakol and Dennick, 2011). The closer to 1 the Cronbach's alpha was, the higher the consistency.

Unweighted and weighted kappa (κ) values were calculated for agreement. K was defined as less than chance agreement if < 0 , slight agreement = 0.01-0.20, fair agreement = 0.21-0.40, moderate agreement = 0.41-0.60, substantial agreement = 0.61-0.80, and almost perfect agreement = 0.81-0.99 (Landis and Koch, 1977, Kundel and Polansky, 2003).

Reliability between histological scoring methods of cartilage damage based on the Janusz method (Janusz et al., 2002) or modified OARSI score (Pritzker et al., 2006) was reported using a Bland-Altman plot (Bland and Altman, 1986). To construct a Bland-Altman plot, the difference between scoring methods (Janusz and OARSI) by an observer was plotted on the y-axis against the average total between scoring methods on the x-axis. Systematic error in terms of bias (mean difference) and random error in terms of precision (Mean \pm 2SD) were also calculated to determine agreements between scores (Hanneman, 2008).

5.4 RESULTS

Two studies were carried out in this chapter. Study 1 investigated the effect of intra-articular 0.1mg and 1mg of MIA for 20 days, while study 2 went up to 42 days for only the 0.1mg MIA injected rats.

5.4.1 Effects of a low 0.1mg and standard 1mg MIA dose

5.4.1.1 Body weight

There was a gradual increase in the weights of all the rats irrespective of the MIA dose or saline injection administered (Fig. 5.3A and B).

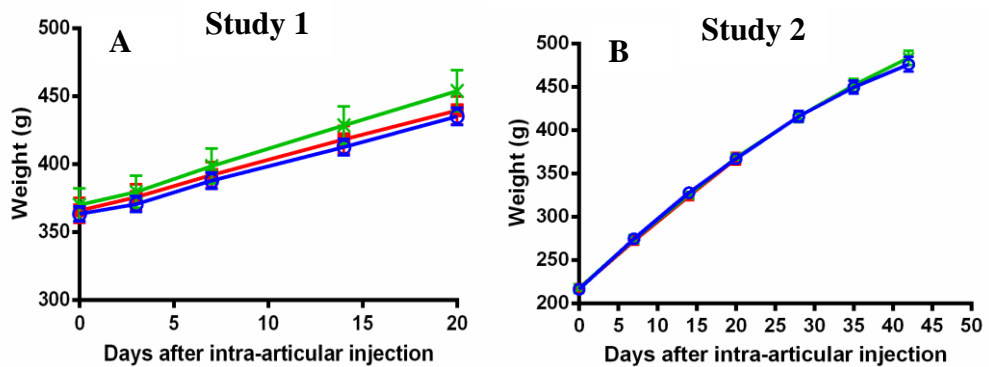


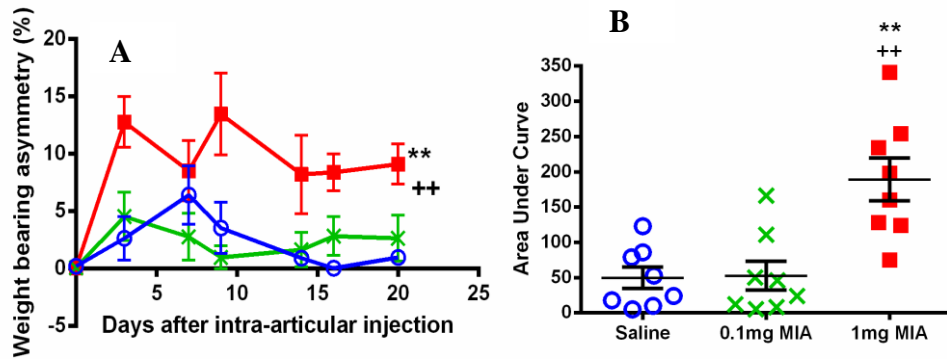
Figure 5.3 Time course of weight gain of rats.

Gradual increase in weight with intra-articular injection of MIA or saline. Study 1 shows data for all groups to day 20 while study 2 shows data for 1mg MIA group to day 20 and the other groups to day 42. Data are mean \pm SEM of weights from 1mg MIA (■), 0.1mg MIA (x) and saline (○) injected rats (n = 8 or 10/group).

5.4.1.2 Intra-articular injection of MIA induces changes in pain behaviour; pain phenotypes depend on severity of disease

Intra-articular injection of 1mg of MIA increased pain behaviour; both an increase in weight bearing asymmetry (1mg; 189 [118 - 261] v saline; 49.8 [14 - 85.5] p<0.01) (Fig. 5.4 A and B) and lowered hind paw withdrawal threshold (1mg; 187 [160 - 215] v saline; 282 [265 - 298] p<0.01) (Fig. 5.5 A and B). Similar results were observed in a subsequent study (Fig. 5.4 C and D, Fig 5.5 C and D). Intra-articular injection of 0.1mg MIA was associated with lowered hind paw withdrawal threshold (0.1mg; 187 [115 - 259] v saline; 282 [265 - 298] p<0.05) in the absence of pronounced weight bearing asymmetry (0.1mg; 52.8 [4.79 - 101] v saline; 49.8 [14 - 85.5] ns) (Fig 5.4 A and B, 5.5 A and B). Similar results were observed in a subsequent (Fig. 5.4 C and D, Fig 5.5 C and D).

Study 1



Study 2

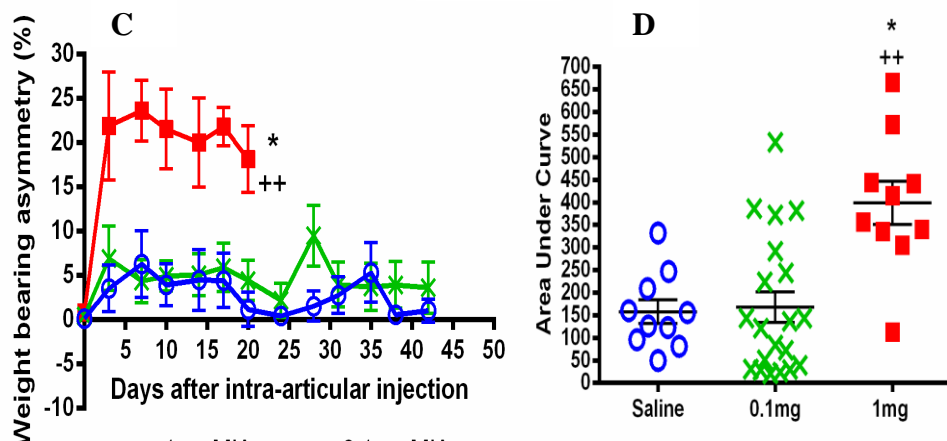


Figure 5.4 Effects of MIA on weight bearing asymmetry

Intra-articular injection of 1mg of MIA induced pain behaviour measured as hind-limb weight bearing asymmetry (A&C). B & D indicate area under the curve data for weight bearing asymmetry. Intra-articular injection of 0.1mg of MIA resulted in minimal weight bearing asymmetry comparable to saline injected control rats (A&C). Study 1 shows data for all groups to day 20 while study 2 shows data for 1mg MIA group to day 20 and the other groups to day 42. Data are expressed as mean \pm SEM, 1mg MIA (■), 0.1mg MIA (x) and saline (○) injected rats (n = 8 or 10/group). Differences between groups were analysed using the area under the curve (A and C) over the time course of the study followed by Kruskal Wallis test with a Dunn's post hoc analysis (B and D). * $p < 0.05$, ** $p < 0.01$ (1mg MIA v saline), ++ $p < 0.01$ (1mg MIA v 0.1mg MIA).

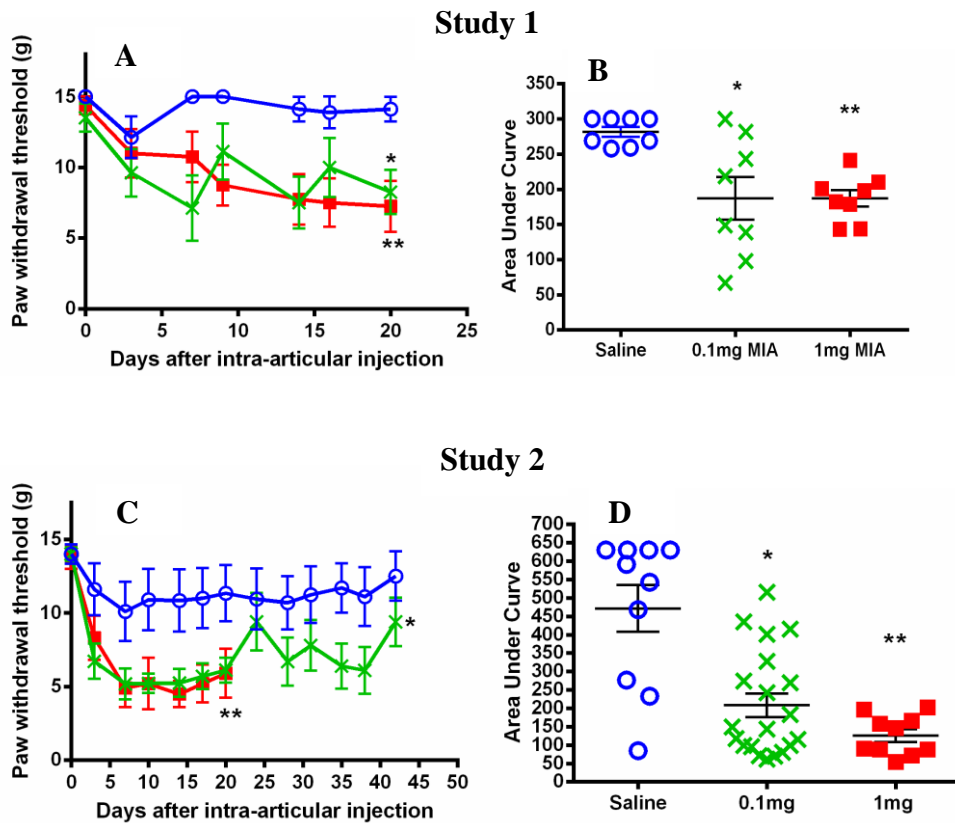


Figure 5.5 Effects of MIA on paw withdrawal threshold

Intra-articular injection of 1mg or 0.1mg of MIA resulted in lowered hind paw withdrawal threshold indicative of allodynia.). B & D indicate area under the curve data for paw withdrawal thresholds. Study 1 shows data for all groups to day 20 while study 2 shows data for 1mg MIA group to day 20 and the other groups to day 42. Data are expressed as mean \pm SEM, 1mg MIA (■), 0.1mg MIA (x) and saline (○) injected rats (n = 8 or 10/group). Differences between groups were analysed using the area under the curve (A and C) over the time course of the study followed by Kruskal Wallis test with a Dunn's post hoc analysis (B and D). * $p < 0.05$, ** $p < 0.01$ (1mg MIA or 0.1mg MIA v saline).

5.4.1.3 Inflammation

Acute inflammation was observed as joint swelling, synovitis and macrophage infiltration into the synovium. Small increases in knee diameter were observed at day 1 following intra-articular MIA injection but did not differ from saline injected control rats (Fig. 5.6A and B). However at day 3, significant differences were observed between MIA and saline injected rats (Fig. 5.6B). Joint swelling returned to baseline levels for all rats by 2 weeks (Fig. 5.6A and B). Intra-articular injection of MIA was associated with increased synovitis detected by histological examination of haematoxylin and eosin stained tissue sections (Figs 5.6C and D) and infiltration by macrophages (Fig 5.6E and F) into the synovium. Synovitis scores 20 days after intra-articular injection of 1mg of MIA [2.5 (2 to 3) Fig. 5.6C], [2 (1 to 3) Fig. 5.6D] and 42 days after intra-articular injection of 0.1mg of MIA [3 (0 to 3) Fig 5.6D] were significantly higher compared to saline injected non-arthritic controls [0 (0 to 2) $p<0.01$ Fig. 5.6C], [1 (0 to 1.3) $p<0.05$, $p<0.001$ Fig. 5.6D]. Macrophage fractional area 20 days after intra-articular injection of 1mg of MIA [16 (11 to 22) Fig. 5.6E], [13 (7.8 to 17) Fig. 5.6F] was significantly higher compared to saline injected [7.1 (2.9 to 11) $p<0.05$ Fig. 5.6E], [4.1 (1.4 to 6.7) $p<0.05$ Fig 5.6F] and 0.1mg MIA injected rats [7.8 (5.1 to 11) $p<0.05$ Fig 5.6E]. Macrophage fractional area 42 days after intra-articular injection of 0.1mg of MIA [16 (11 to 22) Fig. 5.6F] was significantly higher compared to saline injected rats [4.1 (1.4 to 6.7) $p<0.001$ Fig. 5.6F].

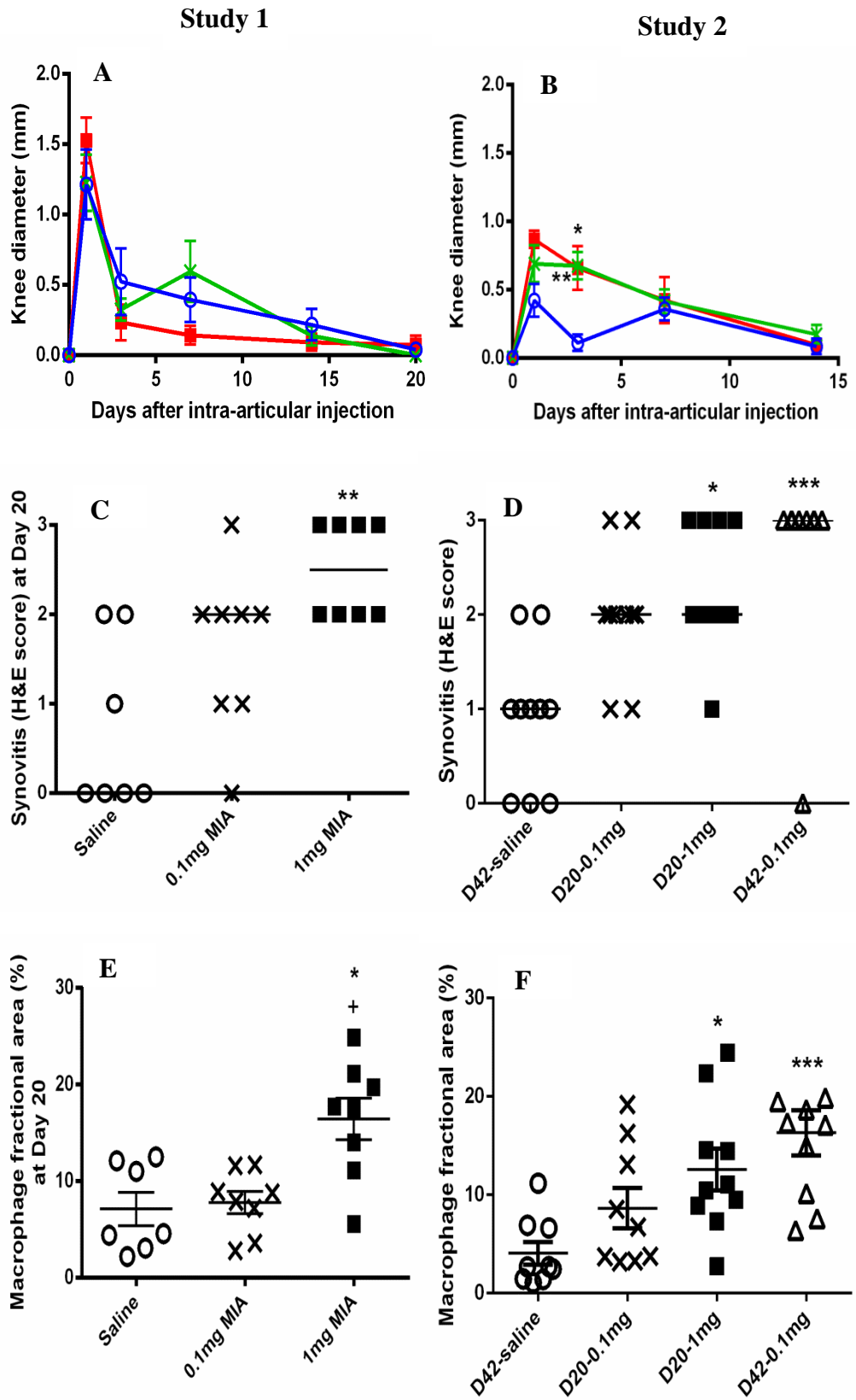


Figure 5.6

Figure 5.6 Evidence of inflammation 20 and 42 days after OA induction.

Study 1 shows data for all groups to day 20 while study 2 shows data for 0.1mg and 1mg MIA groups to day 20 and the saline and 0.1mg groups to day 42. Small changes in knee diameter observed after intra-articular injection of MIA or saline (A and B). Knee joint diameters for MIA injected rats were significantly different to those of saline injected rats (B). Synovitis observed following intra-articular MIA injection was significantly higher in the 1mg MIA injected rats at day 20 (C and D) and 0.1mg MIA injected rats at day 42 (D) compared to saline injected non-arthritic controls. Significantly higher macrophage infiltration into the synovium following 1mg MIA injection at day 20 compared to saline injected (E and F) and 0.1mg MIA injected rats (E). Macrophage infiltration was also observed to be significantly higher in the 0.1mg MIA injected rats at day 42 compared to saline injected rats (F). Data are expressed as mean \pm SEM or median, 1mg MIA (■), 0.1mg MIA (x or Δ) and saline (○) injected rats (n = 8 or 10/group). Differences between groups were analysed using the Kruskal Wallis test with a Dunn's post hoc analysis. *p<0.05, **p<0.01, ***p<0.001 D20-1mg MIA or D42-0.1mg MIA v saline. +p<0.05 D20-1mg MIA v D20-0.1mg MIA.

Synovitis

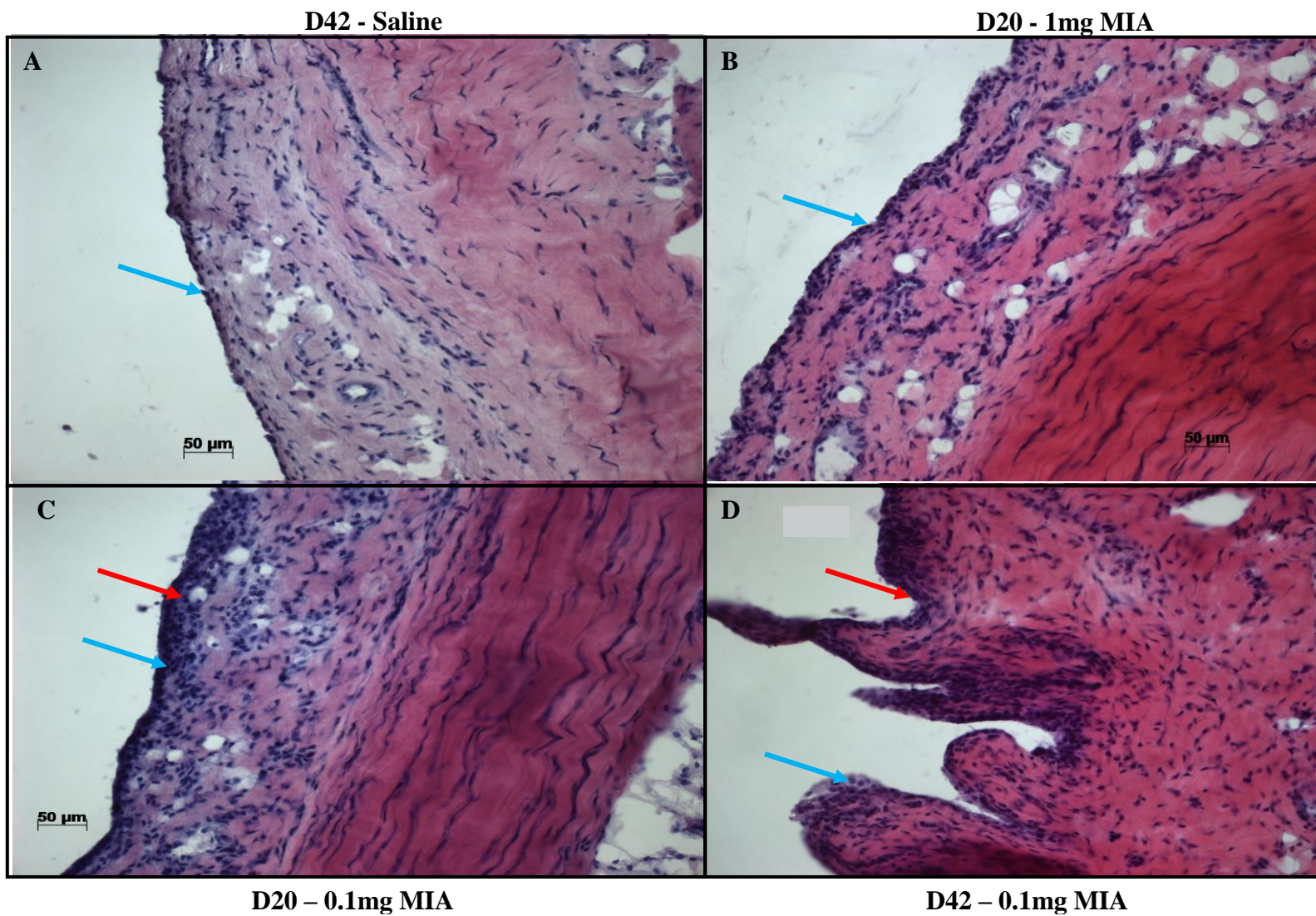
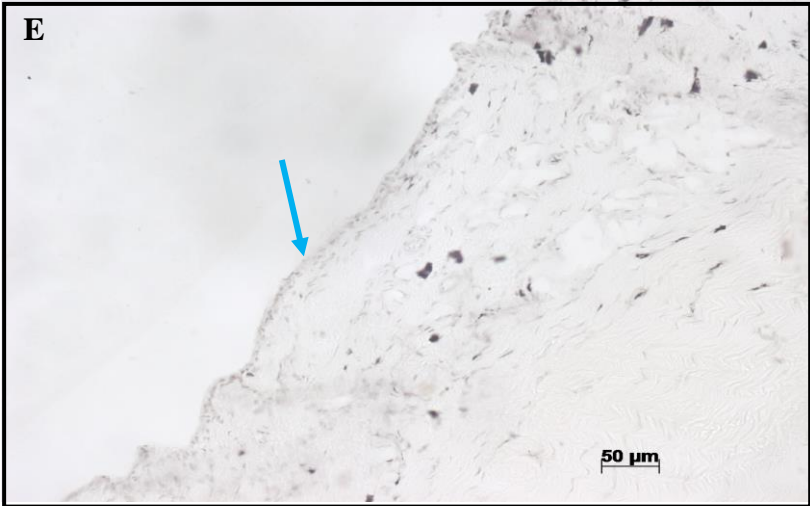


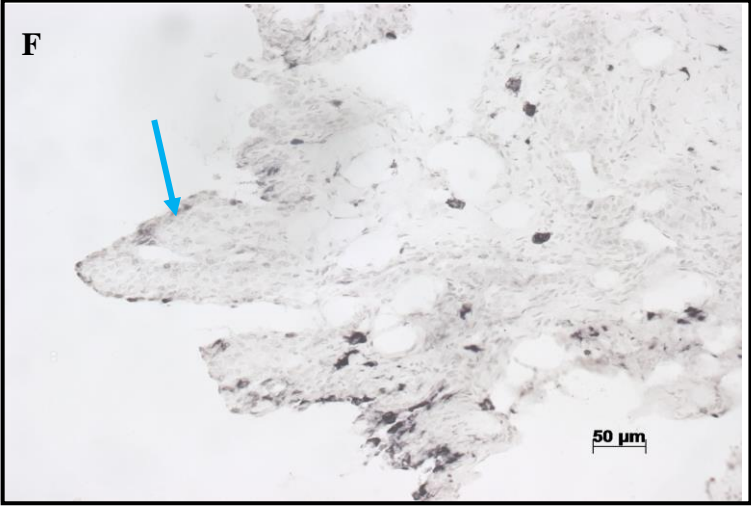
Figure 5.7

Synovial macrophage infiltration

D42 - Saline



D20 - 1mg MIA



D20 - 0.1mg MIA



D42 - 0.1mg MIA



Figure 5.7

Figure 5.7 Mild persistent synovitis is a feature both of standard and low dose MIA model

Synovitis characterised as synovial lining thickness/cellularity (A-D) and macrophage infiltration (E-H). Extensive synovia proliferation (red arrows) in the day 20-1mg and day 42-0.1mg MIA-induced OA rats (C & D) compared with non-arthritic controls (A). Photomicrographs show synovial lining (blue arrows) and cellularity as indicated by the haematoxylin and eosin stain (A-D). Macrophage infiltration-black dots indicate immunoreactivity for CD68, using monoclonal antibody ED1; E-H. Photomicrographs show haematoxylin and eosin stained sections of synovium from a rat with the median synovitis score and mean macrophage fractional area from each group. Scale bar = 50µm.

5.4.1.4 Osteochondral pathology

Intra-articular injection of 0.1mg or 1mg of MIA resulted in structural OA phenotypes as indicated by cartilage damage (microscopic and macroscopic), abnormal chondrocyte morphology, loss of osteochondral junction integrity and matrix proteoglycan loss (Fig. 5.8, Table 5.1 and 5.2). Irrespective of the dose of MIA, cartilage damage, abnormal chondrocyte morphology and proteoglycan loss were significantly higher in these rats compared to the saline-injected non-arthritic controls (Table 5.1; study 1). In study 2, irrespective of the dose of MIA or the duration of MIA (20 and 42 days), macroscopic chondropathy, cartilage damage and abnormal chondrocyte morphology were significantly higher in these rats compared to the saline-injected non-arthritic controls (Table 5.2). Proteoglycan loss was significantly higher only in the day 20 1mg MIA injected rats compared to the saline injected rats (Table 5.2). Vascular channels crossing the osteochondral junction were not significantly different between the groups at day 20 (Table 5.1; study 1) but were significantly higher in the day 20 0.1mg and day 20 1mg MIA injected rats compared to the day 42 saline injected rats and day 42 0.1mg MIA injected rats (Table 5.2; study 2).

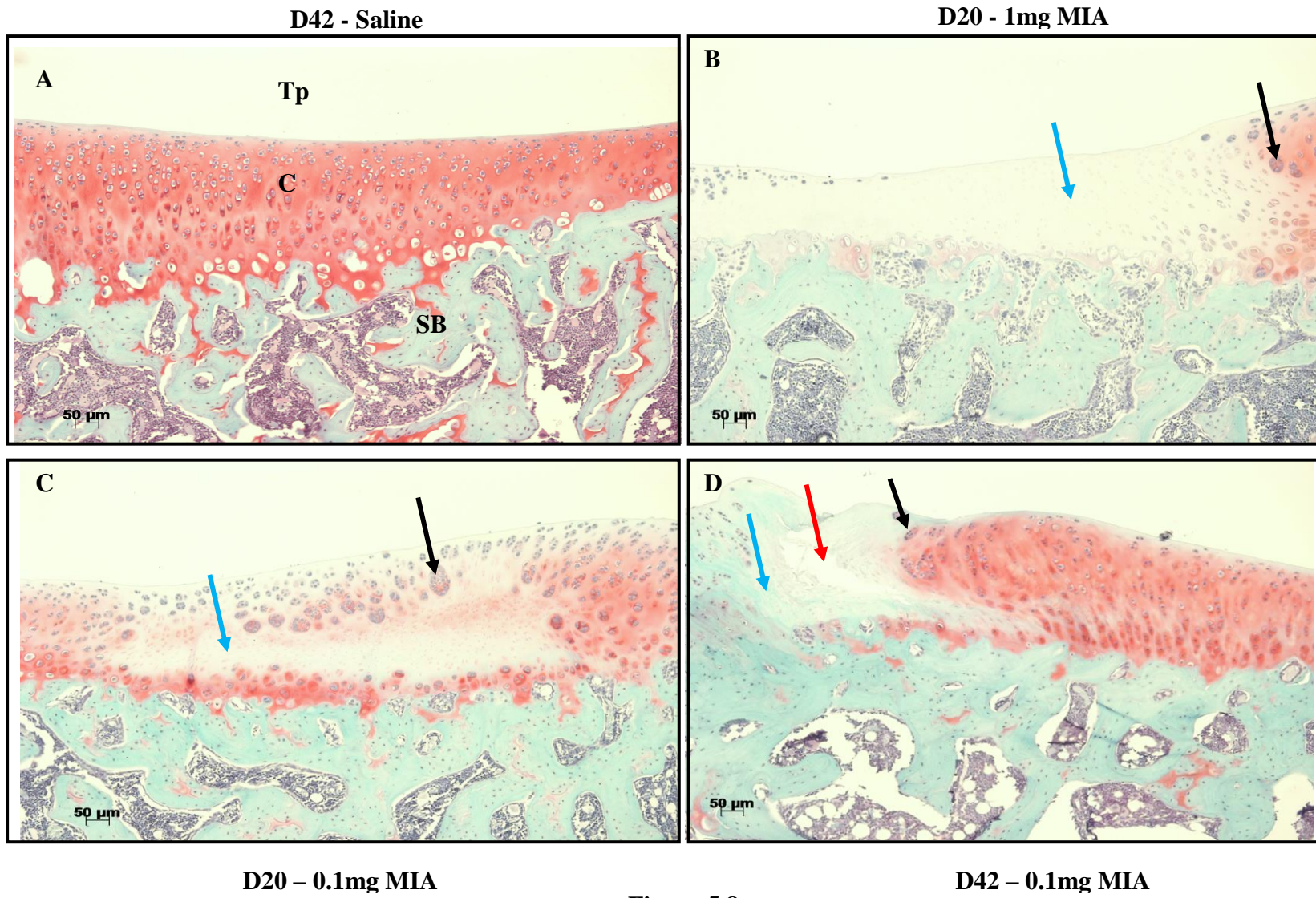


Figure 5.8

Figure 5.8 Structural changes in the articular cartilage in the MIA model

Histological changes of Safranin-O Fast green stained sections showing structural pathology presented as cartilage damage, abnormal morphology of chondrocytes and proteoglycan loss (A-D). Saline-injected control (A) showing smooth cartilage including normal chondrocyte morphology. B & C, 1mg and 0.1mg MIA-treated rats showing thinning of cartilage in weight bearing areas (asterisk), complete chondrocyte death (hypocellularity) (blue arrow) and chondrocyte cloning (black arrow). 0.1mg rat (D) showing cartilage fibrillations (red arrow), hypocellularity (blue arrow) and cloning (black arrow). All arthritic groups (B-D) show loss of proteoglycan content as seen as reduction in staining intensity (red colour) compared to saline controls (A). Photomicrographs (A-D) show tibial plateau from a rat with the median pathology from each group. Tibial plateau (Tp), cartilage (C), subchondral bone (SB). Scale bar = 50 μ m.

Table 5.1 Pathological features in articular cartilage and subchondral bone 20 days after intra-articular injection of MIA (study 1)

Structural changes	D20-Saline	D20-1mg MIA	D20-0.1mg MIA
Cartilage damage	0.38 (0.21 - 1)	2.6 (2.2 – 4.2)***	2.1 (1.6 – 2.8)**
Chondrocyte morphology	0.48 (0.3 – 0.58)	2.2 (1.9 - 2.7)**	2.3 (1.5 – 2.6)**
Osteochondral junction integrity	0.5 (0.33 - 0.7)	0.4 (0.4 – 0.58)	0.5 (0.4 – 0.83)
Proteoglycan loss	1.8 (1.4 - 2.5)	2.7 (2.2 - 3.3)**	2.6 (1.9 – 3.2)*

Histological changes showing structural pathology presented as cartilage damage, abnormal morphology of chondrocytes, channels crossing the osteochondral junction and proteoglycan loss data. Data are presented as median (IQR), * $p < 0.05$, ** $p < 0.01$, *** $p < 0.001$ (all MIA groups v saline).

Table 5.2 Pathological features in articular cartilage and subchondral bone 20 and 42 days after intra-articular injection of MIA (study 2)

Structural changes	D42-Saline	D20-1mg MIA	D20-0.1mg MIA	D42-0.1mg MIA
Macroscopic chondropathy	3.5 (1 - 5.3)	10 (8.5 - 13)***	9 (7 - 11)**	8.5 (7.8 -12)**
Cartilage damage	0.6 (0.18 - 1)	1.8 (1.2 - 4)*	2 (0.83 - 4)**	3 (1.3 - 4)***
Chondrocyte morphology	0.67 (0 – 1.4)	1.8 (1.5 - 2.3)***	2 (1.3 - 2)***	1.7 (0.83 - 2)*
Osteochondral junction integrity	0.5 (0.4 - 0.65)	1.2 (0.92 - 1.4)** ++	1.5 (1.2 - 1.7)**** +++++	0.51 (0.39 -0.87)
Proteoglycan loss	2 (1.2 - 2.5)	2.8 (2.2 - 3.2)**	2.7 (2 - 3)	2 (1.8 - 2.8)

Histological changes showing structural pathology presented as cartilage damage, abnormal morphology of chondrocytes and proteoglycan loss in pictures (Fig.5.8), including macroscopic chondropathy and channels crossing the osteochondral junction data. Data are presented as median (IQR), *p<0.05, **p<0.01, ***p<0.001 (all MIA groups v saline) and ++p<0.01, +++p<0.001 (d20-1mg MIA or d20-0.1mg MIA v d42-0.1mg MIA).

5.4.2 Heterogeneity of OA pathology in the MIA model

Histological scoring of haematoxylin and eosin stained sections for OA structural pathology indicates heterogeneity in the MIA model.

Cartilage damage scored using the Janusz method of scoring was observed to be significantly higher in the ipsilateral posterior (IpP) sections of the day 20 MIA injected rats compared to their corresponding ipsilateral anterior (IpA) sections (Fig. 5.9D). Anterior (IpA) cut sections did not show significant differences between the day 20 MIA injected rats compared to the day 42 saline injected rats (Fig. 5.9A), whereas significant differences were observed in the ipsilateral posterior (IpP) cut sections of the same groups (Fig. 5.9B). When IpA and IpP sections were combined, the total joint scores were significantly different for all MIA groups compared to the saline group of injected rats (Fig. 5.9C). Although the day 42 0.1mg MIA group posterior (IpA) sections were significantly different to the day 42 saline injected (IpA) group, unlike the day 20 MIA group, the cartilage damage scores in the day 42 0.1mg MIA IpP sections were not significantly higher than their corresponding IpA sections (Fig. 5.9D).

Chondrocyte morphology scores for the IpA sections were not significantly different to their corresponding IpP sections (Fig 5.10D), but the scores from the IpP sections only were observed to be significantly higher in the day 20 1mg MIA injected rats compared to day 42 saline injected rats (Fig 5.10A and B). Significant differences were observed for day 20 0.1mg MIA injected rats compared to day 42 saline injected rats in both IpA and IpP cut sections (Fig 5.10A and B). When IpA and IpP sections were combined, the total joint scores for chondrocyte morphology were significantly different for all MIA groups compared to the saline group of injected rats (Fig. 5.10C).

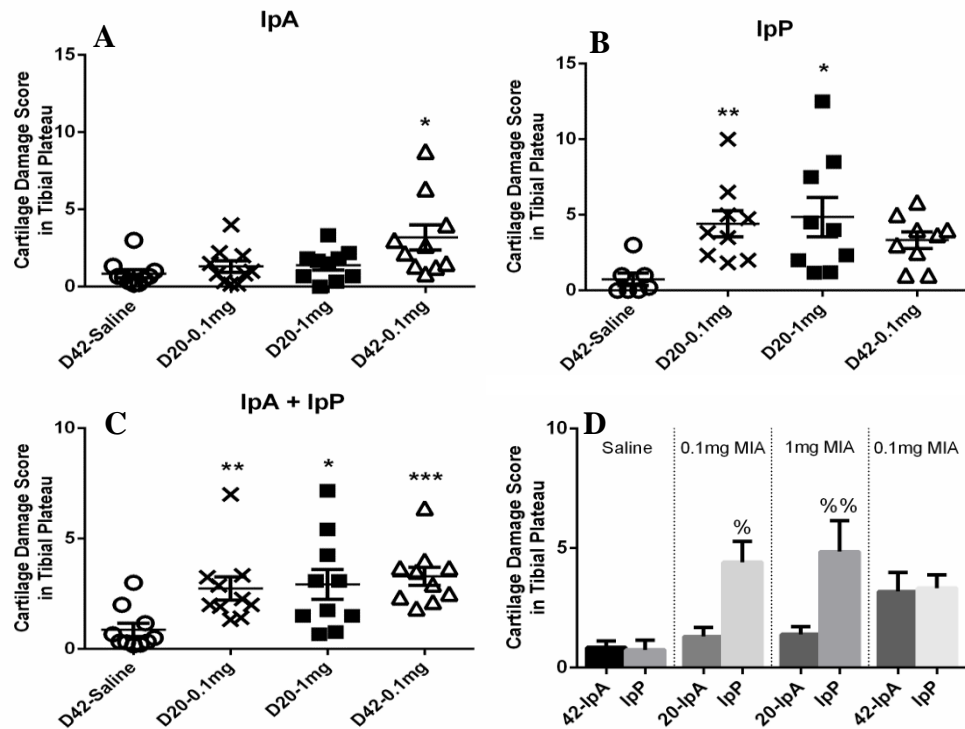


Figure 5.9 IpA and IpP scores for cartilage damage in the MIA model

Significantly higher cartilage damage scores for the day 42-0.1mg MIA injected rats only compared to saline injected rats using IpA sections (A). Significantly higher cartilage damage scores for the day 20-MIA injected rats only compared to saline injected rats using IpP sections (B). Significantly higher cartilage damage scores for all the MIA injected rats compared to saline injected rats for both IpA and IpP sections (C). Significantly higher cartilage damage scores for the IpP-d20-MIA injected rats compared to the corresponding IpA sections (D). Data are expressed as mean \pm SEM, d20-1mg MIA, d20-0.1mg MIA, d42-0.1mgMIA and saline injected rats (n = 10/group). Differences between groups were analysed using the Kruskal Wallis test with a Dunn's post hoc analysis (A-C) or a Wilcoxon matched-pairs signed rank test (D). * $p < 0.05$, ** $p < 0.01$, *** $p < 0.001$ MIA v saline (A-C). % $p < 0.05$, %% $p < 0.01$ IpA v IpP (D).

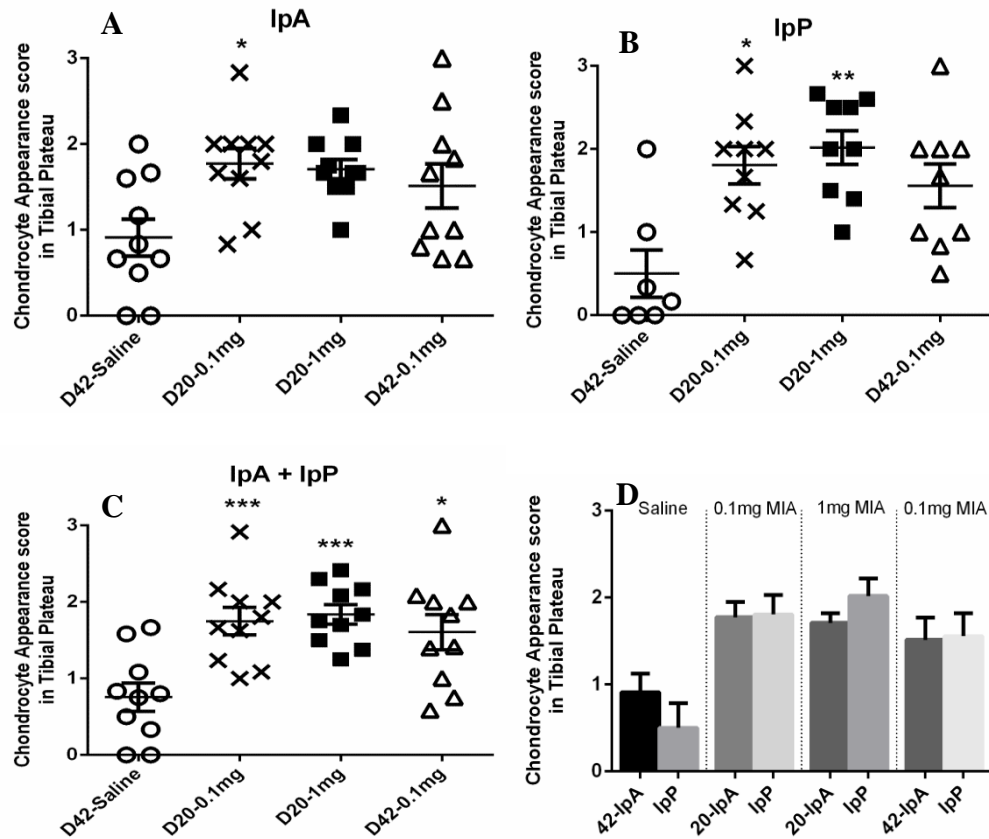


Figure 5.10 IpA and IpP scores for chondrocyte morphology in the MIA model

Significantly higher abnormal chondrocyte appearance scores for the day 20-0.1mg MIA injected rats only compared to saline injected rats using IpA sections (A). Significantly higher abnormal chondrocyte appearance scores for the day 20-MIA injected rats only compared to saline injected rats using IpP sections (B). Significantly higher abnormal chondrocyte appearance scores for all the MIA injected rats compared to saline injected rats for both IpA and IpP sections (C). Data are expressed as mean \pm SEM, d20-1mg MIA, d20-0.1mg MIA, d42-0.1mgMIA and saline injected rats (n = 10/group). Differences between groups were analysed using the Kruskal Wallis test with a Dunn's post hoc analysis (A-C). * $p < 0.05$, ** $p < 0.01$, *** $p < 0.001$ MIA v saline (A-C).

5.4.3 Reliability of histological scoring systems

Reliability measurements were carried out on histological scoring of cartilage damage (Janusz and modified OARSI methods), chondrocyte morphology, osteochondral junction integrity and proteoglycan loss in the cartilage between four investigators. 20 knee joint sections were scored by one investigator (LN) and scoring results compared to the other three investigators (PG, JH and SS). Table 5.3 summarises the analysis for inter observer agreement. The Cronbach's alpha values for the examined parameters (cartilage damage (Janusz and modified OARSI methods), chondrocyte morphology, osteochondral junction integrity and proteoglycan loss) are within the range of 0.55-0.99 with the matching unweighted κ varying from slight to moderate agreement (0.04-0.55) and the weighted κ varying from fair to almost perfect agreement (0.24-0.85).

Chondrocyte morphology scoring was observed to have the lowest Cronbach's alpha value (0.55) while cartilage damage scoring had the highest value (0.99 respectively) (Table 5.3). Osteochondral junction integrity had the lowest unweighted and weighted κ values ranging from slight to moderate agreement (0.04-0.24), while cartilage damage had the highest unweighted and weighted κ values ranging from moderate to almost perfect agreement (0.55-0.85) (Table 5.3).

Investigating the Janusz and modified OARSI histological scoring methods for cartilage damage by one observer (LN) showed statistical significant differences between the arthritic groups compared to their normal saline injected controls (Fig. 5.12A and B). These two methods were also observed to be positively correlated to each other (Fig. 5.12C) and showed no systematic differences to each other as shown by the Bland-Altman plot (Fig 5.12D).

Table 5.3 Inter observer agreement between four histological scoring investigators as measured by two different statistical methods

Reliability (Cronbach's Alpha) v Scorer1	Scorer2	Scorer3	Scorer 4
Cartilage damage (Janusz)	0.99	0.99	NA
Cartilage damage (OARSI)	NA	NA	0.83
Chondrocyte appearance	0.55	0.81	0.84
Number of channels crossing the OCJ	0.8	0.79	NA
Proteoglycan score	0.63	0.84	0.95
Cohen's unweighted kappa v Scorer1	Scorer2	Scorer3	Scorer 4
Cartilage damage (Janusz)	0.55	0.46	NA
Cartilage damage (OARSI)	NA	NA	0.2
Chondrocyte appearance	0.21	0.34	0.31
Number of channels crossing the OCJ	0.04	0.1	NA
Proteoglycan score	0.22	0.34	0.41

Cohen's weighted kappa v Scorer1	Scorer2	Scorer3	Scorer 4
Cartilage damage (Janusz)	0.85	0.79	NA
Cartilage damage (OARSI)	NA	NA	0.5
Chondrocyte appearance	0.26	0.32	0.5
Number of channels crossing the OCJ	0.44	0.24	NA
Proteoglycan score	0.46	0.58	0.74

The closer to 1 the Cronbach's alpha, the higher the consistency of scoring. K was defined as less than chance agreement if < 0 , slight agreement = 0.01-0.20, fair agreement = 0.21-0.40, moderate agreement = 0.41-0.60, substantial agreement = 0.61-0.80, and almost perfect agreement = 0.81-0.99. OCJ – osteochondral junction. Scorer1-LN, scorer2-PG, scorer3-JH, scorer4-SS.

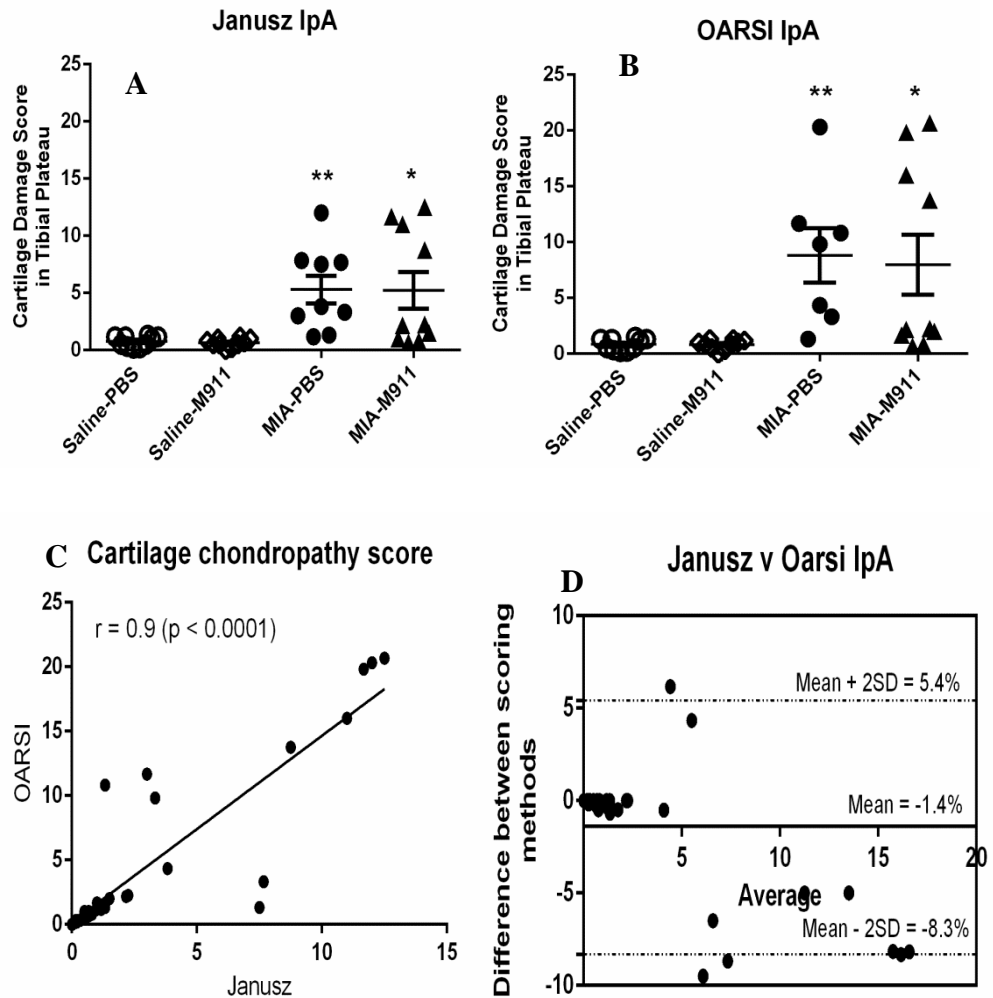


Figure 5.11 Cartilage chondropathy in the MIA model as scored by the Janusz and modified OARSJ classification methods.

Janusz method of scoring (A) shows similar results to the OARSJ classification method (B) and correlates with it (C). D, Bland-Altman plot illustrating agreement between the Janusz and OARSJ scoring methods by an observer. The 95% limits of agreement for the Bland-Altman plot contains 93% (37/40) of the difference scores (D). Mean+2SD (upper limit of agreement), Mean-2SD (lower limit of agreement), Mean (bias – average of the difference values), values outside the limits of agreements are outliers and values within limits of agreements are individual difference values. Scatter plots show mean \pm SEM of $n = 10$ rats/group of their ipsilateral anterior (IpA) sections. Scatter plots with regression line show Spearman's correlation coefficient. * $p < 0.05$, ** $p < 0.01$ MIA-PBS or MIA-M911 versus saline-PBS controls. M911 – anti-NGF monoclonal antibody (more information can be found in chapter 6).

5.4.4 Comparison between Safranin-O and Alcian blue in the detection of matrix proteoglycan

Knee joint sections stained with Safranin-O Fast green or Alcian blue-PAS were scored in order to investigate the sensitivity of these stains to detect proteoglycan content in the cartilage matrix. Proteoglycan loss was scored as the loss of red staining or its intensity (Safranin-O) or loss of blue staining or its intensity (Alcian blue-PAS). A high proteoglycan score equals a high proteoglycan loss or loss of staining intensity. Loss of Safranin-O was significantly higher in the MIA (0.1mg and 1mg) injected rats compared to the saline injected non-arthritic controls as observed in the Safranin-O Fast green stained sections (Fig. 5.13A). Loss of Alcian blue was significantly higher in the 1mg MIA injected rats only compared to the 0.1mg MIA and saline injected rats as observed in the Alcian blue-PAS stained sections (Fig. 5.13B). Comparing both staining methods showed that there was significantly higher loss of Safranin-O in the Safranin-O Fast green stained sections for all groups of rats compared to the loss of Alcian blue in the Alcian blue-PAS stained sections (Fig. 5.13C).

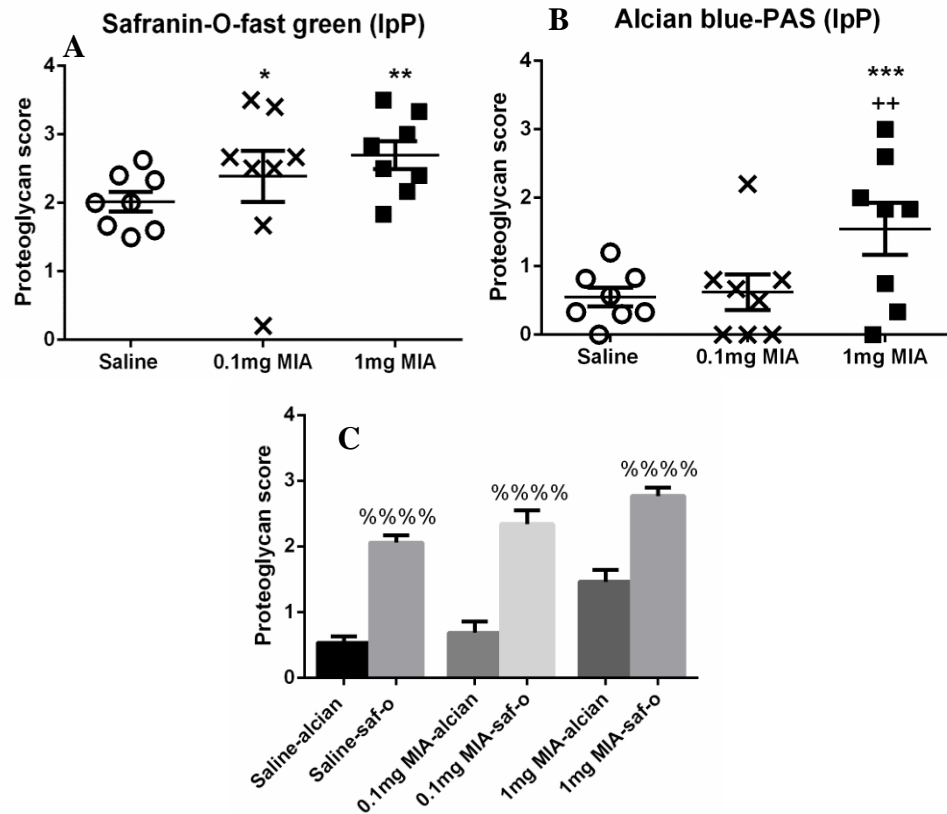


Figure 5.12 Proteoglycan content in the cartilage matrix of the MIA model, comparing the Safranin-O Fast green stain to the Alcian blue-PAS stain

Significantly higher proteoglycan loss (score) for the day 20 MIA (0.1mg and 1mg) injected rats compared to day 20 saline injected rats using Safranin-O Fast green stain (A). 1mg MIA injected rats had a significantly higher loss of proteoglycan compared to the 0.1mg MIA and saline injected rats using Alcian blue-PAS stain (B). Significantly higher proteoglycan loss for the Safranin-O Fast green stained sections compared to the Alcian blue-PAS stained sections (C). Data are expressed as mean \pm SEM (n = 8/group). Differences between groups were analysed using the Kruskal Wallis test with a Dunn's post hoc analysis (A and B) or a Wilcoxon matched-pairs signed rank test (C). *p<0.05, **p<0.01, *** or ****p<0.001 MIA v saline (A and B). %%%p<0.001 alcian v saf-o (C). Ipsilateral posterior (IpP).

5.5 DISCUSSION

The MIA model displays characteristic features of symptomatic knee OA as indicated by pain related behaviours (increased weight bearing asymmetry and reduced hind paw withdrawal threshold), inflammation and joint (macroscopic and microscopic) pathology (Liu et al., 2011, Mapp et al., 2013, Ashraf et al., 2014, Guingamp et al., 1997).

Intra-articular injection of the cellular glycolytic inhibitor MIA brings about pathology by inhibiting the enzyme glyceraldehyde-3-phosphate dehydrogenase (GAPDH) which is responsible for the breakdown of glucose to release energy. This results in lowering chondrocyte metabolism and eventually leads to chondrocyte cell death (Kalbhen, 1987, van der Kraan et al., 1989). Pathological changes to the knee joint begin to occur as a result of progressive loss of chondrocytes (hypocellularity). This includes fibrillations and thinning or loss of the cartilage matrix.

In this chapter, two doses (0.1mg and 1mg) and two time points (day 20 and 42) were examined. The 0.1mg MIA injected rats were sacrificed at either day 20 or day 42 but the 1mg MIA injected rats were all sacrificed at day 20. The reason for this is because the 1mg dose is a widely explored dose, with published reports of pain behaviour and structural pathology from 2 weeks post OA induction. One of the criteria for this thesis was to carry out experiments on a reduced number of rats, while limiting the pain, suffering and distress caused to the rats hence the shorter time point (day 20) for the 1mg MIA dose.

5.5.1 Symptomatic features of OA in the MIA model

Chondropathy is a hallmark of human OA (Walsh et al., 2008). In this study it was observed that both the lower dose (0.1mg) and standard dose (1mg) of MIA showed alterations in pathology which were significantly different to the saline injected non-arthritic rats (Guingamp et al., 1997, Guzman et al., 2003). Cartilage pathology measured by macroscopic scoring or on histological sections did not significantly differ between doses (0.1mg or 1mg) or between duration of OA disease (day 20 and 42). This lack of difference may have been

because this model is a rapidly progressive model and pathology is already established by day 20 (Sagar et al., 2010, Bove et al., 2009). Likewise changes to chondrocyte morphology which is a major feature of this model did not significantly differ between doses or duration of disease. On the other hand the osteochondral junction integrity measured as the number of vessels crossing the osteochondral junction into the calcified cartilage / mm length of cartilage was significantly lower (i.e. the lower the integrity, the more channels crossing the osteochondral junction and vice versa) in the day 20-MIA injected rats compared to the day 42-0.1mg MIA and day 42-saline injected non-arthritic rats in study 2. In study 1 the osteochondral junction integrity was not significantly different between the groups (0.1mg, 1mg and saline) at day 20 i.e. each group of rats had a similar density of vascular channels crossing the osteochondral junction.

The adult healthy cartilage is known to be avascular (Takebe et al., 2014, Hunter et al., 2009), but in OA, vascular growth by angiogenesis has been reported to occur at the osteochondral junction and hence the cartilage is no longer avascular (Walsh et al., 2007, Suri et al., 2007). The findings from the current studies are in line with published work by Mapp et al 2013 which showed a reduction in the number of vascular channels crossing the osteochondral junction (i.e. higher osteochondral junction integrity) with time in the MIA model (Mapp et al., 2013). Increased densities of vascular channels crossing the osteochondral junction may suggest new vessel growth with subchondral bone remodelling. Increased vascular channels may be a source of pain in OA with reports of sensory nerves growing alongside blood vessels in vascular channels associated with angiogenesis (Walsh et al., 2010). It has been reported that angiogenesis may contribute to pain in OA (Ashraf et al., 2011a). The bisphosphonate Zoledronate was reported to reduce pain in both the MIA and medial meniscal tear (MMT) models of OA and one of the potential mechanisms might be through improving subchondral bone integrity as Zoledronate was observed to partially restore bone mineral density and improve subchondral bone remodelling (Strassle et al., 2010, Yu et al., 2012).

Inflammation in the synovium is a feature of human knee OA (Wenham and Conaghan, 2010, Scanzello and Goldring, 2012). Inflammation in the MIA

model includes mild joint swelling which is seen in the early phase of the model, synovial thickening and infiltration into the synovium by immune cells such as macrophages (Bove et al., 2003, Clements et al., 2009). In this study, intra-articular MIA injection either 0.1mg or 1mg did induce an increase in joint swelling which subsided within 7-14 days. Extensive synovial proliferation and increased thickening of the lining layer in both the day 20-1mg and day 42 0.1mg MIA dose were observed. A similar result was observed for macrophage infiltration into the synovium. These results are in-line with data in the literature that showed persistent synovial inflammation in rats injected with 1mg MIA at day 21 (Clements et al., 2009). Synovitis persisting where joint swelling subsides may suggest a move from acute inflammation to chronic inflammation in the standard 1mg dose and the increase in duration for the low dose (d42-0.1mg) making it more persistent. It might also suggest site specificity or localisation of synovitis. Synovitis located at joint margins was reported to subside within 7-14 days post 1mg MIA injection (Bove et al., 2003), this corresponds to reduced joint swelling. In this chapter, synovitis was scored at the infrapatellar fat pad and at this location, synovitis was found to still be present at 20 days post MIA injection.

Peripheral sensitization is a process that can occur as a result of increased activity from peripheral nociceptors by inflammation or joint pathology (Neogi et al., 2013). Increased input from peripheral nociceptors may in turn contribute to central sensitization (Woolf, 2011). Central sensitization increases pain hypersensitivity in inflamed tissue, produces hypersensitivity in non-inflamed tissue (spread of pain) and sustains pain sensitivity after initiating injury is long gone (Latremoliere and Woolf, 2009, Woolf, 2011).

Weight bearing asymmetry, an indicator of standing pain is brought about by the tendency to lean away or put less weight on the affected joint in OA (Christiansen and Stevens-Lapsley, 2010). This phenomenon does occur in animals with unilateral joint injury and can be measured (Bove et al., 2003). Weight bearing asymmetry is associated with peripheral and central sensitization (Graven-Nielsen and Arendt-Nielsen, 2002). On the other hand, mechanical thresholds which indicate widespread pain for example in the affected and non-affected limb (Arendt-Nielsen et al., 2010) can also be

measured in animals (Sagar et al., 2010) and suggests a contribution of central sensitization (Suokas et al., 2012, Graven-Nielsen and Arendt-Nielsen, 2002).

Intra-articular injection of MIA into the knee joint led to a dose dependent increase in pain behaviour as observed as a change in hind limb weight bearing asymmetry. This change in weight bearing asymmetry was only observed following intra-articular injection of 1mg of MIA. This is similar to already published data which have used this dose or higher to represent late severe OA (Kelly et al., 2013b, Combe et al., 2004, Liu et al., 2011). On the other hand the 0.1mg (lower) MIA dose showed minimal changes in weight bearing asymmetry comparable to the saline injected non-arthritic control rats. A similar result of 0.3mg dose not altering weight bearing asymmetry was reported by Sagar et al, (Sagar et al., 2010), although this was not the case reported by another publication using the 0.1mg dose (Bove et al., 2003). The reason for the low dose (0.1mg) MIA not showing any weight bearing asymmetry until the end of the study (day 42) even though they were seen to present with joint pathology is not clear. Joint pathology may contribute to peripheral sensitization which in turn drives weight bearing asymmetry. Intra-articular injection of nerve growth factor (NGF) was reported to augment pain behaviour in OA knees (Ashraf et al., 2014). Structural changes to the joint or on-going pain may be the cause of OA sensitivity to NGF. Further work will be required to investigate if NGF would augment weight bearing asymmetry in the low (0.1mg) dose MIA rats and if this sensitivity to NGF is as a result of structural pathology.

Intra-articular injection of MIA led to a reduction in paw withdrawal threshold in rats treated with either the 0.1mg or 1mg dose compared to the corresponding saline injected non-arthritic rats. These data are in line with already published data which used the 1mg dose or higher (Combe et al., 2004, Burston et al., 2013, Sagar et al., 2015). Another study reports on a reduction in mechanical threshold for a 0.125mg MIA dose (Im et al., 2010). These reductions in thresholds by the MIA injected rats may have been as a result of inputs from inflammation (neurogenic inflammation – see Chapter 1) leading to central sensitization. It can also be as a result of the MIA model reported to be partly neuropathic i.e. presenting with a neuropathic component

(Ivanavicius et al., 2007). Reports comparing the MIA model with other neuropathic pain models showed that OA pain pathways do overlap in some ways with neuropathic pain mechanisms and that MIA injected rats were seen to respond to chronic and neuropathic pain treatments (Fernihough et al., 2004, Ivanavicius et al., 2007, Vonsy et al., 2009). The present study highlights that reduced paw withdrawal thresholds may not be restricted to end stage OA in the higher MIA dose but may also be seen in the lower MIA dose.

5.5.2 Heterogeneity of OA pathology in the MIA model

OA is a heterogeneous disease characterised by multi-tissue failure in synovial joints. This includes the cartilage, bone, synovium, muscle etc. (Driban et al., 2010). The MIA model is also heterogeneous in this aspect as it exhibits failure in different tissues similar to that seen in human knee OA (Little and Zaki, 2012). Although the MIA model can be said to be homogeneous in terms of cartilage pathology as it shows chondropathy on both the lateral and medial tibial plateau (Barve et al., 2007), when assessing chondropathy, it is wrong to generalise the pathology seen in a part of the joint to the whole knee joint. The recommendations by the OARSI histopathology initiative for histological assessments of OA in the rat (Gerwin et al., 2010) suggests the method of frontal sectioning. Here the rat knee joint is split in a frontal plane into two equal anterior and posterior halves. From this, 3 sections per part (anterior or posterior) are cut at 200µm intervals and stained for histopathological assessments.

In this study it was observed that sections from one compartment of the joint alone were not enough to discriminate the diseased groups (MIA-injected rats) from the normal controls (saline-injected rats). For example for chondropathy in the day 20 rats, it was observed that sections from the posterior part of the knee was found to show significant differences between OA and normal controls rather than sections from the anterior part of the knee, and chondropathy was significantly higher in the posterior knees rather than the anterior knees. Combining both parts (anterior and posterior sections) of the knee together to give a total joint score increased the sensitivity to detect chondropathy and thus the discrimination between disease groups and normal

controls increased. In cases like this it would be unwise to score chondropathy on one part of the knee only. This is in contrast to the OARSI recommendation for histopathology in the rat (Gerwin et al., 2010) which suggest assessing pathology in only one part of the knee, although the recommendation was based on the surgically induced MMT model. One of the reasons why chondropathy was observed more in the posterior part of the knee to the anterior part may be because rats like human tend to weight bear more on the posterior part than the anterior part. The day 42 0.1mg MIA injected rats however had equal chondropathy scores for both anterior and posterior knees. This may have been due to the duration of OA development in the MIA model as the day 20 0.1mg and 1mg MIA injected rats showed significantly higher chondropathy in the posterior part but not the anterior, thus it can be said that chondropathy initially arises in the posterior part of the knee before it spreads to the anterior part of the knee.

A similar situation was observed for the measurement of chondrocyte appearance. Significant differences for all MIA groups compared to the saline control group were observed when joint scores from both anterior and posterior parts were combined. Therefore when carrying out histological assessments on rats, this should be taken into consideration so as to obtain true results.

5.5.3 Reliability of histological scoring systems

This study assessed the reliability of the Janusz (Janusz et al., 2002) and modified OARSI scoring systems on rat knees (Pritzker et al., 2006). The Janusz system was reported for use in the surgical meniscal tear rat model and the OARSI system have been used in a few animal models including the MIA model (Sagar et al., 2010) and in human samples (Pearson et al., 2011). One of the reasons for developing the OARSI score was to create a standard scoring system that would enable comparability of results between or across studies, when used independently or in parallel with other systems (Aigner et al., 2010). In this case the modified OARSI system was used in parallel to the Janusz system for scoring cartilage chondropathy. Both systems were able to discriminate between OA groups from normal controls. Also the Janusz system

showed a positive correlation to the modified OARSI system. Results from the Bland-Altman plot comparing the Janusz system to the modified OARSI system show good agreement (Bland and Altman, 1986, Hanneman, 2008). The modified OARSI and Janusz systems including histological scoring for chondrocyte appearance, osteochondral junction integrity and loss of matrix proteoglycan in the cartilage were evaluated between 4 investigators to examine the reliability and reproducibility of histological scoring systems for pathological assessments. Reliability and reproducibility were assessed using the reliability analysis and reported as Cronbach's alpha values and the Cohen's kappa statistic. The Cronbach's alpha which measures internal consistency pertaining to how items within a test measure the same concept or construct can be rated on a scale from 0 to 1, with 1 being near perfect consistency and 0 being poor or no consistency (Spiliotopoulou, 2009, Tavakol and Dennick, 2011). The higher the correlation between two items been measured, the greater the Cronbach's alpha value. There was a good reliability for histological scoring between observers (0.5-0.99), with cartilage chondropathy scoring having the highest Cronbach's alpha (0.99) and abnormal chondrocyte morphology scoring having the least (0.5). The reason for this may be because cartilage scoring may be easier to score than chondrocyte morphology. There is a clear cut for scoring fibrillations in the cartilage. Whereas for chondrocyte morphology assessment, the change from normal (score 0) to hypercellularity (score 1) and the early stages of cloning (score 2) may be hard to judge unlike normal (score 0), the late stages of cloning (score 2) and cell death or hypocellularity (score 3) (see Chapter 2). The cartilage scoring system for example the OARSI system was developed in a way that it could be applied more consistently to less experienced investigators than the HHGS (Pritzker et al., 2006, Rutgers et al., 2010, Custers et al., 2007, Mankin et al., 1971). The chondrocyte morphology scoring system is a subset score of the HHGS (Mankin et al., 1971). Furthermore, the scale of the cartilage scoring system having more items (0-5 with 1-3 cartilage involvement for Janusz method of scoring and 0-6 with 1-4 involvement for the modified OARSI method of scoring) than the chondrocyte morphology scoring system which only scores from a range of (0-3) (see Chapter 2) may be a reason for the lower Cronbach's alpha values.

Although the Cronbach's alpha analysis is an easy way to measure reliability, it does not always mean that a high Cronbach's alpha equals a high degree of consistency as the values analysed may be dependent on factors such as e.g. scale length (the number of items in the scale) (Helms et al., 2006). It has been shown that reliability increases with scale length (Cronbach, 1951, Voss et al., 2000). Therefore results should not be entirely based on Cronbach's alpha values. In this case, reliability was also measured using the Cohen's kappa statistic.

Some observer agreements for rating scoring methods between investigators may be observed as good but this can be due to chance. The Cohen's kappa (κ) was developed as a measure of agreement that corrected or adjusted for chance (Cohen, 1960, Kundel and Polansky, 2003). The κ values for the histological assessments between the 4 investigators were in the range of slight to moderate agreement. κ can be calculated between investigators who report results on multiple categories this is called the weighted κ . It takes into account the actual closeness of measurement between investigators and how close the differences between measurements are. The weighted κ is always greater than the unweighted κ when used for multiple categories but the same when used for only two categories. The weighted κ is commonly used than the κ as it reflects the actual agreement better (Cicchetti, 1981, Kundel and Polansky, 2003). The weighted κ values for the histological assessments between the 4 investigators were in the range of fair to almost perfect agreement.

In both unweighted and weighted κ calculations, the scoring of cartilage chondropathy by Janusz or OARSI methods of scoring were observed to have higher agreement and the osteochondral junction integrity scoring having the least agreement. This may have to do with the cartilage damage being easier to score as mentioned above.

5.5.4 Sensitivity of histological stains in the detection of matrix proteoglycan

The Safranin O-Fast green stain is a widely used stain for assessing loss of proteoglycan in the cartilage of OA animals and in the HHGS in humans

(Gerwin et al., 2010, Mankin et al., 1971). Unlike the Toluidine blue stain which is also widely used, the Safranin O-Fast green stain has been reported as not being a sensitive indicator of proteoglycan content in the cartilage in which GAGs have been depleted (Camplejohn and Allard, 1988). Thus it was suggested that for simple histological scoring of proteoglycan content the Toluidine blue stain should be used (Kraus et al., 2010). The Alcian blue-PAS stain like the toluidine blue stain provides more intense staining as it has a higher affinity for sulphur in the cartilage compared to Safranin-O (Camplejohn and Allard, 1988, Scott, 1973). It was observed that Safranin-O Fast green stained sections were less sensitive in detecting proteoglycan content in the cartilage compared to the Alcian blue-PAS stained sections. This may be as a result of this stain being less sensitive as reported above or it being more sensitive in the detection of proteoglycan loss in the cartilage due to disease or wash-out during fixation or decalcification (Hyllested et al., 2002, Encfeldt and Hjertquist, 1967, Chevrier et al., 2005). The Safranin-O Fast green stained sections were able to discriminate better between OA disease groups and normal saline controls. The MIA (0.1mg and 1mg) injected rats were observed to have significantly higher proteoglycan loss scores compared to the saline injected rats than the Alcian blue-PAS stained sections which showed significantly higher proteoglycan loss in the 1mg MIA injected group only. It can also be argued that the 0.1mg MIA injected rats showed less proteoglycan loss as it may be a milder model and may show progressive loss of proteoglycan with time (d20-0.1mg MIA injected rats). In this case, further work would have to be done to investigate this, to examine the loss of proteoglycan in the 0.1mg MIA model using the Alcian blue-PAS stain and with increasing the duration of OA.

5.6 CONCLUSIONS

The MIA model displayed characteristic features of human knee OA observed as pain behaviour, inflammation and joint pathology. Inflammation and joint pathology did not differ between doses (0.1mg and 1mg MIA) and between duration (day 20 and 42) thus indicating that the low dose MIA model may not be a slow progressive model. Further work may be required to investigate inflammation and structural pathology at earlier time points (day 3, 7 and 14).

Reduced hind paw withdrawal thresholds indicating allodynia in the absence of pronounced weight bearing asymmetry may suggest that mechanisms other than ongoing nociceptive and peripheral input mediate distal allodynia in the lower dose (0.1mg) MIA model. These results show that central augmentation of pain is not restricted to late severe OA (higher MIA doses) following MIA injection in rats.

The MIA model was observed to show heterogeneity in terms of joint pathology, with pathology present in the posterior part of the knee at 3 weeks of arthritis induction but later spreads to the anterior part with time. Therefore pathology seen in a part of the joint should not be generalised to the whole knee joint in this model.

Histological scoring systems are important for assessing of OA pathology. The cartilage scoring systems by Janusz or modified OARSI scoring displayed good agreements between each other and between the 4 investigators. Although one was not better than the other, the OARSI system should be applied over the Janusz system in scoring OA pathology as it is increasingly widely used and was created specifically for use in OA in order to inform a standardized practice.

For the purpose of the detection of proteoglycan loss for OA pathology, the Safranin-O Fast green stain is the better choice. It is important that a stain which can detect proteoglycan loss efficiently is used, as proteoglycan content is considered one of the major characteristics of cartilage integrity in healthy, repaired or tissue-engineered cartilage (Rutgers et al., 2010).

CHAPTER 6; CONTRIBUTION OF NGF IN OA PAIN: TARGETING THE NGF-TRKA PATHWAY IN TWO RAT MODELS OF OA

6.1 INTRODUCTION

For more than half a century, the neurotrophin nerve growth factor (NGF)- β has been known to be responsible for the axonal growth and survival of sensory nerves (Levi-Montalcini and Hamburger, 1951). In the adult, NGF sensitises peripheral nociceptors and might contribute to the development of central sensitisation. NGF effects on sensitisation and nerve growth are predominantly mediated by binding to its high affinity receptor Tropomyosin receptor kinase A (TrkA) (Woolf, 1996). TrkA is a member of a family of receptors with tyrosine kinase activity, including also TrkB and TrkC. NGF can also bind, with lower affinity, to the p75 receptor although the biological relevance of these interactions remains uncertain.

In recent years, NGF has been widely reported to play a role in many acute and chronic pain states, especially those associated with inflammation including rheumatoid arthritis and spondyloarthritis (Watson et al., 2008, McMahon, 1996, Barthel et al., 2009). Increased endogenous NGF levels in the synovial fluid of people with chronic arthritis (Aloe et al., 1992), expression of NGF within the inflamed synovium (Manni et al., 2003) and subchondral bone (Walsh et al., 2010) are all evidence of NGF involvement in OA. In patients matched for severity of chondropathy, synovitis and NGF immunoreactivity was higher in patients who sought joint replacement surgery for symptomatic knee OA than in patients who had not reported symptoms, further indicating that NGF may mediate a contribution of inflammation to OA pain (Stoppiello et al., 2014). As well as sensitising nociceptors, NGF mediated growth of sensory nerve terminals into articular cartilage and into the inner regions of knee menisci might be a potential source of arthritis pain (Ashraf and Walsh, 2008, Suri et al., 2007, Ashraf et al., 2011b). NGF itself can stimulate new

blood vessel growth (angiogenesis), a characteristic of chronic inflammation (Mapp and Walsh, 2012). NGF might also upregulate and increase the release of inflammatory mediators into the joint thereby augmenting inflammation and further exacerbating pain (Štempelj and Ferjan, 2005, Linker et al., 2009).

Sequestering NGF reduces pain in several experimental models (Iwakura et al., 2010, McNamee et al., 2010) and NGF blockade reduces OA pain and improves function in randomised clinical trials (Lane et al., 2010, Sanga et al., 2013, Tiseo et al., 2014). Furthermore, NGF blockade was associated with greater clinical benefit than observed in active treatment control groups using non-steroidal anti-inflammatory drugs (NSAIDs) or opiates (Verburg, 2012). Together these data support targeting of NGF pathways for the relief of OA pain. Randomised controlled trials of NGF blockers, although demonstrating analgesic efficacy, were once put on hold by the Federal Drug Administration due to evidence of an increased risk of rapidly progressive OA (RPOA-osteonecrosis) leading to joint replacement surgery in some treated participants (Hochberg et al., 2012). RPOA was observed in patients receiving either of 2 different NGF blockers, suggesting a class effect, and post hoc analyses have suggested that this increased risk might be associated with concurrent NSAID use, whereas it was not associated with potency of analgesia (Schnitzer et al., 2014).

Blocking TrkA should prevent NGF-mediated sensitisation, while permitting other, less well understood effects of p75 or Trk receptors (B & C), some of which may be beneficial or may potentiate the occurrence of adverse effects if blocked simultaneously (Winston et al., 2003). Evidence of hyperphagia observed in mice may be as a result of BDNF-TrkB blocking (Unger et al., 2007). Small molecular, orally active Trk inhibitors may also be more acceptable and cost effective than monoclonal antibodies (Opar, 2010, Ghilardi et al., 2010). However selectivity of drugs for TrkA over related tyrosine kinase receptors has proved difficult to achieve. AR786 is a novel orally active inhibitor of TrkA kinase activity, with >1000 fold greater potency for TrkA over other tyrosine kinase receptors, including TrkB and TrkC (Andrews, 2014).

Blockade of NGF signalling may reduce OA pain by reducing sensitisation, nerve growth and inflammation, but is not anticipated to be anti-nociceptive per se (Ma and Woolf, 1997). Traditional analgesic agents, such as opiates, also block normal, protective, nociceptive signalling, and display a rapid onset of action, but treatment discontinuation leads to an equally rapid increase in pain. Peripheral sensitisation is mediated, in part, by altered gene expression (Nicol and Vasko, 2007), and analgesic benefits from inhibiting NGF signalling may be expected to be of slower onset and sustained following treatment withdrawal. Preventive analgesia, for example by treating during critical phases during the development of OA or sensitisation, may permit treatment discontinuation with sustained pain reduction.

Subchondral bone remodelling has been implicated to play an important role in OA pain and pathology from clinical and preclinical studies (Kwan Tat et al., 2010, Ogino et al., 2009). Bone remodelling is controlled by the activity of osteoclasts (bone resorption cells) and osteoblasts (bone formation cells) with pathological bone resorption caused by increased osteoclast activity. NGF has been reported to be involved in inducing RANKL-independent osteoclastogenesis and may contribute to normal and pathological subchondral bone remodelling (Hemingway et al., 2011).

The hypothesis was that the NGF-TrkA pathway mediates pain behaviour, synovitis and joint pathology in the MIA and MNX rat models of OA.

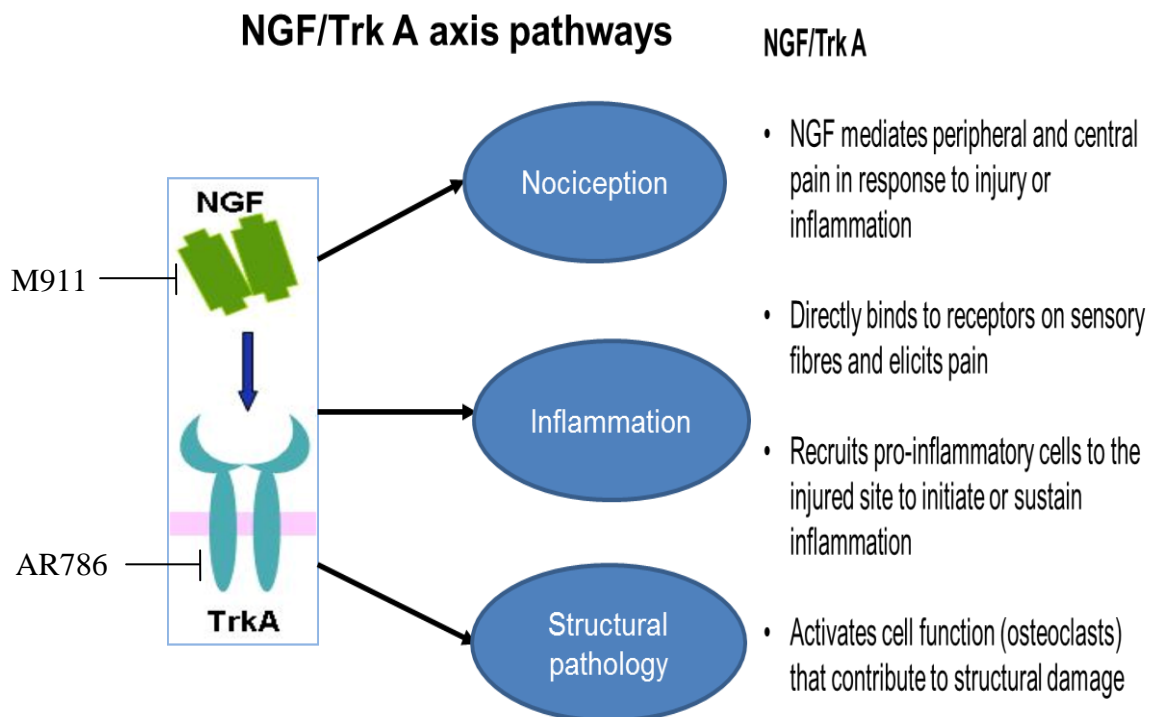


Figure 6.1 NGF-TrkA complex formed by binding of NGF to the TrkA receptor. Downstream signalling of the formation of this complex may alter nociception, inflammation and structural pathology thereby moderating pain.

6.2 AIMS

- To explore the contribution of the NGF-TrkA pathway to pain behaviour, synovitis and joint pathology in the MIA and MNX rat models of OA.
- To evaluate duration of sustained analgesia following discontinuation of AR786 treatment.

6.3 METHODS

Refer to Chapter 2 for general methodology. Experiments were carried out on male Sprague Dawley rats (Charles River, UK) n=100, weighing 200-300g at time of OA induction.

OA induction

Rats were anaesthetised briefly with isoflurane (2% in O₂) and received a single intra-articular injection of MIA (1mg/50µl; Sigma U.K; n = 20) in sterile 0.9% normal saline through the infrapatellar ligament of the knee or underwent transection of the medial meniscus (n = 50). Non osteoarthritic (saline; n =10 or SHAM; n = 20) rats were used as controls. MNX induction was carried out by Paul Mapp.

Behavioural measurements of OA pain

Pain behaviour was measured as hind limb weight-bearing asymmetry and distal allodynia to punctuate stimulation of the hind paw indicated by reduced hind paw withdrawal thresholds. Baseline measurements were obtained immediately prior to intra-articular injection or surgery (day 0) and every 2 to 4 days from day 3 onwards for both therapeutic and preventive studies. Weight bearing asymmetry was assessed as a % difference in weight distribution between hind limbs (non-arthritic knee – arthritic knee) / (non-arthritic knee + arthritic knee) x100 using an incapitance meter (Linton Instruments, U.K). Hind paw withdrawal threshold was assessed using a series of von Frey monofilaments (Semmes-Weinstein monofilaments 1 - 15g) and recorded as the lowest weight of monofilament that elicited a withdrawal of the hind paw.

TrkA inhibitor (AR786) drug therapy

AR786 (kindly provided by Array Biopharma, Boulder, CO) was administered in a therapeutic or preventive protocol as previously described (Ghilardi et al., 2010, Ghilardi et al., 2011).

To evaluate the effects of therapeutic treatment of AR786 in the MIA and MNX models of OA, treatment with AR786 (30mg/kg, p.o., bid) or 5% Gelucire 50/13 vehicle (Gattefosse, Cedex, France) was administered twice

daily for 7 days from 2 weeks after OA induction (after OA was established). Rats were stratified into groups of n = 10 at day 10 (to ensure balanced weight bearing behaviour between groups prior to drug administration) by a researcher not otherwise involved in the study. Rats received either AR786 (MIA or MNX + drug) or vehicle (MIA or MNX + vehicle; saline or SHAM + vehicle).

To evaluate the effects of a preventive treatment and treatment withdrawal of AR786 in the MNX model of OA, AR786 (30mg/kg, p.o., bid) or vehicle (5% Gelucire) was administered 1 h prior to and 8 h following OA induction, and thereafter until the end of the study (day 28 after OA induction). AR786 treatment was discontinued and replaced with vehicle in some rats 2 weeks after continuous treatment. Rats were stratified into treatment groups each comprising 10 rats, 10 days after OA induction (i.e. 4 days before treatment discontinuation on day 14). Stratification was according to weight bearing asymmetry by a researcher not otherwise involved in the study. Rats received either AR786 (MNX + drug; MNX + drug-discontinued) or vehicle (MNX + vehicle; SHAM + vehicle).

Time course of experiment

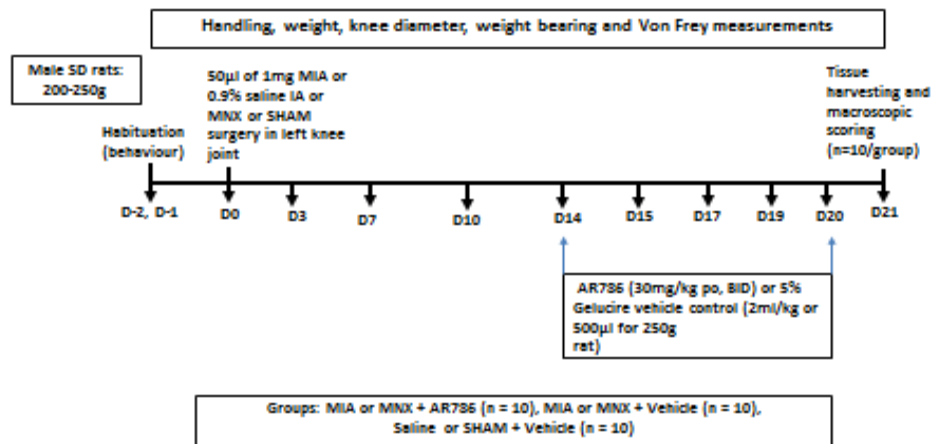


Figure 6.2 Time course of experiment investigating the effect of a therapeutic administration of the TrkA inhibitor AR786 in the MIA and MNX models of OA.

Rats were habituated to pain assessment (incapacitance meter and von Frey box) before baseline measurements were obtained. OA (intra-articular MIA injection or MNX surgery) was induced on day 0. Two weeks (day 14) following OA induction, AR786 was administered by oral gavage twice daily for 7 days (day 20). Rats were handled and scruffed daily prior to oral gavage. Macroscopic scoring and tissue (joint) harvesting were carried out on day 21. Weights, knee diameters, weight bearing and von Frey measurements were carried out at various time points.

Time course of experiment

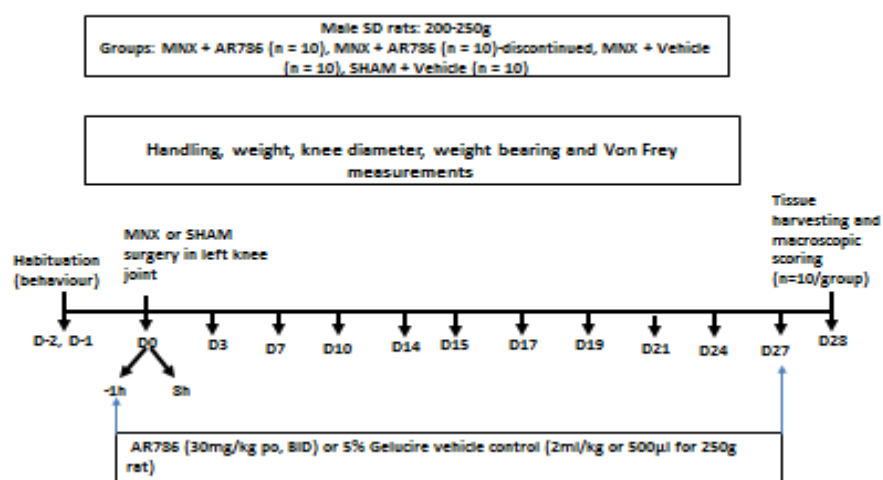


Figure 6.3 Time course of experiment investigating the effect of preventive administration of the TrkA inhibitor AR786 in the MNX model.

AR786 was administered by oral gavage twice daily prior to (day -1), during and after OA induction until the end of the study (day 27). Rats were habituated to pain assessment (incapacitance meter and von Frey box) before baseline measurements were obtained. OA (MNX surgery) was induced on day 0. Macroscopic scoring and tissue (joint) harvesting were carried out on day 28. Weights, knee diameters, weight bearing and von Frey measurements were carried out at various time points.

Anti-NGF (muMab911 or M911) drug therapy

Monoclonal antibody (M911) (Hongo et al., 2000) kindly provided by Rinat/Pfizer, San Francisco, CA was studied in both therapeutic and preventive protocols on pain behaviour, synovitis and osteoclast numbers in the MIA model by Luting Xu and Paul Mapp. Knee joint tissues from this study were then examined by me to investigate the effect of this antibody on histopathology.

For the therapeutic protocol, rats received a weekly dose of M911 (s.c. 10mg/kg) or PBS vehicle on day 14 and 21 after model induction; [M911 (MIA or saline) or PBS (MIA or saline)] or a weekly dose of M911 (s.c. 10ml/kg) or PBS from the day of model induction for the preventive protocol; [M911 (MIA or saline) or PBS vehicle (MIA or saline)].

Inflammation

Inflammation was assessed as joint swelling, synovial histological score and macrophage infiltration.

Joint swelling was measured at the same time as behavioural measurements using digital electronic callipers (Mitutoyo, UK), with values representing difference in knee diameters (mm) between the arthritic (left) and non-arthritic (right) knee joints.

Synovium with patella from each knee was harvested at the end of each study, embedded in OCT and snap frozen over melting isopentane. 5µm thick synovial sections were cut using a motorized cryostat, mounted on glass slides, and briefly air dried before staining. Synovitis grade was assessed on haematoxylin and eosin-stained sections according to lining thickness and cellularity on a scale from 0 to 3. Synovitis scoring was performed using a 20× objective lens of a Zeiss Axioscop-50 microscope (Carl Zeiss Ltd, Welwyn Garden City, UK).

Macrophage infiltration was identified by immunoreactivity for CD68 using the mouse monoclonal antibody clone ED1, and the peroxidase-conjugated avidin-biotin-peroxidase complex (ABC) method. Macrophage infiltration was

quantified using a 20× objective lens of a Zeiss Axioscop-50 microscope (Carl Zeiss Ltd, Welwyn Garden City, UK). Macrophage infiltration was quantified using fractional area and defined as the percentage of synovial area that was CD68-positive.

Macroscopic chondropathy grading of knee joint pathology

At the end of each study, rats were killed either by an overdose in CO₂ (therapeutic study – day 21) or an overdose of pentobarbital (i.p.) (preventive study – day 28). Macroscopic chondropathy scoring of knee joints was based on the Guingamp classification (Guingamp et al., 1997). Macroscopic lesions were graded as: 0 = normal appearance; 1 = slight yellowish discoloration of the chondral surface; 2 = little cartilage erosions in load-bearing areas; 3 = large erosions extending down to the subchondral bone; and 4 = large erosions with large areas of subchondral bone exposure. Each of the chondral compartments of the knee (the medial and lateral femoral condyles, the medial and lateral tibia plateaux, and the femoral groove) was graded. The 5 compartment scores were summated (giving a maximum possible score of 20 per knee).

Osteoclast numbers

Frontal sections (5µm) were stained for tartrate resistant acid phosphatase (TRAP) positive osteoclasts. 6 sections / rat (2 sections at 50µm intervals) from the anterior half of the knee joint were firstly dewaxed in xylene, rehydrated in serial alcohol and distilled water, and finally recalcified in a solution containing 1mM CaCl₂ and 1mM MgCl₂ in PBS before TRAP were stained using the commercially available kits (Sigma-Aldrich, UK). The number of TRAP positive osteoclasts were counted within the subchondral bone area comprising the area between the cartilage/bone junction and the growth plate as previously described (Parfitt et al., 1987, Dempster et al., 2013).

Histopathology

At the end of the M911 study, rats were overdosed with pentobarbital (i.p.). Tibiofemoral joints were removed and post-fixed in neutral buffered formalin

(containing 4% formaldehyde), decalcified in ethylenediaminetetraacetic acid (EDTA). Frontal tissue sections following the Osteoarthritis Research Society International (OARSI) guideline for histological assessment for OA in the rat were cut at 5µm and stained for evaluations (Gerwin et al., 2010).

Articular cartilage surface integrity was scored using the modified OARSI cartilage histopathology assessment system (Pritzker et al., 2006). Cartilage surface integrity and chondrocyte appearance were evaluated using H&E stained sections, and proteoglycan loss was determined using sections stained with Safranin-O Fast green, all of which followed the modified OARSI scoring and were scored on 3 sections / rat. Cartilage histopathology assessment system was scored on a scale from 0 (normal) to 6 (deformation), and a total joint damage score (range 0-24) was calculated as cartilage surface integrity x % of cartilage involved; 0 (no involvement) to 4 (>50% cartilage involvement) as previously described (Pritzker et al., 2006). Chondrocyte appearance was graded from 0 (normal appearance and density), to 3 (chondrocyte hypocellularity). Proteoglycan loss was evaluated on a scale from 0 (normal proteoglycan staining) to 4 (complete loss of proteoglycan staining) on Safranin-O Fast green stained sections (Mankin et al., 1971).

Statistical analysis

Synovial inflammation, lining thickness and cellularity were scored as previously described, one synovial section per animal and overall grade that best represented the section given (Ashraf et al., 2011a). Infiltration by macrophages was quantified on 4 fields of view per synovial section per animal (Walsh et al., 1998a).

Statistical analysis was performed using Prism V.6 (Graph Pad, San Diego, California, USA). All data were analysed using Kruskal Wallis test followed by post hoc Dunn's comparison. Graphs are presented as mean ± SEM or median. Data in text were presented as mean (95% CI) or median (IQR). A two-tailed $p < 0.05$ was considered significant in all cases.

6.4 RESULTS

6.4.1 Effects of AR786 in the MIA and MNX models of OA pain

6.4.1.1 *Body weight*

There was a gradual increase in the weight of all the rats irrespective of model induction or treatment administered (Fig. 6.4 A-C). The MNX vehicle-treated rats had lower weights from the start of the study and thereafter to the end of the study, but this was not significantly different to the rats in the other groups (Fig. 6.4 B).

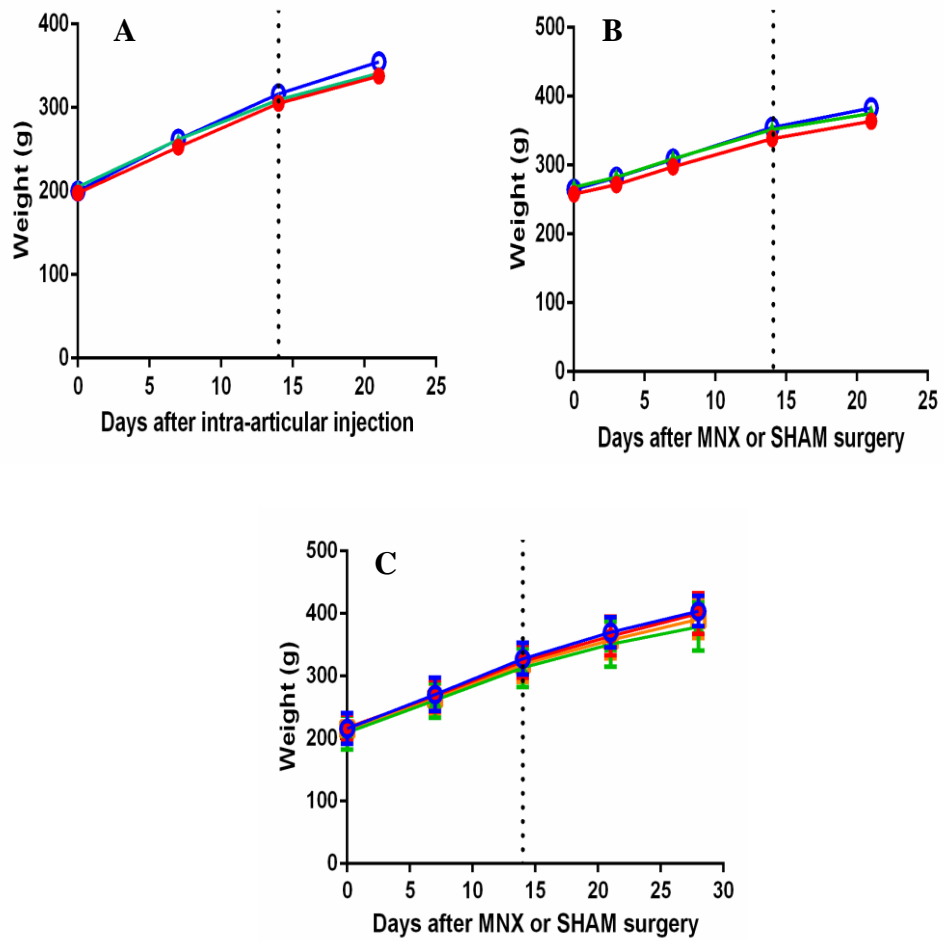


Figure 6.4 Time course of weight gain of rats.

There was a gradual increase in weight in all groups of rats over the course of the study. Oral administration of either AR786 (30mg/kg p.o. bid) or vehicle (5% Gelucire 50/13) control given continuously (A and B) or discontinued (C) from day 14 (**dotted line**) did not alter weight gain. Line graphs show mean \pm SEM over time of $n = 10$ rats/group. Saline- or sham-operated vehicle-treated non-arthritic controls (○). MIA or MNX vehicle treated (●). MIA- or MNX-AR786 (▲). MNX-AR786 discontinued (◻).

6.4.1.2 Pain behaviour

Intra-articular injection of MIA, or MNX surgery, was each followed by increased weight bearing asymmetry from 3 days after arthritis induction, compared with non-arthritic saline-injected or sham operated controls (Figs. 6.5 A-B and 6.6 A). Hind paw withdrawal thresholds ipsilateral to the arthritic knee were reduced (greater sensitivity) by 3 days after arthritis induction in the MIA group and 7-10 days in the MNX group compared with non-arthritic controls (saline; Fig. 6.5 C and sham; Figs. 6.5 D and 6.6 B). Pain behaviour was sustained in arthritic rats through to study termination at 21 or 28 days after arthritis induction (Figs. 6.5 and 6.6).

Effects of TrkA inhibitor on established OA pain behaviour.

Rats received TrkA inhibitor (AR786; 30mg/kg, p.o., bid) from 2 weeks after OA induction (at a time corresponding to fully established OA joint pathology and pain behaviour both in MIA- and MNX-induced models) and continued for 7 days. Weight bearing asymmetry was significantly reduced following 3 days oral administration of AR786 in rats with MIA-induced OA [4.3 (-1.9 to 10) %] and following 5 days treatment in MNX-induced OA [9.2 (5.1 to 13) %]), compared to vehicle-treated arthritic rats at the same time points (MIA [21 (14 to 29) % $p < 0.05$, Fig. 6.5A] and MNX [27 (24 - 30) % $p < 0.05$ Fig. 6.5B]). Hind paw withdrawal thresholds were also significantly increased (less sensitive) following 5 days treatment with AR786 in rats with MIA-induced OA [11 (7 to 15) g] or MNX-induced OA [13 (10 to 15) g]) compared to vehicle treated arthritic rats (MIA [2.7 (1.2 to 4.2) g $p < 0.01$ Fig. 6.5C] and MNX [6.9 (4.3 to 9.5) g $p < 0.05$] Fig. 6.5D). After 7 days treatment with AR786, weight bearing and hind paw withdrawal thresholds in arthritic rats were comparable to those in non-arthritic controls, irrespective of the mode of arthritis induction (Fig.6.5).

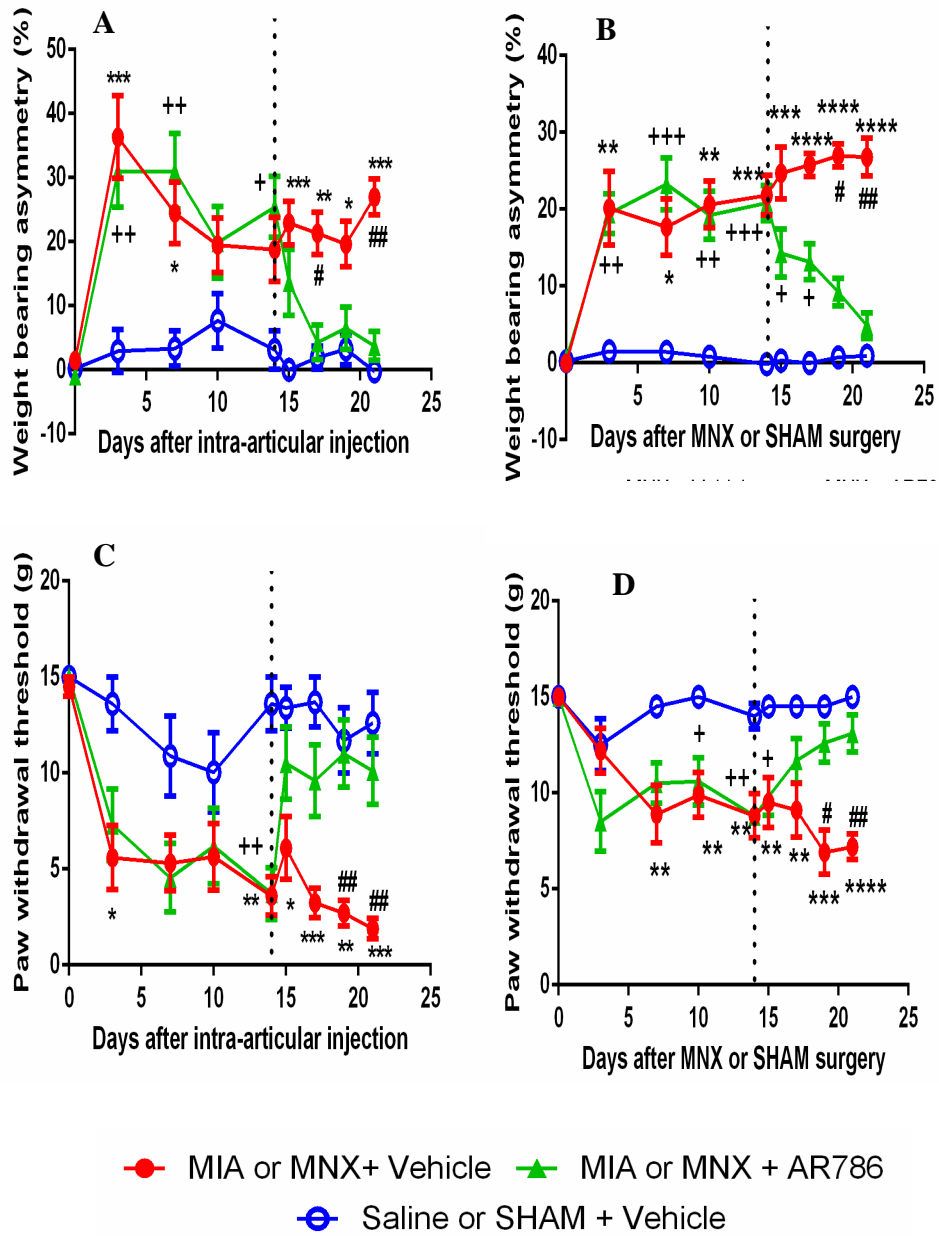


Figure 6.5

Figure 6.5 Effects of therapeutic AR786 on pain behaviour in the MIA and MNX models of OA

MIA injection or MNX surgery was associated with increased pain behaviour (weight bearing asymmetry and lowered hind paw withdrawal thresholds) which was sustained until the end of the study (day 21) (A-D). Administration of AR786 (30mg/kg twice daily) (dotted line) completely abolished pain behaviour by day 17 (3 days after start of treatment) in the MIA-injected rats (A & C). Pain behaviour was attenuated by day 19 (5 days after start of treatment) and completely abolished to control levels by day 21 (7 days after start of treatment) in the MNX-operated rats (B & D). Data indicate mean \pm SEM for n = 10 rats per group. Differences between groups were analysed using Kruskal Wallis test followed by post hoc Dunn's comparison between groups. #p<0.05 MIA or MNX vehicle treated versus MIA- or MNX-drug treated, ++p<0.01 MIA- or MNX-drug treated versus saline- or sham-operated vehicle non-arthritic controls, and ***p<0.001 MIA- or MNX-vehicle versus saline- or SHAM-operated vehicle, non-arthritic controls.

Effects of TrkA inhibition on the development of OA pain behaviour

Rats received TrkA inhibitor (AR786; 30mg/kg, p.o., bid) one day prior to, during and after OA induction by MNX for 28 days. Treatment with AR786 was withdrawn in one group of rats (n = 10) two weeks after arthritis induction and replaced with vehicle treatment. Weight bearing asymmetry did not manifest in MNX-operated rats which received AR786 throughout the study (day 28; [4 (-0.1 to 8.1) %] compared to vehicle-treated, MNX-operated rats [24 (21 to 28) %, $p < 0.001$, Fig. 6.6A]). Likewise hind paw withdrawal thresholds were not altered compared to baseline in arthritic rats that received AR786 throughout the study (day 28; [12 (9.9 to 14) g]) compared to vehicle-treated MNX-operated rats which had significantly lowered thresholds [5.8 (4.2 to 7.4) g, $p < 0.01$, Fig. 6.6B]. Following withdrawal of AR786 treatment 14 days after arthritis induction, weight bearing asymmetry remained attenuated compared to arthritic rats that had never received the drug (Fig. 6.6A). Over time, weight bearing asymmetry gradually increased, but remained significantly different to vehicle-treated control arthritic rats until 4 days before study termination 10 days after treatment withdrawal. Arthritic rats that had their treatment withdrawn did not show a statistical significant difference in weight bearing asymmetry compared to arthritic rats that had continued treatment through to the end of the study (Fig. 6.6A). By contrast, hind paw withdrawal thresholds rapidly decreased (increased sensitivity) following withdrawal of AR786 treatment, and 5 days after treatment withdrawal, thresholds were comparable to those in rats with MNX-induced OA that never received the drug (Fig. 6.6B). The rapid decrease in paw withdrawal threshold in the arthritic rats that had their treatment withdrawn was significantly different to arthritic rats with continued treatment at the end of the study (day 28) (Fig. 6.6B).

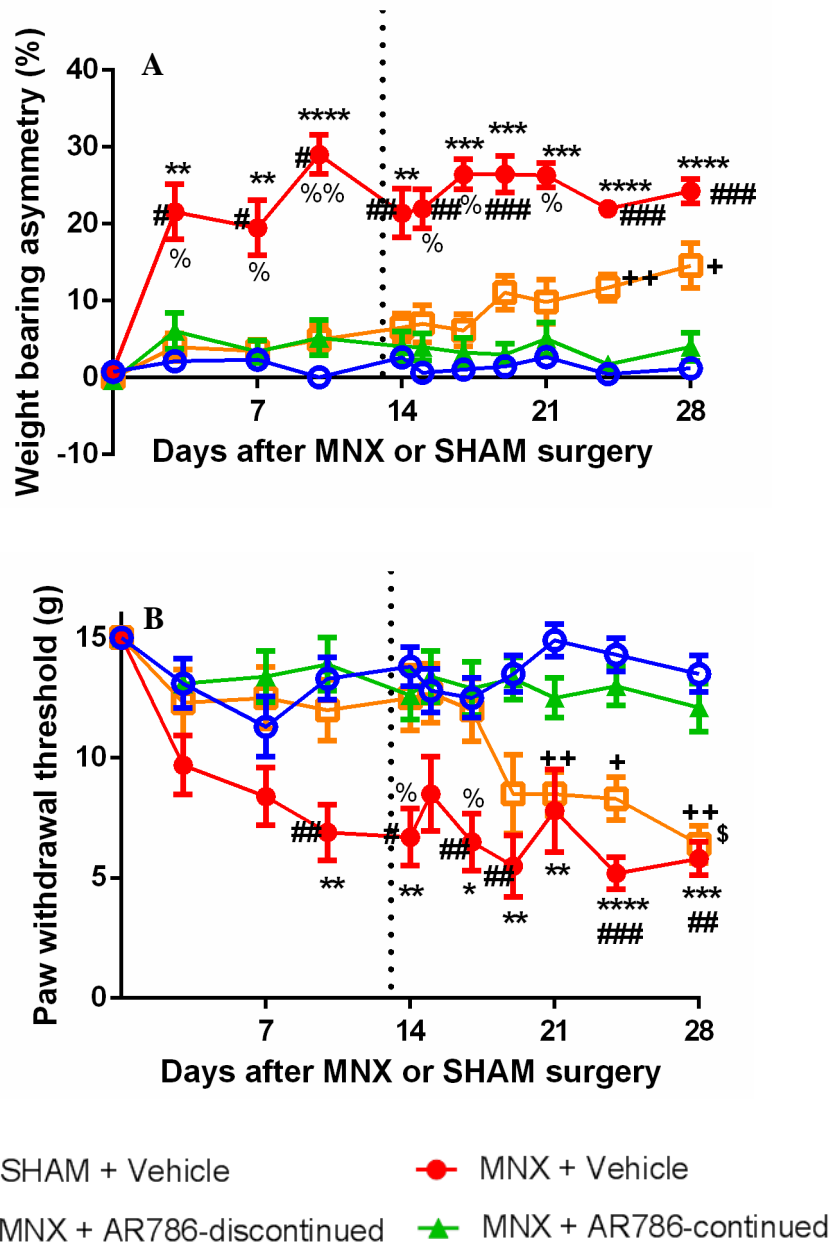


Figure 6.6 Effect of preventive AR786 on pain behaviour in the MNX model of OA

MNX surgery was carried out on day 0. Oral administration of either AR786 (30mg/kg twice daily) or vehicle (5% Gelucire) control was given from a day before OA induction (day -1). AR786 treatment was discontinued in some rats (n = 10) and replaced with vehicle treatment (dotted line) 14 days after OA induction. MNX surgery was followed by an increase in pain behaviour (weight bearing asymmetry and lowered hind paw withdrawal thresholds - A and B) which was sustained until the end of the study (day 28) in rats that were treated with vehicle. Administration of AR786 (30mg/kg twice daily) completely prevented the development of pain

behaviour (A and B). By day 24, 10 days after discontinuation of AR786 treatment in MNX-operated rats, weight bearing asymmetry was significantly greater than in sham-operated rats, but did not reach the levels observed in MNX-operated, vehicle-treated rats and did not differ significantly from rats that continued to receive AR786 through to the end of the study (day 28) (A). Paw withdrawal thresholds were reduced at day 19, 5 days after treatment discontinuation in MNX-operated rats that had received AR786 treatment until day 14. By this time, paw withdrawal thresholds in MNX-operated rats did not differ significantly between those in which AR786 had been discontinued compared with those that had never received AR786 (MNX-operated, vehicle-treated rats). Reduced paw withdrawal threshold was significantly different to sham-operated, vehicle-treated rats by day 21, 7 days after treatment discontinuation and to MNX-operated rats that continued to receive AR786 by day 28, 14 days after treatment discontinuation (B). Data are mean \pm SEM of $n = 10$ rats per group. # $p < 0.05$ MNX vehicle treated versus MNX-drug continued, ++ $p < 0.01$ MNX-drug discontinued versus sham-operated vehicle control, %% $p < 0.01$ MNX vehicle treated versus MNX-drug discontinued, *** $p < 0.001$ MNX vehicle treated versus SHAM-operated vehicle controls and \$ $p < 0.05$ MNX-drug continued versus MNX-drug discontinued.

6.4.1.3 Inflammation

Small increases in knee diameter were observed from 3 days following intra-articular injection of MIA, but did not differ from saline-injected control rats (Fig. 6.7A). MNX or SHAM surgery each resulted in increased knee diameter that persisted in MNX-operated rats, in which knee diameters were significantly greater than sham operated controls from 14 days after surgery (Fig. 6.7B). Intra-articular injection of MIA was followed by increased synovitis detected by histological examination of haematoxylin and eosin stained tissue sections (Figs 6.7C and 6.8B) and infiltration by macrophages (Fig 6.7E) into the synovium. Likewise after MNX surgery, there was an increase in synovitis (Figs 6.7D and 6.8E). Synovitis scores 21 days after intra-articular injection of MIA [2 (2 to 3)] were significantly increased compared to saline-injected, non-arthritic controls [1 (0 to 1.5) $p<0.01$] (Figs. 6.7C and 6.8A - B). Likewise after MNX surgery, synovitis scores were significantly increased compared to sham-operated rats [2 (2 to 3) v 0 (0 to 1) $p<0.01$] (Fig. 6.7D and 8.6D - E). Macrophage fractional area after intra-articular MIA [19 (10 to 29) %] were significantly increased compared to saline injected, non-arthritic controls [5.9 (4.2 to 7.5) %, $p<0.05$, Fig 6.7E].

Effects of TrkA inhibition on OA knee inflammation

Joint swelling, synovial histology and macrophage fractional area were examined to determine whether observed effects of TrkA inhibition on pain behaviour may be mediated or moderated by effects on inflammation.

Administration of AR786 had no significant effect on joint swelling in either the therapeutic or preventive studies (Fig. 6.7A and B), nor on macrophage fractional area in the therapeutic study (Fig. 6.7E). Administration of AR786 from 14 days after intra-articular injection of MIA resulted in a significant reduction in synovitis score 7 days later [1 (0 to 2.3)], compared to vehicle-treated, MIA-injected rats [2 (2 to 3), $p<0.05$, Fig. 6.7C]. However, no significant reductions in synovitis scores were observed at 4 weeks following continuous preventive administration of AR786 in rats with MNX-induced OA (Fig. 6.7D).

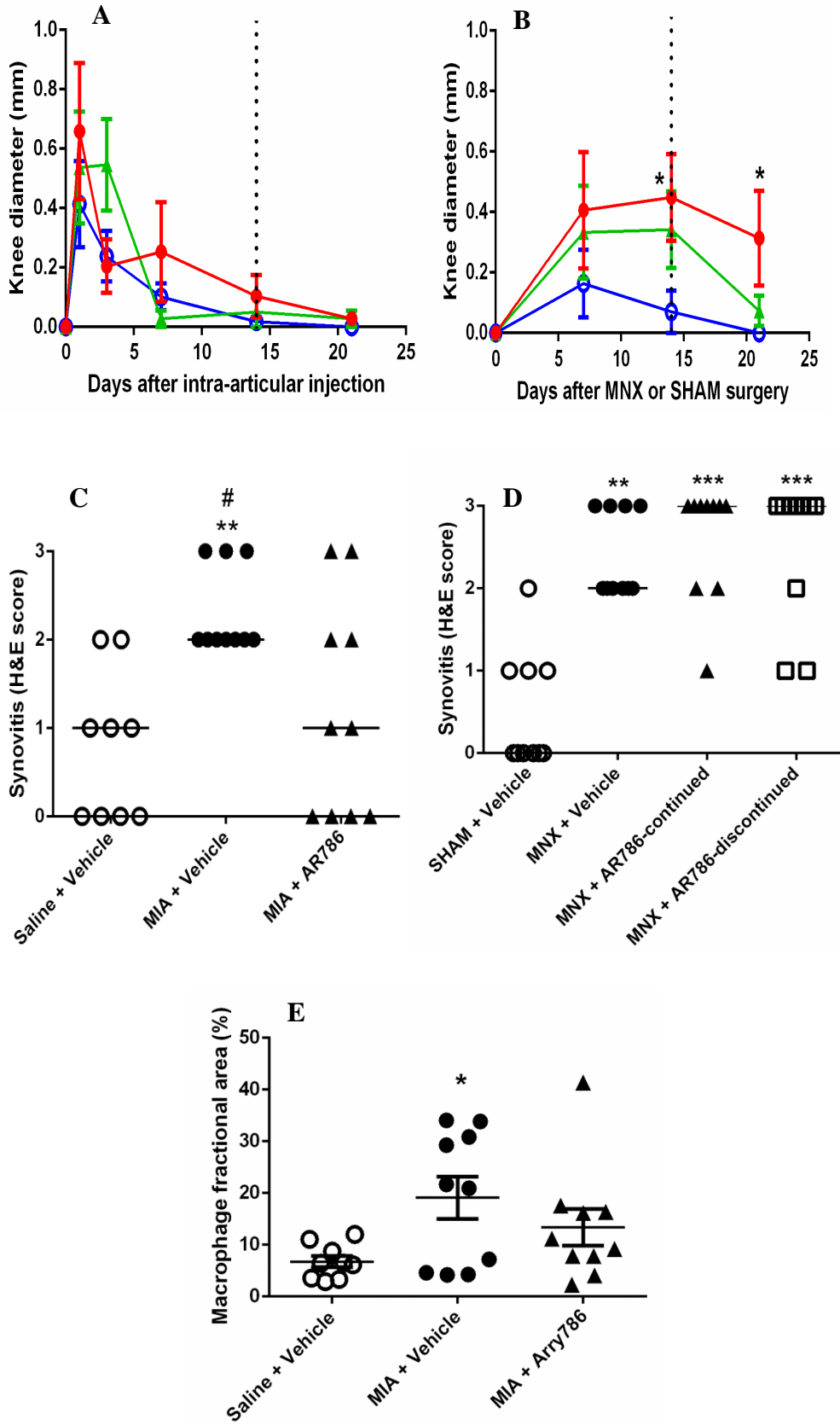


Figure 6.7

Figure 6.7 Effect of AR786 on MIA- or MNX-induced inflammation

Small changes in knee joint diameter were observed after intra-articular injection of MIA or saline (A), or after MNX- or sham surgery (B). Either AR786 (30mg/kg twice daily) or vehicle (5% Gelucire 50/13) control was administered orally from day 14 (dotted line). Knee joint diameters did not differ significantly between MIA- or saline-injected knees, nor between MIA-injected rats treated with either AR786 or Gelucire vehicle (A). MNX-operated knees displayed increased diameters compared with sham-operated knees from 14 days after surgery, when rats were treated with Gelucire vehicle, but not with AR786 (B). Synovitis was reduced in MIA-injected rat knees following day 14 treatment for 7 days with oral AR786 compared to Gelucire vehicle treated controls (C). Synovitis appeared similar after MNX surgery in rats treated either with AR786 or vehicle (D). Macrophage fractional area was increased in MIA-injected rats but not significantly reduced by the 7 day AR786 treatment (E). Knee diameters are given as differences between injected/operated and contralateral knees. Data are mean \pm SEM of n = 10 rats/group (A, B and E) or individual knees and median (C - D). *p<0.05 MIA- or MNX- vehicle versus saline or SHAM-operated controls respectively (A, B and E). #p<0.05 MIA vehicle treated versus MIA-drug treated and **p<0.01 MIA vehicle treated versus saline vehicle controls (C). **p<0.01, ***p<0.001 MNX-all groups versus sham-operated vehicle controls (D).

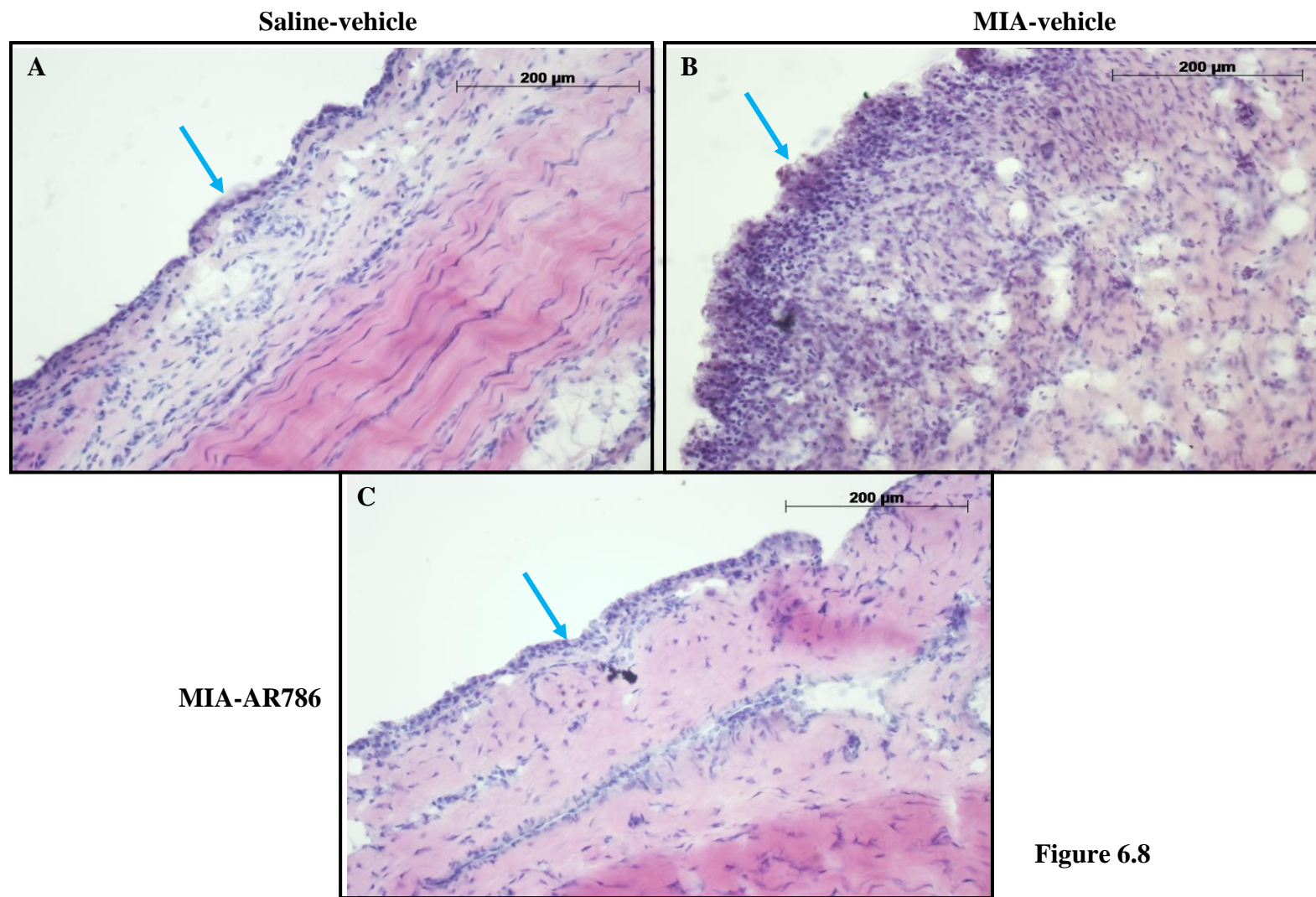


Figure 6.8

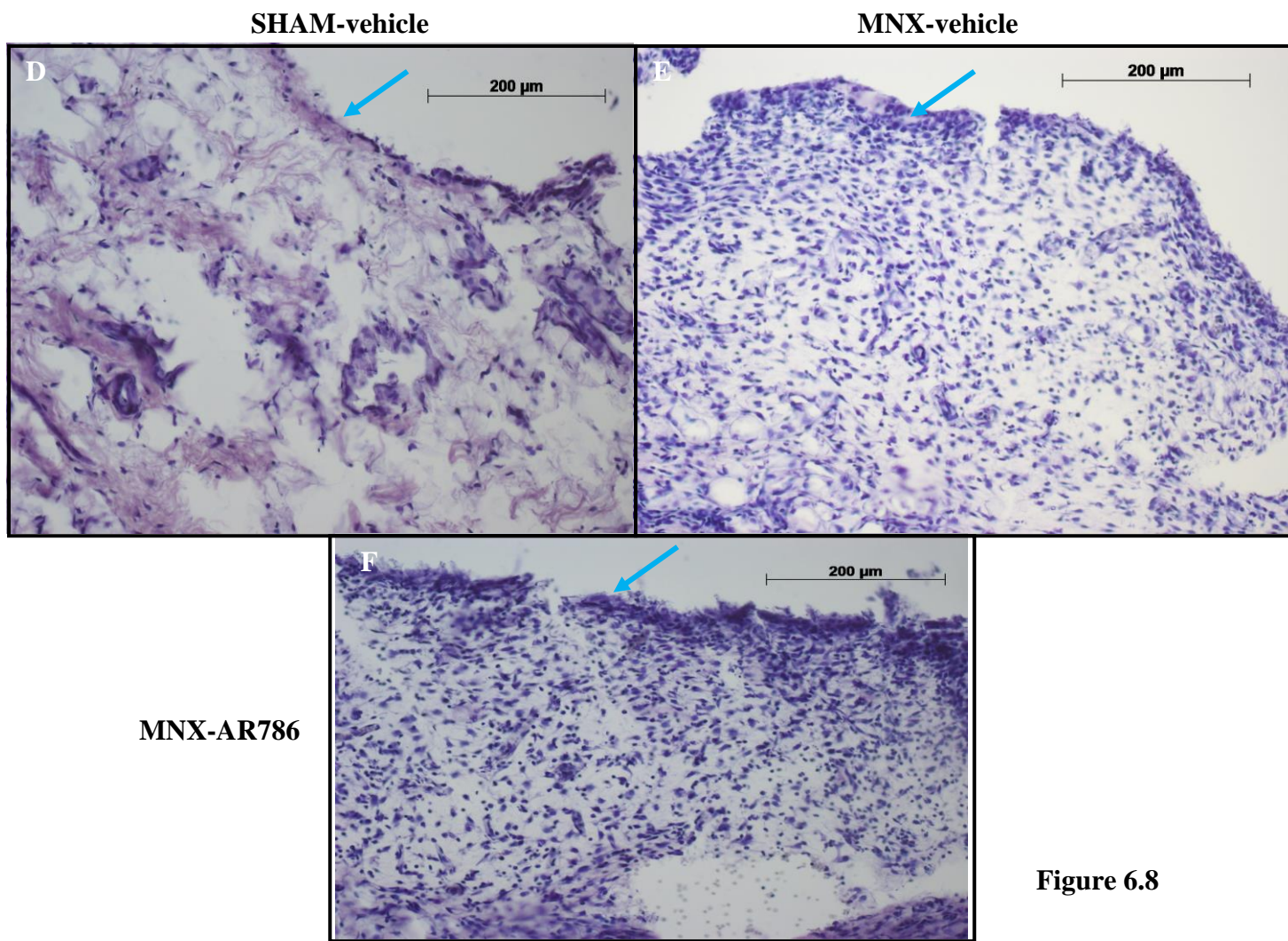


Figure 6.8

Figure 6.8 Synovitis in the MIA and MNX models of OA

Synovia collected 21 days after saline injection and 7 days oral treatment with Gelucire vehicle (A) or 28 days after sham surgery and 28 days oral treatment with Gelucire vehicle (D) display normal microscopic appearances. Both OA models displayed microscopic evidence of synovitis. MIA-injection (B), or MNX surgery (E) resulted in mild synovitis, characterised by increased thickness of the lining layer (blue arrows), and increased sublining cellularity. Synovitis was reduced in MIA-injected rat knees following treatment for 7 days with oral AR786 (C) compared to Gelucire vehicle treated controls (B). Synovitis appeared similar after MNX surgery in rats treated either with AR786 (F) or vehicle (E). Photomicrographs show haematoxylin and eosin stained sections of synovium from a rat with the median synovitis score from each group. Scale bar = 200µm.

6.4.1.4 Macroscopic pathology

Intra-articular injection of MIA or MNX surgery was each followed by increased cartilage damage as indicated by increased macroscopic chondropathy scores (Guingamp scoring method). Macroscopic chondropathy scores 21 days after arthritis induction were significantly higher in vehicle-treated arthritic rats induced by MIA [10 (7.4 to 13)] or MNX [10 (8.6 to 12)], compared to non-arthritic control rats (saline-injected [1 (0.1 to 1.9) $p < 0.001$] and sham-operated [1.5 (0.7 to 2.3) $p < 0.01$] respectively) (Figs. 6.9A and B). Likewise, macroscopic chondropathy scores, 28 days after arthritis induction were significantly higher in vehicle-treated arthritic rats induced by MNX [7.1 (6.2 to 8)] compared to non-arthritic sham-vehicle treated control rats [1.3 (0.5 to 2.1) $p < 0.05$] (Fig. 6.9C). MIA-induced OA was characterised by widespread macroscopic pathology (Figs. 6.9A and 6.11B), whereas chondropathy in MNX-induced OA was predominantly localised to the medial tibiofemoral joint (Figs. 6.9B - C and 6.10E).

Administration of AR786 had no significant effect on macroscopic chondropathy in either OA model, whether administered in treatment or preventive protocols (Fig. 6.9).

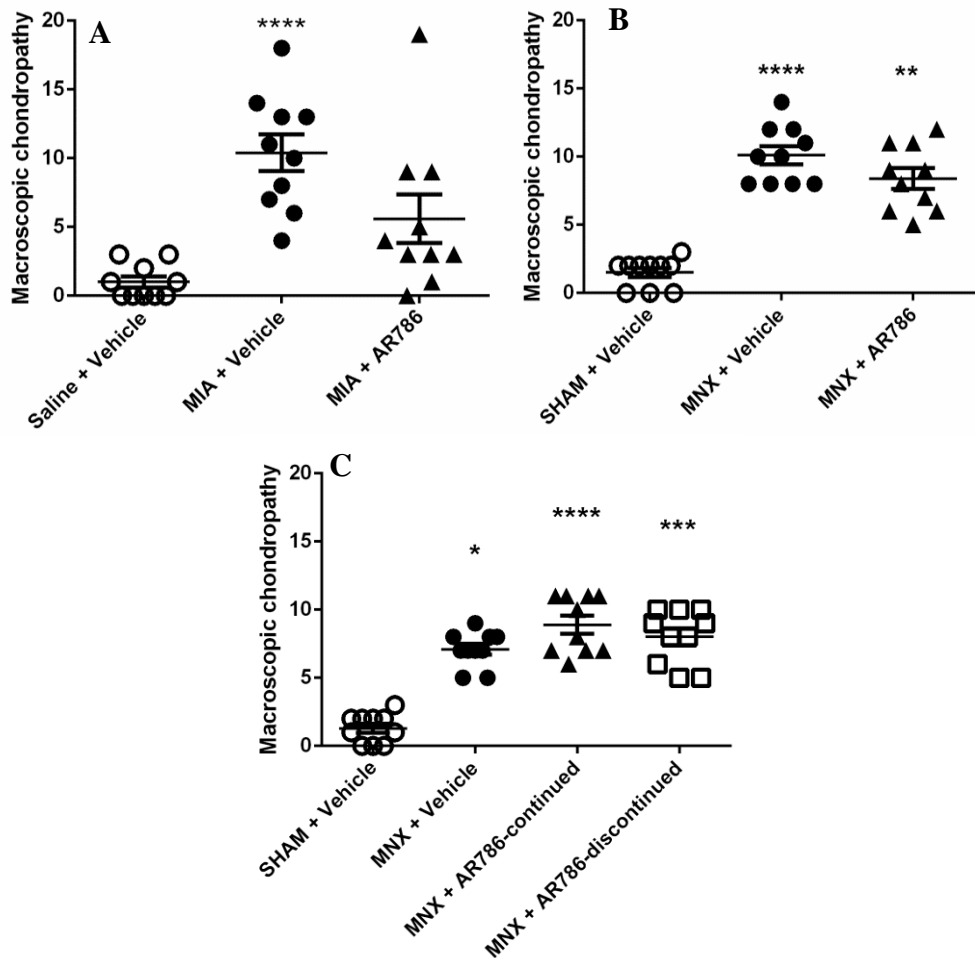


Figure 6.9 Macroscopic chondropathy scoring in the MIA and MNX models of OA.

Both OA models displayed macroscopic evidence of chondropathy (A – C), 21 days (A, B) or 28 days (C) after arthritis induction. Administration of AR786 had no significant effect on macroscopic evidence of chondropathy in either treatment (A, B) or preventive (C) protocols. Scatter plots show mean \pm SEM of $n = 10$ rats/group. * $p < 0.05$, ** $p < 0.01$, *** $p < 0.001$ compared with saline-injected or SHAM-operated vehicle controls. Scoring was done using a dissecting microscope at $\times 10$ magnification.

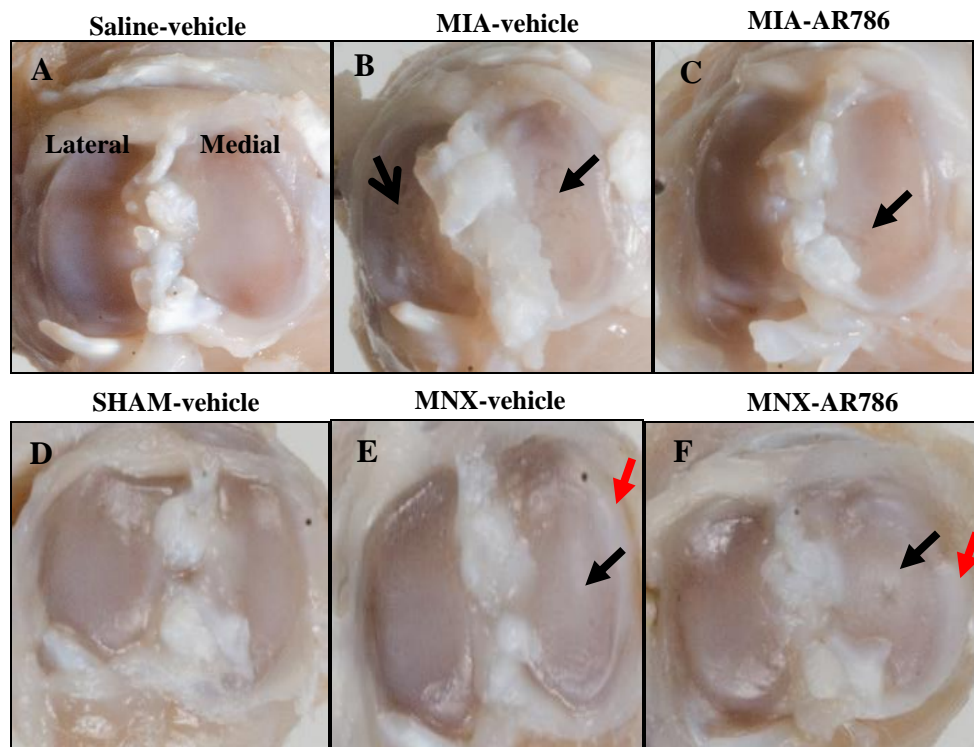


Figure 6.10 Macroscopic appearances of chondropathy in the MIA and MNX models of OA

Tibial plateaux from 21 days after saline-injection (A) or sham-operation (D) show normal appearances with no evidence of cartilage erosion. Tibial plateaux from rats 21 days after MIA-injection (B and C) or MNX (E and F), and following 7 days treatment with Gelucire vehicle (B and E) or AR786 (C and F) display erosions of the articular cartilage in the weight bearing areas (black arrows), some of which extend to the underlying subchondral bone. Osteophytosis (red arrows) is also apparent in the medial tibial plateau of the MNX-operated rats (E and F). Photomicrographs (A-F) show medial and lateral tibial plateaux from a rat with the median chondropathy score from each group.

6.4.1.5 Numbers of TRAP positive osteoclasts

The numbers of tartrate-resistant acid phosphatase (TRAP) positive multinucleated osteoclasts in the subchondral bone of the tibial plateau were increased following either intra-articular injection of MIA or MNX surgery. TRAP positive multinucleated osteoclasts numbers in the subchondral bone 21 days after arthritis induction were significantly higher in MIA [68 (59 to 76)] and MNX [32 (26 to 38)] rats compared to non-arthritic control rats (saline-injected [46 (43 to 50) $p < 0.001$] or sham-operated [23 (19 to 26) $p < 0.05$] respectively) (Fig. 6.11). Administration of AR786 from 14 days after OA induction by intra-articular injection of MIA resulted in significant reductions in the numbers of TRAP positive multinucleated osteoclasts 7 days later [51 (46 to 56)], compared to vehicle-treated, MIA-injected rats [68 (59 to 76), $p < 0.05$, Fig. 6.11A]. However, no significant reductions in numbers of TRAP positive osteoclasts were observed in the MNX-drug treated rats (Fig. 6.11B).

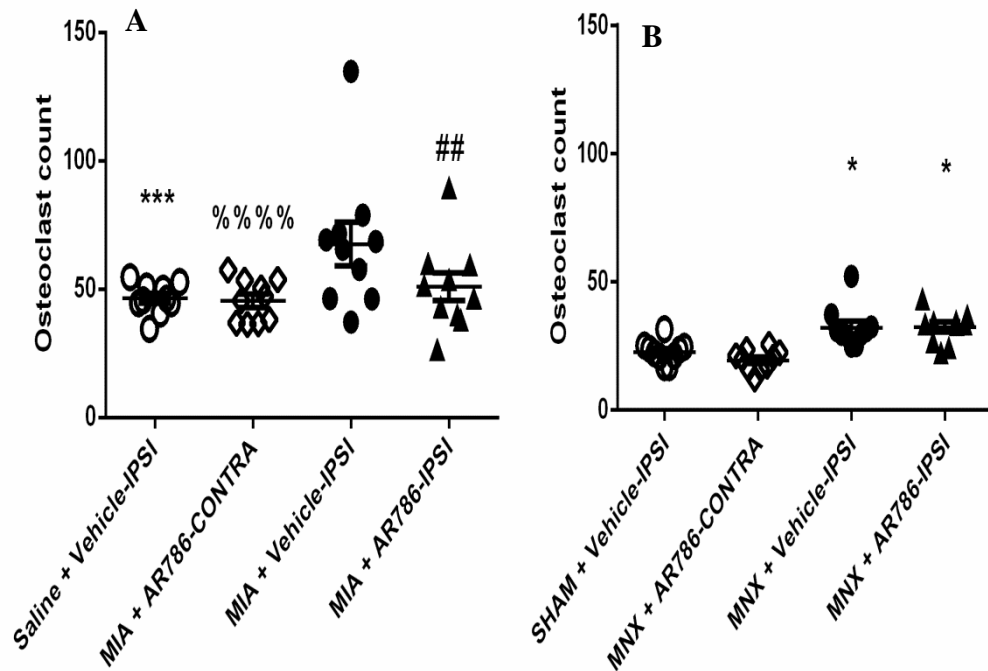


Figure 6.11 TRAP positive multinucleated osteoclasts in MIA and MNX models of OA

Numbers of TRAP positive multinucleated osteoclasts were increased in the joint samples of MIA and MNX-vehicle treated rats at day 21. Numbers of TRAP positive multinucleated osteoclasts were significantly reduced by AR786 therapeutic treatment in MIA-injected rats (A) but not MNX-operated rats (B). Scatter plots show mean \pm SEM of $n = 10$ rats/group on six sections per rat from the anterior half of the knee joint. *** $p < 0.001$ MIA vehicle versus saline-vehicle control, %%% $p < 0.001$ MIA-vehicle versus naïve-drug treated (MIA-CONTRA) and ## $p < 0.01$ MIA-vehicle versus MIA-drug treated (A). * $p < 0.05$ MNX-vehicle or drug treated versus sham-operated vehicle (B). Ipsilateral (IPSI - arthritic knee), contralateral (CONTRA - non-arthritic knee).

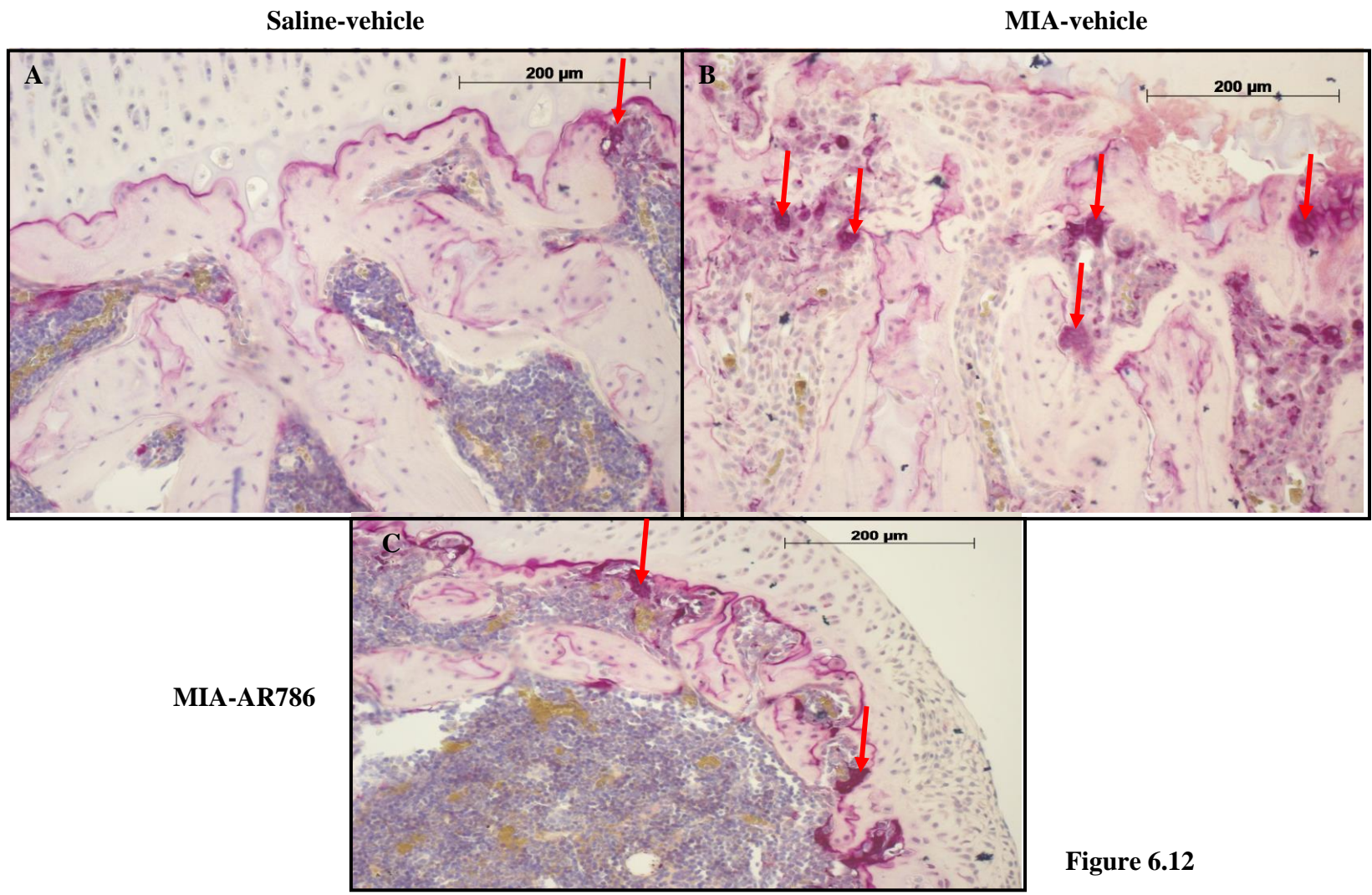


Figure 6.12

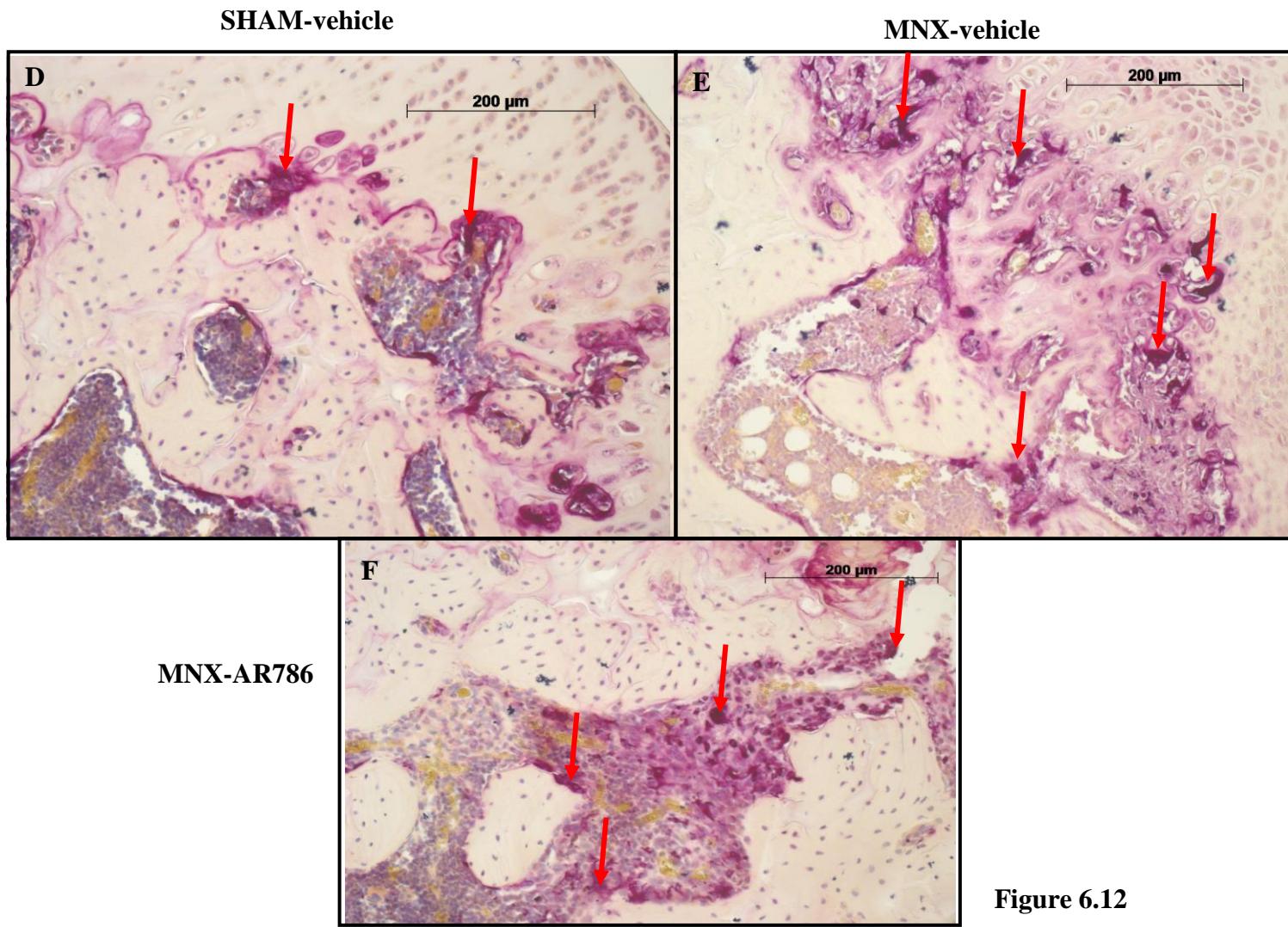


Figure 6.12

Figure 6.12 TRAP positive multinucleated osteoclasts in the MIA and MNX models of OA

Medial tibial plateaux 21 days after saline-injection (A) or sham-operation (D) show minimal numbers of multinucleated osteoclasts (red arrows) in the subchondral bone. Both OA models displayed increased numbers of multinucleated osteoclasts (red arrows), MIA-injection (B), or MNX surgery (E). Numbers of TRAP positive multinucleated osteoclasts were reduced in MIA-injected rat knees following treatment for 7 days with oral AR786 (C) compared to Gelucire vehicle treated controls (B). Numbers of TRAP positive multinucleated osteoclasts were similar after MNX surgery in rats treated either with AR786 (F) or vehicle (E). Photomicrographs show TRAP stained sections of the tibial plateau from a rat with the median osteoclast count from each group. Scale bar = 200 μ m.

6.4.2 Therapeutic and preventive administration of a monoclonal NGF antibody M911 in the MIA model

Knee joint samples from the muMab911 study were kindly provided by Luting Xu to allow me to further explore possible effects of blocking the NGF-TrkA pathway on joint pathology in the MIA model. Pain data are not shown, but the compound had a significant inhibitory effect on pain behaviour in both therapeutic and preventive protocols.

6.4.2.1 Structural (microscopic) pathology

Intra-articular injection of MIA was associated with alterations to the articular cartilage of the knee joint after 28 days, measured as cartilage damage score in the tibial plateau compared to saline-injected rats (Fig 6.13A and B). There was also a significant decrease in matrix proteoglycan in the MIA-injected rats compared to saline controls (Fig 6.13E and F), and abnormal chondrocyte morphology in MIA-injected rats compared to saline-injected rats (Fig 6.13C and D). M911 (s.c. 10mg/kg) did not significantly alter histopathological changes to the cartilage in any of the treatment protocols: 14 days after arthritis induction (therapeutic treatment; Fig 6.13A, C and E) or weekly administration before and after arthritis induction (preventive treatment; Fig 6.13B, D and F).

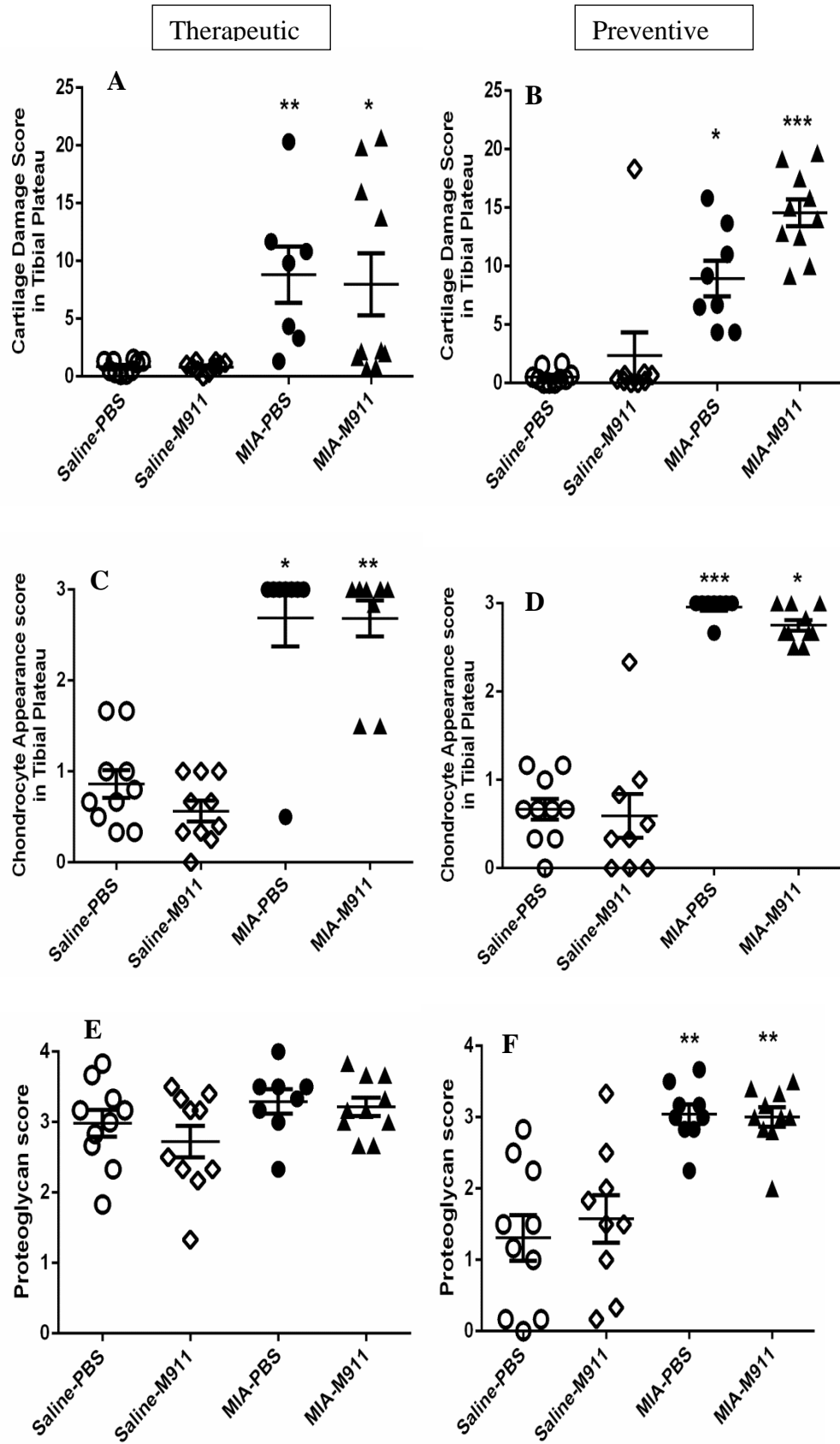


Figure 6.13

Figure 6.13 Microscopic pathology in the MIA model of OA

The MIA model displayed histologic evidence of pathology measured as cartilage chondropathy (A and B), abnormal chondrocyte morphology (C and D) and proteoglycan loss (E and F), 28 days after arthritis induction. Administration of M911 had no significant effect on microscopic pathology in either treatment (A, C and E) or preventive (B, D and F) protocols. Scatter plots show mean \pm SEM of n = 7-10 rats/group. *p<0.05, **p<0.01, ***p<0.001 MIA-PBS or MIA-M911 compared with saline-injected PBS vehicle controls.

Therapeutic

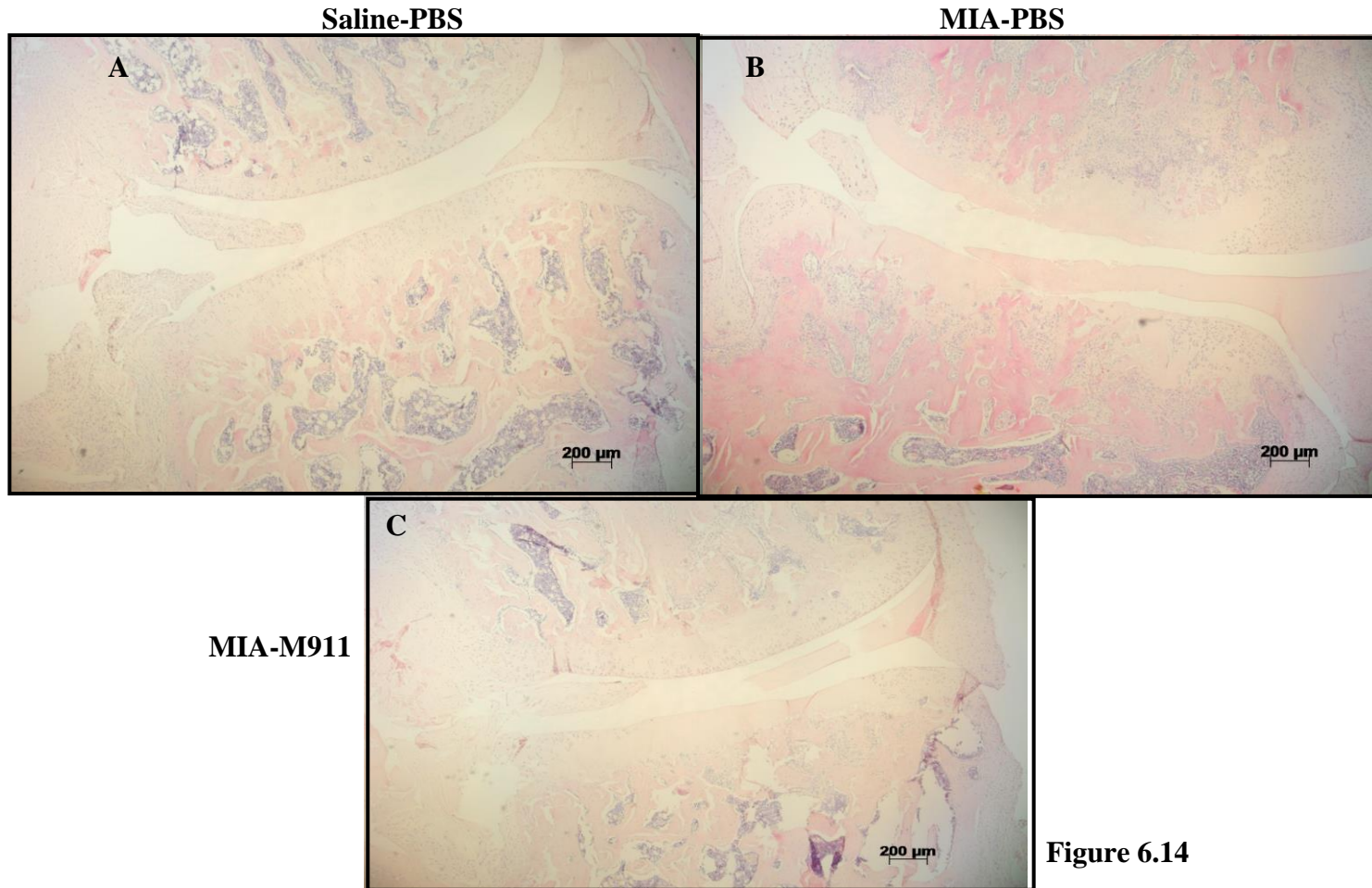
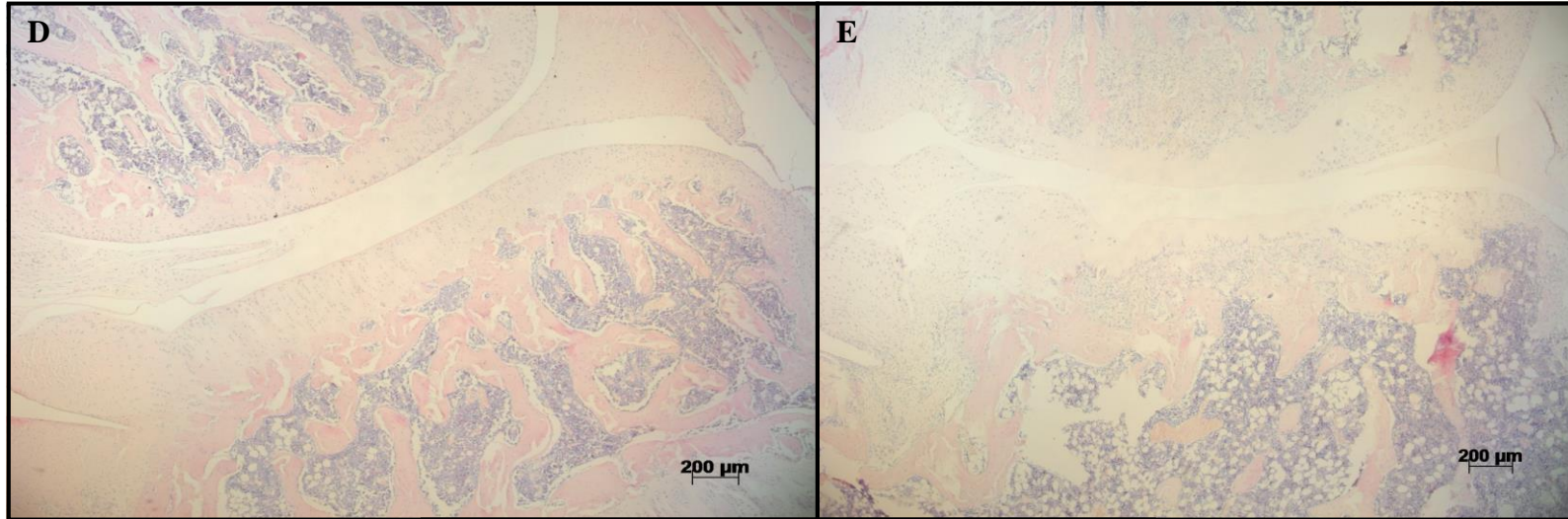


Figure 6.14

Preventive

Saline-PBS

MIA-PBS



MIA-M911

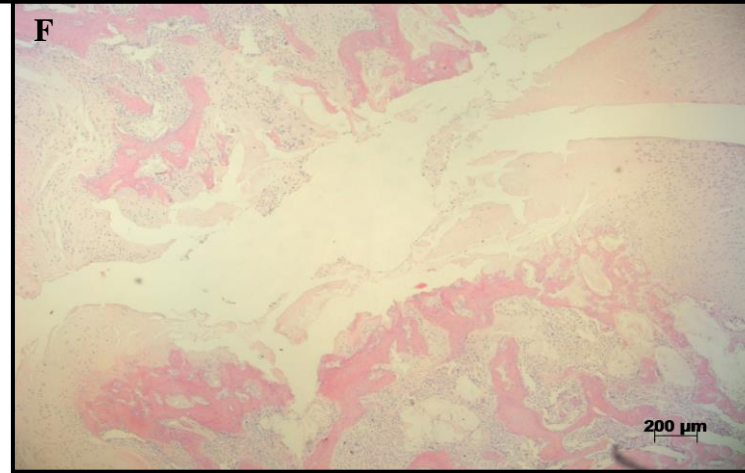


Figure 6.14

Figure 6.14 Microscopic appearances of pathology in the MIA model of OA

Knee joints collected 28 days after saline injection and 2 weeks of weekly subcutaneous injection with PBS vehicle (A) or 4 weeks of weekly subcutaneous injection with PBS vehicle (D) display normal microscopic appearances. The MIA model displayed microscopic evidence of structural pathology in both studies (B, C, E and F). MIA-injection resulted in cartilage fibrillations (E), erosions (B and F), subchondral bone breakdown (F) and abnormal morphology of chondrocytes (B, C, E and F). Structural pathology appeared reduced or mild in the MIA-injected rat knees following 2 weeks of weekly subcutaneous treatment with M911 (C) but this was not significant compared to PBS vehicle treated controls (B). Photomicrographs show haematoxylin and eosin stained sections of the medial tibial plateau from a rat with the median cartilage chondropathy (OARSI) score from each group. Scale bar = 200µm.

6.5 DISCUSSION

The effect of a novel selective TrkA inhibitor, AR786 and an anti-NGF antibody M911 was investigated in two rat models of OA. It was found that pain behaviour associated with OA was inhibited by AR786 using both preventive and therapeutic protocols. AR786 also reduced OA induced synovitis and TRAP positive multinucleated osteoclast numbers in the MIA model, whereas no significant effect on chondropathy was detected in both MIA and MNX models. M911 administration in both preventive and therapeutic protocols did not significantly affect structural pathology assessed by histology. These data suggest the potential of a small molecule, orally available, selective TrkA inhibitor for the treatment of OA pain.

Intra-articular injection of MIA, or MNX surgery, led to pathological features of OA (chondropathy and mild synovitis), and increased pain behaviours, as previously reported (Ashraf et al., 2014, Sagar et al., 2013). Weight bearing asymmetry, comparable to standing pain in people with OA (Christiansen and Stevens-Lapsley, 2010) might result from a combination of nociception, peripheral and central sensitisation (Suokas et al., 2012). Reductions in hind paw withdrawal thresholds to punctate mechanical stimulation are indicative of allodynia, and are associated with the development of central sensitisation in rats with OA (Sagar et al., 2010). Central sensitisation may augment joint pain, and contribute to more widespread pain sensitivity in people with OA (Suokas et al., 2012). These data support a sequential progression from peripheral to central nociceptive mechanisms during the induction of OA in rats, with early weight bearing asymmetry followed by the establishment of distal allodynia. Sequential development of augmented pain processing during OA development is further indicated by electrophysiological, cellular and molecular studies in rat models of OA (Sagar et al., 2011, Burston et al., 2013). By 14 days after OA induction, either by MIA or MNX, an OA phenotype is established which resembles that seen in humans, including chondropathy, synovitis, weight bearing asymmetry and reduced mechanical pain thresholds at sites distant from the affected joint (Mapp et al., 2013). These characteristics change little during the following 35 days in the absence of therapeutic

intervention. Minor differences in pain phenotypes reported between MIA and MNX OA models may reflect heterogeneity also observed between different people with OA. Reductions in hind paw withdrawal threshold in MIA-induced OA were more pronounced than in MNX-induced OA, as previously reported (Mapp et al., 2013), consistent with a greater contribution from central pain processing (Ivanavicius et al., 2007, Orita et al., 2011). Consistency of TrkA inhibitor analgesic effects between models suggests that findings may be relevant to OA in general, rather than being specific to the mode of OA induction.

Oral administration of the TrkA inhibitor AR786 abolished pain behaviour in both MIA and MNX models in preventive and therapeutic studies. These findings extend previous reports of analgesic effects of Trk inhibitors in non-malignant skeletal and bone cancer pain (Ghilardi et al., 2010, Ghilardi et al., 2011), to indicate that analgesic effects of Trk inhibition may be mediated specifically by TrkA. NGF blockade using a TrkA-immunoglobulin G (TrkA-IgG) fusion protein also reduced pain behaviour in rodent OA (McNamee et al., 2010). Analgesic efficacy of NGF blockade using monoclonal antibodies in clinical trials confirms the importance of NGF to OA pain. These findings indicate a role also for the high affinity NGF receptor, TrkA, and demonstrate the potential for a small molecule selective inhibitor of TrkA as a novel therapeutic strategy in OA. NGF is released during inflammation, and increased expression of NGF within the synovium (Stoppiello et al., 2014) or subchondral bone (Walsh et al., 2010) may mediate OA pain by binding to TrkA on adjacent unmyelinated and thinly myelinated sensory neurones. NGF binding to TrkA initiates phosphorylation and increased sensitivity of the calcium channel TRPV1, increased expression of neuropeptides substance P, and calcitonin gene-related peptide (CGRP) and of brain derived neurotrophic factor (BDNF) (Pezet and McMahon, 2006, Basbaum et al., 2009). Increased neuropeptide release into the joint can facilitate neurogenic inflammation and angiogenesis, and further sensitise articular nociceptors (Mapp et al., 2012, Bullock et al., 2014). Release of BDNF within the spinal cord may contribute to central sensitisation (Lu et al., 2009). Rats with OA are particularly sensitive to the effects of NGF on pain behaviour, and display increased TrkA

expression in DRGs not only ipsilateral, but also contralateral to the arthritic joint (Ashraf et al., 2014).

AR786 displays low CNS penetration, with plasma : CSF ratios approximately 10:1 (Andrews, 2014). However, TrkA inhibition attenuated distal allodynia to punctuate stimulation, a behavioural correlate of abnormal central pain processing. NGF may induce central sensitisation indirectly by increasing BDNF expression in primary afferent neurons (Apfel et al., 1996). Furthermore, synovitis may be a stimulus to the generation of central sensitisation during arthritis (Ashraf et al., 2014). Reductions in distal allodynia relapsed more quickly after treatment withdrawal than did weight bearing asymmetry, suggesting that TrkA inhibition has a more sustained effect on peripheral pain processing, than on central sensitisation. Referred pain (distal allodynia) results from both central and peripheral input (Suokas et al., 2012). It is likely, therefore that reduction of distal allodynia following TrkA inhibition results from blocking peripheral actions of NGF.

It was observed that rats with OA that received 14 days pre-emptive treatment continued to display improved weight bearing asymmetry for at least 10 days after treatment withdrawal. These sustained analgesic effects are consistent with a reduction in peripheral sensitisation that requires further sustained stimulus from the arthritic joint in order to relapse. This raises the potential that TrkA inhibition might prevent the transition to a sensitised state if administered for short periods during critical phases of OA development, or during active phases of disease. This contrasts, for example, with NSAIDs such as indomethacin, which, while reducing weight bearing asymmetry in MNX-induced OA, requires continued treatment for maintenance of effect, with a relapse of weight bearing asymmetry to levels that are comparable to those seen in arthritic rats that have never received indomethacin only 3 days after treatment withdrawal (Ashraf et al., 2014, Sagar et al., 2011).

On the other hand, the discontinued NSAID nimesulide being able to show a sustained effect in attenuating allodynia (but not weight bearing asymmetry) where the TrkA inhibitor didn't, further expands on the fact that TrkA inhibition has a more sustained effect on peripheral pain processing, than on

central sensitisation and that other mechanisms which may or may not be involving the NGF-TrkA pathway are at work here (Sagar et al., 2011). For example other central mechanisms of pain i.e. inputs from the spinal cord, such as increased expression of cyclooxygenases (COX) maybe involved as spinal COX-2 expression has been known to be increased and plays a crucial role in pain (Prochazkova et al., 2009, Seybold et al., 2003).

Synovitis is a characteristic feature of human knee OA that is associated with pain (Hill et al., 2007). Inflammation itself might mediate pain through the generation of factors that activate or sensitise joint nociceptors, including NGF (Fischer et al., 2010). Furthermore, synovitis might contribute to progressive cartilage damage (Scanzello and Goldring, 2012, Hill et al., 2007, Loeuille et al., 2005). TrkA activation increases inflammatory neuropeptide release from sensory nerves, including substance P and calcitonin gene-related peptide, these may mediate neurogenic inflammation (Kidd and Urban, 2001). Furthermore, TrkA might be expressed by mast cells (Nilsson et al., 1997), synovial fibroblasts (Manni et al., 2003), macrophages (Barouch et al., 2001) and chondrocytes (Pecchi et al., 2014), and inflammatory cell activation by NGF leads to the upregulation and release of histamine, bradykinin or prostaglandins, which might further activate or sensitise joint nociceptors (Štempelj and Ferjan, 2005, Linker et al., 2009). AR786 reduced synovitis in rats with MIA-induced OA, but did not significantly reduce either knee swelling or synovitis in rats with MNX-induced OA. Different effects of AR786 on synovitis between the 2 models may reflect different mechanisms of inflammation, or a more intense (and less responsive) synovitis in the MNX model (Mapp et al., 2013).

Chondropathy is a hallmark of human OA (Walsh et al., 2008), and cartilage changes have been associated with pain severity (Torres et al., 2006). Clinical trials of NGF-blocking antibodies were once put on hold by the Federal Drug Administration due to the rare occurrence of RPOA in patients receiving these agents (Schnitzer et al., 2014). Small reductions in macroscopic chondropathy scores observed following treatment with AR786 did not reach statistical significance and are unlikely to have made any major contribution to the observed reductions in pain behaviour. Likewise the minimal reductions in

microscopic chondropathy scores with therapeutic administrations of M911 also not reaching significance may not have contributed to the analgesic effect of this compound (pain data are not shown). In both AR786 and M911 studies, there was no evidence of OA exacerbation following treatment, but the occurrence of rare effects seen in predisposed individuals to NGF blockade cannot be excluded. It is possible that RPOA associated with NGF-blockade using monoclonal antibodies is due to effects of NGF that are not mediated by TrkA, or occur only in association with concomitant cyclooxygenase inhibition or other predisposing factors (Schnitzer et al., 2014). These studies were not designed to investigate rare adverse events as they were limited by small n numbers and the experiments were carried out on a species that share a relatively homogenous genetic background and dosing regimens have been undertaken for a short period of time and without concomitant medications. Therefore, more extensive toxicological studies would need to be undertaken with anti-NGF antibodies and TrkA inhibitors to investigate effects of NGF-TrkA blockade on structural pathology and contribution of these effects to rare adverse events.

Subchondral bone remodelling plays an important role in OA pain and pathology. Bone remodelling may occur before cartilage degeneration in OA, at which stage potential pain mediators (cyclooxygenase 2, substance P, TNF- α) may be detected in the subchondral bone (Kwan Tat et al., 2010, Ogino et al., 2009). Reports from the Boston Osteoarthritis Knee study reported that bone marrow lesions, detected by MRI, were strongly associated with OA knee pain and recent clinical trials using the bisphosphonate zoledranate confirms this association (Felson et al., 2001, Laslett et al., 2012). The outgrowth of sensory nerves following blood vessel growth within the subchondral bone may be a cause of pain in OA as these nerves are usually prone to sensitisation and have been reported to express the TrkA receptor (Suri et al., 2007, Castañeda-Corral et al., 2011). Bone remodelling is controlled by the activity of osteoclasts (bone resorption cells) and osteoblasts (bone formation cells). Osteoclastogenesis, development of osteoclasts is regulated by the osteoprotegerin (OPG)/receptor activator of NF- κ B (RANK)/receptor activator of NF- κ B ligand (RANKL) system. Associations between pain and bone

marrow lesions and the analgesic effects of zoledronic acid may suggest effects mediated by osteoclast activity in the subchondral bone. AR786 reduced numbers of TRAP positive multinucleated osteoclasts in the subchondral bone of rats with MIA-induced OA but did not significantly reduce numbers of TRAP positive multinucleated osteoclasts in rats with MNX-induced OA. The effects of AR786 in reducing pain behaviour and osteoclast numbers in the MIA model is similar to reports on the RANKL inhibitor, osteoprotegerin Fc (OPG-Fc) in inhibiting pain behaviour by targeting osteoclasts (Sagar et al., 2014). This suggests involvement of NGF-TrkA pathway not just in mediating nociception and inflammation but also in mediating pathology by activating function of cells (osteoclast) that contribute to structural pathology.

6.6 CONCLUSIONS

Inhibition of NGF activity by blocking TrkA reduced pain behaviour in two rat models of OA. Analgesic mechanisms of TrkA inhibition might include reductions in synovitis, osteoclast activity as well as reducing nociceptor sensitisation.

Reductions in pain behaviour were observed both using preventive and treatment protocols, and were sustained for up to 10 days despite treatment discontinuation. Clinical trials of NGF blockade have demonstrated potential for blocking the NGF-TrkA pathway for the relief of OA pain.

Further research should address possible differences between NGF-blockade and selective TrkA inhibition, and the potential for sustained benefit from discontinuous treatment, in order to help realise the potential of NGF-TrkA pathway inhibition for OA pain relief.

CHAPTER 7; GENERAL DISCUSSION

7.1 MAIN STUDY FINDINGS

Using animal models of arthritis, these data show that the NGF-TrkA pathway may play a role in mediating inflammation, osteochondral pathology and pain behaviour. These data also show validated methods for assessing joint pathology in these rat models.

The carrageenan model of inflammatory arthritis exhibited pain behaviour and acute inflammation observed as joint swelling, synovitis and macrophage infiltration into the synovium. The macrophage infiltration observed consisted of all activated macrophages displaying features of both M1 and M2 subtypes.

The MIA and MNX models of OA exhibited inflammation (joint swelling, synovitis and macrophage infiltration) and pain behaviour. The MIA and MNX models displayed structural pathology both macroscopically and microscopically. The pain phenotypes (weight bearing asymmetry and hind paw withdrawal threshold) observed in the MIA model were dependent on the MIA dose. The 0.1mg MIA injected rats displayed reduced hind paw withdrawal threshold but not weight bearing asymmetry whereas the 1mg MIA injected rats displayed both.

The Guingamp method of macroscopic scoring permitted discrimination between OA disease group (MIA and MNX) and normal controls (saline and sham). This method of scoring had a higher reliability and reproducibility than other macroscopic scoring methods (Indian ink and modified SFA).

The Janusz and modified OARSI histopathology scoring systems for cartilage damage were reliable and reproducible with similar variability and had strong correlations to each other. For histopathological assessment in the MIA model at earlier time points, the total joint score (anterior and posterior part) gave sufficient power to enable discrimination between the diseased group and the non-arthritic saline-injected controls. This finding is original as it contradicts

what was published for OARSI histopathological assessments in the rat (Gerwin et al., 2010), which encourages assessing only one part of the joint.

Following preventive or therapeutic treatment with the tropomyosin receptor kinase (Trk) A inhibitor, AR786, pain behaviour was inhibited in both MIA and MNX models, while inflammation was attenuated only in the MIA model. Analgesia was sustained for up to 10 days in the MNX model following AR786 treatment discontinuation. AR786 administration reduced the numbers of tartrate resistant acid phosphatase (TRAP) positive multinucleated osteoclasts in the MIA model, although it did not significantly alter macroscopic measures of structural pathology in either models of OA. These findings are novel as this thesis first reports the use of the TrkA inhibitor AR786 in reducing OA associated pain behaviour in the MIA and MNX models of OA. It also reports on the sustained analgesic effect of this compound in the MNX model. Preventive and therapeutic treatment with the anti-NGF monoclonal antibody M911 also did not alter changes to cartilage pathology.

Collectively these findings support the hypothesis that pain behaviour and structural pathology are features of OA models that are mediated by NGF and TrkA. NGF may mediate OA pain by altering joint function and structure, including neuronal sensitisation, inflammation and subchondral osteoclast activation. Therefore inhibition of the NGF-TrkA signalling has therapeutic potential in ameliorating structural pathology and associated pain in OA.

7.2 NGF; A MEDIATOR OF INFLAMMATION, OSTEOCHONDRAL PATHOLOGY AND PAIN IN OSTEOARTHRITIS

To date there are no effective structure modifying treatments, and available analgesic treatments are limited in efficacy and have associated adverse side effects (Matthews and Hunter, 2011, Goldring and Berenbaum, 2015). These two areas of unmet clinical need (structural joint degeneration and pain) co-exist but may not necessarily coincide as treatments that attenuate pain are rarely able to alter structural pathology and in some cases may exacerbate joint pathology (Reijman et al., 2005, Brown et al., 2012). On the other hand, structure modifying treatments (e.g. doxycycline) often fail to provide effective pain relief (Brandt et al., 2005, Nuesch et al., 2009). Given the complexity of OA, a single therapy may not be effective and therefore future research requires addressing both symptoms and structural changes (Mobasheri, 2013, Pulsatelli et al., 2013, Thakur et al., 2014).

The findings from this thesis show the symptomatic features of OA (inflammation, osteochondral pathology and pain behaviour), evidence of NGF-TrkA involvement in contributing to these features and the potential of targeting the TrkA receptor.

7.2.1 Inflammation

In this thesis, inflammation was observed as joint swelling, synovitis and infiltration into the synovium by inflammatory macrophages.

Intra-articular injection of λ carrageenan has been shown previously to induce acute inflammation (Walsh et al., 1998a, Valenti et al., 2012), similarly in this thesis, intra-articular injection of 2% carrageenan induced acute inflammation (joint swelling and synovitis). With this model, joint swelling begins within minutes of injection and therefore permits an accurate definition of the time of onset of acute inflammation. Intra-articular injection of 1mg of MIA or MNX surgery have also been shown to induce synovitis (Mapp et al., 2013), similarly in this thesis, intra-articular injection of 1mg of MIA or MNX

surgery induced inflammation. Oral administration of AR786 was observed to reduce synovitis in the MIA model, the mechanism of this inhibition is not entirely clear but it highlights the possible involvement of the NGF-TrkA in mediating inflammation. Increased expression of NGF has been reported in human OA synovium (Stoppiello et al., 2014) produced by synovial fibroblasts or macrophages. Synovial cells express TrkA and are therefore sensitive to NGF. NGF can also stimulate the proliferation of the synoviocytes (Raychaudhuri and Raychaudhuri, 2009).

Synovitis is reported to contribute to OA pain in both preclinical and clinical studies (Orita et al., 2012, Hunter et al., 2013). Inflammatory cells are also reported to contribute to OA (de Lange-Brokaar et al., 2012). For example, activated macrophages were detected in OA patients and were associated with clinical OA symptoms (Byers Kraus et al., 2013, Daghestani et al., 2015).

In this thesis it was demonstrated that macrophages of the M1 and M2 subtypes were present in the carrageenan model of inflammatory arthritis. ED macrophage markers were used to stain for all activated phagocytic macrophages (ED1 – CD68), macrophages involved in tissue healing (ED2 – CD163) and chronic inflammatory macrophages (ED3 – CD169). Likewise in the MIA model of OA, macrophages expressing ED1 were present in the synovium. As reported in other studies, macrophages that express these markers were observed in the joint of intra-articular injected carrageenan and antigen induced arthritis rats (Walsh et al., 1998a, Dijkstra et al., 1987). AR786 was observed to have no significant effect in reducing ED1 expressing macrophages although it significantly reduced synovitis score. This would suggest that NGF-TrkA may contribute to the regulation of inflammatory mediators that contribute to the inflammatory process or other inflammatory cells. NGF was reported to play a role in the stimulation of inflammatory cytokines (IL-1, -2, -6, -8 and TNF) and leukocyte activation or migration (Seidel et al., 2010). TrkA is expressed by most immune cells (B and T lymphocytes, mast cells, monocytes, neutrophils, basophils and eosinophils) thus allowing NGF to modulate cell differentiation and regulate the immune response (Aloe et al., 2012, Bracci-Laudiero, 2010, Prencipe et al., 2014).

7.2.2 Osteochondral pathology

Characteristic features of structural pathology in OA can be observed macroscopically and by histology on joint tissue sections. The features observed in humans are cartilage fibrillations and eventual loss of cartilage, loss of proteoglycan, loss of osteochondral junction integrity (increased breaching of the osteochondral junction by vascular channels), subchondral bone remodelling (Walsh et al., 2008, Stoppiello et al., 2014). In rat models of OA, structural changes in the joint consists of cartilage fibrillations, abnormal morphology of chondrocytes, proteoglycan loss, loss of osteochondral junction integrity, subchondral bone remodelling and increased numbers of activated osteoclasts in the subchondral bone (Mapp et al., 2013, Ashraf et al., 2011a, Sagar et al., 2014, Yu et al., 2013). Similarly in this thesis the MIA and MNX models also demonstrated the above features of OA structural pathology. In this respect the MIA and MNX models used in this thesis were shown to effectively mimic the human condition.

Although the TrkA inhibitor did not significantly reduce macroscopic chondropathy changes in the MIA model, it does not discount that there might be a small biologic effect on chondropathy. Irrespective of the lack of effect in altering chondropathy, it was observed to reduce the numbers of TRAP positive osteoclasts in the MIA model. NGF was reported to play a role in inducing RANKL-independent osteoclastogenesis (Hemingway et al., 2011). NGF induced both osteoclast differentiation and activation. These NGF-induced cells were positive for TRAP and capable of bone resorption (Hemingway et al., 2011). Other reports point to the involvement of osteoclasts in chondropathy and pain as their inhibition prevented cartilage pathology and pain behaviour in the MIA model (Strassle et al., 2010, Sagar et al., 2014). The results in this thesis support the involvement of NGF-TrkA in regulating osteoclast function and points to important effects on OA pathology.

7.2.3 Pain

Chronic pain represents a major public health burden with evident socioeconomic impact on its sufferers, for example, in people with OA.

OA pain can be either localised and/or referred. Localised pain may be associated with peripheral sensitization while referred pain may be associated with both peripheral and central sensitization (Suokas et al., 2012, Hucho and Levine, 2007). Central sensitization is implicated in advanced OA as evidenced by the presence of persistent pain even after knee replacement surgery and spread of pain beyond the affected joint (Lundblad et al., 2008, Lluch et al., 2014). Pain behaviours in this thesis, weight bearing asymmetry (pain on loading) and lowered paw withdrawal threshold at remote sites broadly represent peripheral and central sensitization in OA (Sagar et al., 2010, Ashraf et al., 2014).

One of the main findings from this thesis was that reduced paw withdrawal thresholds was not restricted to the higher 1mg MIA dose but was present in the low 0.1mg MIA dose. Indeed, hind paw withdrawal thresholds were lowered following both the 0.1mg dose of MIA and the 1mg dose of MIA, in the absence of weight bearing asymmetry in the 0.1mg dose. This might offer a model of a different pain phenotype which suggests that there may be different subgroups of people in OA which present with central pain only, and the separation of these subgroups of people would allow for the development of targeted treatments for OA pain.

Recent clinical studies suggest that NGF may represent a good target for the development of innovative analgesic treatments. Evidence from both clinical and preclinical research indicates that NGF is an important mediator of inflammatory nociceptive and neuropathic pain (Watson et al., 2008, Seidel et al., 2010, Seidel et al., 2013, Ashraf et al., 2014). NGF signals through TrkA or p75, and although p75 can interact with TrkA, most of NGF-induced sensitisation is reported to occur through TrkA (Eibl et al., 2012, Watson et al., 2008).

To confirm the role of the NGF-TrkA in mediating pain, the TrkA inhibitor AR786 was used. It was observed that AR786 attenuated already established pain behaviour when administered therapeutically and prevented the development of pain behaviour when given as a pre-emptive treatment in OA models. These results observed in this thesis are in line with already published

work that report that inhibition of NGF function reduces hyperalgesia and pain behaviour in models of acute local inflammation, chronic inflammatory arthritis and OA (McNamee et al., 2010, Seidel et al., 2010, Seidel et al., 2013). Other studies report the attenuation of non-malignant skeletal or bone cancer pain with inhibition of TrkA function (Ghilardi et al., 2010, Ghilardi et al., 2011), although the Trk inhibitor used in both studies blocks the other two Trk (TrkB, C) receptors in addition to TrkA. In this thesis, there is evidence for TrkA involvement in mediating OA pain as the inhibitor used here was selective for TrkA. Also in the above studies, they report that early or sustained administration but not late or acute administration was effective in inhibiting pain behaviour, while in this thesis late or acute administration was just as effective as the early or sustained administration of AR786. Thus implying that this inhibitor would be beneficial for use in both early and late OA pain states.

AR786 reduced synovitis and numbers of TRAP positive osteoclast, which indicates this therapeutic approach may reduce the mechanisms underlying the pain behaviour in these models. It is likely that synovitis contributes to pain through the synthesis and release of factors (neuropeptides; substance P, CGRP, other inflammatory mediators; ILs, TNF, histamine, bradykinin, prostaglandins and NGF) that activate or sensitise joint nociceptors (Fischer et al., 2010, Kidd and Urban, 2001). TrkA activation is reported to contribute to increased neuropeptide release (Mantyh et al., 2011). Osteoclasts might contribute to pain by creating an acidic environment in the subchondral bone (Jimenez-Andrade et al., 2010) and the release of proteases such as cathepsin K (Teitelbaum, 2007). The released protons (H^+) can directly activate and sensitise sensory neurones thus increasing pain signalling (Jimenez-Andrade et al., 2010). Osteoclasts are able to cut channels through the osteochondral junction (Mapp and Walsh, 2012), and loss of osteochondral junction integrity may expose sensory nerves in the subchondral bone to sensitising factors from the cartilage and synovium (Mapp and Walsh, 2012).

NGF-blocking antibodies sequester NGF and prevent it binding to its receptors, therefore it is not known if NGF contributes to pain through p75 or only through TrkA, although NGF binding to p75 has been reported to cause

pain (Watanabe et al., 2008). The p75 receptor was associated with inflammatory pain in the CFA model. The findings in this thesis suggest that the majority of the pain behaviour exhibited by the OA models is dependent on NGF binding to TrkA, and not through the p75 receptor as AR786 specifically blocks TrkA. Nevertheless, NGF binding to p75 modulates or increases binding of NGF to TrkA (Toni et al., 2014, Lachance et al., 1997) and blocking NGF binding to p75 on sympathetic neurones transiently reduces TrkA activation (Lachance et al., 1997). Therefore NGF-p75 signalling may be influenced by AR786 and contribute to the effect reported herein. TrkA is expressed by DRGs in the spinal cord and there is increased expression with intra-articular NGF injection (Ashraf et al., 2014). Although the compound used here does not cross the blood brain barrier (Andrews, 2014), the effect of this compound in reducing central sensitization might be through effect of blocking TrkA expressed on DRGs thus preventing or dampening the ascending of sensory input to the brain.

7.2.4 Targeting NGF or TrkA for OA

Despite the successes of molecules targeting TrkA for controlling pain in animal models, there are still no clinical trials for it. As mAbs carry the risk of immune reactions such as acute anaphylaxis, serum sickness and the generation of antibodies against the therapeutic agent, the use of Trk inhibitors may be a better choice. Adverse events such as peripheral oedema, arthralgia, pain in extremity and neurosensory symptoms were reported with anti-NGF mAbs in clinical trials (Pokrovnichka, 2012). On the other hand, if drug development were to begin for Trk inhibitors, investigators will need to take into account the lack of selectivity of pan Trk inhibitors. Blocking of other Trk receptors may result in adverse effects (Winston et al., 2003). These include hyperphagia, obesity and ataxia (in greater doses) which have been reported to be attributed to inhibition of BDNF/TrkB signalling (Unger et al., 2007).

In this thesis the importance of the selective targeting of TrkA is highlighted from evidence of its involvement in contributing to nociception, inflammation and pathology.

7.3 LIMITATIONS OF CURRENT RESEARCH

The results presented in this thesis support the evidence of symptomatic features of arthritis in animal models and the involvement of the NGF-TrkA in contributing to these features. These conclusions are limited by a number of factors and are outlined for each chapter below;

Firstly one of the main limitations is the use of animal models. Rat OA models used in this thesis and elsewhere display similar histological and pain behavioural characteristics to those observed in chronic human OA (Sagar et al., 2013). The consistent analgesic effects of AR786 between models suggest that findings from this thesis might be relevant to OA in general, rather than being specific to the mode of OA induction. However, caution must be exercised before generalising from laboratory findings to human OA. Rat models develop rapidly and pain mechanisms might differ in early compared to long established OA. The efficacy of drugs may not directly reflect that observed in humans due to the rapidity of disease progression or the low/minute concentrations of drug treatment administered in clinical trials following toxicological studies (Lampropoulou-Adamidou et al., 2014). OA animal models are for the most part driven by mechanical factors than in the naturally occurring OA in humans, therefore some factors that contribute to human OA may not be affected in certain animals. Treatment may be effective in animals because they are initiated at or close to the time of injury in contrast to human clinical trials (Martel-Pelletier and Pelletier, 2013). However, preclinical research plays a major role in understanding the mechanisms of disease and the identification of potential treatment targets.

CHAPTER 3

The present study reports on characteristic features of acute inflammation to include acute joint swelling and acute synovitis. It does not however report on infiltration by neutrophils which are the cardinal cells of acute inflammation but rather reports on macrophage infiltration, the signature cells of chronic inflammation. However, this thesis reports that macrophages are involved and present in the early stages of inflammation in the carrageenan model.

The study is also limited to acute inflammation and is important for therapeutics targeting acute inflammation but not persistent or chronic inflammation. Mechanisms underlying the shift from acute to persistent chronic inflammation in humans is not entirely clear and in OA, and patients may present with both acute and chronic inflammation (Bonnet and Walsh, 2005).

Rats used in this chapter did not have equal body weights at the time of arthritis induction. The carrageenan injected rats had higher body weights than the naïve rats. This might have occurred as a result of the random selection of rats for induction not based on body weights but on baseline behaviour (weight bearing asymmetry) by an independent researcher.

CHAPTER 4

The disadvantage of the macroscopic chondropathy scoring (either by direct scoring or photographic scoring) like histological scoring is that the scoring methods did not include the patella. Patellofemoral OA is a known source of pain and disability. During tissue harvesting, the patella was always removed in attachment to the synovium as this aids for histological assessment of synovitis. Radiography, although not carried out in this thesis may be another method of investigating associations between patellofemoral OA and histological synovitis.

Another limitation to this study was that reliability tests were carried out between observers with different levels of experience. Therefore, reliability and validity estimates may have limited generalizability and that inter-observer variation may be less with more experienced operators.

Synovitis was associated with radiological joint space narrowing (JSN), which is normally regarded as an important marker of OA structural severity (Altman et al., 1987). This association between JSN and synovitis may suggest that association between OA severity and synovitis may be as a result of cartilage pathology (Walsh et al., 2008). This thesis does not have any radiological measurements to back up the associations observed between OA severity and synovitis.

CHAPTER 5

The study from this chapter showed that central sensitization represented by a reduction in hind paw withdrawal threshold indicative of allodynia was observed also in the low 0.1mg MIA dose which may represent early mild OA. This conclusion was based just on the pain behaviour data only and did not include data from other factors involved in central sensitization i.e. spinal glia cells (astrocytes, microglia).

This chapter consisted of two studies; study 1 had 3 groups of rats (0.1mg, 1mg and saline) all stopped at day 20, while in the second study, there were 4 groups (day 42 – saline, day 42 – 0.1mg MIA, day 20 – 0.1mg MIA and day 20 – 1mg MIA). The lack of the day 20 – saline and the day 42 – 1mg MIA might be limitations to the current study as direct comparisons for time in the saline and 1mg MIA rats could not be made. Specifically, the effect of time on the number of vascular channels crossing the osteochondral junction in the saline group. Was the reduction in vascular densities observed in both the day 42 saline and day 42 - 0.1mg MIA injected rats really due to ageing?

CHAPTER 6

The experiments with AR786 did not investigate microscopic pathology (histopathology). Effect of drug not significantly altering pathology was entirely based on macroscopic grading. This explores the outer appearance of the knee joint but not the underlying appearance i.e. looking down the microscope with pathology highlighted or intensified by histological stains. Due to this, other effects of the compound for example on subchondral bone remodelling which is known to play an important role in OA pain and pathology were not investigated. On the other hand, the experiment with M911 did not investigate macroscopic pathology but only microscopic pathology. Investigating the effect of both compounds on microscopic and macroscopic pathology could further increase the understanding of the contributions of NGF-TrkA to OA joint pathology.

NGF is responsible for sensory nerve growth, and pain in OA is mediated by sensory nerves. NGF produced by vascular cells may contribute to the growth

of fine, unmyelinated sensory nerves along newly formed vessels (Walsh et al., 2010, Nico et al., 2008). Exposure of these vessels in the subchondral bone to sensitizing factors or their ingrowth into the cartilage or meniscus may be a potential source of pain (Mapp and Walsh, 2012, Suri et al., 2007, Ashraf et al., 2011b). This thesis did not investigate sensory nerve growth in the OA models and thus effect of AR786 on nerve growth was not explored.

Despite the above limitations, the work presented in this thesis supports the view that blocking the TrkA receptor may be beneficial in relieving structural pathology and pain in OA. The above limitations therefore form a basis for future work that should help in further investigating the mechanisms of structural pathology and associated pain in OA.

7.4 DIRECTIONS FOR FUTURE RESEARCH

This thesis provides a platform for further research into the mechanisms of structural pathology and associated pain in OA.

The presence of joint swelling, synovitis and macrophage infiltration confirmed the induction of acute inflammation in the carrageenan model of monoarthritis. It also confirmed the presence of different subtypes of macrophages in acute inflammation. Further work should determine whether this distribution of macrophage subtypes resembles that in chronic inflammation in the OA synovium using the MIA and MNX models, and their associations to synovitis and pain behaviour in the models. Equally, further work should test the specificity of the ED macrophage markers in labelling their specific macrophage subsets by either using double immunofluorescence to co-localise the markers on macrophages.

Synovitis is associated with radiological joint space narrowing (JSN), which is normally regarded as an important marker of OA progression (Altman et al., 1987). This association between JSN and synovitis may suggest that association between OA severity and synovitis may be as a result of cartilage pathology (Walsh et al., 2008). This thesis does not have any radiological measurements to back up the associations observed between OA severity and synovitis. Further work including radiological measurement should address association between OA severity and synovitis.

Central sensitization represented by a reduction in hind paw withdrawal threshold indicative of allodynia was observed also in the low 0.1mg MIA dose which represent early mild OA. This conclusion was based just on the pain behaviour data only. Future work to back up these results would require research into investigating cells in the spinal cord e.g. astrocytes, microglia and neurones which have been reported to show increased excitability of spinal neurones and are associated with pain behaviour (allodynia) showing central sensitization in the 1mg MIA dose (Sagar et al., 2010, Kelly et al., 2013b, Sagar et al., 2011). Furthermore another pain behaviour measurement for example, gait analysis system (CatWalk) can be used to test the sensitivity of

the incapacitance meter in detecting weight bearing asymmetry in the 0.1mg MIA model.

Reductions in distal allodynia relapsed more quickly after treatment withdrawal than did weight bearing asymmetry, suggesting that TrkA inhibition has a more sustained effect on peripheral pain processing, than on central sensitisation. Further research should determine whether low concentrations of AR786 in CSF could alter central pain processing in the brain.

Reports on the discontinued NSAID nimesulide being able to show a sustained effect in attenuating allodynia (but not weight bearing asymmetry) where the TrkA inhibitor didn't, further expands on the above statement that TrkA inhibition has a more sustained effect on peripheral pain processing, than on central sensitisation and that other mechanisms which may or may not be involving the NGF-TrkA pathway are at work here (Sagar et al., 2011). For example other central mechanisms of pain such as, increased expression of cyclooxygenases (COX) maybe involved as spinal COX-2 expression is increased and plays a crucial role in pain (Prochazkova et al., 2009, Seybold et al., 2003). Further work would be required to investigate if TrkA inhibition has an effect in altering central processing which would include electrophysiological, cellular and molecular studies.

AR786 reduced synovitis in rats with MIA-induced OA, but did not significantly reduce either knee swelling or synovitis in rats with MNX-induced OA. Different effects of AR786 on synovitis between the 2 models may reflect different mechanisms of inflammation, or a more intense (and less responsive) synovitis in the MNX model (Mapp et al., 2013). Further research should determine whether anti-inflammatory effects of AR786 are mediated by direct actions on inflammatory cells or by reducing neurogenic inflammation (effect on SP and CGRP synthesis and release), and whether AR786-sensitive inflammation is generalizable to arthritis in man.

NGF plays a role in inducing RANKL-independent osteoclastogenesis (Hemingway et al., 2011). Further research should investigate if effect of

AR786 on osteoclast numbers would reduce their effects in contributing to joint pathology and pain.

Reductions in pain behaviour were observed both using preventive and treatment protocols with AR786, and were sustained for up to 10 days despite treatment discontinuation. Clinical trials of NGF blockade have demonstrated potential for blocking the NGF-TrkA pathway for the relief of OA pain. Further research should address possible differences between NGF-blockade and selective TrkA inhibition, and the potential for sustained benefit from discontinuous treatment, in order to help realise the potential of NGF-TrkA pathway inhibition for OA pain relief.

A study using the pan Trk inhibitor reported the attenuation of sarcoma induced nerve sprouting and neuroma formation and bone cancer pain in the mouse (Ghilardi et al., 2010). The role of NGF is to facilitate nerve growth. Further work should investigate the effect of AR786 on sensory nerve growth in the OA models and also explore whether inhibiting nerve growth would have an effect on joint pain.

Reports of RPOA (osteonecrosis) with anti-NGF treatments encourage more research for better NGF blockers. On the other hand, given the many unresolved issues around anti-NGF mAbs, their further research is discouraged. The occurrence of RPOA was mostly in association with NSAIDs (Brown et al., 2012). Future studies should investigate the effect of TrkA inhibitors in addition to NSAIDs on joint pathology in OA.

7.5 CONCLUSION

In OA, there is progressive joint degeneration with eventual loss of joint function accompanied by associated pain. The symptoms of OA are well characterised and although the pathophysiology underlying the symptoms are extensively studied, it is still an area that presents a significant challenge to OA researchers. The lack of disease modifying OA drugs results in the treatment of pain to relieve OA symptoms. A better understating of the mechanisms by which structural pathology results in pain is encouraged for the development of new targeted therapies.

The results presented in this thesis using models of OA support the hypothesis that pain behaviour and structural pathology are features of OA models that are mediated by NGF and TrkA. NGF-TrkA signalling contributes to inflammation, osteoclast activation and associated pain. TrkA inhibition therefore holds therapeutic potential for OA treatment.

The occurrence of RPOA with Tanezumab encourages alternative targeting of NGF-TrkA signalling for OA pain relief (Brown et al., 2012). The issues of the occurrence of the unexpected adverse effects for example with blocking NGF make known the significant gaps in our current understanding of the broader roles of NGF in the pathogenesis of OA pathology and pain.

Bridging the gap in our knowledge of OA and OA associated pain requires that clinical research in OA patients is complemented by preclinical research in disease-specific OA models. Clinical studies provide useful information on associations between clinical symptoms (i.e., pain) and particular tissue pathologies, genetic differences (e.g., single nucleotide polymorphisms - SNPs), psychosocial determinants, etc. In contrast preclinical studies provide information on causal relationships between specific molecular, cellular or pathological events and OA pain using therapeutic or prophylactic interventions in the absence of such interventions for OA patients (Malfait et al., 2013). The proper design, execution and reporting of results from preclinical animal research help to make data from these studies more reproducible and translatable to clinical research. Despite this, preclinical

studies can only guide, rather than accurately predict results of research in man.

REFERENCES

- Abdiche, Y. N., Malashock, D. S. & Pons, J. 2008. Probing the binding mechanism and affinity of tanezumab, a recombinant humanized anti-NGF monoclonal antibody, using a repertoire of biosensors. Protein Science : A Publication of the Protein Society, **17**, 1326-1335.
- Agnihotri, A. 2009. *Osteoarthritis pathology* [Online]. joint-pain-expert.net. Available: <http://www.joint-pain-expert.net/osteoarthritis-pathology.html> [Accessed 02/04/15 2015].
- Aigner, T., Cook, J. L., Gerwin, N., Glasson, S. S., Lavery, S., Little, C. B., McIlwraith, W. & Kraus, V. B. 2010. Histopathology atlas of animal model systems – overview of guiding principles. Osteoarthritis and Cartilage, **18, Supplement 3**, S2-S6.
- Aloe, L. & Levi-Montalcini, R. 1977. Mast cells increase in tissues of neonatal rats injected with the nerve growth factor. Brain Research, **133**, 358-366.
- Aloe, L., Rocco, M., Bianchi, P. & Manni, L. 2012. Nerve growth factor: from the early discoveries to the potential clinical use. Journal of Translational Medicine, **10**, 239.
- Aloe, L., Tuveri, M. A., Carcassi, U. & Levi-Montalcini, R. 1992. Nerve growth factor in the synovial fluid of patients with chronic arthritis. Arthritis Rheum, **35**, 351-5.
- Altman, R., Alarcon, G., Appelrouth, D., Bloch, D., Borenstein, D., Brandt, K., Brown, C., Cooke, T. D., Daniel, W., Feldman, D. & Et Al. 1991. The American College of Rheumatology criteria for the classification and reporting of osteoarthritis of the hip. Arthritis Rheum, **34**, 505-14.
- Altman, R., Alarcon, G., Appelrouth, D., Bloch, D., Borenstein, D., Brandt, K., Brown, C., Cooke, T. D., Daniel, W., Gray, R. & Et Al. 1990. The American College of Rheumatology criteria for the classification and reporting of osteoarthritis of the hand. Arthritis Rheum, **33**, 1601-10.
- Altman, R., Asch, E., Bloch, D., Bole, G., Borenstein, D., Brandt, K., Christy, W., Cooke, T. D., Greenwald, R., Hochberg, M. & Et Al. 1986. Development of criteria for the classification and reporting of osteoarthritis. Classification of osteoarthritis of the knee. Diagnostic and Therapeutic Criteria Committee of the American Rheumatism Association. Arthritis Rheum, **29**, 1039-49.
- Altman, R. D. 2010. Early management of osteoarthritis. Am J Manag Care, **16 Suppl Management**, S41-7.
- Altman, R. D., Fries, J. F., Bloch, D. A., Carstens, J., Cooke, T. D., Genant, H., Gofton, P., Groth, H., Mcshane, D. J., Murphy, W. A. & Et Al. 1987. Radiographic assessment of progression in osteoarthritis. Arthritis Rheum, **30**, 1214-25.
- Altman, R. D. & Gold, G. E. 2007. Atlas of individual radiographic features in osteoarthritis, revised. Osteoarthritis Cartilage, **15 Suppl A**, A1-56.
- Amos, N., Lauder, S., Evans, A., Feldmann, M. & Bondeson, J. 2006. Adenoviral gene transfer into osteoarthritis synovial cells using the endogenous inhibitor IkappaBalpha reveals that most, but not all,

- inflammatory and destructive mediators are NFkappaB dependent. *Rheumatology (Oxford)*. England.
- Anand, P. 1995. Nerve growth factor regulates nociception in human health and disease. *Br J Anaesth*, **75**, 201-8.
- Andrews, S. W. 2014. *Allosteric Small Molecule Inhibitors of the NGF/TrkA Pathway: A New Approach to Treating Inflammatory Pain* [Online]. Available: <http://www.arraybiopharma.com/files/6313/9810/8021/PubAttachment587.pdf> [Accessed 29/01/2014 2014].
- Andruski, B., Mccafferty, D. M., Ignacy, T., Millen, B. & Mcdougall, J. J. 2008. Leukocyte trafficking and pain behavioral responses to a hydrogen sulfide donor in acute monoarthritis. *Am J Physiol Regul Integr Comp Physiol*. United States.
- Anemaet, W. K. 2008. *The effects of non-surgical interventions on osteoarthritis-like changes in the mouse knee*. PhD, University of South Florida.
- Apfel, S. C., Wright, D. E., Wiideman, A. M., Dormia, C., Snider, W. D. & Kessler, J. A. 1996. Nerve Growth Factor Regulates the Expression of Brain-Derived Neurotrophic Factor mRNA in the Peripheral Nervous System. *Molecular and Cellular Neuroscience*, **7**, 134-142.
- Appleton, C. T., Mcerlain, D. D., Pitelka, V., Schwartz, N., Bernier, S. M., Henry, J. L., Holdsworth, D. W. & Beier, F. 2007. Forced mobilization accelerates pathogenesis: characterization of a preclinical surgical model of osteoarthritis. *Arthritis Res Ther*, **9**, R13.
- Arden, N. K., Reading, I. C., Jordan, K. M., Thomas, L., Platten, H., Hassan, A. & Ledingham, J. 2008. A randomised controlled trial of tidal irrigation vs corticosteroid injection in knee osteoarthritis: the KIVIS Study. *Osteoarthritis Cartilage*, **16**, 733-9.
- Arendt-Nielsen, L., Nie, H., Laursen, M. B., Laursen, B. S., Madeleine, P., Simonsen, O. H. & Graven-Nielsen, T. 2010. Sensitization in patients with painful knee osteoarthritis. *Pain*, **149**, 573-81.
- Ashraf, S. 2011. *Contributions of inflammation and angiogenesis to structural damage and pain in osteoarthritis*. Doctor of Philosophy, University of Nottingham.
- Ashraf, S., Mapp, P. I., Burston, J., Bennett, A. J., Chapman, V. & Walsh, D. A. 2014. Augmented pain behavioural responses to intra-articular injection of nerve growth factor in two animal models of osteoarthritis. *Ann Rheum Dis*, **73**, 1710-1718.
- Ashraf, S., Mapp, P. I. & Walsh, D. A. 2010. Angiogenesis and the persistence of inflammation in a rat model of proliferative synovitis. *Arthritis & Rheumatism*, **62**, 1890-1898.
- Ashraf, S., Mapp, P. I. & Walsh, D. A. 2011a. Contributions of angiogenesis to inflammation, joint damage, and pain in a rat model of osteoarthritis. *Arthritis & Rheumatism*, **63**, 2700-2710.
- Ashraf, S. & Walsh, D. A. 2008. Angiogenesis in osteoarthritis. *Curr Opin Rheumatol*, **20**, 573-80.
- Ashraf, S., Wibberley, H., Mapp, P. I., Hill, R., Wilson, D. & Walsh, D. A. 2011b. Increased vascular penetration and nerve growth in the meniscus: a potential source of pain in osteoarthritis. *Annals of the Rheumatic Diseases*, **70**, 523-529.

- Atukorala, I., Kwoh, C. K., Guermazi, A., Roemer, F. W., Boudreau, R. M., Hannon, M. J. & Hunter, D. J. 2014. Synovitis in knee osteoarthritis: a precursor of disease? Annals of the Rheumatic Diseases.
- Awhla. 2005-2014. *Practical Animal Handling in Small Animals* [Online]. Newcastle University. Available: <http://www.ahwla.org.uk/site/tutorials/BVA/BVA06-Rat/Rat.html> [Accessed 7th August 2014].
- Ayral, X., Dougados, M., Listrat, V., Bonvarlet, J. P., Simonnet, J. & Amor, B. 1996. Arthroscopic evaluation of chondropathy in osteoarthritis of the knee. J Rheumatol, **23**, 698-706.
- Ayral, X., Pickering, E. H., Woodworth, T. G., Mackillop, N. & Dougados, M. 2005. Synovitis: a potential predictive factor of structural progression of medial tibiofemoral knee osteoarthritis – results of a 1 year longitudinal arthroscopic study in 422 patients. Osteoarthritis and Cartilage, **13**, 361-367.
- Baker, K., Grainger, A., Niu, J., Clancy, M., Guermazi, A., Crema, M., Hughes, L., Buckwalter, J., Wooley, A., Nevitt, M. & Felson, D. T. 2010. Relation of synovitis to knee pain using contrast-enhanced MRIs. Ann Rheum Dis, **69**, 1779-83.
- Barouch, R., Kazimirsky, G., Appel, E. & Brodie, C. 2001. Nerve growth factor regulates TNF- α production in mouse macrophages via MAP kinase activation. Journal of Leukocyte Biology, **69**, 1019-1026.
- Barthel, C., Yeremenko, N., Jacobs, R., Schmidt, R., Bernateck, M., Zeidler, H., Tak, P.-P., Baeten, D. & Rihl, M. 2009. Nerve growth factor and receptor expression in rheumatoid arthritis and spondyloarthritis. Arthritis Research & Therapy, **11**, R82.
- Barve, R. A., Minnerly, J. C., Weiss, D. J., Meyer, D. M., Aguiar, D. J., Sullivan, P. M., Weinrich, S. L. & Head, R. D. 2007. Transcriptional profiling and pathway analysis of monosodium iodoacetate-induced experimental osteoarthritis in rats: relevance to human disease. Osteoarthritis and Cartilage, **15**, 1190-1198.
- Basbaum, A. I., Bautista, D. M., Scherrer, G. & Julius, D. 2009. Cellular and Molecular Mechanisms of Pain. Cell, **139**, 267-284.
- Bellamy, N., Campbell, J., Robinson, V., Gee, T., Bourne, R. & Wells, G. 2006. Intraarticular corticosteroid for treatment of osteoarthritis of the knee. Cochrane Database Syst Rev, CD005328.
- Bendele, A., McComb, J., Gould, T., Mcabee, T., Sennello, G., Chlipala, E. & Guy, M. 1999. Animal models of arthritis: relevance to human disease. Toxicol Pathol, **27**, 134-42.
- Bendele, A. M. 2001. Animal models of osteoarthritis. J Musculoskeletal Neuronal Interact, **1**, 363-76.
- Bendele, A. M. & Hulman, J. F. 1991. Effects of body weight restriction on the development and progression of spontaneous osteoarthritis in guinea pigs. Arthritis Rheum, **34**, 1180-4.
- Benelli, R., Lorusso, G., Albini, A. & Noonan, D. M. 2006. Cytokines and chemokines as regulators of angiogenesis in health and disease. Curr Pharm Des, **12**, 3101-15.
- Benguin, J. & Locker, B. 1983. Chondropathie rotulienne. In: 2ème journée d'arthroscopie du genou., Vol. 1. Lyon: Lyon méd, 89–90.

- Benito, M. J., Veale, D. J., Fitzgerald, O., Van Den Berg, W. B. & Bresnihan, B. 2005. Synovial tissue inflammation in early and late osteoarthritis. *Ann Rheum Dis*. England.
- Berenbaum, F. 2010. Targeted therapies in osteoarthritis: a systematic review of the trials on www.clinicaltrials.gov. *Best Pract Res Clin Rheumatol*, **24**, 107-19.
- Berg, W. 2009. Lessons from animal models of arthritis over the past decade. *Arthritis Research & Therapy*, **11**, 250.
- Bland, J. M. & Altman, D. G. 1986. Statistical methods for assessing agreement between two methods of clinical measurement. *Lancet*, **1**, 307-10.
- Bland, J. M. & Altman, D. G. 1995. Comparing methods of measurement: why plotting difference against standard method is misleading. *Lancet*, **346**, 1085-7.
- Boers, M., Brooks, P., Strand, C. V. & Tugwell, P. 1998. The OMERACT filter for Outcome Measures in Rheumatology. *J Rheumatol*, **25**, 198-9.
- Bondeson, J., Blom, A. B., Wainwright, S., Hughes, C., Caterson, B. & Van Den Berg, W. B. 2010. The role of synovial macrophages and macrophage-produced mediators in driving inflammatory and destructive responses in osteoarthritis. *Arthritis Rheum*, **62**, 647-57.
- Bondeson, J., Wainwright, S. D., Lauder, S., Amos, N. & Hughes, C. E. 2006. The role of synovial macrophages and macrophage-produced cytokines in driving aggrecanases, matrix metalloproteinases, and other destructive and inflammatory responses in osteoarthritis. *Arthritis Res Ther*, **8**, R187.
- Bonnet, C. S. & Walsh, D. A. 2005. Osteoarthritis, angiogenesis and inflammation. *Rheumatology* **44**, 17-16.
- Bove, S. E., Calcaterra, S. L., Brooker, R. M., Huber, C. M., Guzman, R. E., Juneau, P. L., Schrier, D. J. & Kilgore, K. S. 2003. Weight bearing as a measure of disease progression and efficacy of anti-inflammatory compounds in a model of monosodium iodoacetate-induced osteoarthritis. *Osteoarthritis Cartilage*, **11**, 821-30.
- Bove, S. E., Flatters, S. J. L., Inglis, J. J. & Mantyh, P. W. 2009. New advances in musculoskeletal pain. *Brain Research Reviews*, **60**, 187-201.
- Bracci-Laudiero, L. 2010. *NGF and inflammation: a complex bidirectional interaction*. [Online]. Available: <http://brainimmune.com/nerve-growth-factor-and-inflammation-a-complex-bidirectional-interaction/> [Accessed 16/05/2015].
- Brain, S. D. 2011. TRPV1 and TRPA1 channels in inflammatory pain: elucidating mechanisms. *Annals of the New York Academy of Sciences*, **1245**, 36-37.
- Brandt, K. D., Mazzuca, S. A. & Buckwalter, K. A. 2006. Acetaminophen, like conventional NSAIDs, may reduce synovitis in osteoarthritic knees. *Rheumatology (Oxford)*, **45**, 1389-94.
- Brandt, K. D., Mazzuca, S. A., Katz, B. P., Lane, K. A., Buckwalter, K. A., Yocum, D. E., Wolfe, F., Schnitzer, T. J., Moreland, L. W., Manzi, S., Bradley, J. D., Sharma, L., Oddis, C. V., Hugenberg, S. T. & Heck, L. W. 2005. Effects of doxycycline on progression of osteoarthritis:

- results of a randomized, placebo-controlled, double-blind trial. Arthritis Rheum, **52**, 2015-25.
- Breivik, H., Collett, B., Ventafridda, V., Cohen, R. & Gallacher, D. 2006. Survey of chronic pain in Europe: Prevalence, impact on daily life, and treatment. European Journal of Pain, **10**, 287-287.
- Brown, J. W. & Podosin, R. 1966. A syndrome of the neural crest. Arch Neurol, **15**, 294-301.
- Brown, M. T., Murphy, F. T., Radin, D. M., Davignon, I., Smith, M. D. & West, C. R. 2012. Tanezumab Reduces Osteoarthritic Knee Pain: Results of a Randomized, Double-Blind, Placebo-Controlled Phase III Trial. The Journal of Pain, **13**, 790-798.
- Bruton, A., Conway, J. H. & Holgate, S. T. 2000. Reliability: What is it, and how is it measured? Physiotherapy, **86**, 94-99.
- Buckwalter, J. A. & Mankin, H. J. 1998. Articular cartilage: degeneration and osteoarthritis, repair, regeneration, and transplantation. Instr Course Lect, **47**, 487-504.
- Buckwalter, J. A. & Martin, J. A. 2006. Osteoarthritis. Adv Drug Deliv Rev, **58**, 150-67.
- Bullock, C. M., Wookey, P., Bennett, A., Mobasheri, A., Dickerson, I. & Kelly, S. 2014. Peripheral Calcitonin Gene-Related Peptide Receptor Activation and Mechanical Sensitization of the Joint in Rat Models of Osteoarthritis Pain. Arthritis & Rheumatology, **66**, 2188-2200.
- Bullough, P. G. 2004. The role of joint architecture in the etiology of arthritis. Osteoarthritis Cartilage, **12 Suppl A**, S2-9.
- Bulstra, S. K., Drukker, J., Kuijer, R., Buurman, W. A. & Linden, A. J. V. D. 1993. Thionin Staining of Paraffin and Plastic Embedded Sections of Cartilage. Biotechnic & Histochemistry, **68**, 20-28.
- Buma, P., Elmans, L., Van Den Berg, W. B. & Schrama, L. H. 2000. Neurovascular plasticity in the knee joint of an arthritic mouse model. Anat Rec, **260**, 51-61.
- Burr, D. B. 2004. Anatomy and physiology of the mineralized tissues: Role in the pathogenesis of osteoarthrosis. Osteoarthritis and Cartilage, **12**, 20-30.
- Burston, J. J., Sagar, D. R., Shao, P., Bai, M., King, E., Brailsford, L., Turner, J. M., Hathway, G. J., Bennett, A. J., Walsh, D. A., Kendall, D. A., Lichtman, A. & Chapman, V. 2013. Cannabinoid CB2 Receptors Regulate Central Sensitization and Pain Responses Associated with Osteoarthritis of the Knee Joint. PLoS ONE, **8**, e80440.
- Byers Kraus, V., Mcdaniel, G., Huebner, J. L., Stabler, T., Pieper, C., Coleman, R. E., Petry, N. A., Low, P. S., Shen, J. & Mitchell, P. 2013. Direct in vivo evidence of activated macrophages in human osteoarthritis. Osteoarthritis and Cartilage, **21, Supplement**, S42.
- Camplejohn, K. L. & Allard, S. A. 1988. Limitations of safranin 'O' staining in proteoglycan-depleted cartilage demonstrated with monoclonal antibodies. Histochemistry, **89**, 185-188.
- Canetta, S. E. 2010. *Type III Neuregulin1 Signaling in Peripheral Sensory Neurons Affects Thermal Pain Sensation and Hyperalgesia*. Doctor of Philosophy, Columbia University.

- Castañeda-Corral, G., Jimenez-Andrade, J. M., Bloom, A. P., Taylor, R. N., Mantyh, W. G., Kaczmarek, M. J., Ghilardi, J. R. & Mantyh, P. W. 2011. The majority of myelinated and unmyelinated sensory nerve fibers that innervate bone express the tropomyosin receptor kinase A. Neuroscience, **178**, 196-207.
- Cattaneo, A. 2010. Tanezumab, a recombinant humanized mAb against nerve growth factor for the treatment of acute and chronic pain. Curr Opin Mol Ther, **12**, 94-106.
- Chamberlain, P., Compston, J., Cox, T. M., Hayman, A. R., Imrie, R. C., Reynolds, K. & Holmes, S. D. 1995. Generation and characterization of monoclonal antibodies to human type-5 tartrate-resistant acid phosphatase: development of a specific immunoassay of the isoenzyme in serum. Clinical Chemistry, **41**, 1495-9.
- Chaplan, S. R., Bach, F. W., Pogrel, J. W., Chung, J. M. & Yaksh, T. L. 1994. Quantitative assessment of tactile allodynia in the rat paw. J Neurosci Methods, **53**, 55-63.
- Chevrier, A., Rossomacha, E., Buschmann, M. D. & Hoemann, C. D. 2005. Optimization of Histoprocessing Methods to Detect Glycosaminoglycan, Collagen Type II, and Collagen Type I in Decalcified Rabbit Osteochondral Sections. Journal of Histotechnology, **28**, 165-175.
- Christiansen, C. L. & Stevens-Lapsley, J. E. 2010. Weight-Bearing Asymmetry in Relation to Measures of Impairment and Functional Mobility for People With Knee Osteoarthritis. Archives of Physical Medicine and Rehabilitation, **91**, 1524-1528.
- Cicchetti, D. V. 1981. Testing the Normal Approximation and Minimal Sample Size Requirements of Weighted Kappa When the Number of Categories is Large. Applied Psychological Measurement, **5**, 101-104.
- Cicutini, F. M. & Spector, T. D. 1997. Evidence for the increasing prevalence of osteoarthritis with aging; does this pertain to the oldest old? . In: HAMERMAN, D. (ed.) *Osteoarthritis – public health implications for an aging population*. Baltimore, MD: The Johns Hopkins University Press.
- Clements, K. M., Ball, A. D., Jones, H. B., Brinckmann, S., Read, S. J. & Murray, F. 2009. Cellular and histopathological changes in the infrapatellar fat pad in the monoiodoacetate model of osteoarthritis pain. Osteoarthritis and Cartilage, **17**, 805-812.
- Cohen, J. 1960. A Coefficient of Agreement for Nominal Scales. Educational and Psychological Measurement, **20**, 37-46.
- Collins, H. D. 1950. The Pathology of Articular and Spinal Diseases. Annals of Internal Medicine, **33**, 260-260.
- Combe, R., Bramwell, S. & Field, M. J. 2004. The monosodium iodoacetate model of osteoarthritis: a model of chronic nociceptive pain in rats? Neurosci Lett, **370**, 236-40.
- Conaghan, P. G., Felson, D., Gold, G., Lohmander, S., Totterman, S. & Altman, R. 2006. MRI and non-cartilaginous structures in knee osteoarthritis. Osteoarthritis Cartilage, **14 Suppl A**, A87-94.
- Coons, A. H. & Kaplan, M. H. 1950. Localization of antigen in tissue cells; improvements in a method for the detection of antigen by means of fluorescent antibody. J Exp Med, **91**, 1-13.

- Cooper, C., Dennison, E., Edwards, M. & Litwic, A. 2013. Epidemiology of osteoarthritis. Medicographia, **35**, 145-151.
- Cronbach, L. 1951. Coefficient alpha and the internal structure of tests. Psychometrika, **16**, 297-334.
- Crowley, C., Spencer, S. D., Nishimura, M. C., Chen, K. S., Pitts-Meek, S., Armanini, M. P., Ling, L. H., McMahon, S. B., Shelton, D. L., Levinson, A. D. & Et Al. 1994. Mice lacking nerve growth factor display perinatal loss of sensory and sympathetic neurons yet develop basal forebrain cholinergic neurons. Cell, **76**, 1001-11.
- Custers, R. J. H., Creemers, L. B., Verbout, A. J., Van Rijen, M. H. P., Dhert, W. J. A. & Saris, D. B. F. 2007. Reliability, reproducibility and variability of the traditional Histologic/Histochemical Grading System vs the new OARSI Osteoarthritis Cartilage Histopathology Assessment System. Osteoarthritis and Cartilage, **15**, 1241-1248.
- Da, R. R., Qin, Y., Baeten, D. & Zhang, Y. 2007. B cell clonal expansion and somatic hypermutation of Ig variable heavy chain genes in the synovial membrane of patients with osteoarthritis. J Immunol, **178**, 557-65.
- Daghestani, H. N., Pieper, C. F. & Kraus, V. B. 2015. Soluble macrophage biomarkers indicate inflammatory phenotypes in patients with knee osteoarthritis. Arthritis Rheumatol, **67**, 956-65.
- Dallegrì, F. & Ottonello, L. 1997. Tissue injury in neutrophilic inflammation. Inflamm Res, **46**, 382-91.
- Damoiseaux, J. G., Dopp, E. A., Calame, W., Chao, D., Macpherson, G. G. & Dijkstra, C. D. 1994. Rat macrophage lysosomal membrane antigen recognized by monoclonal antibody ED1. Immunology, **83**, 140-7.
- Danneman, P. J., Stein, S. & Walshaw, S. O. 1997. Humane and practical implications of using carbon dioxide mixed with oxygen for anesthesia or euthanasia of rats. Lab Anim Sci, **47**, 376-85.
- Davidson, R. K., Waters, J. G., Kevorkian, L., Darrah, C., Cooper, A., Donell, S. T. & Clark, I. M. 2006. Expression profiling of metalloproteinases and their inhibitors in synovium and cartilage. Arthritis Res Ther, **8**, R124.
- Day, J. S., Ding, M., Van Der Linden, J. C., Hvid, I., Sumner, D. R. & Weinans, H. 2001. A decreased subchondral trabecular bone tissue elastic modulus is associated with pre-arthritis cartilage damage. J Orthop Res, **19**, 914-8.
- De Lange-Brokaar, B. J. E., Ioan-Facsinay, A., Van Osch, G. J. V. M., Zuurmond, A. M., Schoones, J., Toes, R. E. M., Huizinga, T. W. J. & Kloppenburg, M. 2012. Synovial inflammation, immune cells and their cytokines in osteoarthritis: a review. Osteoarthritis and Cartilage, **20**, 1484-1499.
- Delcroix, J.-D., Valletta, J. S., Wu, C., Hunt, S. J., Kowal, A. S. & Mobley, W. C. 2003. NGF Signaling in Sensory Neurons: Evidence that Early Endosomes Carry NGF Retrograde Signals. Neuron, **39**, 69-84.
- Dempster, D. W., Compston, J. E., Drezner, M. K., Glorieux, F. H., Kanis, J. A., Malluche, H., Meunier, P. J., Ott, S. M., Recker, R. R. & Parfitt, A. M. 2013. Standardized nomenclature, symbols, and units for bone histomorphometry: A 2012 update of the report of the ASBMR Histomorphometry Nomenclature Committee. Journal of Bone and Mineral Research, **28**, 2-17.

- Denham, S., Barfoot, R. & Sills, J. 1990. The rat FcR for monomeric IgG is preferentially expressed on red pulp macrophages in the spleen. Immunology, **69**, 329-331.
- Dijkstra, C. D., Dopp, E. A., Joling, P. & Kraal, G. 1985. The heterogeneity of mononuclear phagocytes in lymphoid organs: distinct macrophage subpopulations in the rat recognized by monoclonal antibodies ED1, ED2 and ED3. Immunology, **54**, 589-99.
- Dijkstra, C. D., Dopp, E. A., Vogels, I. M. & Van Noorden, C. J. 1987. Macrophages and dendritic cells in antigen-induced arthritis. An immunohistochemical study using cryostat sections of the whole knee joint of rat. Scandinavian journal of immunology, **26**, 513-523.
- Donnerer, J., Schuligoi, R. & Stein, C. 1992. Increased content and transport of substance P and calcitonin gene-related peptide in sensory nerves innervating inflamed tissue: evidence for a regulatory function of nerve growth factor in vivo. Neuroscience, **49**, 693-8.
- Dougados, M., Ayrat, X., Lustrat, V., Gueguen, A., Bahuaud, J., Beaufils, P., Beguin, J. A., Bonvarlet, J. P., Boyer, T., Coudane, H. & Et Al. 1994. The SFA system for assessing articular cartilage lesions at arthroscopy of the knee. Arthroscopy, **10**, 69-77.
- Dray, A. & Read, S. J. 2007. Arthritis and pain. Future targets to control osteoarthritis pain. Arthritis Res Ther, **9**, 212.
- Driban, J., Sitler, M., Barbe, M. & Balasubramanian, E. 2010. Is osteoarthritis a heterogeneous disease that can be stratified into subsets? Clinical Rheumatology, **29**, 123-131.
- Eger, E. I., 2nd 1984. The pharmacology of isoflurane. Br J Anaesth, **56 Suppl 1**, 71s-99s.
- Eibl, J. K., Strasser, B. C. & Ross, G. M. 2012. Structural, biological, and pharmacological strategies for the inhibition of nerve growth factor. Neurochemistry International, **61**, 1266-1275.
- Encfeldt, B. & Hjertquist, S. O. 1967. The effect of various fixatives on the preservation of acid aminoglycans in tissues. Acta Pathologica Microbiologica Scandinavica, **71**, 219-232.
- Fabriek, B. O., Dijkstra, C. D. & Van Den Berg, T. K. 2005. The macrophage scavenger receptor CD163. Immunobiology, **210**, 153-60.
- Fahnestock, M., Yu, G. & Coughlin, M. D. 2004. ProNGF: a neurotrophic or an apoptotic molecule? Prog Brain Res, **146**, 101-10.
- Felson, D. T., Chaisson, C. E., Hill, C. L., Totterman, S. M., Gale, M. E., Skinner, K. M., Kazis, L. & Gale, D. R. 2001. The association of bone marrow lesions with pain in knee osteoarthritis. Ann Intern Med, **134**, 541-9.
- Fernihough, J., Gentry, C., Malcangio, M., Fox, A., Rediske, J., Pellas, T., Kidd, B., Bevan, S. & Winter, J. 2004. Pain related behaviour in two models of osteoarthritis in the rat knee. Pain, **112**, 83-93.
- Fischer, A. G. T. 1929. Chronic (non-tuberculous) arthritis: Pathology and principles of modern treatment. Journal of the American Medical Association, **93**, 1245-1246.
- Fischer, M. J. M., Mak, S. W. Y. & Mcnaughton, P. A. 2010. Sensitisation of Nociceptors – What are Ion Channels Doing? Open Pain Journal, 82-96.

- Fleiss, J. L. 1999. Reliability of Measurement. *The Design and Analysis of Clinical Experiments*. John Wiley & Sons, Inc.
- Franses, R. E., McWilliams, D. F., Mapp, P. I. & Walsh, D. A. 2010. Osteochondral angiogenesis and increased protease inhibitor expression in OA. *Osteoarthritis Cartilage*, **18**, 563-71.
- Freeman, M. A. & Wyke, B. 1967. The innervation of the knee joint. An anatomical and histological study in the cat. *J Anat*, **101**, 505-32.
- Freemont, A. J., Watkins, A., Le Maitre, C., Baird, P., Jeziorska, M., Knight, M. T., Ross, E. R., O'Brien, J. P. & Hoyland, J. A. 2002. Nerve growth factor expression and innervation of the painful intervertebral disc. *J Pathol*, **197**, 286-92.
- Garraway, S. M., Petruska, J. C. & Mendell, L. M. 2003. BDNF sensitizes the response of lamina II neurons to high threshold primary afferent inputs. *Eur J Neurosci*, **18**, 2467-76.
- Gerwin, N., Bendele, A. M., Glasson, S. & Carlson, C. S. 2010. The OARSI histopathology initiative - recommendations for histological assessments of osteoarthritis in the rat. *Osteoarthritis Cartilage*, **18 Suppl 3**, S24-34.
- Ghilardi, J., Freeman, K., Jimenez-Andrade, J., Mantyh, W., Bloom, A., Kuskowski, M. & Mantyh, P. 2010. Administration of a tropomyosin receptor kinase inhibitor attenuates sarcoma-induced nerve sprouting, neuroma formation and bone cancer pain. *Molecular Pain*, **6**, 1-12.
- Ghilardi, J. R., Freeman, K. T., Jimenez-Andrade, J. M., Coughlin, K., Kaczmarek, M. J., Castaneda-Corral, G., Bloom, A. P., Kuskowski, M. A. & Mantyh, P. W. 2012. Neuroplasticity of sensory and sympathetic nerve fibers in the painful arthritic joint. *Arthritis Rheum*.
- Ghilardi, J. R., Freeman, K. T., Jimenez-Andrade, J. M., Mantyh, W. G., Bloom, A. P., Bouhana, K. S., Trollinger, D., Winkler, J., Lee, P., Andrews, S. W., Kuskowski, M. A. & Mantyh, P. W. 2011. Sustained blockade of neurotrophin receptors TrkA, TrkB and TrkC reduces non-malignant skeletal pain but not the maintenance of sensory and sympathetic nerve fibers. *Bone*, **48**, 389-398.
- Gignac, M. A., Davis, A. M., Hawker, G., Wright, J. G., Mahomed, N., Fortin, P. R. & Badley, E. M. 2006. "What do you expect? You're just getting older": A comparison of perceived osteoarthritis-related and aging-related health experiences in middle- and older-age adults. *Arthritis Rheum*, **55**, 905-12.
- Gineyts, E., Mo, J. A., Ko, A., Henriksen, D. B., Curtis, S. P., Gertz, B. J., Garner, P. & Delmas, P. D. 2004. Effects of ibuprofen on molecular markers of cartilage and synovium turnover in patients with knee osteoarthritis. *Ann Rheum Dis*, **63**, 857-61.
- Giorno, R. 1984. A comparison of two immunoperoxidase staining methods based on the avidin-biotin interaction. *Diagn Immunol*, **2**, 161-6.
- Goldring, M. B. 2001. Anticytokine therapy for osteoarthritis. *Expert Opin Biol Ther*, **1**, 817-29.
- Goldring, M. B. & Berenbaum, F. 2015. Emerging targets in osteoarthritis therapy. *Current Opinion in Pharmacology*, **22**, 51-63.
- Goldring, M. B. & Goldring, S. R. 2010a. Articular cartilage and subchondral bone in the pathogenesis of osteoarthritis. *Ann N Y Acad Sci*, **1192**, 230-7.

- Goldring, M. B. & Marcu, K. B. 2009. Cartilage homeostasis in health and rheumatic diseases. Arthritis Res Ther, **11**, 224.
- Goldring, S. R. & Goldring, M. B. 2010b. Bone and cartilage in osteoarthritis: is what's best for one good or bad for the other? Arthritis Res Ther, **12**, 143.
- Gordon, S. & Taylor, P. R. 2005. Monocyte and macrophage heterogeneity. Nat Rev Immunol, **5**, 953-64.
- Graven-Nielsen, T. & Arendt-Nielsen, L. 2002. Peripheral and central sensitization in musculoskeletal pain disorders: an experimental approach. Curr Rheumatol Rep, **4**, 313-21.
- Guermazi, A., Roemer, F. W. & Genant, H. K. 2013. Role of imaging in osteoarthritis: diagnosis, prognosis, and follow-up. Medicographia, **35**, 164-171.
- Guesdon, J. L., Ternynck, T. & Avrameas, S. 1979. The use of avidin-biotin interaction in immunoenzymatic techniques. Journal of Histochemistry & Cytochemistry, **27**, 1131-9.
- Guingamp, C., Gegout-Pottie, P., Philippe, L., Terlain, B., Netter, P. & Gillet, P. 1997. Mono-iodoacetate-induced experimental osteoarthritis: a dose-response study of loss of mobility, morphology, and biochemistry. Arthritis Rheum, **40**, 1670-9.
- Guzman, R. E., Evans, M. G., Bove, S., Morenko, B. & Kilgore, K. 2003. Mono-iodoacetate-induced histologic changes in subchondral bone and articular cartilage of rat femorotibial joints: an animal model of osteoarthritis. Toxicol Pathol, **31**, 619-24.
- Gwilym, S. E., Keltner, J. R., Warnaby, C. E., Carr, A. J., Chizh, B., Chessell, I. & Tracey, I. 2009. Psychophysical and functional imaging evidence supporting the presence of central sensitization in a cohort of osteoarthritis patients. Arthritis Care & Research, **61**, 1226-1234.
- Halliday, D. A., Zettler, C., Rush, R. A., Scicchitano, R. & Mcneil, J. D. 1998. Elevated nerve growth factor levels in the synovial fluid of patients with inflammatory joint disease. Neurochem Res, **23**, 919-22.
- Hanneman, S. K. 2008. Design, analysis, and interpretation of method-comparison studies. AACN Adv Crit Care, **19**, 223-34.
- Hansel, T. T., Kropshofer, H., Singer, T., Mitchell, J. A. & George, A. J. 2010. The safety and side effects of monoclonal antibodies. Nat Rev Drug Discov, **9**, 325-38.
- Haraoui, B., Pelletier, J. P., Cloutier, J. M., Faure, M. P. & Martel-Pelletier, J. 1991. Synovial membrane histology and immunopathology in rheumatoid arthritis and osteoarthritis. In vivo effects of antirheumatic drugs. Arthritis Rheum, **34**, 153-63.
- Hartnell, A., Steel, J., Turley, H., Jones, M., Jackson, D. G. & Crocker, P. R. 2001. Characterization of human sialoadhesin, a sialic acid binding receptor expressed by resident and inflammatory macrophage populations. Blood, **97**, 288-96.
- Hassan, H. & Walsh, D. A. 2014. Central pain processing in osteoarthritis: implications for treatment. Pain Manag, **4**, 45-56.
- Hassanali, S. H. & Oyoo, G. O. 2011. Osteoarthritis: a look at pathophysiology and approach to new treatments: a review. East African Orthopaedic Journal, **5**.

- Hayami, T., Pickarski, M., Zhuo, Y., Wesolowski, G. A., Rodan, G. A. & Duong Le, T. 2006a. Characterization of articular cartilage and subchondral bone changes in the rat anterior cruciate ligament transection and meniscectomized models of osteoarthritis. Bone, **38**, 234-43.
- Hayami, T., Pickarski, M., Zhuo, Y., Wesolowski, G. A., Rodan, G. A. & Duong, L. T. 2006b. Characterization of articular cartilage and subchondral bone changes in the rat anterior cruciate ligament transection and meniscectomized models of osteoarthritis. Bone, **38**, 234-243.
- Haywood, L., McWilliams, D. F., Pearson, C. I., Gill, S. E., Ganesan, A., Wilson, D. & Walsh, D. A. 2003. Inflammation and angiogenesis in osteoarthritis. Arthritis Rheum, **48**, 2173-7.
- Hechelhammer, L., Pfirrmann, C. W., Zanetti, M., Hodler, J., Boos, N. & Schmid, M. R. 2007. Imaging findings predicting the outcome of cervical facet joint blocks. Eur Radiol, **17**, 959-64.
- Helmick, C. G., Felson, D. T., Lawrence, R. C., Gabriel, S., Hirsch, R., Kwoh, C. K., Liang, M. H., Kremers, H. M., Mayes, M. D., Merkel, P. A., Pillemer, S. R., Reveille, J. D. & Stone, J. H. 2008. Estimates of the prevalence of arthritis and other rheumatic conditions in the United States. Part I. Arthritis Rheum, **58**, 15-25.
- Helms, J. E., Henze, K. T., Sass, T. L. & Mifsud, V. A. 2006. Treating Cronbach's Alpha Reliability Coefficients as Data in Counseling Research. The Counseling Psychologist, **34**, 630-660.
- Hemingway, F., Taylor, R., Knowles, H. J. & Athanasou, N. A. 2011. RANKL-independent human osteoclast formation with APRIL, BAFF, NGF, IGF I and IGF II. Bone, **48**, 938-944.
- Heppelmann, B. 1997. Anatomy and histology of joint innervation. J Peripher Nerv Syst, **2**, 5-16.
- Hewett, T. A., Kovacs, M. S., Artwohl, J. E. & Bennett, B. T. 1993. A comparison of euthanasia methods in rats, using carbon dioxide in prefilled and fixed flow rate filled chambers. Lab Anim Sci, **43**, 579-82.
- Hill, C. L., Hunter, D. J., Niu, J., Clancy, M., Guermazi, A., Genant, H., Gale, D., Grainger, A., Conaghan, P. & Felson, D. T. 2007. Synovitis detected on magnetic resonance imaging and its relation to pain and cartilage loss in knee osteoarthritis. Ann Rheum Dis, **66**, 1599-603.
- Hochberg, M. C. 2013. Osteoarthritis: new approaches. Medicographia, **35**, 139-144.
- Hochberg, M. C., Abramson, S. B., Hungerford, D. S., McCarthy, E., Vignon, E. P. & Smith, M. D., Et Al 2012. Adjudication of Reported Serious Adverse Joint Events in the Tanezumab Clinical Development Program. Arthritis Rheum, **64**, 260.
- Hochberg, M. C., Lethbridge-Cejku, M., Scott, W. W., Jr., Reichle, R., Plato, C. C. & Tobin, J. D. 1995. Upper extremity bone mass and osteoarthritis of the knees: data from the Baltimore Longitudinal Study of Aging. J Bone Miner Res, **10**, 432-8.
- Holdenpaul, H., Asopa, V., Robertson, A. G. S., Clarke, A. R., Tyler, S., Bennett, G. S., Brain, S. D., Wilcock, G. K., Allen, S. J., Smith, S. K. F. & Dawbarn, D. 1997. Immunoglobulin-like domains define the

- nerve growth factor binding site of the TrkA receptor. *Nat Biotech*, **15**, 668-672.
- Hongo, J.-a. S., Laramee, G. R., Urfer, R., Shelton, D. L., Restivo, T., Sadick, M., Galloway, A., Chu, H. & Winslow, J. W. 2000. Antibody Binding Regions on Human Nerve Growth Factor Identified by Homolog- and Alanine-Scanning Mutagenesis. *Hybridoma*, **19**, 215-227.
- Honore, P. & Mantyh, P. W. 2000. Bone cancer pain: from mechanism to model to therapy. *Pain Med*, **1**, 303-9.
- Hsu, S. M. & Raine, L. 1981. Protein A, avidin, and biotin in immunohistochemistry. *J Histochem Cytochem*, **29**, 1349-53.
- Hucho, T. & Levine, J. D. 2007. Signaling pathways in sensitization: toward a nociceptor cell biology. *Neuron*, **55**, 365-76.
- Hudspith, M. J., Siddall, P. J. & Munglani, R. 2006. Physiology of pain. *In: HOPKINS, H. A. (ed.) Foundations of Anesthesia*. 2nd ed.: Elsevier Mosby.
- Hukkanen, M., Gronblad, M., Rees, R., Kottinen, Y. T., Gibson, S. J., Hietanen, J., Polak, J. M. & Brewerton, D. A. 1991. Regional distribution of mast cells and peptide containing nerves in normal and adjuvant arthritic rat synovium. *J Rheumatol*, **18**, 177-83.
- Hukkanen, M., Konttinen, Y. T., Rees, R. G., Santavirta, S., Terenghi, G. & Polak, J. M. 1992. Distribution of nerve endings and sensory neuropeptides in rat synovium, meniscus and bone. *Int J Tissue React*, **14**, 1-10.
- Hunter, D. J., Guermazi, A., Roemer, F., Zhang, Y. & Neogi, T. 2013. Structural correlates of pain in joints with osteoarthritis. *Osteoarthritis and Cartilage*, **21**, 1170-1178.
- Hunter, D. J., Mcdougall, J. J. & Keefe, F. J. 2008. The symptoms of osteoarthritis and the genesis of pain. *Rheum Dis Clin North Am*, **34**, 623-43.
- Hunter, D. J., Mcdougall, J. J. & Keefe, F. J. 2009. The Symptoms of Osteoarthritis and the Genesis of Pain. *Medical Clinics of North America*, **93**, 83-100.
- Hyllested, J. L., Veje, K. & Ostergaard, K. 2002. Histochemical studies of the extracellular matrix of human articular cartilage—a review. *Osteoarthritis and Cartilage*, **10**, 333-343.
- Iannone, F., De Bari, C., Dell'accio, F., Covelli, M., Patella, V., Lo Bianco, G. & Lapadula, G. 2002. Increased expression of nerve growth factor (NGF) and high affinity NGF receptor (p140 TrkA) in human osteoarthritic chondrocytes. *Rheumatology (Oxford)*, **41**, 1413-8.
- Im, H.-J., Kim, J.-S., Li, X., Kotwal, N., Sumner, D. R., Van Wijnen, A. J., Davis, F. J., Yan, D., Levine, B., Henry, J. L., Desevré, J. & Kroin, J. S. 2010. Alteration of sensory neurons and spinal response to an experimental osteoarthritis pain model. *Arthritis & Rheumatism*, **62**, 2995-3005.
- Imai, S., Tokunaga, Y., Maeda, T., Kikkawa, M. & Hukuda, S. 1997. Calcitonin gene-related peptide, substance P, and tyrosine hydroxylase-immunoreactive innervation of rat bone marrows: An immunohistochemical and ultrastructural investigation on possible efferent and afferent mechanisms. *Journal of Orthopaedic Research*, **15**, 133-140.

- Indo, Y., Tsuruta, M., Hayashida, Y., Karim, M. A., Ohta, K., Kawano, T., Mitsubuchi, H., Tonoki, H., Awaya, Y. & Matsuda, I. 1996. Mutations in the TRKA/NGF receptor gene in patients with congenital insensitivity to pain with anhidrosis. Nat Genet, **13**, 485-488.
- Ippolito, E., Pedrini, V. A. & Pedrini-Mille, A. 1983. Histochemical properties of cartilage proteoglycans. Journal of Histochemistry & Cytochemistry, **31**, 53-61.
- Ito, T., Kaneko, T., Yamanaka, Y., Shigetani, Y., Yoshiba, K. & Okiji, T. 2014. M2 macrophages participate in the biological tissue healing reaction to mineral trioxide aggregate. J Endod, **40**, 379-83.
- Ivanavicius, S. P., Ball, A. D., Heapy, C. G., Westwood, F. R., Murray, F. & Read, S. J. 2007. Structural pathology in a rodent model of osteoarthritis is associated with neuropathic pain: Increased expression of ATF-3 and pharmacological characterisation. Pain, **128**, 272-282.
- Iwakura, N., Ohtori, S., Orita, S., Yamashita, M., Takahashi, K. & Kuniyoshi, K. 2010. Role of Low-Affinity Nerve Growth Factor Receptor Inhibitory Antibody in Reducing Pain Behavior and Calcitonin Gene-Related Peptide Expression in a Rat Model of Wrist Joint Inflammatory Pain. Journal of Hand Surgery, **35**, 267-273.
- Jaffer, S. & Bleiweiss, I. J. 2004. Beyond hematoxylin and eosin--the role of immunohistochemistry in surgical pathology. Cancer Invest, **22**, 445-65.
- Janusz, M. J., Bendele, A. M., Brown, K. K., Taiwo, Y. O., Hsieh, L. & Heitmeyer, S. A. 2002. Induction of osteoarthritis in the rat by surgical tear of the meniscus: Inhibition of joint damage by a matrix metalloproteinase inhibitor. Osteoarthritis and Cartilage, **10**, 785-791.
- Janusz, M. J., Hookfin, E. B., Heitmeyer, S. A., Woessner, J. F., Freemont, A. J., Hoyland, J. A., Brown, K. K., Hsieh, L. C., Almstead, N. G., De, B., Natchus, M. G., Pikul, S. & Taiwo, Y. O. 2001. Moderation of iodoacetate-induced experimental osteoarthritis in rats by matrix metalloproteinase inhibitors. Osteoarthritis Cartilage, **9**, 751-60.
- Ji, R.-R., Xu, Z.-Z. & Gao, Y.-J. 2014. Emerging targets in neuroinflammation-driven chronic pain. Nat Rev Drug Discov, **13**, 533-548.
- Jimenez-Andrade, J. M., Mantyh, W. G., Bloom, A. P., Ferng, A. S., Geffre, C. P. & Mantyh, P. W. 2010. Bone cancer pain. Annals of the New York Academy of Sciences, **1198**, 173-181.
- Jones, A. & Doherty, M. 1996. Intra-articular corticosteroids are effective in osteoarthritis but there are no clinical predictors of response. Annals of the Rheumatic Diseases, **55**, 829-832.
- Jones, K. 2012. *Oral Dosing (Gavage) in Mice and Rats SOP* [Online]. University of British Columbia. Available: <http://www.animalcare.ubc.ca/sop/ACS-2012-Tech09.pdf> [Accessed 29th August 2013].
- Jordan, J. M. 2012. Impact of Race/Ethnicity in OA Treatment. HSS Journal, **8**, 39-41.
- Jordan, J. M., Helmick, C. G., Renner, J. B., Luta, G., Dragomir, A. D., Woodard, J., Fang, F., Schwartz, T. A., Abbate, L. M., Callahan, L. F., Kalsbeek, W. D. & Hochberg, M. C. 2007. Prevalence of knee symptoms and radiographic and symptomatic knee osteoarthritis in

- African Americans and Caucasians: the Johnston County Osteoarthritis Project. *J Rheumatol*, **34**, 172-80.
- Kalbhen, D. & Blum, U. 1977. Theoretisches Konzept und experimentelle bestatigung fur ein neues arthrosemmodell am versuchstier. *Arzneimittelforschung Drug Res*, 527-31.
- Kalbhen, D. A. 1987. Chemical model of osteoarthritis--a pharmacological evaluation. *J Rheumatol*, **14 Spec No**, 130-1.
- Kamisan, N., Naveen, S. V., Ahmad, R. E. & Tunku, K. 2013. Chondrocyte density, proteoglycan content and gene expressions from native cartilage are species specific and not dependent on cartilage thickness: a comparative analysis between rat, rabbit and goat. *BMC Veterinary Research*, **9**, 62.
- Kashiwagi, M., Tortorella, M., Nagase, H. & Brew, K. 2001. TIMP-3 is a potent inhibitor of aggrecanase 1 (ADAM-TS4) and aggrecanase 2 (ADAM-TS5). *J Biol Chem*, **276**, 12501-4.
- Kawai, T. & Akira, S. 2010. The role of pattern-recognition receptors in innate immunity: update on Toll-like receptors. *Nat Immunol*, **11**, 373-84.
- Kawamoto, K., Aoki, J., Tanaka, A., Itakura, A., Hosono, H., Arai, H., Kiso, Y. & Matsuda, H. 2002. Nerve growth factor activates mast cells through the collaborative interaction with lysophosphatidylserine expressed on the membrane surface of activated platelets. *J Immunol*, **168**, 6412-9.
- Kelly, S., Chapman, R. J., Woodhams, S., Sagar, D. R., Turner, J., Burston, J. J., Bullock, C., Paton, K., Huang, J., Wong, A., McWilliams, D. F., Okine, B. N., Barrett, D. A., Hathway, G. J., Walsh, D. A. & Chapman, V. 2013a. Increased function of pronociceptive TRPV1 at the level of the joint in a rat model of osteoarthritis pain. *Annals of the Rheumatic Diseases*.
- Kelly, S., Dobson, K. L. & Harris, J. 2013b. Spinal nociceptive reflexes are sensitized in the monosodium iodoacetate model of osteoarthritis pain in the rat. *Osteoarthritis Cartilage*, **21**, 1327-35.
- Kerr, B. J., Bradbury, E. J., Bennett, D. L., Trivedi, P. M., Dassan, P., French, J., Shelton, D. B., McMahon, S. B. & Thompson, S. W. 1999. Brain-derived neurotrophic factor modulates nociceptive sensory inputs and NMDA-evoked responses in the rat spinal cord. *J Neurosci*, **19**, 5138-48.
- Kerr, B. J., Souslova, V., McMahon, S. B. & Wood, J. N. 2001. A role for the TTX-resistant sodium channel Nav 1.8 in NGF-induced hyperalgesia, but not neuropathic pain. *Neuroreport*, **12**, 3077-80.
- Kidd, B. L. & Urban, L. A. 2001. Mechanisms of inflammatory pain. *British Journal of Anaesthesia*, **87**, 3-11.
- King, D. F. & King, L. A. 1986. A brief historical note on staining by hematoxylin and eosin. *Am J Dermatopathol*, **8**, 168.
- Kiraly, K., Lammi, M., Arokoski, J., Lapvetalainen, T., Tammi, M., Helminen, H. & Kiviranta, I. 1996. Safranin O reduces loss of glycosaminoglycans from bovine articular cartilage during histological specimen preparation. *Histochem J*, **28**, 99-107.
- Kissin, E. Y., Freitas, C. F. & Kissin, I. 2005. The effects of intraarticular resiniferatoxin in experimental knee-joint arthritis. *Anesthesia and analgesia*, **101**, 1433-1439.

- Ko, E. & Co, I. 2008. Pain in Osteoarthritis. African Journal of Biomedical Research, **11**, 119 - 128.
- Kontinen, Y. T., Tiainen, V. M., Gomez-Barrena, E., Hukkanen, M. & Salo, J. 2006. Innervation of the joint and role of neuropeptides. Ann N Y Acad Sci, **1069**, 149-54.
- Kool, J., Gerrits-Boeye, M. Y., Severijnen, A. J. & Hazenberg, M. P. 1992. Immunohistology of joint inflammation induced in rats by cell wall fragments of *Eubacterium aerofaciens*. Scand J Immunol, **36**, 497-506.
- Krasnokutsky, S., Belitskaya-Levy, I., Bencardino, J., Samuels, J., Attur, M., Regatte, R., Rosenthal, P., Greenberg, J., Schweitzer, M., Abramson, S. B. & Rybak, L. 2011. Quantitative magnetic resonance imaging evidence of synovial proliferation is associated with radiographic severity of knee osteoarthritis. Arthritis Rheum, **63**, 2983-91.
- Kraus, V. B., Huebner, J. L., Degroot, J. & Bendele, A. 2010. The OARSI histopathology initiative " recommendations for histological assessments of osteoarthritis in the guinea pig. Osteoarthritis and Cartilage, **18**, Supplement 3, S35-S52.
- Kundel, H. L. & Polansky, M. 2003. Measurement of observer agreement. Radiology, **228**, 303-8.
- Kwan Tat, S., Lajeunesse, D., Pelletier, J.-P. & Martel-Pelletier, J. 2010. Targeting subchondral bone for treating osteoarthritis: what is the evidence? Best Practice & Research Clinical Rheumatology, **24**, 51-70.
- Lachance, C., Belliveau, D. J. & Barker, P. A. 1997. Blocking nerve growth factor binding to the p75 neurotrophin receptor on sympathetic neurons transiently reduces trkA activation but does not affect neuronal survival. Neuroscience, **81**, 861-71.
- Lam, F. Y. & Ferrell, W. R. 1989. Inhibition of carrageenan induced inflammation in the rat knee joint by substance P antagonist. Ann Rheum Dis, **48**, 928-32.
- Lam, F. Y. & Ferrell, W. R. 1991. Neurogenic component of different models of acute inflammation in the rat knee joint. Ann Rheum Dis, **50**, 747-51.
- Lampropoulou-Adamidou, K., Lelovas, P., Karadimas, E. V., Liakou, C., Triantafillopoulos, I. K., Dontas, I. & Papaioannou, N. A. 2014. Useful animal models for the research of osteoarthritis. Eur J Orthop Surg Traumatol, **24**, 263-71.
- Landis, J. R. & Koch, G. G. 1977. The measurement of observer agreement for categorical data. Biometrics, **33**, 159-74.
- Lane, N. E., Schnitzer, T. J., Birbara, C. A., Mokhtarani, M., Shelton, D. L., Smith, M. D. & Brown, M. T. 2010. Tanezumab for the Treatment of Pain from Osteoarthritis of the Knee. New England Journal of Medicine, **363**, 1521-1531.
- Laslett, L. L., Doré, D. A., Quinn, S. J., Boon, P., Ryan, E., Winzenberg, T. M. & Jones, G. 2012. Zoledronic acid reduces knee pain and bone marrow lesions over 1 year: a randomised controlled trial. Annals of the Rheumatic Diseases, **71**, 1322-1328.
- Latremoliere, A. & Woolf, C. J. 2009. Central sensitization: a generator of pain hypersensitivity by central neural plasticity. J Pain, **10**, 895-926.
- Lau, K. H., Onishi, T., Wergedal, J. E., Singer, F. R. & Baylink, D. J. 1987. Characterization and assay of tartrate-resistant acid phosphatase

- activity in serum: potential use to assess bone resorption. Clinical Chemistry, **33**, 458-62.
- Le, A. P. & Friedman, W. J. 2012. Matrix Metalloproteinase-7 Regulates Cleavage of Pro-Nerve Growth Factor and Is Neuroprotective following Kainic Acid-Induced Seizures. The Journal of neuroscience : the official journal of the Society for Neuroscience, **32**, 10.1523/JNEUROSCI.4128-11.2012.
- Lee, A. S., Ellman, M. B., Yan, D., Kroin, J. S., Cole, B. J., Van Wijnen, A. J. & Im, H. J. 2013a. A current review of molecular mechanisms regarding osteoarthritis and pain. Gene, **527**, 440-7.
- Lee, K. S., Park, E. H., Cho, H.-Y., Kim, Y. I. & Han, H. C. 2013b. Peripheral group II and III metabotropic glutamate receptors in the knee joint attenuate carrageenan-induced nociceptive behavior in rats. Neuroscience Letters, **542**, 21-25.
- Leigh, J. P., Seavey, W. & Leistikow, B. 2001. Estimating the costs of job related arthritis. J Rheumatol, **28**, 1647-54.
- Leong, A. S. & Wright, J. 1987. The contribution of immunohistochemical staining in tumour diagnosis. Histopathology, **11**, 1295-305.
- Levi-Montalcini, R. & Hamburger, V. 1951. Selective growth stimulating effects of mouse sarcoma on the sensory and sympathetic nervous system of the chick embryo. J Exp Zool, **116**, 321-61.
- Linker, R., Gold, R. & Luhder, F. 2009. Function of Neurotrophic Factors Beyond the Nervous System: Inflammation and Autoimmune Demyelination. **29**, 43-68.
- Little, B. C. & Smith, M. M. **2008**. Animal Models of Osteoarthritis. Current Rheumatology Reviews, **4**.
- Little, C. B. & Zaki, S. 2012. What constitutes an "animal model of osteoarthritis"--the need for consensus? Osteoarthritis Cartilage, **20**, 261-7.
- Liu, P., Okun, A., Ren, J., Guo, R.-C., Ossipov, M. H., Xie, J., King, T. & Porreca, F. 2011. Ongoing pain in the MIA model of osteoarthritis. Neuroscience Letters, **493**, 72-75.
- Liu, T., Van Rooijen, N. & Tracey, D. J. 2000. Depletion of macrophages reduces axonal degeneration and hyperalgesia following nerve injury. Pain, **86**, 25-32.
- Lluch, E., Torres, R., Nijs, J. & Van Oosterwijck, J. 2014. Evidence for central sensitization in patients with osteoarthritis pain: A systematic literature review. European Journal of Pain, **18**, 1367-1375.
- Loeser, R. F., Goldring, S. R., Scanzello, C. R. & Goldring, M. B. 2012. Osteoarthritis: a disease of the joint as an organ. Arthritis Rheum, **64**, 1697-707.
- Loeuille, D., Chary-Valckenaere, I., Champigneulle, J., Rat, A.-C., Toussaint, F., Pinzano-Watrin, A., Goebel, J. C., Mainard, D., Blum, A., Pourel, J., Netter, P. & Gillet, P. 2005. Macroscopic and microscopic features of synovial membrane inflammation in the osteoarthritic knee: Correlating magnetic resonance imaging findings with disease severity. Arthritis & Rheumatism, **52**, 3492-3501.
- Lorenz, H. & Richter, W. 2006. Osteoarthritis: Cellular and molecular changes in degenerating cartilage. Progress in Histochemistry and Cytochemistry, **40**, 135-163.

- Lu, V. B., Biggs, J. E., Stebbing, M. J., Balasubramanyan, S., Todd, K. G., Lai, A. Y., Colmers, W. F., Dawbarn, D., Ballanyi, K. & Smith, P. A. 2009. Brain-derived neurotrophic factor drives the changes in excitatory synaptic transmission in the rat superficial dorsal horn that follow sciatic nerve injury. The Journal of Physiology, **587**, 1013-1032.
- Lundblad, H., Kreicbergs, A. & Jansson, K. A. 2008. Prediction of persistent pain after total knee replacement for osteoarthritis. J Bone Joint Surg Br, **90**, 166-71.
- Ma, Q. P. & Woolf, C. J. 1997. The progressive tactile hyperalgesia induced by peripheral inflammation is nerve growth factor dependent. Neuroreport, **8**, 807-10.
- Mackay, J. L. 1947. Effects of a narcotic level of carbon dioxide on the plasma potassium and respiration of cats. Am J Physiol, **151**, 469-78.
- Malemud, C. J. 2010. Anticytokine therapy for osteoarthritis: evidence to date. Drugs Aging, **27**, 95-115.
- Malfait, A. M., Little, C. B. & Mcdougall, J. J. 2013. A commentary on modelling osteoarthritis pain in small animals. Osteoarthritis Cartilage, **21**, 1316-26.
- Malfait, A. M., Ritchie, J., Gil, A. S., Austin, J. S., Hartke, J., Qin, W., Tortorella, M. D. & Mogil, J. S. 2010. ADAMTS-5 deficient mice do not develop mechanical allodynia associated with osteoarthritis following medial meniscal destabilization. Osteoarthritis Cartilage, **18**, 572-80.
- Mamet, J., Baron, A., Lazdunski, M. & Voilley, N. 2002. Proinflammatory mediators, stimulators of sensory neuron excitability via the expression of acid-sensing ion channels. J Neurosci, **22**, 10662-70.
- Mankin, H. J., Dorfman, H., Lippiello, L. & Zarins, A. 1971. Biochemical and Metabolic Abnormalities in Articular Cartilage from Osteo-Arthritic Human Hips II. CORRELATION OF MORPHOLOGY WITH BIOCHEMICAL AND METABOLIC DATA. The Journal of Bone & Joint Surgery, **53**, 523-537.
- Manni, L., Lundeberg, T., Fiorito, S., Bonini, S., Vigneti, E. & Aloe, L. 2003. Nerve growth factor release by human synovial fibroblasts prior to and following exposure to tumor necrosis factor-alpha, interleukin-1 beta and cholecystokinin-8: the possible role of NGF in the inflammatory response. Clin Exp Rheumatol, **21**, 617-24.
- Mantyh, P. W., Koltzenburg, M., Mendell, L. M., Tive, L. & Shelton, D. L. 2011. Antagonism of Nerve Growth Factor-TrkA Signaling and the Relief of Pain. Anesthesiology, **115**, 189-204
10.1097/ALN.0b013e31821b1ac5.
- Mapp, P. I. 1995. Innervation of the synovium. Ann Rheum Dis, **54**, 398-403.
- Mapp, P. I., Avery, P. S., Mcwilliams, D. F., Bowyer, J., Day, C., Moores, S., Webster, R. & Walsh, D. A. 2008. Angiogenesis in two animal models of osteoarthritis. Osteoarthritis Cartilage, **16**, 61-9.
- Mapp, P. I., Kerslake, S., Brain, S. D., Blake, D. R. & Cambridge, H. 1996. The effect of intra-articular capsaicin on nerve fibres within the synovium of the rat knee joint. J Chem Neuroanat, **10**, 11-8.
- Mapp, P. I., Mcwilliams, D. F., Turley, M. J., Hargin, E. & Walsh, D. A. 2012. A role for the sensory neuropeptide calcitonin gene-related peptide in

- endothelial cell proliferation in vivo. British Journal of Pharmacology, **166**, 1261-1271.
- Mapp, P. I., Sagar, D. R., Ashraf, S., Burston, J. J., Suri, S., Chapman, V. & Walsh, D. A. 2013. Differences in structural and pain phenotypes in the sodium monoiodoacetate and meniscal transection models of osteoarthritis. Osteoarthritis and Cartilage, **21**, 1336-1345.
- Mapp, P. I. & Walsh, D. A. 2012. Mechanisms and targets of angiogenesis and nerve growth in osteoarthritis. *Nat Rev Rheumatol*. United States.
- Mapp, P. I., Walsh, D. A., Bowyer, J. & Maciewicz, R. A. 2010. Effects of a metalloproteinase inhibitor on osteochondral angiogenesis, chondropathy and pain behavior in a rat model of osteoarthritis. Osteoarthritis Cartilage, **18**, 593-600.
- Mardy, S., Miura, Y., Endo, F., Matsuda, I. & Indo, Y. 2001. Congenital insensitivity to pain with anhidrosis (CIPA): effect of TRKA (NTRK1) missense mutations on autophosphorylation of the receptor tyrosine kinase for nerve growth factor. Human Molecular Genetics, **10**, 179-188.
- Martel-Pelletier, J. 2004. Pathophysiology of osteoarthritis. Osteoarthritis and Cartilage, **12, Supplement**, 31-33.
- Martel-Pelletier, J. & Pelletier, J. 2013. Use of animal models for testing drugs targeting osteoarthritis symptoms and articular tissue structural changes. OA Musculoskeletal Medicine, **1**, 25.
- Martinek, V. 2003. Anatomy and pathophysiology of articular cartilage. Dtsch Z Sportmed, **54**, 166-70.
- Matos, L. L., Trufelli, D. C., De Matos, M. G. & Da Silva Pinhal, M. A. 2010. Immunohistochemistry as an important tool in biomarkers detection and clinical practice. Biomark Insights, **5**, 9-20.
- Matthews, G. L. & Hunter, D. J. 2011. Emerging drugs for osteoarthritis. Expert Opin Emerg Drugs, **16**, 479-91.
- Mcalindon, T. E., Snow, S., Cooper, C. & Dieppe, P. A. 1992. Radiographic patterns of osteoarthritis of the knee joint in the community: the importance of the patellofemoral joint. Annals of the Rheumatic Diseases, **51**, 844-849.
- Mcdougall, J. J. 2006. Arthritis and pain. Neurogenic origin of joint pain. Arthritis Res Ther, **8**, 220.
- McGarry, J. G. & Daruwalla, Z. J. 2011. The efficacy, accuracy and complications of corticosteroid injections of the knee joint. Knee Surg Sports Traumatol Arthrosc, **19**, 1649-54.
- McIlwraith, C. W. & Van Sickle, D. C. 1981. Experimentally induced arthritis of the equine carpus: histologic and histochemical changes in the articular cartilage. Am J Vet Res, **42**, 209-17.
- Mckelvey, L., Shorten, G. D. & O'keeffe, G. W. 2013. Nerve growth factor-mediated regulation of pain signalling and proposed new intervention strategies in clinical pain management. J Neurochem, **124**, 276-89.
- Mckenna, F., Borenstein, D., Wendt, H., Wallemark, C., Lefkowitz, J. B. & Geis, G. S. 2001. Celecoxib versus diclofenac in the management of osteoarthritis of the knee. Scand J Rheumatol, **30**, 11-8.
- Mcmahon, S., Koltzenburg, M., Tracey, I. & Turk, D. C. 2013. Wall & Melzack's Textbook of Pain. 6 ed. London: Elsevier Health Sciences UK.

- McMahon, S. B. 1996. NGF as a Mediator of Inflammatory Pain. Philosophical Transactions of the Royal Society of London. Series B: Biological Sciences, **351**, 431-440.
- McMahon, S. B. & Bevan, S. 2005. Inflammatory mediators and the modulators of pain. [Accessed 25/03/12].
- McNamee, K. E., Burleigh, A., Gompels, L. L., Feldmann, M., Allen, S. J., Williams, R. O., Dawbarn, D., Vincent, T. L. & Inglis, J. J. 2010. Treatment of murine osteoarthritis with TrkA5 reveals a pivotal role for nerve growth factor in non-inflammatory joint pain. Pain, **149**, 386-392.
- Meachim, G. 1972. Light microscopy of Indian ink preparations of fibrillated cartilage. Ann Rheum Dis, **31**, 457-64.
- Mendmeshop.Com. 2006-2015. *What Causes Osteoarthritis in the Knee?* [Online]. MendMeShop. Available: http://www.mendmeshop.com/knee/knee_osteoarthritis_causes.php [Accessed 10/08/2015].
- Mephram, B. L. 1991. Theory and practice of histological techniques, 3rd ed. J. D. Bancroft, A. Stevens (Eds). Churchill Livingstone, Edinburgh, 1990. No. of pages: 740. Price: £55. ISBN: 0 443 03559 8. The Journal of Pathology, **164**, 281-281.
- Merskey, H. & Bogduk, N. 1994. Classification of Chronic Pain, IASP Task Force on Taxonomy. Seattle: IASP press.
- Mert, T., Gunay, I., Ocal, I., Guzel, A. I., Inal, T. C., Sencar, L. & Polat, S. 2009. Macrophage depletion delays progression of neuropathic pain in diabetic animals. Naunyn Schmiedebergs Arch Pharmacol, **379**, 445-52.
- Michael, J. W. P., Schlüter-Brust, K. U. & Eysel, P. 2010. The Epidemiology, Etiology, Diagnosis, and Treatment of Osteoarthritis of the Knee. Deutsches Arzteblatt International, **107**, 152-162.
- Miller, R. D. 2010. *Miller's Anaesthesia*, Philadelphia, USA, Churchill Livingstone Elsevier.
- Miller, R. E., Tran, P. B., Obeidat, A. M., Raghu, P., Ishihara, S., Miller, R. J. & Malfait, A. M. 2015. The Role of Peripheral Nociceptive Neurons in the Pathophysiology of Osteoarthritis Pain. Curr Osteoporos Rep.
- Millikin, P. D. 2005. *Haematoxylin Staining: Some Technical Notes* [Online].
- Min, S. S., Han, J. S., Kim, Y. I., Na, H. S., Yoon, Y. W., Hong, S. K. & Han, H. C. 2001. A novel method for convenient assessment of arthritic pain in voluntarily walking rats. Neurosci Lett, **308**, 95-8.
- Minkin, C. 1982. Bone acid phosphatase: Tartrate-resistant acid phosphatase as a marker of osteoclast function. Calcified Tissue International, **34**, 285-290.
- Mobasheri, A. 2013. The future of osteoarthritis therapeutics: emerging biological therapy. Curr Rheumatol Rep, **15**, 385.
- Mokbel, A. N., El Tookhy, O. S., Shamaa, A. A., Rashed, L. A., Sabry, D. & El Sayed, A. M. 2011. Homing and reparative effect of intra-articular injection of autologous mesenchymal stem cells in osteoarthritic animal model. BMC Musculoskelet Disord, **12**, 259.
- Murat, N., Karadam, B., Ozkal, S., Karatosun, V. & Gidener, S. 2007. [Quantification of papain-induced rat osteoarthritis in relation to time with the Mankin score]. Acta Orthop Traumatol Turc, **41**, 233-7.

- Murphy, G. & Nagase, H. 2008. Reappraising metalloproteinases in rheumatoid arthritis and osteoarthritis: destruction or repair? Nat Clin Pract Rheumatol, **4**, 128-35.
- Musumeci, G., Aiello, F., Szychlinska, M., Di Rosa, M., Castrogiovanni, P. & Mobasher, A. 2015. Osteoarthritis in the XXIst Century: Risk Factors and Behaviours that Influence Disease Onset and Progression. International Journal of Molecular Sciences, **16**, 6093-6112.
- Myers, R. R., Heckman, H. M. & Rodriguez, M. 1996. Reduced hyperalgesia in nerve-injured WLD mice: relationship to nerve fiber phagocytosis, axonal degeneration, and regeneration in normal mice. Exp Neurol, **141**, 94-101.
- Myers, S. L., Brandt, K. D., Ehlich, J. W., Braunstein, E. M., Shelbourne, K. D., Heck, D. A. & Kalasinski, L. A. 1990. Synovial inflammation in patients with early osteoarthritis of the knee. J Rheumatol, **17**, 1662-9.
- Neogi, T., Frey-Law, L., Scholz, J., Niu, J., Arendt-Nielsen, L., Woolf, C., Nevitt, M., Bradley, L., Felson, D. T. & Study, F. T. M. O. 2013. Sensitivity and sensitisation in relation to pain severity in knee osteoarthritis: trait or state? Annals of the Rheumatic Diseases.
- Neugebauer, V., Han, J. S., Adwanikar, H., Fu, Y. & Ji, G. 2007. Techniques for assessing knee joint pain in arthritis. Mol Pain, **3**, 8.
- Neugebauer, V. & Schaible, H. G. 1988. Peripheral and spinal components of the sensitization of spinal neurons during an acute experimental arthritis. Agents Actions, **25**, 234-6.
- Neugebauer, V. & Schaible, H. G. 1990. Evidence for a central component in the sensitization of spinal neurons with joint input during development of acute arthritis in cat's knee. J Neurophysiol, **64**, 299-311.
- Nice, N. I. F. H. a. C. E. *Osteoarthritis: Care and management in adults* [Online]. Available: <http://www.nice.org.uk/guidance/cg177/chapter/1-recommendations> [Accessed 15/05/2015].
- Nico, B., Mangieri, D., Benagiano, V., Crivellato, E. & Ribatti, D. 2008. Nerve growth factor as an angiogenic factor. Microvascular Research, **75**, 135-141.
- Nicol, G. D. & Vasko, M. R. 2007. Unraveling the story of NGF-mediated sensitization of nociceptive sensory neurons: ON or OFF the Trks? Mol Interv, **7**, 26-41.
- Nilsson, G., Forsberg-Nilsson, K., Xiang, Z., Hallböök, F., Nilsson, K. & Metcalfe, D. D. 1997. Human mast cells express functional TrkA and are a source of nerve growth factor. European Journal of Immunology, **27**, 2295-2301.
- Nuesch, E., Rutjes, A. W., Trelle, S., Reichenbach, S. & Juni, P. 2009. Doxycycline for osteoarthritis of the knee or hip. Cochrane Database Syst Rev, CD007323.
- Oakley, S. P. & Lassere, M. N. 2003. A critical appraisal of quantitative arthroscopy as an outcome measure in osteoarthritis of the knee. Seminars in Arthritis and Rheumatism, **33**, 83-105.
- Oakley, S. P., Portek, I., Szomor, Z., Appleyard, R. C., Ghosh, P., Kirkham, B. W., Murrell, G. A. & Lassere, M. N. 2005. Arthroscopy -- a potential "gold standard" for the diagnosis of the chondropathy of early osteoarthritis. Osteoarthritis Cartilage, **13**, 368-78.

- Obata, K., Yamanaka, H., Dai, Y., Tachibana, T., Fukuoka, T., Tokunaga, A., Yoshikawa, H. & Noguchi, K. 2003. Differential activation of extracellular signal-regulated protein kinase in primary afferent neurons regulates brain-derived neurotrophic factor expression after peripheral inflammation and nerve injury. *J Neurosci*, **23**, 4117-26.
- Ogino, S., Sasho, T., Nakagawa, K., Suzuki, M., Yamaguchi, S., Higashi, M., Takahashi, K. & Moriya, H. 2009. Detection of pain-related molecules in the subchondral bone of osteoarthritic knees. *Clinical Rheumatology*, **28**, 1395-1402.
- Ohnishi, K., Komohara, Y., Saito, Y., Miyamoto, Y., Watanabe, M., Baba, H. & Takeya, M. 2013. CD169-positive macrophages in regional lymph nodes are associated with a favorable prognosis in patients with colorectal carcinoma. *Cancer Sci*, **104**, 1237-44.
- Okamura, Y., Watari, M., Jerud, E. S., Young, D. W., Ishizaka, S. T., Rose, J., Chow, J. C. & Strauss, J. F., 3rd 2001. The extra domain A of fibronectin activates Toll-like receptor 4. *J Biol Chem*, **276**, 10229-33.
- Opar, A. 2010. Kinase inhibitors attract attention as oral rheumatoid arthritis drugs. *Nat Rev Drug Discov*, **9**, 257-258.
- Orita, S., Ishikawa, T., Miyagi, M., Ochiai, N., Inoue, G., Eguchi, Y., Kamoda, H., Arai, G., Suzuki, M., Sakuma, Y., Oikawa, Y., Toyone, T., Aoki, Y., Takahashi, K. & Ohtori, S. 2012. Percutaneously absorbed NSAIDs attenuate local production of proinflammatory cytokines and suppress the expression of c-Fos in the spinal cord of a rodent model of knee osteoarthritis. *Journal of Orthopaedic Science*, **17**, 77-86.
- Orita, S., Ishikawa, T., Miyagi, M., Ochiai, N., Inoue, G., Eguchi, Y., Kamoda, H., Arai, G., Toyone, T., Aoki, Y., Kubo, T., Takahashi, K. & Ohtori, S. 2011. Pain-related sensory innervation in monoiodoacetate-induced osteoarthritis in rat knees that gradually develops neuronal injury in addition to inflammatory pain. *BMC Musculoskeletal Disorders*, **12**, 134.
- Ostergaard, K., Andersen, C., Petersen, J., Bendtzen, K. & Salter, D. 1999. Validity of histopathological grading of articular cartilage from osteoarthritic knee joints. *Annals of the Rheumatic Diseases*, **58**, 208-213.
- Ostergaard, K., Petersen, J., Andersen, C. B., Bendtzen, K. & Salter, D. M. 1997. Histologic/histochemical grading system for osteoarthritic articular cartilage. Reproducibility and validity. *Arthritis & Rheumatism*, **40**, 1766-1771.
- Outerbridge, R. E. 1961. The etiology of chondromalacia patellae. *J Bone Joint Surg Br*, **43-B**, 752-7.
- Pandit, J. J. 2014. Monitoring (un)consciousness: the implications of a new definition of 'anaesthesia'. *Anaesthesia*, **69**, 801-807.
- Parfitt, A. M., Drezner, M. K., Glorieux, F. H., Kanis, J. A., Malluche, H., Meunier, P. J., Ott, S. M. & Recker, R. R. 1987. Bone histomorphometry: Standardization of nomenclature, symbols, and units: Report of the asbmr histomorphometry nomenclature committee. *Journal of Bone and Mineral Research*, **2**, 595-610.
- Pasquali Ronchetti, I., Guerra, D., Taparelli, F., Boraldi, F., Bergamini, G., Mori, G., Zizzi, F. & Frizziero, L. 2001. Morphological analysis of knee synovial membrane biopsies from a randomized controlled

- clinical study comparing the effects of sodium hyaluronate (Hyalgan) and methylprednisolone acetate (Depomedrol) in osteoarthritis. Rheumatology (Oxford), **40**, 158-69.
- Pastoureau, P. C., Chomel, A. C. & Bonnet, J. 1999. Evidence of early subchondral bone changes in the meniscectomized guinea pig. A densitometric study using dual-energy X-ray absorptiometry subregional analysis. Osteoarthritis Cartilage, **7**, 466-73.
- Pauli, C., Whiteside, R., Heras, F. L., Nesic, D., Koziol, J., Grogan, S. P., Matyas, J., Pritzker, K. P. H., D'lima, D. D. & Lotz, M. K. 2012. COMPARISON OF CARTILAGE HISTOPATHOLOGY ASSESSMENT SYSTEMS ON HUMAN KNEE JOINTS AT ALL STAGES OF OSTEOARTHRITIS DEVELOPMENT. Osteoarthritis and Cartilage, **20**, 476-485.
- Pearle, A. D., Scanzello, C. R., George, S., Mandl, L. A., Dicarolo, E. F., Peterson, M., Sculco, T. P. & Crow, M. K. 2007. Elevated high-sensitivity C-reactive protein levels are associated with local inflammatory findings in patients with osteoarthritis. Osteoarthritis Cartilage, **15**, 516-23.
- Pearson, R. G., Kurien, T., Shu, K. S. S. & Scammell, B. E. 2011. Histopathology grading systems for characterisation of human knee osteoarthritis – reproducibility, variability, reliability, correlation, and validity. Osteoarthritis and Cartilage, **19**, 324-331.
- Pecchi, E., Priam, S., Gosset, M., Pigenet, A., Sudre, L., Laiguillon, M.-C., Berenbaum, F. & Houard, X. 2014. Induction of nerve growth factor expression and release by mechanical and inflammatory stimuli in chondrocytes: possible involvement in osteoarthritis pain. Arthritis Research & Therapy, **16**, R16.
- Pedersen, D. R., Goetz, J. E., Kurriger, G. L. & Martin, J. A. 2013. Comparative digital cartilage histology for human and common osteoarthritis models. Orthopedic Research and Reviews, **2013:5**, 13-20.
- Pelletier, J. P. & Martel-Pelletier, J. 1989. Protective effects of corticosteroids on cartilage lesions and osteophyte formation in the Pond-Nuki dog model of osteoarthritis. Arthritis Rheum, **32**, 181-93.
- Penraat, J. H., Allen, A. L., Fretz, P. B. & Bailey, J. V. 2000. An evaluation of chemical arthrodesis of the proximal interphalangeal joint in the horse by using monoiodoacetate. Canadian Journal of Veterinary Research, **64**, 212-221.
- Pessler, F., Dai, L., Diaz-Torne, C., Gomez-Vaquero, C., Paessler, M. E., Zheng, D. H., Einhorn, E., Range, U., Scanzello, C. & Schumacher, H. R. 2008. The synovitis of "non-inflammatory" orthopaedic arthropathies: a quantitative histological and immunohistochemical analysis. Ann Rheum Dis, **67**, 1184-7.
- Pezet, S. & McMahon, S. B. 2006. Neurotrophins: mediators and modulators of pain. Annu Rev Neurosci, **29**, 507-38.
- Pinto, M., Lima, D. & Tavares, I. 2007. Neuronal activation at the spinal cord and medullary pain control centers after joint stimulation: a c-fos study in acute and chronic articular inflammation. Neuroscience, **147**, 1076-89.

- Pokrovnichka, A. 2012. *Anti-NGF Drug Class Efficacy and Safety* [Online]. Available: <http://www.fda.gov/downloads/AdvisoryCommittees/CommitteesMeetingMaterials/Drugs/ArthritisDrugsAdvisoryCommittee/UCM301302.pdf> [Accessed 30/04/2015].
- Poole, R., Blake, S., Buschmann, M., Goldring, S., Lavery, S., Lockwood, S., Matyas, J., Mcdougall, J., Pritzker, K., Rudolph, K., Van Den Berg, W. & Yaksh, T. 2010. Recommendations for the use of preclinical models in the study and treatment of osteoarthritis. *Osteoarthritis Cartilage*, **18 Suppl 3**, S10-6.
- Prencipe, G., Minnone, G., Strippoli, R., De Pasquale, L., Petrini, S., Caiello, I., Manni, L., De Benedetti, F. & Bracci-Laudiero, L. 2014. Nerve Growth Factor Downregulates Inflammatory Response in Human Monocytes through TrkA. *The Journal of Immunology*, **192**, 3345-3354.
- Pritzker, K. P. H., Gay, S., Jimenez, S. A., Ostergaard, K., Pelletier, J. P., Revell, P. A., Salter, D. & Van Den Berg, W. B. 2006. Osteoarthritis cartilage histopathology: grading and staging. *Osteoarthritis and Cartilage*, **14**, 13-29.
- Prochazkova, M., Zanvit, P., Dolezal, T., Prokesova, L. & Krsiak, M. 2009. Increased gene expression and production of spinal cyclooxygenase 1 and 2 during experimental osteoarthritis pain. *Physiol Res*, **58**, 419-25.
- Prys-Roberts, C. 1987. ANAESTHESIA: A PRACTICAL OR IMPRACTICAL CONSTRUCT? *British Journal of Anaesthesia*, **59**, 1341-1345.
- Pulsatelli, L., Addimanda, O., Brusi, V., Pavloska, B. & Meliconi, R. 2013. New findings in osteoarthritis pathogenesis: therapeutic implications. *Therapeutic Advances in Chronic Disease*, **4**, 23-43.
- Radin, E. L. & Rose, R. M. 1986. Role of subchondral bone in the initiation and progression of cartilage damage. *Clin Orthop Relat Res*, 34-40.
- Ramsey, I. S., Delling, M. & Clapham, D. E. 2006. An introduction to TRP channels. *Annu Rev Physiol*, **68**, 619-47.
- Raychaudhuri, S. P. & Raychaudhuri, S. K. 2009. The regulatory role of nerve growth factor and its receptor system in fibroblast-like synovial cells. *Scand J Rheumatol*, **38**, 207-15.
- Raychaudhuri, S. P., Raychaudhuri, S. K., Atkuri, K. R. & Herzenberg, L. A. 2011. Nerve growth factor: A key local regulator in the pathogenesis of inflammatory arthritis. *Arthritis Rheum*, **63**, 3243-52.
- Ready, L. B. & Edwards, W. T. 1992. Management of Acute Pain: a Practical Guide. *Taskforce on Acute Pain*. Seattle: IASP Publications.
- Reginster, J. Y. 2002. The prevalence and burden of arthritis. *Rheumatology (Oxford)*, **41 Supp 1**, 3-6.
- Reijman, M., Bierma-Zeinstra, S. M., Pols, H. A., Koes, B. W., Stricker, B. H. & Hazes, J. M. 2005. Is there an association between the use of different types of nonsteroidal antiinflammatory drugs and radiologic progression of osteoarthritis? The Rotterdam Study. *Arthritis Rheum*, **52**, 3137-42.
- Renshaw, S. (ed.) 2007. *Immunochemical staining techniques*, Bloxham, UK: Scion Publishing Ltd.

- Richards, P. J., Williams, A. S., Goodfellow, R. M. & Williams, B. D. 1999. Liposomal clodronate eliminates synovial macrophages, reduces inflammation and ameliorates joint destruction in antigen-induced arthritis. *Rheumatology (Oxford)*, **38**, 818-25.
- Richardson C, Bae W, Fazeli B, Filvaroff E & R, S. 2001. Quantitative characterization of osteoarthritis in the guinea pig. *Trans Orthop Res Soc*, 26.
- Rickert, R. R. & Maliniak, R. M. 1989. Intralaboratory quality assurance of immunohistochemical procedures. Recommended practices for daily application. *Arch Pathol Lab Med*, **113**, 673-9.
- Roach, H. I., Aigner, T., Soder, S., Haag, J. & Welkerling, H. 2007. Pathobiology of osteoarthritis: pathomechanisms and potential therapeutic targets. *Curr Drug Targets*, **8**, 271-82.
- Robertson, A. G., Banfield, M. J., Allen, S. J., Dando, J. A., Mason, G. G., Tyler, S. J., Bennett, G. S., Brain, S. D., Clarke, A. R., Naylor, R. L., Wilcock, G. K., Brady, R. L. & Dawbarn, D. 2001. Identification and structure of the nerve growth factor binding site on TrkA. *Biochem Biophys Res Commun*, **282**, 131-41.
- Roemer, F. W., Guermazi, A., Felson, D. T., Niu, J., Nevitt, M. C., Crema, M. D., Lynch, J. A., Lewis, C. E., Torner, J. & Zhang, Y. 2011. Presence of MRI-detected joint effusion and synovitis increases the risk of cartilage loss in knees without osteoarthritis at 30-month follow-up: the MOST study. *Ann Rheum Dis*, **70**, 1804-9.
- Roemer, F. W., Zhang, Y., Niu, J., Lynch, J. A., Crema, M. D., Marra, M. D., Nevitt, M. C., Felson, D. T., Hughes, L. B., El-Khoury, G. Y., Englund, M. & Guermazi, A. 2009. Tibiofemoral joint osteoarthritis: risk factors for MR-depicted fast cartilage loss over a 30-month period in the multicenter osteoarthritis study. *Radiology*, **252**, 772-80.
- Roman-Blas, J. A. & Herrero-Beaumont, G. 2013. Osteoarthritis pathophysiology: similarities and dissimilarities with other rheumatological diseases and the role of subchondral bone. *Medicographia*, **35**, 158-163.
- Rosenberg, L. 1971. *Chemical Basis for the Histological Use of Safranin O in the Study of Articular Cartilage*.
- Roubille, C., Martel -Pelletier, J. & Pelletier, J. P. 2013. Osteoarthritis treatments: where do we stand at the moment? *Medicographia*, **35**, 172-180.
- Rueff, A. & Mendell, L. E. 1996. Nerve Growth Factor and Inflammatory Pain. *Technical Corner from IASP Newsletter* [Online]. [Accessed 31/03/12].
- Russell, N. L. 1963. A RAPID METHOD FOR DECALCIFICATION OF BONE FOR HISTOLOGICAL EXAMINATION USING THE "HISTETTE". *J Med Lab Technol*, **20**, 299-301.
- Rutgers, M., Van Pelt, M. J. P., Dhert, W. J. A., Creemers, L. B. & Saris, D. B. F. 2010. Evaluation of histological scoring systems for tissue-engineered, repaired and osteoarthritic cartilage. *Osteoarthritis and Cartilage*, **18**, 12-23.
- Sagar, D. R., Ashraf, S., Xu, L., Burston, J. J., Menhinick, M. R., Poulter, C. L., Bennett, A. J., Walsh, D. A. & Chapman, V. 2014. Osteoprotegerin reduces the development of pain behaviour and joint pathology in a

- model of osteoarthritis. *Annals of the Rheumatic Diseases*, **73**, 1558-1565.
- Sagar, D. R., Burston, J. J., Hathway, G. J., Woodhams, S. G., Pearson, R. G., Bennett, A. J., Kendall, D. A., Scammell, B. E. & Chapman, V. 2011. The contribution of spinal glial cells to chronic pain behaviour in the monosodium iodoacetate model of osteoarthritic pain. *Mol Pain*, **7**, 88.
- Sagar, D. R., Nwosu, L., Walsh, D. A. & Chapman, V. 2015. Dissecting the contribution of knee joint NGF to spinal nociceptive sensitization in a model of OA pain in the rat. *Osteoarthritis and Cartilage*, **23**, 906-13.
- Sagar, D. R., Staniaszek, L. E., Okine, B. N., Woodhams, S., Norris, L. M., Pearson, R. G., Garle, M. J., Alexander, S. P., Bennett, A. J., Barrett, D. A., Kendall, D. A., Scammell, B. E. & Chapman, V. 2010. Tonic modulation of spinal hyperexcitability by the endocannabinoid receptor system in a rat model of osteoarthritis pain. *Arthritis Rheum*, **62**, 3666-76.
- Sagar, D. R., Suokas, A. K., Walsh, D. A. & Chapman, V. 2013. Translational Relevance of Animal Models of Osteoarthritic Pain. *HERMANN O. HANDWERKER and LARS ARENDT-NIELSEN, eds., Pain Models: Translational Relevance and Applications*. IASP Press.
- Saito, T. 2003. Neurogenic inflammation in osteoarthritis of the knee. *Modern Rheumatology*, **13**, 301-304.
- Samuel, E. P. 1952. The autonomic and somatic innervation of the articular capsule. *The Anatomical Record*, **113**, 53-70.
- Sanga, P., Katz, N., Polverejan, E., Wang, S., Kelly, K. M., Haeussler, J. & Thippawong, J. 2013. Efficacy, safety, and tolerability of fulranumab, an anti-nerve growth factor antibody, in the treatment of patients with moderate to severe osteoarthritis pain. *PAIN®*, **154**, 1910-1919.
- Scanzello, C. R. & Goldring, S. R. 2012. The role of synovitis in osteoarthritis pathogenesis. *Bone*, **51**, 249-257.
- Scanzello, C. R., Mckee, B., Swaim, B. H., Dicarlo, E., Asomugha, E. U., Kanda, V., Nair, A., Lee, D. M., Richmond, J. C., Katz, J. N., Crow, M. K. & Goldring, S. R. 2011. Synovial inflammation in patients undergoing arthroscopic meniscectomy: molecular characterization and relationship to symptoms. *Arthritis Rheum*, **63**, 391-400.
- Scanzello, C. R., Plaas, A. & Crow, M. K. 2008. Innate immune system activation in osteoarthritis: is osteoarthritis a chronic wound? *Curr Opin Rheumatol*, **20**, 565-72.
- Schaible, H.-G., Ebersberger, A. & Natura, G. 2011. Update on peripheral mechanisms of pain: beyond prostaglandins and cytokines. *Arthritis Research & Therapy*, **13**, 210.
- Mechanisms of Pain in Arthritis*, 2002. Directed by Schaible, H.-G., Ebersberger, A. & Von Banchet, G. S.: Blackwell Publishing Ltd.
- Schaible, H.-G. & Grubb, B. D. 1993. Afferent and spinal mechanisms of joint pain. *Pain*, **55**, 5-54.
- Schaible, H.-G., Schmelz, M. & Tegeder, I. 2006. Pathophysiology and treatment of pain in joint disease. *Advanced Drug Delivery Reviews*, **58**, 323-342.
- Schaible, H.-G. & Straub, R. H. 2014. Function of the sympathetic supply in acute and chronic experimental joint inflammation. *Autonomic Neuroscience*, **182**, 55-64.

- Schaible, H. G. 2007. Peripheral and Central Mechanisms of Pain Generation. *In: STEIN, C. (ed.) Analgesia*. Springer Berlin Heidelberg.
- Schindelmeiser, J., Gullotta, F. & Münsterman, D. 1989. Purple Acid Phosphatase of Human Brain Macrophages in AIDS Encephalopathy. *Pathology - Research and Practice*, **185**, 184-186.
- Schmitz, N., Laverty, S., Kraus, V. B. & Aigner, T. 2010. Basic methods in histopathology of joint tissues. *Osteoarthritis and Cartilage*, **18**, S113-S116.
- Schnitzer, T. J., Ekman, E. F., Spierings, E. L. H., Greenberg, H. S., Smith, M. D., Brown, M. T., West, C. R. & Verburg, K. M. 2014. Efficacy and safety of tanezumab monotherapy or combined with non-steroidal anti-inflammatory drugs in the treatment of knee or hip osteoarthritis pain. *Annals of the Rheumatic Diseases*.
- Scott, J. E. 1973. Affinity, competition and specific interactions in the biochemistry and histochemistry of polyelectrolytes. *Biochem. Soc. Trans.*, **1**, 787-806.
- Scott, J. E. & Dorling, J. 1965. Differential staining of acid glycosaminoglycans (mucopolysaccharides) by Alcian blue in salt solutions. *Histochemie*, **5**, 221-233.
- Seegers, H. C., Hood, V. C., Kidd, B. L., Cruwys, S. C. & Walsh, D. A. 2003. Enhancement of angiogenesis by endogenous substance P release and neurokinin-1 receptors during neurogenic inflammation. *J Pharmacol Exp Ther*, **306**, 8-12.
- Seidel, M. F., Herguijuela, M., Forkert, R. & Otten, U. 2010. Nerve growth factor in rheumatic diseases. *Semin Arthritis Rheum*, **40**, 109-26.
- Seidel, M. F., Wise, B. L. & Lane, N. E. 2013. Nerve growth factor: an update on the science and therapy. *Osteoarthritis Cartilage*, **21**, 1223-8.
- Sellam, J. & Berenbaum, F. 2008. Clinical features of osteoarthritis. *In: Firestein GS, Budd RC, Harris Jr ED, McInnes IB, Ruddy S, Sargent JS, Eds. Kelley's Textbook of Rheumatology*. Philadelphia: Elsevier Inc.
- Sellam, J. & Berenbaum, F. 2010. The role of synovitis in pathophysiology and clinical symptoms of osteoarthritis. *Nat Rev Rheumatol*, **6**, 625-635.
- Seybold, V. S., Jia, Y. P. & Abrahams, L. G. 2003. Cyclo-oxygenase-2 contributes to central sensitization in rats with peripheral inflammation. *Pain*, **105**, 47-55.
- Sharif Naeni, R., Cahill, C. M., Ribeiro-Da-Silva, A., Menard, H. A. & Henry, J. L. 2005. Remodelling of spinal nociceptive mechanisms in an animal model of monoarthritis. *Eur J Neurosci*, **22**, 2005-15.
- Shelton, D. L., Zeller, J., Ho, W.-H., Pons, J. & Rosenthal, A. 2005. Nerve growth factor mediates hyperalgesia and cachexia in auto-immune arthritis. *Pain*, **116**, 8-16.
- Shi, S. R., Liu, C. & Taylor, C. R. 2007. Standardization of immunohistochemistry for formalin-fixed, paraffin-embedded tissue sections based on the antigen-retrieval technique: from experiments to hypothesis. *J Histochem Cytochem*, **55**, 105-9.
- Shu, S. Y., Ju, G. & Fan, L. Z. 1988. The glucose oxidase-DAB-nickel method in peroxidase histochemistry of the nervous system. *Neurosci Lett*, **85**, 169-71.

- Smeyne, R. J., Klein, R., Schnapp, A., Long, L. K., Bryant, S., Lewin, A., Lira, S. A. & Barbacid, M. 1994. Severe sensory and sympathetic neuropathies in mice carrying a disrupted Trk/NGF receptor gene. Nature, **368**, 246-249.
- Smith, W. & Harrap, S. B. 1997. Behavioural and cardiovascular responses of rats to euthanasia using carbon dioxide gas. Lab Anim, **31**, 337-46.
- Sohn, D. H., Sokolove, J., Sharpe, O., Erhart, J. C., Chandra, P. E., Lahey, L. J., Lindstrom, T. M., Hwang, I., Boyer, K. A., Andriacchi, T. P. & Robinson, W. H. 2012. Plasma proteins present in osteoarthritic synovial fluid can stimulate cytokine production via Toll-like receptor 4. Arthritis Res Ther, **14**, R7.
- Sokolove, J. & Lepus, C. M. 2013. Role of inflammation in the pathogenesis of osteoarthritis: latest findings and interpretations. Ther Adv Musculoskelet Dis, **5**, 77-94.
- Soren, A., Klein, W. & Huth, F. 1976. Microscopic comparison of the synovial changes in posttraumatic synovitis and osteoarthritis. Clin Orthop Relat Res, 191-5.
- Spector, T. D. & Macgregor, A. J. 2004. Risk factors for osteoarthritis: genetics. Osteoarthritis Cartilage, **12 Suppl A**, S39-44.
- Spiliotopoulou, G. 2009. Reliability reconsidered: Cronbach's alpha and paediatric assessment in occupational therapy. Aust Occup Ther J, **56**, 150-5.
- Spinnler, K., Fröhlich, T., Arnold, G. J., Kunz, L. & Mayerhofer, A. 2011. Human Trypsin Cleaves Pro-Nerve Growth Factor (Pro-NGF): HINTS OF LOCAL, MAST CELL-DEPENDENT REGULATION OF NGF/PRO-NGF ACTION. The Journal of Biological Chemistry, **286**, 31707-31713.
- Štempelj, M. & Ferjan, I. 2005. Signaling pathway in nerve growth factor induced histamine release from rat mast cells. Inflammation Research, **54**, 344-349.
- Steward, A., Liu, Y. & Wagner, D. 2011. Engineering cell attachments to scaffolds in cartilage tissue engineering. JOM, **63**, 74-82.
- Stoppioello, L. A., Mapp, P. I., Wilson, D., Hill, R., Scammell, B. E. & Walsh, D. A. 2014. Structural associations of symptomatic knee osteoarthritis. Arthritis & Rheumatology, **66**, 3018-3027.
- Stoward, P. J. 1967. The histochemical properties of some periodate-reactive mucosubstances of the pregnant Syrian hamster before and after methylation with methanolic thionyl chloride. Journal of the Royal Microscopical Society, **87**, 77-103.
- Strassle, B. W., Mark, L., Leventhal, L., Piesla, M. J., Jian Li, X., Kennedy, J. D., Glasson, S. S. & Whiteside, G. T. 2010. Inhibition of osteoclasts prevents cartilage loss and pain in a rat model of degenerative joint disease. Osteoarthritis and Cartilage, **18**, 1319-1328.
- Streefkerk, J. G. 1972. INHIBITION OF ERYTHROCYTE PSEUDOPEROXIDASE ACTIVITY BY TREATMENT WITH HYDROGEN PEROXIDE FOLLOWING METHANOL. Journal of Histochemistry & Cytochemistry, **20**, 829-831.
- Summers, T. A. & Jaffe, E. S. 2011. Hairy cell leukemia diagnostic criteria and differential diagnosis. Leuk Lymphoma, **52 Suppl 2**, 6-10.

- Sun, Y., Mauerhan, D. R., Kneisl, J. S., James Norton, H., Zinchenko, N., Ingram, J., Hanley, E. N. & Gruber, H. E. 2012. Histological Examination of Collagen and Proteoglycan Changes in Osteoarthritic Menisci. The Open Rheumatology Journal, **6**, 24-32.
- Suokas, A. K., Walsh, D. A., McWilliams, D. F., Condon, L., Moreton, B., Wylde, V., Arendt-Nielsen, L. & Zhang, W. 2012. Quantitative sensory testing in painful osteoarthritis: a systematic review and meta-analysis. Osteoarthritis and Cartilage, **20**, 1075-1085.
- Suri, S., Gill, S. E., Massena De Camin, S., Wilson, D., McWilliams, D. F. & Walsh, D. A. 2007. Neurovascular invasion at the osteochondral junction and in osteophytes in osteoarthritis. Ann Rheum Dis, **66**, 1423-8.
- Szolcsányi, J. & Sándor, Z. 2012. Multimeric TRPV1 nociceptor: a target for analgesics. Trends in Pharmacological Sciences, **33**, 646-655.
- Taiwo, Y. O., Levine, J. D., Burch, R. M., Woo, J. E. & Mobley, W. C. 1991. Hyperalgesia induced in the rat by the amino-terminal octapeptide of nerve growth factor. Proceedings of the National Academy of Sciences, **88**, 5144-5148.
- Takebe, T., Kobayashi, S., Suzuki, H., Mizuno, M., Chang, Y.-M., Yoshizawa, E., Kimura, M., Hori, A., Asano, J., Maegawa, J. & Taniguchi, H. 2014. Transient vascularization of transplanted human adult-derived progenitors promotes self-organizing cartilage. The Journal of Clinical Investigation, **124**, 4325-4334.
- Tavakol, M. & Dennick, R. 2011. Making sense of Cronbach's alpha. International Journal of Medical Education, **2**, 53-55.
- Teitelbaum, S. L. 2007. Osteoclasts: What Do They Do and How Do They Do It? The American Journal of Pathology, **170**, 427-435.
- Termeer, C., Benedix, F., Sleeman, J., Fieber, C., Voith, U., Ahrens, T., Miyake, K., Freudenberg, M., Galanos, C. & Simon, J. C. 2002. Oligosaccharides of Hyaluronan activate dendritic cells via toll-like receptor 4. J Exp Med, **195**, 99-111.
- Tessier, J. J., Bowyer, J., Brownrigg, N. J., Peers, I. S., Westwood, F. R., Waterton, J. C. & Maciewicz, R. A. 2003. Characterisation of the guinea pig model of osteoarthritis by in vivo three-dimensional magnetic resonance imaging. Osteoarthritis and Cartilage, **11**, 845-853.
- Thakur, M., Dickenson, A. H. & Baron, R. 2014. Osteoarthritis pain: nociceptive or neuropathic? Nat Rev Rheumatol, **10**, 374-380.
- Thompson, S. W. N., Bennett, D. L. H., Kerr, B. J., Bradbury, E. J. & McMahon, S. B. 1999. Brain-derived neurotrophic factor is an endogenous modulator of nociceptive responses in the spinal cord. Proceedings of the National Academy of Sciences, **96**, 7714-7718.
- Tiseo, P. J., Kivitz, A. J., Ervin, J. E., Ren, H. & Mellis, S. J. 2014. Fasinumab (REGN475), an antibody against nerve growth factor for the treatment of pain: Results from a double-blind, placebo-controlled exploratory study in osteoarthritis of the knee. Pain, **155**, 1245-1252.
- Toni, T., Dua, P. & Van Der Graaf, P. H. 2014. Systems Pharmacology of the NGF Signaling Through p75 and TrkA Receptors. CPT Pharmacometrics Syst Pharmacol, **3**, e150.

- Tonussi, C. R. & Ferreira, S. H. 1992. Rat knee-joint carrageenin incapacitation test: an objective screen for central and peripheral analgesics. *Pain*, **48**, 421-7.
- Tore, F. & Tuncel, N. 2009. Mast cells: target and source of neuropeptides. *Curr Pharm Des*, **15**, 3433-45.
- Torelli, S. R., Rahal, S. C., Volpi, R. S., Yamashita, S., Mamprim, M. J. & Crocci, A. J. 2004. Radiography, computed tomography and magnetic resonance imaging at 0.5 Tesla of mechanically induced osteoarthritis in rabbit knees. *Brazilian Journal of Medical and Biological Research*, **37**, 493-501.
- Torres, L., Dunlop, D. D., Peterfy, C., Guermazi, A., Prasad, P., Hayes, K. W., Song, J., Cahue, S., Chang, A., Marshall, M. & Sharma, L. 2006. The relationship between specific tissue lesions and pain severity in persons with knee osteoarthritis. *Osteoarthritis and Cartilage*, **14**, 1033-1040.
- Trelle, S., Reichenbach, S., Wandel, S., Hildebrand, P., Tschannen, B., Villiger, P. M., Egger, M. & Juni, P. 2011. Cardiovascular safety of non-steroidal anti-inflammatory drugs: network meta-analysis. *BMJ*, **342**, c7086.
- Unger, T. J., Calderon, G. A., Bradley, L. C., Sena-Esteves, M. & Rios, M. 2007. Selective deletion of Bdnf in the ventromedial and dorsomedial hypothalamus of adult mice results in hyperphagic behavior and obesity. *J Neurosci*, **27**, 14265-74.
- Vad, V. B. & Dysart, S. H. 2012. Managing Knee Osteoarthritis: Systemic Pharmacotherapy and Intra-Articular Treatments. Available: <http://www.rheumatologynetwork.com/osteoarthritis/managing-knee-osteoarthritis-systemic-pharmacotherapy-and-intra-articular-treatments> [Accessed 03/04/2015].
- Valdes, A. M., Van Oene, M., Hart, D. J., Surdulescu, G. L., Loughlin, J., Doherty, M. & Spector, T. D. 2006. Reproducible genetic associations between candidate genes and clinical knee osteoarthritis in men and women. *Arthritis & Rheumatism*, **54**, 533-539.
- Valenti, C., Giuliani, S., Cialdai, C., Tramontana, M. & Maggi, C. A. 2010a. Anti-inflammatory synergy of MEN16132, a kinin B2 receptor antagonist, and dexamethasone in carrageenan-induced knee joint arthritis in rats. *British Journal of Pharmacology*, **161**, 1616-1627.
- Valenti, C., Giuliani, S., Cialdai, C., Tramontana, M. & Maggi, C. A. 2010b. Anti-inflammatory synergy of MEN16132, a kinin B(2) receptor antagonist, and dexamethasone in carrageenan-induced knee joint arthritis in rats. *British Journal of Pharmacology*, **161**, 1616-1627.
- Valenti, C., Giuliani, S., Cialdai, C., Tramontana, M. & Maggi, C. A. 2012. Fasitibant chloride, a kinin B(2) receptor antagonist, and dexamethasone interact to inhibit carrageenan-induced inflammatory arthritis in rats. *British Journal of Pharmacology*, **166**, 1403-1410.
- Van Der Kraan, P. M., Vitters, E. L., Van Beuningen, H. M., Van De Putte, L. B. & Van Den Berg, W. B. 1990. Degenerative knee joint lesions in mice after a single intra-articular collagenase injection. A new model of osteoarthritis. *Journal of experimental pathology (Oxford, England)*, **71**, 19-31.
- Van Der Kraan, P. M., Vitters, E. L., Van De Putte, L. B. & Van Den Berg, W. B. 1989. Development of osteoarthritic lesions in mice by "metabolic"

- and "mechanical" alterations in the knee joints. The American Journal of Pathology, **135**, 1001-1014.
- Van Der Kuyl, A. C., Van Den Burg, R., Zorgdrager, F., Groot, F., Berkhout, B. & Cornelissen, M. 2007. Sialoadhesin (CD169) Expression in CD14+ Cells Is Upregulated Early after HIV-1 Infection and Increases during Disease Progression. PLoS ONE, **2**, e257.
- Van Der Sluijs, J. A., Geesink, R. G., Van Der Linden, A. J., Bulstra, S. K., Kuyser, R. & Drukker, J. 1992. The reliability of the Mankin score for osteoarthritis. J Orthop Res, **10**, 58-61.
- Van Lent, P. L., Blom, A. B., Schelbergen, R. F., Sloetjes, A., Lafeber, F. P., Lems, W. F., Cats, H., Vogl, T., Roth, J. & Van Den Berg, W. B. 2012. Active involvement of alarmins S100A8 and S100A9 in the regulation of synovial activation and joint destruction during mouse and human osteoarthritis. Arthritis Rheum, **64**, 1466-76.
- Van Lent, P. L. E. M., Blom, A. B., Van Der Kraan, P., Holthuysen, A. E. M., Vitters, E., Van Rooijen, N., Smeets, R. L., Nabbe, K. C. a. M. & Van Den Berg, W. B. 2004. Crucial role of synovial lining macrophages in the promotion of transforming growth factor β -mediated osteophyte formation. Arthritis & Rheumatism, **50**, 103-111.
- Verburg, K. 2012. *Monoclonal Antibodies Targeted Against Nerve Growth Factor For the Treatment of Chronic Pain* [Online]. Available: <http://www.fda.gov/downloads/advisorycommittees/committeesmeetinmaterials/drugs/arthritisadvisorycommittee/ucm301305.pdf> [Accessed 12/10/2014 2014].
- Vonsy, J. L., Ghandehari, J. & Dickenson, A. H. 2009. Differential analgesic effects of morphine and gabapentin on behavioural measures of pain and disability in a model of osteoarthritis pain in rats. Eur J Pain, **13**, 786-93.
- Voss, K., Stem, D., Jr. & Fotopoulos, S. 2000. A Comment on the Relationship between Coefficient Alpha and Scale Characteristics. Marketing Letters, **11**, 177-191.
- Walsh, D. A., Bonnet, C. S., Turner, E. L., Wilson, D., Situ, M. & McWilliams, D. F. 2007. Angiogenesis in the synovium and at the osteochondral junction in osteoarthritis. Osteoarthritis Cartilage, **15**, 743-51.
- Walsh, D. A., McWilliams, D. F., Turley, M. J., Dixon, M. R., Franses, R. E., Mapp, P. I. & Wilson, D. 2010. Angiogenesis and nerve growth factor at the osteochondral junction in rheumatoid arthritis and osteoarthritis. Rheumatology (Oxford), **49**, 1852-61.
- Walsh, D. A., Rodway, H. A. & Claxson, A. 1998a. Vascular turnover during carrageenan synovitis in the rat. Lab Invest, **78**, 1513-21.
- Walsh, D. A., Salmon, M., Wharton, J., Mapp, P. I. & Polak, J. M. 1993. Autoradiographic localisation and characterisation of substance P binding sites in rat knees. Regulatory Peptides, **46**, 189-192.
- Walsh, D. A., Wade, M., Mapp, P. I. & Blake, D. R. 1998b. Focally regulated endothelial proliferation and cell death in human synovium. Am J Pathol, **152**, 691-702.
- Walsh, D. A., Yousef, A., McWilliams, D. F., Hill, R., Hargin, E. & Wilson, D. 2008. Evaluation of a Photographic Chondropathy Score (PCS) for pathological samples in a study of inflammation in tibiofemoral osteoarthritis. Osteoarthritis and Cartilage, **17**, 304-312.

- Watanabe, T., Ito, T., Inoue, G., Ohtori, S., Kitajo, K., Doya, H., Takahashi, K. & Yamashita, T. 2008. The p75 receptor is associated with inflammatory thermal hypersensitivity. J Neurosci Res, **86**, 3566-74.
- Watson, J., Allen, S. & Dawbarn, D. 2008. Targeting Nerve Growth Factor in Pain. BioDrugs, **22**, 349-359.
- Wei, L., Fleming, B. C., Sun, X., Teeple, E., Wu, W., Jay, G. D., Elsaid, K. A., Luo, J., Machan, J. T. & Chen, Q. 2010. A Comparison of Differential Biomarkers of Osteoarthritis with and without Post-traumatic Injury in the Hartley Guinea Pig Model. Journal of orthopaedic research : official publication of the Orthopaedic Research Society, **28**, 900-906.
- Wenham, C. Y. J. & Conaghan, P. G. 2010. The role of synovitis in osteoarthritis. Therapeutic Advances in Musculoskeletal Disease, **2**, 349-359.
- Werner, B., Antonio Carlosnadj, Mehdadorres, Luiz Fernando Bleggi 2005. Practical use of Immunohistochemistry in surgical pathology. Jornal Brasileiro de Patologia e Medicina Laboratorial, **41**, 353-364.
- Werner, M., Chott, A., Fabiano, A. & Battifora, H. 2000. Effect of formalin tissue fixation and processing on immunohistochemistry. Am J Surg Pathol, **24**, 1016-9.
- Williams, J. M. & Brandt, K. D. 1984. Exercise increases osteophyte formation and diminishes fibrillation following chemically induced articular cartilage injury. Journal of Anatomy, **139**, 599-611.
- Williams, J. M. & Brandt, K. D. 1985. Triamcinolone hexacetonide protects against fibrillation and osteophyte formation following chemically induced articular cartilage damage. Arthritis Rheum, **28**, 1267-74.
- Winston, J. H., Toma, H., Shenoy, M., He, Z. J., Zou, L., Xiao, S. Y., Micci, M. A. & Pasricha, P. J. 2003. Acute pancreatitis results in referred mechanical hypersensitivity and neuropeptide up-regulation that can be suppressed by the protein kinase inhibitor k252a. J Pain, **4**, 329-37.
- Wise, B. L., Niu, J., Yang, M., Lane, N. E., Harvey, W., Felson, D. T., Hietpas, J., Nevitt, M., Sharma, L., Torner, J., Lewis, C. E. & Zhang, Y. 2012. Patterns of compartment involvement in tibiofemoral osteoarthritis in men and women and in whites and African Americans. Arthritis Care Res (Hoboken), **64**, 847-52.
- Wolfensohn, S. & Lloyd, M. 2003. Handbook of Laboratory Animal Management and Welfare, Third Edition. Blackwell Publishing Ltd.
- Woolf, C. J. *Pain hypersensitivity* [Online]. Wellcome trust. Available: <http://www.wellcome.ac.uk/en/pain/microsite/science4.html> [Accessed 12/08/2015 2015].
- Woolf, C. J. 1991. Generation of acute pain: central mechanisms. Br Med Bull, **47**, 523-33.
- Woolf, C. J. 1996. Phenotypic Modification of Primary Sensory Neurons: The Role of Nerve Growth Factor in the Production of Persistent Pain. Philosophical Transactions of the Royal Society of London. Series B: Biological Sciences, **351**, 441-448.
- Woolf, C. J. 2011. Central sensitization: Implications for the diagnosis and treatment of pain. PAIN, **152**, S2-S15.
- Woolf, C. J. & Costigan, M. 1999. Transcriptional and posttranslational plasticity and the generation of inflammatory pain. Proceedings of the

National Academy of Sciences of the United States of America, **96**, 7723-7730.

- Yaziji, H. & Barry, T. 2006. Diagnostic Immunohistochemistry: what can go wrong? Adv Anat Pathol, **13**, 238-46.
- Yorimitsu, M., Nishida, K., Shimizu, A., Doi, H., Miyazawa, S., Komiyama, T., Nasu, Y., Yoshida, A., Watanabe, S. & Ozaki, T. 2008. Intra-articular injection of interleukin-4 decreases nitric oxide production by chondrocytes and ameliorates subsequent destruction of cartilage in instability-induced osteoarthritis in rat knee joints. Osteoarthritis and Cartilage, **16**, 764-771.
- Yoshioka, M., Coutts, R. D., Amiel, D. & Hacker, S. A. 1996. Characterization of a model of osteoarthritis in the rabbit knee. Osteoarthritis and Cartilage, **4**, 87-98.
- Yu, D.-G., Yu, B., Mao, Y.-Q., Zhao, X., Wang, X.-Q., Ding, H.-F., Cao, L., Liu, G.-W., Nie, S.-B., Liu, S. & Zhu, Z.-A. 2012. Efficacy of zoledronic acid in treatment of teoarthritis is dependent on the disease progression stage in rat medial meniscal tear model. Acta Pharmacol Sin, **33**, 924-934.
- Yu, D. G., Ding, H. F., Mao, Y. Q., Liu, M., Yu, B., Zhao, X., Wang, X. Q., Li, Y., Liu, G. W., Nie, S. B., Liu, S. & Zhu, Z. A. 2013. Strontium ranelate reduces cartilage degeneration and subchondral bone remodeling in rat osteoarthritis model. Acta Pharmacol Sin, **34**, 393-402.
- Yu, Y. C., Koo, S. T., Kim, C. H., Lyu, Y., Grady, J. J. & Chung, J. M. 2002. Two variables that can be used as pain indices in experimental animal models of arthritis. J Neurosci Methods, **115**, 107-13.
- Yusuf, E., Kortekaas, M. C., Watt, I., Huizinga, T. W. J. & Kloppenburg, M. 2011. Do knee abnormalities visualised on MRI explain knee pain in knee osteoarthritis? A systematic review. Annals of the Rheumatic Diseases, **70**, 60-67.
- Zegarska, B., Lelinska, A. & Tyrakowski, T. 2006. Clinical and experimental aspects of cutaneous neurogenic inflammation. Pharmacol Rep, **58**, 13-21.
- Zhang, G. H., Min, S. S., Lee, K. S., Back, S. K., Yoon, S. J., Yoon, Y. W., Kim, Y. I., Na, H. S., Hong, S. K. & Han, H. C. 2004. Intraarticular pretreatment with ketamine and memantine could prevent arthritic pain: relevance to the decrease of spinal c-fos expression in rats. Anesth Analg, **99**, 152-8.
- Zhang, W., Doherty, M., Peat, G., Bierma-Zeinstra, M. A., Arden, N. K., Bresnihan, B., Herrero-Beaumont, G., Kirschner, S., Leeb, B. F., Lohmander, L. S., Mazieres, B., Pavelka, K., Punzi, L., So, A. K., Tuncer, T., Watt, I. & Bijlsma, J. W. 2010a. EULAR evidence-based recommendations for the diagnosis of knee osteoarthritis. Ann Rheum Dis, **69**, 483-9.
- Zhang, W., Moskowitz, R. W., Nuki, G., Abramson, S., Altman, R. D., Arden, N., Bierma-Zeinstra, S., Brandt, K. D., Croft, P., Doherty, M., Dougados, M., Hochberg, M., Hunter, D. J., Kwoh, K., Lohmander, L. S. & Tugwell, P. 2008. OARSI recommendations for the management of hip and knee osteoarthritis, Part II: OARSI evidence-based, expert consensus guidelines. Osteoarthritis Cartilage, **16**, 137-62.

- Zhang, W., Nuki, G., Moskowitz, R. W., Abramson, S., Altman, R. D., Arden, N. K., Bierma-Zeinstra, S., Brandt, K. D., Croft, P., Doherty, M., Dougados, M., Hochberg, M., Hunter, D. J., Kwoh, K., Lohmander, L. S. & Tugwell, P. 2010b. OARSI recommendations for the management of hip and knee osteoarthritis: part III: Changes in evidence following systematic cumulative update of research published through January 2009. Osteoarthritis Cartilage, **18**, 476-99.
- Zhu, W., Galoyan, S. M., Petruska, J. C., Oxford, G. S. & Mendell, L. M. 2004. A developmental switch in acute sensitization of small dorsal root ganglion (DRG) neurons to capsaicin or noxious heating by NGF. Journal of neurophysiology, **92**, 3148-52.
- Zimmermann, M. 1983. Ethical guidelines for investigations of experimental pain in conscious animals. Pain, **16**, 109-10.

APPENDICES

Materials and Reagents

Acetic acid	VWR Ltd. Lutterworth, UK
Acetone	VWR Ltd. Lutterworth, UK
Accu-Edge disposable microtome blades	University of Nottingham stores
Albumin, Bovine (A-4503)	Sigma Aldrich, Poole, UK
Alcian blue (A5268)	Sigma Aldrich, Poole, UK
Ammonium Chloride	VWR Ltd. Lutterworth, UK
Axio Vision Imaging system	Carl Zeiss Ltd. Welwyn Garden City, UK
Axiocam	Carl Zeiss Ltd. Welwyn Garden City, UK
Beta-D-glucose (G5250)	Sigma Aldrich, Poole, UK
Cork Blocks 20mm x 3mm (E7.15/CD)	Raymond Lamb, Eastbourne, UK
Coverslips 22mm x 64mm	VWR Ltd. Lutterworth, UK
DePeX™	VWR Ltd. Lutterworth, UK
Diaminobenzidine (D5637)	Sigma Aldrich, Poole, UK
Diammonium Nickle II Sulphate (A1827)	Sigma Aldrich, Poole, UK
Disodium phosphate heptahydrate (S9390)	Sigma Aldrich, Poole, UK
EDTA Disodium Salt (E5134)	University of Nottingham stores
Electronic Calliper	Miyutoyo UK Ltd. Andover, UK
Eosin (1%)	Raymond Lamb, Eastbourne, UK
Ethanol absolute (32221)	Sigma Aldrich, Poole, UK
Fast Green (F-7258)	Sigma Aldrich, Poole, UK
Formalin Neutral buffered pH 7.0	VWR Ltd. Lutterworth, UK
Formic Acid (399388)	Sigma Aldrich, Poole, UK
Glucose Oxidase Aspergillus Niger (G2133)	Sigma Aldrich, Poole, UK
Harris Haematoxylin	Raymond Lamb, Eastbourne, UK
Haematoxylin (H3136)	Sigma Aldrich, Poole, UK
Horse Serum (H1270)	Sigma Aldrich, Poole, UK
Hydrochloric Acid	VWR Ltd. Lutterworth, UK
Hydrogen peroxide (H1009)	Sigma Aldrich, Poole, UK
Incapacitance Meter	Linton Instruments, Norfolk, UK
Iron (III) Chloride (157740)	Sigma Aldrich, Poole, UK
Isopentane	VWR Ltd. Lutterworth, UK
KS300 image analysis software	Imaging Associates Ltd. Thame, UK
Lambda Carrageenan (C-3889)	Sigma Aldrich, Poole, UK
Sprague Dawley rats	Charles River, Kent, UK
Mayers Haematoxylin	Raymond Lamb, Eastbourne, UK
Methanol	Sigma Aldrich, Poole, UK
Novasapa cold steriliser	Pfizer Animal Health, Surrey, UK
Paraformaldehyde (P6148)	Sigma Aldrich, Poole, UK
Periodic acid	Sigma Aldrich, Poole, UK
Phosphate Buffered Saline pH 7.4 (43711)	VWR Ltd. Lutterworth, UK
Polysine™ Microscope adhesion slides (10219280)	Fischer Scientific Ltd. Loughborough, UK
Polyvinylpyrrolidone (PVP40T)	Sigma Aldrich, Poole, UK
Safranin-O (S-2255)	Sigma Aldrich, Poole, UK
Schiff reagent (1090330500)	VWR Ltd. Lutterworth, UK

Shandon Pathcentre Tissue Processor
SLS Slides Immunofl Wht 3 Well 10mm^o
(MIC3410)

Sodium acetate trihydrate (236500)
Sodium Chloride (S-3014)
Sodium Chloride Solution, 0.9% (S8776)
Sodium iodoacetate (I9148)
Sony DSC-s85 CyberShot digital camera
Sterile Op-Cover
Sterile scalpel blades no.11
Surgical Instruments
Syringe insulin-0.5ml 29G (6134897)
Tissue Tek® embedding centre
Tissue Tek OCT® mounting medium
TRAP Kit
Tris base (T1509)
Vectastain® *Elite* ABC Kit (PK6100)
Vetasept Povidone-Iodine Scrub
Xylene
Zeiss Axioscop-50 microscope

Shandon Thermo Scientific, Leicester, UK

Scientific Laboratory Supplies Ltd.
Nottingham, UK

Sigma Aldrich, Poole, UK
Sigma Aldrich, Poole, UK
Sigma Aldrich, Poole, UK
Sigma Aldrich, Poole, UK
Carl Zeiss Ltd. Welwyn Garden City, UK
Kruuse Ltd. Sherburn in Elmet, North Yorkshire
Swann-Morton Sheffield, UK
Interfocus Ltd. Cambridge, UK
VWR Ltd. Lutterworth, UK
Sakura Finetek Europe, The Netherlands
Raymond Lamb, Eastbourne, UK
Sigma Aldrich, Poole, UK
Sigma Aldrich, Poole, UK
Vector Laboratories Ltd. Peterborough, UK
Animalcare Ltd. Dunnington, York
Sigma Aldrich, Poole, UK
Carl Zeiss Ltd. Welwyn Garden City, UK

Buffers and solutions used for immunohistochemistry

Acid Alcohol	Hydrochloric Acid (1.0 M) Ethanol dH ₂ O	5.0ml 350ml 145ml
Acetic acid solution	Acetic acid (glacial) dH ₂ O	4ml 396ml
Cryoprotectant	PBS Sucrose: 1xPBS Sucrose Sodium Azide	 2.5L 375g 0.25g
Decalcification fluid	dH ₂ O Tris (trizma) base EDTA (10% w/v) PVP (7.5% w/v) NaOH pellets pH	2.5L 3.35g 250g 187.5g 20-25g 6.95
Fast Green Solution	Fast Green dH ₂ O	0.1g 500ml
Fixative	Formalin Zamboni's: 16% PFA Picric Acid 0.2M Phosphate buffer dH ₂ O	 250ml 150ml 500ml 100ml
Horse Blocking Buffer	BSA (5%) Horse serum (3.3%) PBS (0.1ml) dH ₂ O	0.01g 0.7ml 2.0ml 17.3ml
Hydrochloric acid (1.0M)	HCL (37%) dH ₂ O	0.5ml 4.5ml
Hydrogen Peroxide in Methanol	Hydrogen Peroxide (0.33%) Methanol	3.0ml 300ml

PBS (10 x concentrated at 0.1 M) Working dilution (1x)	Sodium chloride	70.1g
	Sodium dihydrogen Orthophosphate	4.4g
	Di-sodium hydrogen Orthophosphate	12.8g
	Potassium chloride	2.0g
	pH	7.4
Safranin-O Solution	Safranin-O	0.04g
	dH ₂ O	400ml
Sodium Acetate (0.1M)	Sodium acetate trihydrate	5.64g
	Glacial acetic acid	3.51ml
	dH ₂ O	1L
Sodium Acetate (0.2M)	Sodium acetate trihydrate	25.77 g
	Glacial acetic acid	0.6ml
	dH ₂ O	1L
Weigert's Haematoxylin; Reagent A	Haematoxylin	
Reagent B	Ethanol	2.0g
	dH ₂ O	200ml
Note: Add equal volumes of A to B to make Weigert's Haematoxylin		10ml
	Iron (III) Chloride (2.9g in 10ml dH ₂ O)	8ml
	HCL (37%)	2ml
	dH ₂ O	190ml
TRAP kit	Acetate solution	50ml
	Citrate solution	50ml
	Fast Garnet GBC Base solution	10nl
	Naphthol AS-BI Phosphoric acid	10ml
	Sodium Nitrate solution	10ml
	Tartrate solution	10ml
	Gill's Haematoxylin solution	50ml

Antibody list

Primary antibodies

Description	Specificity	Other names	Clone	Isotype	Product type	Code	Company	Reference	Dilution
Mouse Anti-rat CD68	CD68	ED1, macrosialin	ED1	IgG1	Monoclonal	MCA341GA	Serotec Ltd. Oxford, UK	Dijkstra et al., 1985	1:1000
Mouse Anti-rat CD163	CD163	ED2	ED2	IgG1	Monoclonal	MCA342GA	Serotec Ltd. Oxford, UK	Dijkstra et al., 1985	1:1000
Mouse Anti-rat CD169	CD169	ED3	ED3	IgG2a	Monoclonal	MCA343GA	Serotec Ltd. Oxford, UK	Dijkstra et al., 1985	1:1000

Secondary antibody

Description	Antigen	Donor	Label	Code	Company	Dilution
Anti-Mouse IgG Affinity Purified, Rat Absorbed	Mouse IgG	Horse	Biotinylated	BA- 2001	Vector Laboratories Ltd. Peterborough, UK	1:100